The regulation of STIM1 translocation to the plasma membrane

Ciara Mary Elizabeth Walsh

UNIVERSITY OF LIVERPOOL

Thesis submitted in accordance with the requirements of the University of Liverpool for the degree of Doctor in Philosophy

September 2010

The regulation of STIM1 translocation to the plasma membrane

Ciara Mary Elizabeth Walsh

Abstract

A rise in intracellular Ca^{2+} concentration is key to controlling both short term and long term Ca^{2+} dependent processes which include secretion, metabolism and gene expression, cell growth and proliferation. Store operated Ca^{2+} channels (SOCs), which are activated by the depletion of Ca^{2+} from internal Ca^{2+} stores, the main store being the endoplasmic reticulum (ER), are the major route for Ca^{2+} influx in non-excitable cell types. Stromal interacting molecule 1 (STIM1) is a Ca^{2+} sensing protein located in the endoplasmic reticulum (ER). Depletion of ER calcium stores triggers oligomerisation and subsequent translocation of STIM1 from its reticular location to specialized endoplasmic reticulum-plasma membrane (ER-PM) junctions where it forms STIM1 puncta and interacts with the SOC channel, Orai1. This induces the clustering of Orai1 into a functional tetrameric pore which is permeable to Ca^{2+} ions, enabling Ca^{2+} entry into the cell. The precise mechanism by which STIM1 is recruited to the plasma membrane to activate SOCs and the plasma membrane components involved in targeting STIM1 to the plasma membrane are largely unknown. In this study the mechanisms underlying movement of STIM1 to the plasma membrane and its accumulation at ER-plasma membrane junctions was explored in HeLa cells.

In the initial part of this study I investigated whether the movement of STIM1 to the plasma membrane is an ATP-dependent process. I found that depletion of cytosolic ATP can stimulate STIM1 puncta formation in HeLa cells and

that the formation of STIM1-Orai1 complexes at the plasma membrane is unaffected in these conditions. Inhibition of ATP synthesis also initiated the loss of phosphatidylinositol 4,5-bisphosphate (PtdIns(4,5)P_2) from the plasma membrane. ATP depletion did not affect the structure of the microtubule cytoskeleton. These results suggest that the translocation of STIM1 and the formation of STIM1-Orai1 complexes is an ATP independent process which is not due to the disruption of microtubules and support a diffusional model for STIM1 puncta formation.

It has been suggested that an additional interaction of the C-terminal polybasic domain of STIM1 with plasma membrane phosphoinositides could contribute to STIM1 puncta formation prior to binding to Orai1. I investigated the role of phosphoinositides in the formation of STIM1 puncta and SOCE in response to store depletion. Treatment of HeLa cells with inhibitors of the phosphatidylinositol 3-kinase (PI3K) and phosphatidylinositol 4-kinase (wortmannin and LY294002) partially inhibited formation of STIM1 puncta. Additional rapid depletion of PtdIns(4,5)P_2 resulted in more substantial inhibition of the translocation of STIM1-EYFP into puncta. The inhibition was extensive at a concentration of LY294002 (50 μM) that should primarily inhibit PI3K consistent with a major role for PtdIns(4,5)P_2 and PtdIns(3,4,5)P_3 in puncta formation. Depletion of phosphoinositides also partially inhibited SOCE. Overexpression of Orai1 resulted in a recovery of translocation of STMI1 into puncta following phosphoinositide depletion and under these conditions SOCE was increased to above control levels. These observations support the idea that phosphoinositides are not essential but contribute to STIM1 accumulation at ER-PM junctions with a second translocation mechanism involving direct STIM1/Orai1 interactions.

It was recently reported that STIM1 and Orai1 may function within a macromolecular complex involving other unidentified proteins. In this study I have identified that Golli-BG21, a member of the myelin basic protein (MBP) family, can directly interact with STIM1. Golli interacts with the C-terminal domain of STIM1 in both *in vitro* and *in vivo* binding assays and this interaction may be modulated by intracellular Ca^{2+} concent554ration. Golli also colocalises with full length STIM1 and Orai1 complexes in HeLa cells following store depletion. Overexpression of Golli reduces SOCE in HeLa cells but this inhibition is overcome by overexpressing STIM1. We therefore suggest that Golli binds to STIM1-Orai1 complexes to negatively regulate the activity of SOCs.

Publications

Work presented in this thesis has been published in part in the following papers:

Walsh C.M., Doherty M.K., Tepikin A.V. and Burgoyne R.D. (2010). Evidence for an interaction between STIM1 and Golli in store operated calcium entry. *Biochem. J.*, **430(3)**:453-460.

Walsh, C.M., Chvanov, M., Haynes, L.P., Petersen, O.H., Tepikin, A.V. and Burgoyne, R.D. (2009). Role of phosphoinositides in STIM1 dynamics and store operated calcium entry. *Biochem. J.*, **425(1)**:159-168.

*Chvanov M, *Walsh C.M., Haynes LP, Voronina SG, Lur G, Gerasimenko OV, Barraclough R, Rudland PS, Petersen OH, Burgoyne RD & Tepikin AV. (2008). ATP depletion induces translocation of STIM1 to puncta and formation of STIM1-Orai1 clusters: translocation and re-translocation of STIM1 does not require ATP. *Pflugers. Arch.* **457**:505-517. *equal first authors

Table of Contents

Abbreviations

µg	Microgram
µl	Microlitre
µM	Micromolar
2-APB	2-aminoethoxydiphenyl-borate
2DG	2-Deoxy-D-glucose
Å	Angstrom
aa	Amino acid
AC	Adenylyl cyclase
AMPA	α-amino-3-hydroxy-5-methyl-isoxalole-5-prioponic acid
ARC	Arachidonic-acid-regulated-Ca^{2+}-selective
ATP	Adenosine triphosphate
Ba^{2+}	Barium
BiFC	Bimolecular fluorescence complementation
Ca^{2+}	Calcium
CAD	Ca^{2+}-activating domain
CaM	Calmodulin
CDI	Ca^{2+}-dependent inactivation
cEF	Canonical EF hand
CFP	Cyan fluorescent protein
CICR	Calcium-induced calcium release
CMD	CRAC modulatory domain
$cPLA_2$	cytoplasmic phospholipase A_2

CRAC	Calcium release-activated calcium
CRACR2A	CRAC regulator 2A
Cs^{2+}	Caesium
CTD	C-terminal domain
DAG	Diacylglycerol
dNTP	Deoxyribonucleotide triphosphate
EM	Electron microscopy
ER	Endoplasmic reticulum
ERM	Ezrin-radixin-moesin
EYFP	Enhanced yellow fluorescent protein
FAPP1	Phosphoinositol 4-phosphate adaptor protein 1
FKBP	FK506 binding protein
FRB	FKBP12-rapamycin binding protein
FRET	Förster resonance energy transfer
fS	Femtosecond
Gd^{3+}	Gadolinium
GFP	Green fluorescent protein
GST	Glutathione S-transferase
hEF	Hidden EF hand
His_6	Hexahistidine peptide
HRP	Horseradish peroxidise
IA	Iodoacetate
I_{CRAC}	CRAC channel current
IL-2	Interleukin 2

IP_3	Inositol 1,4,5-trisphosphate
IP_3R	Inositol 1,4,5-trisphosphate receptor
KA	Kainate
K_d	Dissociation constant
kD	Kilodaltons
L	Litre
LTC_4	cysteinyl leukotriene C_4
MALDI-ToF	Matrix-assisted laser desorption/ionisation-time of flight mass spectrometry
MBP	Myelin basic protein
mCherry	Monomeric cherry protein
mg	Milligram
ml	Millilitre
mM	Millimolar
ms	Milliseconds
MβCD	methyl-β-cyclodextrin
NAADP	Nicotinic acid adenine dinucleotide phosphate
NCX	Na^+/Ca^{2+} exchanger
ng	Nanogram
nm	Nanometer
nM	Nanomolar
NMDA	N-methyl-D-aspartate
NTD	N-terminal domain
Olig	Oligomycin

PCR	Polymerase chain reaction
PFO-PAGE	Perfluoro-octanoic acid polyacrylamide gel *electrophoresis*
PI3K	Phosphatidylinositol 3-Kinase
PI4K	Phosphatidylinositol 4-Kinase
PKC	Protein kinase C
PLC	Phospholipase C
PM	Plasma membrane
PMCA	Plasma membrane Ca^{2+}-ATPase
Ptase	Phosphatase
PtdIns(3,4,5)P_3	Phosphatidylinositol 3,4,5-trisphosphate
PtdIns(4)P	Phosphatidylinositol 4-phosphate
PtdIns(4,5)P_2	Phosphatidylinositol 4,5-bisphosphate
RFP	Red fluorescent protein
RNAi	Ribonucleic acid interference
RyR	Ryanodine receptor
SAM	Sterile-α motif
SCID	Severe combined immune deficiency
SDS-PAGE	Sodium dodecyl sulfate polyacrylamide gel electrophoresis
SERCA	Sarco-endoplasmic reticulum Ca^{2+}-ATPase
SHD	STIM1 homomerisation domain
siRNA	Short-interfering ribonucleic acid
SNAP-25	Synaptosomal-associated protein of 25 kD
SNARE	soluble N-ethyl-*maleimide*-sensitive attachment receptor protein

SOAR	STIM1 Orai1 activating region
SOC	Store-operated calcium
SOCE	Store-operated calcium entry
SR	Sarcoplasmic reticulum
Sr^{2+}	Strontium
STIM1	Stromal interacting molecule 1
STIM2	Stromal interacting molecule 2
TIRF	Total internal reflection fluorescence
TM	Transmembrane
TPC	Two pore channel
TPEN	N,N,N,N-Tetrakis(2-pyridylmethyl)ethylenediamine
TRP	Transient receptor potential
TRPC	Transient receptor potential channel
U	Units
v/w	volume by weight
VAMP-2	Vesicle-associated membrane protein 2
Y2H	Yeast 2-hybrid
YC	C-terminal fragment of EYFP
YFP	Yellow fluorescent protein
YN	N-terminal fragment of EYFP
αSNAP	αSynaptosomal-associated protein

Acknowledgements

First and foremost I would like to thank my supervisors Prof Bob Burgoyne and Prof Alexei Tepikin for their excellent supervision, encouragement and guidance throughout my PhD. I would also like to thank Dr Lee Haynes for his incredible patience and guidance in the lab and for his spontaneous science pop quizzes (which I won't miss!) and to Hannah McCue for her continuous support, encouragement and (above all) friendship. To all Red Block members past and present, including Alan, Jeff, Helen, Margaret, Mark H, James, Sarah, Michele, Matt, Gerald, Zoe and Neil, thanks for putting up with my rants and raves, for answering my silly questions and for tolerating the stick insects. Thanks also to my fellow PhD peers: Jonathan, Chris, Gyuri, Dave and Sarah who were always free for a drink or a drop-in chat during our 4 years together.

Thanks goes to the housemates who I've lived with throughout my time in Liverpool, especially my topsie David for sticking with me in the Dublin AND Liverpool times, and Ryan who spent tireless hours with me listening (intently!) about STIM proteins and nearly as many with me forgetting about it in the Raz. Thanks also to all of my many housemates for tolerating the collection of disabled pets that I managed to acquire and for making me feel completely happy and at home in Liverpool.

A huge thank you to all of the countless friends I've come to know and love in Liverpool, especially to Robo and Gibo for the not so politically correct board game nights, David L for the all the gin times in Penny Lane, Naomi (never a dull

minute!), to dysfunctional Becky for her inspirational moments of brilliance and to the RCSI girlies in Dublin who have always stuck by me. Also thank you to the skydiving crew who made me take a massive leap of faith and never look back!

A very special thanks goes to my siblings Áine, Simon and Niall, to my new sisters Orlaith and Lorraine and to my incredible parents for their never ending love and support and for not losing the rag with me during my PhD and write up, I couldn't have done this without you.

Thanks also to all of the people who I've met in "The Pool" whose names are too many to mention here but who made my time in Liverpool, both inside and outside of the lab, an incredible experience which was a joy to share with them.

CHAPTER ONE

Introduction

1.1 Calcium Signalling

Calcium (Ca^{2+}) ions influence nearly every aspect of cellular life. Spatial and temporal modulation of cytoplasmic Ca^{2+} levels is a key signalling mechanism in virtually all cell types for the control of a multitude of both short and long term cellular processes (Parekh and Putney, 2005). Changes in intracellular Ca^{2+} regulate a range of functions such as enzyme activity and secretion. Cellular events as diverse as fertilisation and muscle contraction are controlled by cytosolic Ca^{2+} oscillations. Long term responses to spatial and temporal Ca^{2+} fluctuations include changes in gene transcription, mitochondrial ATP production, cell cycle control and apoptosis. The importance of Ca^{2+} signalling is highlighted by the range of human disorders caused by defects in Ca^{2+} homeostasis, which include severe combined immunodeficiency (SCID), acute pancreatitis, allergy, inflammatory bowel disease, thrombosis, breast cancer and Alzheimer's disease (Parekh, 2010; Parekh and Putney, 2005).

In most cases, Ca^{2+} signalling is initiated by a rise in cytoplasmic Ca^{2+} levels stimulated by external factors such as neurotransmitters, hormones or growth factors. Following this, Ca^{2+} can be sequestered by mitochondria or diffuse into the nucleus (Ashby and Tepikin, 2001). Eukaryotic cells have developed two distinct mechanisms for increasing their cytoplasmic Ca^{2+} concentration: Ca^{2+} release from intracellular stores or Ca^{2+} influx across the plasma membrane into the cell.

The equilibrium between Ca^{2+} influx and extrusion is critical for the maintenance of Ca^{2+} homeostasis. Mechanisms involved in increasing cytosolic Ca^{2+} include plasma membrane channels which regulate the influx of Ca^{2+} from the extracellular space, and channels located on the endoplasmic reticulum (ER) and sacroplasmic reticulum (SR) that regulate the release of Ca^{2+} from intracellular stores. Ca^{2+} release into the cytosplasm is offset by plasma membrane Ca^{2+}-ATPases (PMCAs) that transport Ca^{2+} across the plasma membrane and out of the cell, and by sarco-endoplasmic reticulum Ca^{2+}-ATPases (SERCAs) that pump Ca^{2+} from the cytoplasm into the lumen of the ER or SR. Additionally, ion exchangers, such as the Na^{+}/Ca^{2+} exchanger use the gradients of other ions to pump Ca^{2+} out of the cell. Mitochondria also play a role in buffering cytosolic Ca^{2+} through their low-affinity but high capacity Ca^{2+} uniporter (Bootman et al., 2001). An overview of Ca^{2+} signalling is illustrated in Figure 1.1.

At resting levels, the equilibrium between Ca^{2+} influx and extrusion maintains the concentration of intracellular free Ca^{2+} ($[Ca^{2+}]_i$) at ~100 nM or less, while extracellular Ca^{2+} concentration ($[Ca^{2+}]_o$) is approximately 1 – 2 mM. Stimulation by, for example, an extracellular agonist or depolarisation, induces an increase in $[Ca^{2+}]_i$ globally of up to 1 µM via Ca^{2+} influx through plasma membrane channels or Ca^{2+} release from stores (Bootman et al., 2001). Distinct PMCAs, SERCAs, Ca^{2+} sensor proteins and Ca^{2+} channels are expressed in varying levels in different cell types which confer cell-type specific Ca^{2+} signalling characteristics, accounting for the immense variability in the properties of Ca^{2+} signals observed within cellular systems (Berridge et al., 2000).

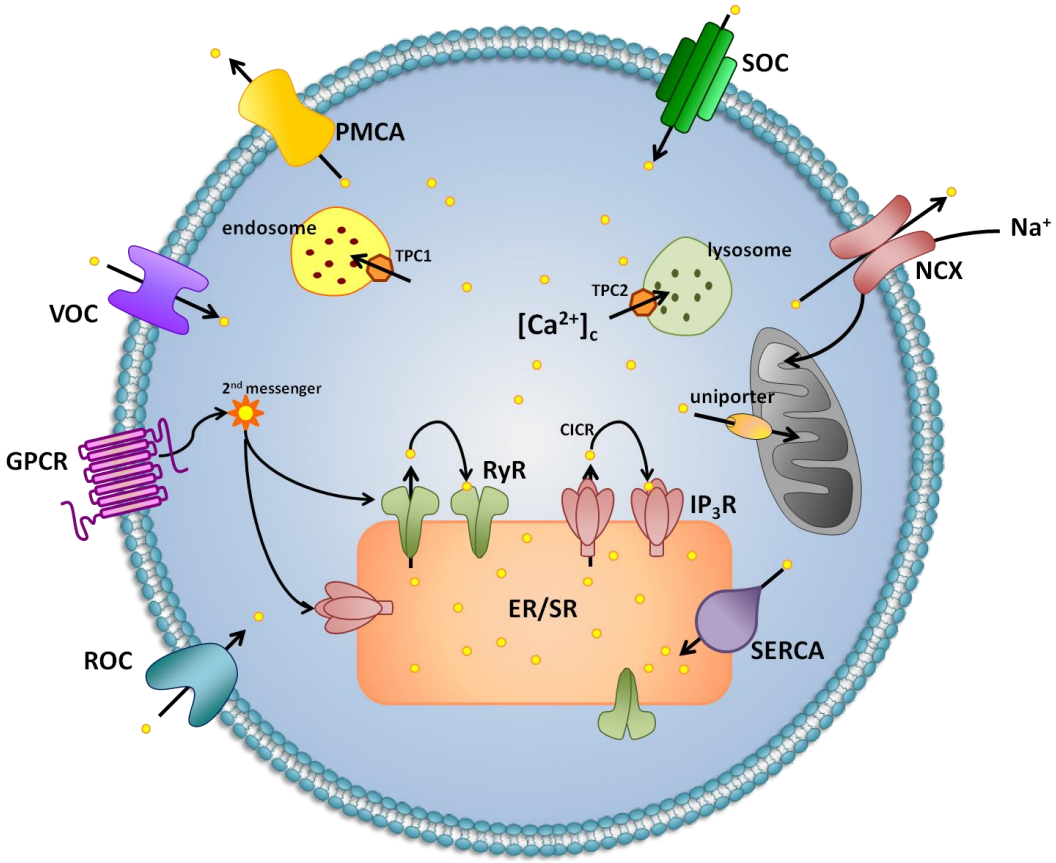

Figure 1.1. Overview of Ca^{2+} Signalling. Ca^{2+} influx into the cell is mediated by voltage-operated (or voltage-gated) channels (VOC), receptor operated channels (ROC), or store-operated channels (SOC). Ca^{2+} entry through ROCs are controlled by intracellular and extracellular agonists. SOCs are controlled by extracellular agonists which bind to G-protein coupled receptors (GPCRs) to stimulate the formation of second messengers, including inositol 1,4,5-trisphosphate (IP_3), to release Ca^{2+} from the endoplasmic reticulum or sarcoplasmic reticulum store (ER/SR) through the activation of IP_3 receptors (IP_3R) on the ER/SR membrane. Ryanodine receptors (RyR) on the ER/SR membrane are activated to release Ca^{2+} by second messengers including cyclic ADP ribose. Since IP_3R and RyR are both sensitive to Ca^{2+}, the Ca^{2+} signal can be propagated by the process of Ca^{2+}-induced Ca^{2+} release (CICR). The Ca^{2+} signal is attenuated by several mechanisms, including the transport of Ca^{2+} back into the ER by the action of the sarco/endoplasmic reticulum Ca^{2+}-ATPase (SERCA) or by the efflux of Ca^{2+} from the cell by the plasma membrane Ca^{2+}-ATPase (PMCA). The plasma membrane Na^+/Ca^{2+} exchanger (NCX) transports Ca^{2+} from the cell by exchanging three Na^+ ions for one Ca^{2+} ion from the cytosol. Additionally, cellular organelles such as the mitochondria can sequester Ca^{2+} via the mitochondrial uniporter and acidic stores such as the endosomes and lysosomes can release Ca^{2+} via the NAADP-sensitive two pore channels, TPC1 and TPC2, respectively.

However, very few Ca^{2+} signalling protein families are involved in regulating the diversity of Ca^{2+}-dependent processes, and these proteins are very well conserved and ubiquitously expressed throughout eukaryotes (Petersen et al., 2005).

Cells express various families of Ca^{2+}-permeable plasma membrane channels that each activates Ca^{2+} influx via different mechanisms. Voltage gated Ca^{2+} channels are the key signal transducers of electrical signalling, e.g. neurons and muscle, and activate Ca^{2+} influx in response to plasma membrane depolarisation to initiate cellular responses such as contraction, secretion and neurotransmission (Catterall et al., 2007). These Ca^{2+} selective pores are activated briefly in response to action potentials and generate an inward Ca^{2+} current. Several classes of voltage gated Ca^{2+} channels, namely L-, T-, N-, P-, Q- and R-type channels, have been characterised. The Ca_v1 subfamily ($Ca_v1.1$ – $Ca_v1.4$) conduct L-type Ca^{2+} currents that instigate endocrine secretion, contraction and synaptic transmission in the ribbon synapses of the ear and eye (Hofmann et al., 1994; Striessnig, 1999). The Ca_v2 subfamily ($Ca_v2.1$ – $Ca_v2.3$) conduct N- and P/Q-type Ca^{2+} currents required for fast synaptic transmission in neurons of the central and peripheral nervous system (Catterall, 2000; Dunlap et al., 1995; Olivera et al., 1994; Snutch and Reiner, 1992). Finally, the Ca_v3 subfamily ($Ca_v3.1$-$Ca_v3.3$) conduct T-type currents which are activated by small depolarisations of the plasma membrane and trigger low-threshold Ca^{2+} spiking which is important for repetitive action potential firing of neurons in the brain and in pacemaker cells in the heart (Perez-Reyes, 2003). Ligand operated channels, e.g. the vanilloid transient receptor potential (TRPV) channels, are a family of Ca^{2+} entry channels gated by a variety of stimuli, e.g. TRPV4 which is

expressed in a wide variety of tissues, is activated by synthetic 4α-phorbols, and also by endogenous substances including arachidonic acid, the endocannabinoids anandamide and 2-AG, and cytochrome P-450 metabolites of arachidonic acid (Nilius et al., 2004). Ca^{2+} influx through TRPV4 is thought to be involved in the regulation of terminal differentiation in osteoclasts by sustaining NFATc1-dependent gene expression (Masuyama et al., 2008). Finally, store-operated Ca^{2+} channels are activated by Ca^{2+} release from intracellular stores and since they are ubiquitously expressed are considered the major mechanism of Ca^{2+} influx in non-excitable cells (Parekh, 2007).

Ca^{2+} release from endoplasmic reticulum (ER), sarcoplasmic reticulum (SR) or acidic organelles can occur by the release of Ca^{2+} through messenger-activated channels located on the ER/SR and acidic membranes or by the activation of the mitochondrial permeability transition pore. Ca^{2+} can pass through the ER membrane into the cytosol via two distinct families of ion transport channels, inositol trisphosphate receptors (IP_3Rs) and ryanodine receptors (RyRs). IP_3Rs are ubiquitously expressed whereas RyRs are found mainly in excitable tissues such as skeletal and cardiac muscle where they are important for excitation-contraction coupling (Fill and Copello, 2002; Takeshima et al., 1994; Takeshima et al., 1998) but are also present in some non-excitable cell types including hepatocytes (Komazaki et al., 1998) and have been implicated in the stimulation of insulin secretion in excitable pancreatic beta cells (Johnson et al., 2004). IP_3R activation is initiated by the binding of various hormones and growth factors to specific cell surface receptors which culminate in phosphorylation and activation of phospholipase C

(PLC). Active PLC hydrolyses phosphatidylinositol 4,5-bisphosphate (PtdIns(4,5)P_2) to the second messengers inositol 1,4,5-trisphosphate (IP_3) and diacylglycerol (DAG). DAG is known to activate protein kinase C (PKC) isoforms but can also regulate ion channels independently of PKC (Potier and Trebak, 2008). IP_3 is mobile and diffuses through the cytosol until it binds to IP_3Rs on the ER/SR membrane. IP_3 binding induces a conformational change within the IP_3R resulting in the opening of the integral channel and the efflux of Ca^{2+} into the cytoplasm causing the resting ER Ca^{2+} concentration to drop below its resting levels of ~400—600 μM. Three IP_3R isoforms have been identified, each of which has a different affinity for Ca^{2+} (Mikoshiba, 2007). These receptors function as tetramers and can consist of homomeric and heteromeric subunits, suggesting that a range of functionally distinct IP_3Rs may exist in cells (Bootman et al., 2001). IP_3Rs are regulated by both IP_3 and cytosolic Ca^{2+}, where increases in local Ca^{2+} concentration stimulates further Ca^{2+}-induced Ca^{2+} release (CICR) from the stores. High concentrations of IP_3 and low (<1 μM) cytosolic Ca^{2+} concentrations synergistically activate IP_3Rs. However, the sensitivity of the IP_3R decreases at higher Ca^{2+} concentrations, and cytosolic Ca^{2+} concentrations of 1-10 μM inhibit the channels (Bootman and Lipp, 1999). The bell shaped dependence of IP_3R activity on cytosolic Ca^{2+} is critical for modulating the activity of IP_3Rs and for the production of the complex patterns of Ca^{2+} signals produced in cells (Bootman et al., 2001).

RyRs are structurally and functionally similar to IP_3Rs but exhibit twice the Ca^{2+} conductance of IP_3Rs. Like IP_3Rs, RyRs are sensitive to regulation by Ca^{2+} and exhibit a bell shaped dependence on Ca^{2+}, although they are activated at 1 – 10 μM and

inhibited at 10-100 µM cytosolic Ca^{2+} (Bootman et al., 2001). There are three RyR isoforms which each carry out specific functions in distinct cell types. Low concentrations (1-10 µM) of ryanodine stimulate, while higher concentrations (100 µM) inhibit RyRs. Millimolar concentrations of caffeine also increase the sensitivity of RyRs to Ca^{2+} so that RyRs become active at lower concentrations of Ca^{2+} (Bootman et al., 2001).

There are a number of different types of Ca^{2+} signalling events. Ca^{2+} signals can be small or large in amplitude, confined to small Ca^{2+} microdomains or extended global Ca^{2+} signals across the whole cell. Following the opening of IP_3Rs or RyRs, Ca^{2+} enters the cytosol to form an "elementary release event" (Laude and Simpson, 2009). Ca^{2+} "blips" arise from the opening of a single IP_3R or RyR, have a small amplitude of <30 nM, last for ~200 ms and typically don't spread beyond a few micrometres. Ca^{2+} "puffs" (known as "quarks" for RyRs) occur as a result of coordinated release of Ca^{2+} from a cluster of IP_3Rs (or RyRs). Ca^{2+} puffs have amplitudes of ~200 nM and last for ~500 ms (Laude and Simpson, 2009). A Ca^{2+} "wave" occurs as a result of the spatio-temporal summation of Ca^{2+} puffs and can spread globally throughout the cell. Ca^{2+} diffuses slowly through a cell (at a rate of 10-50 $\mu m^2/s$) (Laude and Simpson, 2009) and Ca^{2+} signals can be significantly modulated by Ca^{2+} release or uptake by cellular organelles.

Mitochondria can modulate both Ca^{2+} entry and release from internal stores, via the low-affinity, rapid uniporter which is powered by the mitochondrial membrane potential. Mitochondria located in close proximity to IP_3Rs and RyRs are exposed to

Ca^{2+} microdomains. These pockets of high Ca^{2+} concentrations enable the low-affinity uniporter to accumulate Ca^{2+} effectively, which decreases the local Ca^{2+} concentration and further stimulates store depletion (Duszynski et al., 2006).

Other cellular compartments are also capable of Ca^{2+} uptake and release, including the Golgi apparatus, lysosomes, acidic endosomes and secretory granules (Rizzuto and Pozzan, 2006). Recent evidence has suggested a role for acidic compartments in the regulation of Ca^{2+} signalling (Zhu et al., 2010). The second messenger, nicotinic acid adenine dinucleotide phosphate (NAADP), has been implicated as a potent second messenger which can modulate Ca^{2+} release at very low (nanomolar) concentrations from internal stores which are insensitive to IP_3 and cADPR (Chini et al., 1995; Galione and Petersen, 2005; Lee and Aarhus, 1995). A recent report identified that a novel class of voltage gated ion channels called two-pore channels (TPCs) may be the NAADP-sensitive Ca^{2+} release channels on acidic membranes. Three TPC genes exist in vertebrates, although TPC3 is absent from most primates and rodents. TPC1 and TPC2 mRNAs are expressed in most human tissues, with highest expression reported in kidneys and liver. TPC1 localises to endosomal membranes, whereas TPC2 is found on lysosomal membranes. It seems that TPC2 may control NAADP-stimulated Ca^{2+} release from lysosome-related stores, since NAADP fails to mobilise Ca^{2+} in β-cells from *Tpcn2* knockout mice (Calcraft et al., 2009). Recent evidence suggests that Ca^{2+} release through endolysosomal TPCs may trigger subsequent Ca^{2+} mobilisation from the ER/SR stores. Overexpression of TPC2 in HEK293 cells results in biphasic Ca^{2+} transients, with a slow release followed by a large transient (Calcraft et al., 2009). This large transient is selectively blocked by

both thapsigargin treatment and the IP_3R inhibitor, heparin, indicating that the second large transient was due to Ca^{2+} release through IP_3Rs. Pretreatment of cells with bafilomycin A, which depletes acidic Ca^{2+} stores, abolishes both the initial NAADP-dependent Ca^{2+} mobilisation and the secondary large transient, indicating that the initial Ca^{2+} mobilisation is indeed release from acidic stores and also implying that the secondary Ca^{2+} transient from ER/SR stores is dependent on the prior mobilisation of Ca^{2+} from acidic stores. It seems likely therefore, that local Ca^{2+} release from endolysosomal TPCs may serve to trigger a global Ca^{2+} response by activating CICR from the ER/SR stores via IP_3Rs and/or RyRs (Calcraft et al., 2009).

The primary mechanism of Ca^{2+} influx into non-excitable cells is store operated Ca^{2+} entry. Following the depletion of intracellular stores, Ca^{2+} influx through SOC channels is crucial for replenishing the stores and also for maintaining high cytosolic Ca^{2+} concentrations for downstream signalling events. However, despite over two decades of intensive investigations, the molecular identities of the SOCE mediators and the mechanism for SOC activation remained unknown. Only recently, with the introduction of RNAi screening technologies, have the elusive SOC channel components been uncovered, with the identification of the ER Ca^{2+}-sensor protein, STIM1 and the plasma membrane Ca^{2+} channel subunit, Orai1 as the key modulators of SOCE.

1.2 Biophysical properties of store operated Ca^{2+} channels

A family of store operated Ca^{2+} channels may exist since SOCs with distinct biophysical properties have been recorded in different cell types. The most

commonly studied SOC is the Ca^{2+}-release activated Ca^{2+} (CRAC) channel, which was discovered in the early 1990s (Hoth and Penner, 1992; Parekh and Penner, 1995). The characteristics of the CRAC channel current (I_{CRAC}) are unique and readily discernible from currents associated with other Ca^{2+} channels. CRAC channels are highly Ca^{2+} selective and can discriminate between divalent cations, with lesser permeability to Ba^{2+} and SR^{2+} but negligible permeability to monovalent cations. However, in the absence of divalent cations, the channel exhibits increased permeability to monovalent cations. The channel has a tiny single-channel conductance, estimated by fluctuation analysis to be 24 fS in 100 mM extracellular calcium {Zweifach, 1993 #268}**.** The narrow pore size of the channel may contribute to its high selectivity, since the pore itself is an estimated 3.9 Å, similar to the size of a Cs^{2+} ion (~3.8 Å) (Yamashita et al., 2007). CRAC channels are sensitive to fast Ca^{2+}-dependent inactivation, where local feedback of Ca^{2+} following Ca^{2+} influx through the channels reduces further influx (Fierro and Parekh, 1999). The combination of fast inactivation and the large differences in Ca^{2+} concentrations on either side of the plasma membrane result in a sharp inwardly rectifying current-voltage relationship. Channel currents with these unique properties have been recorded in a wide variety of cell types, ranging from immune cells such as T-lymphocytes and mast cells, to hepatocytes and fibroblasts (Parekh, 2007). CRAC channel currents have also been detected in cells from *Drosophila* and *Caenorhabditis elegans*, suggesting that this conserved current fulfils an important function.

1.3 Physiological functions of SOC channels

In addition to maintaining Ca^{2+} homeostasis, SOC channels have been implicated in the regulation of a variety of short-term and long-term responses in mammalian cells, including secretion, adhesion, motility, growth, the regulation of Ca^{2+}-dependent enzymes and modulation of gene expression via the activation of nuclear transcription factors (Parekh, 2007). Short term responses mediated by SOCE in T cells include the regulation of T cell motility and the formation of immunological synapses. A rise in intracellular concentration through SOCE is required for the maintenance of an interaction between cytotoxic T lymphocytes and antigen presenting cells, forming an immunological synapse, and Ca^{2+} buffers or SOCE inhibitors have been shown to prevent immunological synapse formation (Bhakta et al., 2005; Delon et al., 1998).

The amplitude and spatiotemporal dynamics of Ca^{2+} signals are crucial in controlling the specificity of Ca^{2+} dependent processes in cells. For example, in neurons, the frequency of Ca^{2+} transients mediates axon growth, growth cone turning and differentiation (Gomez et al., 2001; Spitzer et al., 2000). Ca^{2+} signalling within local microdomains plays an important role in generating the specificity of a Ca^{2+} response. Ca^{2+} microdomains near the CRAC channel rather than a bulk rise in cytoplasmic Ca^{2+} may be responsible for eliciting local effects on nearby targets, such as the PMCA, to compensate for the rise in cytosolic Ca^{2+} ((Bautista and Lewis, 2004), and Ca^{2+}-sensitive adenylyl cyclases (including AC1 and AC8) (Martin et al., 2009), nitric oxide synthase (Lin et al., 2000) and mitochondia (Hoth et al., 1997). In mast cells, the formation of Ca^{2+} microdomains through store-operated Ca^{2+} entry

(SOCE) are crucial in the activation of intracellular enzymes, e.g. cytoplasmic phospholipase A_2 ($cPLA_2$) and 5-lipoxygenase, which are required for arachidonic acid production and subsequent secretion of the pro-inflammatory LTC_4 (Chang et al., 2006). Increases in cytosolic Ca^{2+} are detected by the tyrosine kinase, SYK, which triggers a phosphorylation cascade ultimately resulting in the translocation of $cPLA_2$ to the Golgi apparatus and the hydrolysis of arachidonate-containing phospholipids to produce arachidonic acid (Parekh, 2007). 5-lipoxygenase metabolises arachidonic acid to synthesise cysteinyl leukotriene C_4 (LTC_4) which is subsequently secreted from cells and activates cysteinyl leukotriene type 1 receptors on adjacent cells to produce IP_3. In this way, Ca^{2+} microdomains from a single cell are capable of activating a feed-forward loop resulting in the transfer of information over large distances and the production of a global immune response (Parekh, 2010).

It was recently reported that the spatial Ca^{2+} gradient within the Ca^{2+} oscillations that occur as a result of SOCE is the key mechanism for controlling Ca^{2+}-dependent gene expression in mast cells. DiCapite *et al* compared the ability of SOCE-dependent Ca^{2+} oscillations to activate *c-fos* gene expression and found that stimulations of mast cells with LTC_4 activates *c-fos* expression only in the presence of external Ca^{2+}. *c-fos* expression was inhibited in the absence of external Ca^{2+} or by pretreating cells with the CRAC channel inhibitor, Synta, suggesting that Ca^{2+} influx is required for the activation of gene expression (Di Capite et al., 2009). Moreover, treatment of cells with EGTA to buffer cytosolic Ca^{2+} did not inhibit the activation of *c-fos* expression by LTC_4, thereby indicating that local Ca^{2+} influx drives gene expression and that global Ca^{2+} oscillations are not essential for this process (Di

Capite et al., 2009). This study was the first to demonstrate that Ca^{2+} influx through SOC channels does not serve to simply generate Ca^{2+} oscillations but rather that Ca^{2+} oscillations are required to activate SOCs and the local influx through SOCs provides the Ca^{2+} signal that is required for the activation of downstream gene expression.

Ca^{2+} microdomains mediate long term changes in gene expression through SOCs. SOCE is the main mechanism used by T lymphocytes to increase intracellular Ca^{2+} concentrations, resulting in the activation of downstream signalling proteins, including the serine/ threonine phosphatase calcineurin and its target transcription factor NFAT (nuclear factor of activated T cells); CaMK (Ca^{2+}- calmodulin-dependent kinase) and its target CREB (cyclic-AMP-responsive-element-binding protein); MEF2 (myocyte enhancer factor 2) which is activated by both calcineurin and CaMK, and NFκB (nuclear factor κB) (Feske et al., 2001; Hogan et al., 2003). Of these pathways, the calcineurin/NFAT pathway is to date the most thoroughly studied. Following a rise in cytoplasmic Ca^{2+} levels, calcineurin dephophorylates NFAT to expose a nuclear localisation sequence which binds to importins and shuttles to the nucleus to activate expression of immune response genes. NFAT is part of a positive feedback pathway where it functions with the transcription factor Foxp3 to stimulate the development and maintain the function of regulatory T cells (Wu et al., 2006b). Several groups have shown that T cells from SCID patients with an R91W mutation in the *Orai1* gene have massive reductions in SOCE and I_{CRAC} and consequently fail to proliferate in response to T cell stimulation, to activate NFAT or produce NFAT-dependent cytokines (Feske et al., 2000; Feske et al., 2001; Feske et

al., 1996). SOCE is also involved in regulating gene expression in mast cells. Store depletion induced by receptor stimulation activates expression of the *c-fos* gene, which forms part of the AP-1 transcription factor complex required for regulating the expression of chemokines and cytokines that are involved in inflammatory responses (Chang et al., 2006; Parekh, 2007).

Studies on *Orai1*, *Stim1* and *Stim2* knockout mice have been invaluable in elucidating the physiological roles of SOC channels, particularly with regards to immune system function. The *Stim1* and *Orai1* genes are required for survival in mice with varying genetic backgrounds since mice lacking either of these genes die prenatally or soon after birth, and *Stim2* knockout mice die within ~5 weeks (Baba et al., 2008; Bergmeier et al., 2009; Oh-Hora et al., 2008; Vig et al., 2008). Mice lacking *Orai1* exhibit eyelid irritation and sporadic hair loss which is similar to the cyclical alopecia seen in mice with a keratinocyte-specific deletion in the *Cnb1* gene, which encodes a regulatory subunit of calcineurin (Gwack et al., 2008). Both I_{CRAC} currents and SOCE are strongly inhibited in mast cells and T cells from *Orai1* deficient mice (Gwack et al., 2008; Vig et al., 2008). Numerous studies have shown that mast cells, T cells and B cells function abnormally in *Orai1*$^{-/-}$ mice as a result of impaired SOCE. Mast cells from *Orai1* knockout mice develop normally but exhibit defective degranulation and leukotreine C4 production in response to antigen IgE stimulation (Vig et al., 2008). *Orai1*$^{-/-}$ B cell display reduced proliferation in response to B cell receptor stimulation, suggesting that SOCE is involved in the expansion of B cells following antigenic stimulation (Gwack et al., 2008). T cells from *Orai1* deficient mice displayed complex phenotypes in several studies. Proliferation and

development of *Orai1* deficient naive T cells was normal and these cells displayed only moderate inhibition of IL-2 and IFN-γ secretion, suggesting that Orai1 is not essential for T cell function in mice (Gwack et al., 2008; Vig et al., 2008). However, differentiated *Orai1* $^{-/-}$ T cells have been shown to express lower levels of *Orai2* and *Orai3* mRNA and a much stronger decrease in cytokine production when compared with naive T cells, suggesting that *Orai2* and/or *Orai3* may compensate for the lack of *Orai1* in differentiated or activated T cells (Gwack et al., 2008). Although cytokine production is inhibited in *Orai1* deficient B, T and mast cells, the finding that these cells still proliferate in the absence of *Orai1* suggests that SOCE may not be essential for normal lymphocyte development. However, it has yet to be determined whether a lack of *Orai1* affects T, B and mast cell function *in vivo*.

Stim1 knockout mice, like mice lacking *Orai1*, die early postnatally. Mast cells, macrophages and naive and differentiated $CD4^+$ and $CD8^+$ T-cells from *Stim1*-deficient mice have impaired SOCE when stimulated by the IgE receptor FcεRI or the Ag receptor complex (Baba et al., 2008; Beyersdorf et al., 2009; Brandman et al., 2007; Braun et al., 2009). *Stim1* deficient mast cells also have much reduced degranulation and cytokine production after FcεRI stimulation (Baba et al., 2008). In contrast, *Stim2* deficient mice exhibit only a minor reduction in SOCE following T cell stimulation and display a pronounced inhibition of sustained Ca^{2+} influx and NFAT translocation, suggesting that STIM1 alone is not sufficient to sustain Ca^{2+} influx in T cells lacking *Stim2* (Brandman et al., 2007). Both *Stim1* and *Stim2* deficient T cells show reduced production of the cytokines IL-2, IL-4 and IFN-γ, suggesting that both STIM proteins are involved in stimulating T cell activation

(Brandman et al., 2007). Macrophages from *Stim1* deficient mice fail to activate FcεR-induced Ca^{2+} entry and phagocytosis, resulting in impaired macrophage function (Braun et al., 2009). These mice were protected from IgG-induced elimination of red blood cells in anaemia and also from thrombocytopenia, indicating that STIM1 is a mediator of the pathology of these diseases (Braun et al., 2009).

1.4 The discovery of SOC machinery

Following the discovery of I_{CRAC} in the early 1990s (Hoth and Penner, 1992), considerable research was carried out to characterise the biophysical properties and pharmacological profile of the CRAC channel, creating a unique channel "fingerprint" (Hogan et al., 2010; Prakriya and Lewis, 2003). These studies revealed CRAC as a store-dependent, highly Ca^{2+}-selective, low conductance, inwardly rectifying channel with slow activation and fast inactivation kinetics. However, the major goal and possibly the biggest challenge of these studies was to find the molecular identity of the channel itself. The CRAC channel "fingerprint" was a valuable tool in selecting potential candidate genes which fulfil the collection of properties associated with the CRAC channel.

Members of the transient receptor potential (TRP) gene family (including TRPC1, TRPC3, TRPC4, TRPC5, TRPV5 and TRPV6) have been proposed to be the CRAC channel (Ramsey et al., 2006). However, although some TRPs have been described as SOC channels, the biophysical fingerprints for many of these channels do not match that of the CRAC channel. The interaction between TRPCs and SOCE is

discussed in more detail in Section 1.12. The elusive CRAC channel mediators were finally discovered in 2005 from two RNAi screens which were carried out in order to identify potential genes which are involved in SOCE. Roos *et al* chose a target group of 170 proteins which contain channel-like or transmembrane domains, Ca^{2+}-binding regions or have been implicated in SOC function, and designed a system to specifically suppress expression of each target protein in Drosophila S2 cells to evaluate its potential role in thapsigargin-evoked Ca^{2+} influx (Roos et al., 2005). Liou *et al* adopted a similar RNAi approach to test 2,304 proteins with known signalling domains for their involvement in store-dependent Ca^{2+} entry in HeLa cells (Liou et al., 2005). These studies identified the ER-transmembrane protein, stromal interacting molecule (STIM) 1 as a protein which is essential for SOCE (Liou et al., 2005; Roos et al., 2005).

STIM1 is a conserved and ubiquitously expressed type I transmembrane protein (Oritani and Kincade, 1996; Williams et al., 2001) with several predicted protein interacting domains and is localised primarily to the ER (Liou et al., 2005; Wu et al., 2006a; Zhang et al., 2005) but is also present at lower levels in the plasma membrane (Manji et al., 2000; Soboloff et al., 2006a; Williams et al., 2002; Zhang et al., 2005). Many studies following from the RNAi screens confirmed that RNAi knockdown of STIM1 suppresses both SOCE and I_{CRAC} (Huang et al., 2006; Mercer et al., 2006; Spassova et al., 2006), indicating that it is essential for the activity of SOCs. Investigations into the distribution of STIM1 using confocal (Baba et al., 2006; Liou et al., 2005; Soboloff et al., 2006a; Xu et al., 2006; Zhang et al., 2005), TIRF (Luik et al., 2006; Wu et al., 2006a) and transmission electron microscopy (Wu et

al., 2006a; Zhang et al., 2005) found that when intracellular Ca^{2+} stores are full, STIM1 is distributed throughout the ER, colocalising with ER markers but in response to store depletion it redistributes to aggregates known as "puncta" at ER-PM junctions (Baba et al., 2006; Liou et al., 2005; Soboloff et al., 2006a; Xu et al., 2006; Zhang et al., 2005). Although the translocation of STIM1 to ER-PM junctions occurs over a long period of time, with translocation beginning at less than 1 minute (Liou et al., 2005) and maximal puncta formation observed at approximately 5 minutes after store depletion (Chvanov et al., 2008; Liou et al., 2005; Zhang et al., 2005), TIRF microscopy and electrophysiology experiments showed that STIM1 puncta formation precedes CRAC activation by a number of seconds (Wu et al., 2006a), suggesting that STIM1 redistribution is an essential step in CRAC activation.

Following the initial RNAi screens, Feske *et al* performed a genome-wide modified linkage analysis in patients suffering from severe combined immune deficiency (SCID) in which T cell receptor engagement or store depletion failed to activate SOCE and I_{CRAC} and traced this defect to a single point mutation at residue 91 (R91W) in the Orai1 protein which was common to these patients (Feske et al., 2006). Notably, retroviral delivery of wild type Orai1 into T cells from these SCID patients rescued both SOCE and I_{CRAC} (Feske et al., 2006), establishing Orai1 as a key regulator for SOCE. At the same time, two independent studies using RNAi screening technology to identify novel proteins involved in SOCE also discovered Orai1 as a SOCE regulator (Vig et al., 2006b; Zhang et al., 2006). Like STIM1, Orai1 is a widely expressed protein, suggesting that it may be involved in a general

mechanism for mediating SOCE. It is a plasma membrane protein with four transmembrane domains and intracellular N- and C-termini and shares no homology to known ion channel proteins which, with its known involvement in SOCE, made it a possible candidate for the CRAC channel or a CRAC channel subunit. Expression of either STIM1 or Orai1 alone has little effect on SOCE (Peinelt et al., 2006; Soboloff et al., 2006b; Xu et al., 2006). However, overexpression of both proteins together results in the potentiation of SOCE in a variety of cell types (Mercer et al., 2006; Peinelt et al., 2006; Soboloff et al., 2006b; Zhang et al., 2005), reaching up to 100-fold higher in amplitude than endogenous SOCE in some cell types (Soboloff et al., 2006b). STIM1 has also been shown to gate Orai1 *in vitro* indicating that the two proteins interact functionally (Zhou et al., 2010). TIRF and confocal microscopy have shown that overexpression of STIM1 induces the redistribution of Orai1 into plasmalemmal clusters in response to store depletion which are directly opposite STIM1 puncta (Chvanov et al., 2008; Luik et al., 2006; Xu et al., 2006). Moreover, dual imaging of fluorescently labelled STIM1 and cytosolic Ca^{2+} levels revealed that STIM1-Orai1 puncta colocalise with sites of Ca^{2+} influx (Luik et al., 2006), revealing that STIM1 and Orai1 are the key molecular components required for SOCE.

1.5 STIM proteins

STIM1 (originally called SIM) was identified in a library screen as a cell surface protein that enables stromal cells to bind to pre-lymphocytes (Oritani and Kincade, 1996). STIM1 was initially described as a candidate tumour suppressor protein. The STIM1 gene localises to a region on chromosome 11p15.5 which is associated with

a variety of paediatric cancers and overexpression of STIM1 (GOK) was found to induce cell death when expressed in rhabdoid tumour and rhabdomyosarcoma cells (Sabbioni et al., 1997). Immunofluorescence and cell surface biotinylation studies characterised STIM1 as a ubiquitously expressed cell surface protein in K562 cells and it was shown to undergo post-translational modifications such as N-linked glycosylation and phosphorylation on serine and threonine residues within its C-terminus (Manji et al., 2000). Further screens for STIM1 related sequences revealed that STIM proteins are expressed in species from *Drosophila* and *C. elegans* to *Homo sapiens* (Williams et al., 2001). Vertebrates also contain a second STIM gene, STIM2, which shares 61% homology with STIM1, suggesting that STIM2 arose as a result of gene duplication in early vertebrates (Williams et al., 2001).

STIM1 has been established as a Ca^{2+} sensor which can activate or deactivate CRAC channels in response to Ca^{2+} store depletion or repletion, respectively (Liou et al., 2005; Roos et al., 2005; Zhang et al., 2005). The N-terminus of STIM1 is located within the ER lumen and consists of a signal peptide, an EF-hand domain and a sterile-α motif which contains two N-linked glycosylation sites, followed by a transmembrane domain that spans the ER membrane (Stathopulos et al., 2009; Stathopulos et al., 2008). The C-terminal domain of STIM1 is cytosolic and contains two coiled-coiled domains which overlap with an ezrin-radixin-moesin (ERM)-like segment, a serine/proline and a lysine-rich region (Baba et al., 2006; Huang et al., 2006; Liou et al., 2005). The structures of STIM1 and STIM2 are illustrated in Figure 1.2.

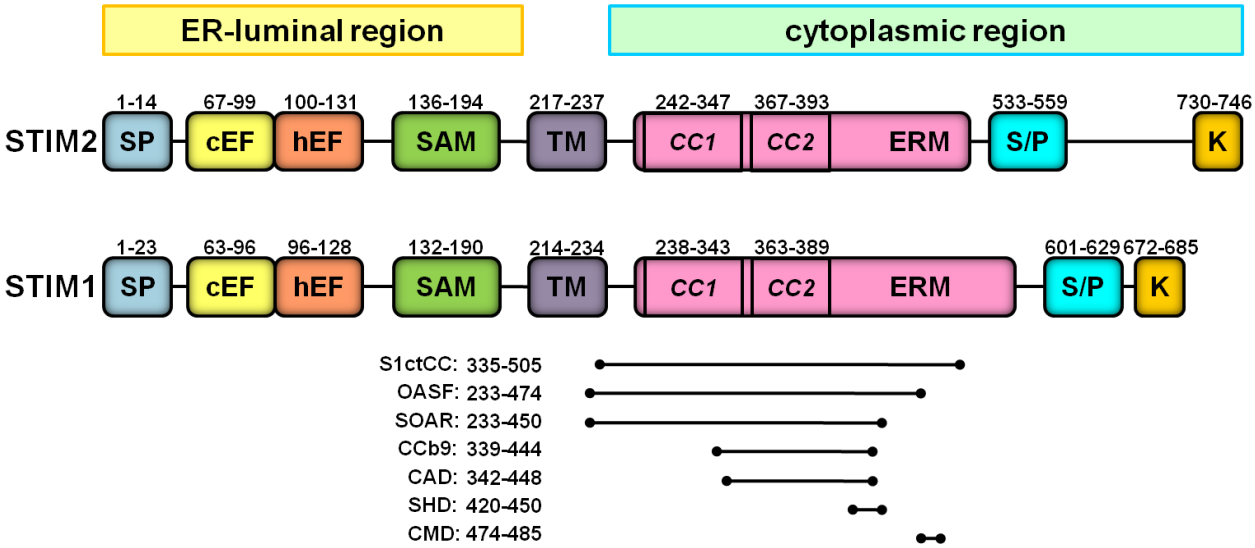

Figure 1.2. Schematic representation of the structures of the STIM proteins. Comparison of the structural domains within STIM1 and STIM2. Both proteins contain an N-terminal canonical EF and hidden EF hand pair (cEF and hEF), sterile-α motif (SAM), transmembrane region (TM), ERM domain containing two putative coiled-coil regions (CC1 and CC2), serine/proline-rich domain (S/P) and lysine-rich domain (K). The proteins diverge at their N-termini before the EF-hand pair and also in the C-terminus downstream of the coiled-coiled domains. The various domains within the STIM1 C-terminus which have been found to mediate SOCE are also outlined below the schematic.

1.6 STIM1 as a Ca^{2+} sensor

The EF-hand and SAM domains of STIM1 are responsible for sensing Ca^{2+} within the ER lumen, which is required for coupling store depletion to SOC activation (Liou et al., 2007; Roos et al., 2005; Stathopulos et al., 2009; Stathopulos et al., 2008; Zhang et al., 2005). This is the only region of STIM1 which is conserved from *C. elegans* and *Drosophila* through to humans (Strange et al., 2007). The EF-hand domain contains a canonical EF hand (cEF1) (Liou et al., 2005; Roos et al., 2005; Stathopulos et al., 2009; Stathopulos et al., 2008) with a conventional helix-loop-helix EF motif. The cEF1 has a low affinity for Ca^{2+}, with a K_d of 0.2-0.6 mM, so that it can sense changes in the ER luminal Ca^{2+} range of ~0.1 – 0.8 mM (Feske et al., 2006; Hogan and Rao, 2007; Stathopulos et al., 2008). NMR structural analysis revealed that the EF-SAM domain also contains a second hidden EF-hand (hEF2) which cannot bind Ca^{2+} but stabilises the cEF1 hand through hydrogen bonding to form an EF-hand pair (Stathopulos et al., 2008). The paired EF-hands together mediate a tight interaction with an α-helix from the SAM domain to form a stable EF-SAM structure which, due to the presence of the non-functional hEF2 hand, has a relatively low affinity of ~250 μM for Ca^{2+} (Stathopulos et al., 2008). When Ca^{2+} is bound to the EF-SAM region, the protein fragment is well folded and monomeric (Stathopulos et al., 2006; Stathopulos et al., 2008). Although the structure of the recombinant EF-SAM domain in the absence of Ca^{2+} has not yet been solved, Ikura and colleagues performed various biophysical measurements which suggest that Ca^{2+} depletion from the EF-SAM domain results in extensive disruption of the tertiary protein structure and the dissociation of the SAM domain from the EF-hands (Stathopulos et al., 2006; Stathopulos et al., 2008). Depletion of Ca^{2+} from the EF-SAM domain

exposes hydrophobic residues within both the EF hands and SAM domains resulting in unfolding and destabilisation of the protein fragment and the formation of aggregates (Stathopulos et al., 2006; Stathopulos et al., 2008), which correlates with the oligomerisation of full length STIM1 in response to ER store depletion. Addition of Ca^{2+} results in the reformation of stably folded EF-SAM monomers (Stathopulos et al., 2008), which is concurrent with the dissipation of STIM1 puncta and its redistribution to bulk ER following store repletion. STIM1 proteins that contain Ca^{2+}-binding mutations in the EF-hand domain are constitutively distributed in puncta in cells and SOCE is constitutively active irrespective of the ER Ca^{2+} content (Liou et al., 2005; Mercer et al., 2006; Spassova et al., 2006; Zhang et al., 2005) whereas SAM deletion mutants lack the ability to form puncta (Baba et al., 2006). Moreover, mutations that disrupt the cEF1 hand, the EF-SAM stability or the SAM hydrophobic core all induce EF-SAM aggregation (Stathopulos et al., 2008), suggesting that destabilisation of the EF-SAM interaction is crucial for the oligomerisation of the luminal portion of STIM1. These studies provided experimental evidence that STIM1 is an ER Ca^{2+} sensor that can respond to changes in the Ca^{2+} content within the stores to activate SOCE.

1.7 Store depletion leads to oligomerisation of STIM1

When ER stores are filled, STIM1 is distributed diffusely throughout bulk ER (Liou et al., 2007; Liou et al., 2005; Wu et al., 2006a). The luminal EF-SAM region of STIM1 senses changes in ER Ca^{2+} content from resting levels (400 – 800 μm) down to ~200 μM (Brandman et al., 2007). This depletion induces further oligomerisation of STIM1 within the ER. STIM1 oligomers then translocate within the ER to the plasma

membrane (to sites known as ER-PM junctions) in order to activate SOC influx (Liou et al., 2005; Wu et al., 2006a). In spite of the fact that the EF-SAM region aggregates in the absence of Ca^{2+}, full length STIM1 does not seem to exist as a monomer in cells where the stores are replete. Several studies have shown that STIM proteins form heteromultimers in resting conditions (Baba et al., 2006; Williams et al., 2001). Endogenous or overexpressed STIM1-STIM1 and STIM1-STIM2 complexes co-immunoprecipitate in lysates from cells with replete stores (Williams et al., 2001), while the isolated C-terminal domain or EF-hand region of STIM1 have also been shown to form dimers (Ji et al., 2008; Muik et al., 2009; Yuan et al., 2009), as does full length STIM1 (Penna et al., 2008). STIM1 may therefore exist as a dimer in resting cells (Penna et al., 2008; Williams et al., 2002). Interestingly, although the EF-SAM domain is involved in the oligomerisation of STIM1 in response to store depletion, oligomerisation is not dependent on this region since STIM1 can still interact with a chimeric STIM1 protein in which the EF-SAM region is replaced with granulocyte colony stimulating factor (GCSF) receptor, suggesting that a domain within the C-terminal cytosolic portion of STIM1 plays an additional role in the formation of STIM1 oligomers (Williams et al., 2002). In a recent study investigating C-terminal STIM1 deletion mutants, Muik et al demonstrated using FRET analysis and perfluoro-octanoic acid (PFO)-PAGE that STIM1 fragments comprising aa233-450 or aa233-474 form homo-oligomers but that shorter C-terminal fragments (aa233-420) exhibit reduced potential to homomerise. Interestingly, a fragment (aa400-474) which is C-terminal to the coiled-coil region still displays the ability to homomerise, suggesting that the coiled-coil region is not required for oligomerisation (Muik et al., 2009). This led to the

identification of a cytosolic assembly domain within the STIM1 C-terminus, termed the STIM1 homomerisation domain (SHD), which is essential for oligomerisation of the STIM1 C-terminus and for STIM1 coupling to Orai1 (Muik et al., 2009). A further domain within STIM1, termed the CRAC activation domain (CAD, discussed in further detail in Section 1.21) has also been shown to contribute to stabilising STIM1 oligomers once they have formed since mutation of CAD affect STIM1 function and oligomerisation (Covington et al., 2010).

1.8 Redistribution of STIM1

Upon store depletion, STIM1 forms oligomers before it translocates into punctate clusters near the plasma membrane, thereby signalling to the plasma membrane that the store has been depleted. Live cell imaging revealed an increase in FRET between a CFP-STIM1 donor and a YFP-STIM1 acceptor immediately following store depletion, demonstrating that STIM1 oligomerisation occurs within 5 seconds of store depletion, which precedes the accumulation of STIM1 puncta near the plasma membrane (Liou et al., 2007). Many studies have demonstrated that STIM1 oligomers translocate to puncta immediately adjacent to the plasma membrane (Baba et al., 2006; Liou et al., 2005; Mercer et al., 2006; Wu et al., 2006a; Zhang et al., 2005). TIRF microscopy revealed that YFP-STIM1 puncta form within 100-200 nm of the cell surface (Hewavitharana et al., 2008; Liou et al., 2005), whereas ultrastructural analysis of HRP-tagged STIM1 and chemical crossbridging studies have independently revealed that STIM1 puncta form to within 9-25 nm of the plasma membrane (Varnai et al., 2007; Wu et al., 2006a).

The formation of puncta is considered to involve the local diffusion of STIM1 within the ER membrane to junctional ER sites that are in close apposition to the plasma membrane (termed ER-PM junctions). ER found in these regions is ribosome-free, allowing the ER to come within an estimated 11-17 nm distance of the plasma membrane, close enough to the cell surface to allow for possible interactions between STIM1 and plasma membrane structures (Lur et al., 2009; Orci et al., 2009; Wu et al., 2006a). Interestingly, electron micrographs from several studies have shown that store depletion increases the number of ER-PM by ~30% in Jurkat cells (Wu et al., 2006a) and 250% in HeLa cells (Orci et al., 2009). Overexpression of STIM1 results in a similar increase in both the number and size of ER-PM junctions in pancreatic acinar cells, suggesting that STIM1 itself may be involved in the formation of these junctions (Lur et al., 2009).

1.9 STIM1 in the plasma membrane

Although STIM1 localises predominantly to ER structures, surface biotinylation studies demonstrated that a substantial portion of STIM1 (~25%) is detected in the plasma membrane (Hewavitharana et al., 2008; Manji et al., 2000; Soboloff et al., 2006a). Furthermore, several studies have reported an increase in the levels of plasma membrane STIM1 upon thapsigargin treatment, suggesting that STIM1 is inserted into the plasma membrane following translocation, resulting in the externalisation of the STIM1 N-terminus (Lopez et al., 2006; Zhang et al., 2005). In biotinylation and streptavidin pull down experiments which utilised a STIM1 E76A/D87A double mutant with defective EF-hand binding, the mutant was found

to be absent from the cell surface despite the fact that it was permanently punctate (Hewavitharana et al., 2008).

Further studies have demonstrated that chimeric STIM1 proteins which are N-terminally fused with fluorescent proteins such as CFP, YFP, or tags such as HRP or haemagglutinin, can translocate to puncta near the plasma membrane but fail to incorporate into the plasma membrane, since antibodies fail to detect any surface exposed N-terminal tags following store depletion (Hauser and Tsien, 2007; Liou et al., 2005; Mercer et al., 2006). Moreover, a GFP-STIM1 protein failed to be quenched by extracellular acidification, demonstrating that the N-terminal tag does not become externalised after thapsigargin treatment (Wu et al., 2006a; Xu et al., 2006). Electron microscropy revealed on an ultrastructural level that HRP-STIM1 remains subplasmalemmal upon translocation (Wu et al., 2006a). However, when a CFP tag was fused to the C-terminus of STIM1, the N-terminus becomes extracellular after store depletion, suggesting that STIM1 insertion into the plasma membrane is not disrupted by C-terminal tags (Hauser and Tsien, 2007). Additionally, when a very small hexahistidine tag was added to the N-terminus of STIM1, it was reported to be exposed following store depletion (Hauser and Tsien, 2007). It was not shown however that the exposure was a consequence of store depletion and surprisingly, no data was shown for cells before store depletion. Together these results indicate that the addition of bulky N-terminal protein tags may block STIM1 trafficking and insertion into to the plasma membrane and suggest that endogenous STIM1 may be inserted into the plasma membrane following store depletion, although this remains to be conclusively determined.

1.10 The role of plasma membrane STIM1 in SOCE

It is still unclear whether plasma membrane STIM1 has a role in the regulation of SOCs. One group has shown that STIM1 is present in the plasma membrane independent of store depletion and can regulate SOC activity since external application of antibodies to the N-terminal EF-hand domain of STIM1 reduces I_{CRAC} in haematopoietic cells and SOCE in HEK293 cells (Spassova et al., 2006). However, a separate study using this approach failed to observe I_{CRAC} inhibition in HEK293 cells (Mignen et al., 2008b). Additionally, N-terminally tagged STIM1 proteins which are not detected at the cell surface retain the ability to activate SOCE to a similar level when compared with C-terminally tagged STIM1 proteins, suggesting that plasma membrane insertion of STIM1 is not essential for SOC activation (Muik et al., 2008) but may possibly contribute to SOCE through an interaction with ER-resident STIM1 or with Orai1 (Spassova et al., 2006). However, it is still possible that the major role for plasma membrane STIM1 is as a cell surface adhesion protein, as originally suggested in early STIM1 (SIM) reports where it was characterised as a protein required for adhesion to stroma (Oritani and Kincade, 1996). Additionally, plasma membrane STIM1 has been implicated in the regulation of arachidonic-acid-regulated-Ca^{2+}-selective (ARC) channels which is discussed in more detail in section 1.12.

1.11 STIM1 targeting to the plasma membrane

Despite the fact that a portion of STIM1 is found in the plasma membrane, the wide body of evidence available suggests that ER-localised STIM1 does not insert into the plasma membrane following store depletion but rather remains subplasmalemmal

in ER-PM junctions. However, the interactions that direct STIM1 to these junctions and retain puncta at the plasma membrane following translocation are unclear. Plasma membrane lipid rafts which are enriched in cholesterol, lipids and glycoproteins have been found to determine the clustering of STIM1 aggregates in ER-PM junctions since STIM1 co-migrates with lipid raft domains in density gradient fractionation studies and co-immunoprecipitates with caveolin-1 (Pani et al., 2008). Confocal microscopy has shown that YFP-STIM1 puncta also colocalise with the caveolar marker protein, GM1 (Pani et al., 2008). Additionally, disruption of lipid rafts with the cholesterol extractor, methyl-β-cyclodextrin (MβCD), results in an inhibition of STIM1 puncta formation and a decrease in SOCE in both HSG cells and platelets (Pani et al., 2008). Disruption of lipid rafts with MβCD also reduces the interaction between STIM1 and Orai1, suggesting that lipid rafts may function as a scaffold to support an interaction between STIM1 and Orai1 (Galan et al., 2010; Jardin et al., 2008c).

Several domains within STIM1 have been found to be involved in making plasma membrane contacts. Huang et al conducted a study using various STIM1 C-terminal deletion mutants and found that deletion of the cationic polybasic domain in a constitutively active STIM1 (D76A) mutant results in a dominant negative mutant that blocks NFAT1-GFP translocation to the nucleus and I_{CRAC} in HEK293 cells, suggesting that the polybasic region is necessary for STIM1 function (Huang et al., 2006). The polybasic domain is a lysine-rich region of 14 amino acids that are predicted to fold into a two-turn α-helix. Mutation of these lysines to either alanines or glutamates, which respectively should disrupt or retain the helical

structure, inhibits GFP-NFAT translocation to the nucleus, suggesting that the lysine residues within this region are required for SOCE activation (Huang et al., 2006). Further studies revealed that STIM1 mutants lacking the polybasic domain oligomerise within the ER following store depletion, as shown by FRET between CFP-STIM1 and a YFP-STIM1-ΔK mutant in RBL cells, but that these oligomers fail to translocate, indicating a crucial role for the polybasic domain in recruiting STIM1 to ER-PM junctions, possibly through an interaction with some components within the plasma membrane (Liou et al., 2007; Park et al., 2009).

In a recent report investigating the mechanism of targeting of 48 small GTPases to the plasma membrane, 37 of these were found to contain polybasic targeting motifs comprising 4 or more lysine or arginine residues at their C-termini, similar to that found in STIM1, which are sufficient for plasma membrane targeting when expressed alone (Heo et al., 2006). Using an inducible chemical phosphatase method, it was shown that polybasic clusters dissociate from the plasma membrane following simultaneous depletion of the plasma membrane phosphoinositides, PtdIns(4,5)P_2 and PtdIns(3,4,5)P_3, but not upon singular depletion of either species, suggesting that both PtdIns(4,5)P_2 and PtdIns(3,4,5)P_3 jointly regulate recruitment of polybasic clusters to the plasma membrane (Heo et al., 2006).

Plasma membrane phosphoinositides regulate the activity of a variety of ion channels and transporters, including voltage gated potassium and calcium channels and transient receptor potential channels (Gamper and Shapiro, 2007). There are several lines of evidence to indicate that phosphoinositides may also regulate the

activity of store operated calcium channels. Firstly, inhibition of phosphotidylinositol (PI) 3- and 4-kinases with either wortmannin or LY294002 inhibits SOCE in platelets (Jenner et al., 1996; Rosado and Sage, 2000). Wortmannin treatment has also been shown to block I_{CRAC} in rat basophilic leukemia cells, a phenomenon which is independent of the levels of IP_3 present, since direct application IP_3 into the cells fails to restore the I_{CRAC} current (Broad et al., 2001). Similarly, joint depletion of PtdIns(4,5)P_2 using a chemically inducible phosphatase and PtdIns(3,4,5)P_3 with wortmannin or LY294002 also reduces SOCE in COS-7 cells but depletion of either phosphoinositide species alone has little effect on SOCE activity, suggesting that multiple phosphoinositides are involved in SOCE (Korzeniowski et al., 2009).

Since PtdIns(4,5)P_2 and PtdIns(3,4,5)P_3 are required for SOCE and both species regulate the plasma membrane localisation of proteins containing a C-terminal cluster of polybasic amino acids (Heo et al., 2006), it has been suggested that the polybasic region of STIM1 may function as a membrane-targeting domain via binding to phosphoinositides (Liou et al., 2007). The C-termini of both STIM1 and STIM2 have been shown to bind directly to phosphoinositide-containing liposomes, where the STIM1 C-terminus interacts preferentially with PtdIns(4,5)P_2 over other phosphoinositide species (Ercan et al., 2009). Interestingly, when the polybasic domain or the coiled coil region were deleted from the STIM1 C-terminus, no phosphoinositide binding was observed, confirming that the STIM1 polybasic domain is required for STIM1 recruitment to the plasma membrane, but these results also suggest that STIM1 requires its oligomerisation domains for

phosphoinositide binding (Ercan et al., 2009). It is possible that the increased positive charge of the STIM1 oligomers increases the affinity of STIM1 for the negatively charged phosphoinositides.

Depleting PtdIns(4,5)P_2 from the plasma membrane does not prevent STIM1 puncta formation but results in a small reduction in the numbers of puncta, which is consistent with a role for multiple phosphoinositides in tethering STIM1 to the plasma membrane (Korzeniowski et al., 2009; Varnai et al., 2007). However, depletion of PtdIns(4,5)P_2 and PtdIns(3,4,5)P_3 did not dissociate preformed puncta, suggesting that once formed other protein interactions may stabilise puncta at the plasma membrane (Korzeniowski et al., 2009; Varnai et al., 2007).

A second region within STIM1 may also contribute to plasma membrane targeting of puncta, since a STIM1 deletion mutant lacking the polybasic domain retains the ability to form puncta only when Orai1 is overexpressed in the same cell, suggesting that an interaction with the Orai1 channel in the plasma membrane is sufficient to target STIM1 to ER-PM junctions (Park et al., 2009). It may be the case that in physiological conditions, phosphoinositides are initially required to anchor STIM1 to the plasma membrane, thereby increasing the likelihood of an interaction with diffusing Orai1 molecules in the plasma membrane. The molecular coupling between STIM1 and Orai1 is discussed further in Section 1.21.

1.12 Additional STIM1-mediated channels

The involvement of members of the mammalian canonical TRP (TRPC) superfamily of ion channels in SOCE has been the focus of intensive investigation and controversy in recent years. The TRPC channels are activated by receptor stimulation and PLC hydrolysis and of the seven members, six (TRPC1-6) have been suggested to function as SOCs. siRNA knockdown and mouse knockout studies have implicated TRPC1 and TRPC4 as SOCs (Dietrich et al., 2005; Freichel et al., 2001; Zagranichnaya et al., 2005). TRPC3, C6 and C7 are all activated by diacylglycerol (Hofmann et al., 1999; Okada et al., 1999). STIM1 has been shown to interact with and activate Ca^{2+} influx through these channels (Alicia et al., 2008; Cheng et al., 2008; Huang et al., 2006; Jardin et al., 2008a; Kim et al., 2009; Liao et al., 2008; Ma et al., 2008; Ong et al., 2007; Pani et al., 2008; Yuan et al., 2009). The C-terminus of STIM1 activates TRPC1 and TRPC3 and coimmunoprecipitates with TRPC1, TRPC2, TRPC4 and TRPC5, suggesting that STIM1 heteromultimerises TRPC channels, enabling them to function as SOCs (Huang et al., 2006; Yuan et al., 2007). Association of TRPC1 with STIM1 has been shown to promote TRPC1 insertion into lipid rafts, thereby converting it from a receptor-operated to a store-operated channel and this association is dynamically regulated by the status of the ER store (Alicia et al., 2008; Pani et al., 2008). Additionally, biochemical and functional studies have pointed towards an interaction between Orai1 and the TRPCs (Liao et al., 2007; Liao et al., 2009; Ong et al., 2007). The R91W Orai1 mutant blocks DAG-activated Ca^{2+} entry in cells that transiently or stably express TRPC proteins and it has been suggested that Orai1 forms complexes with TRPCs recruited to lipid rafts by STIM1 which form functional SOCs (Liao et al., 2009). It seems that TRPC

isoforms may form ternary complexes with STIM1 and Orai1 and possibly form part of the SOC channel itself. However, unlike Orai1 which fulfils all of the biophysical criteria of the bone fide CRAC channel, TRPCs are less selective to Ca^{2+} with higher single-channel conductance and more linear current-voltage relationships. Furthermore, it is not clear how Orai1 could confer the high Ca^{2+} selectivity characteristic of CRAC when complexed with TRPCs. It seems that further studies are required to determine the dynamics of STIM1/Orai1/TRPC interactions and how these complexes function to mediate Ca^{2+} signalling.

STIM1 has also been implicated in the regulation of arachidonic-acid-regulated-Ca^{2+}-selective (ARC) channels. ARC channels are receptor operated Ca^{2+} channels that function independently of store depletion and STIM1 translocation. ARC channels are inhibited by STIM1 antibodies that recognise the extracellular N-terminus (Mignen et al., 2007). Similarly, mutation of the N-linked glycosylation site that prevents the plasma membrane insertion of STIM1 inhibits ARC channels without affecting SOC channel activity (Mignen et al., 2007). It seems therefore that, unlike SOCs which require translocation of ER-resident STIM1 to the plasma membrane for activation, the constitutive pool of plasma membrane STIM1 is critical for the activation of ARCs. ARC channel activity is absolutely dependent on low levels of arachidonic acid and STIM1 fails to activate ARCs in the absence of arachidonic acid (Mignen et al., 2007), suggesting that STIM1 may either enable the activation of ARCs by arachidonic acid or modulate it in some way. The activity of ARC channels also requires Orai1 and Orai3. Expression of dominant negative Orai1 and Orai3 mutant constructs (E106Q-Orai1 and E81Q-Orai3) inhibits native ARC

channel currents, suggesting that Orai1 and Orai3 may be ARC channel subunits (Mignen et al., 2008a). This was confirmed by expressing preassembled heteromeric Orai1 and Orai3 multimers in cells which determined that the functional ARC channel consists of a pentameric assembly of three Orai1 subunits and two Orai3 subunits (Mignen et al., 2008a). However, the molecular mechanism underlying the activation of ARC channels by STIM1 remains to be determined.

1.13 Additional proteins affecting STIM1 function

Several studies have suggested a role for the microtubule cytoskeleton in STIM1 dynamics (Baba et al., 2006; Grigoriev et al., 2008; Smyth et al., 2007). EYFP- or GFP-tagged STIM1 exhibits a tubulovesicular distribution which colocalises with α-tubulin, suggesting that STIM1 associates with the microtubule cytoskeleton (Baba et al., 2006; Smyth et al., 2007). Microtubule depolymerisation with nocodazole results in a loss of vesicular distribution of EYFP-STIM1 to an expression pattern which is similar to that of the ER in HEK293 cells (Smyth et al., 2007). GFP-STIM1 was also observed to form puncta in HeLa cells under similar conditions (Baba et al., 2006). The association between STIM1 and microtubules has been shown to be mediated by the microtubule-plus-end-tracking protein, EB1 (Grigoriev et al., 2008). STIM1 binds EB1 via a short microtubule binding motif (SxIP) in its C-terminal domain and forms comet-like aggregates at sites where polymerising microtubules meet the ER network through its interaction with EB1 (Grigoriev et al., 2008; Honnappa et al., 2009). However, it is unclear whether STIM1 association with extending microtubule tips plays a physiological role in Ca^{2+} signalling since nocodazole or taxol treatment has been shown to completely abolish SOCE and

I_{CRAC} in HEK293 cells (Smyth et al., 2007) but had no effect on Ca^{2+} influx in DT40 or HeLa cells (Baba et al., 2006). Additionally, EB1 depletion had no effect on thapsigargin-induced SOCE in HeLa cells, suggesting that the microtubule growth-dependent concentration of STIM1 is not required for STIM1-mediated SOCE (Grigoriev et al., 2008).

The polybasic domains of STIM1 and STIM2 have both been shown to interact directly with calmodulin (CaM) in a Ca^{2+} dependent manner using isothermal titration calorimetry (Bauer et al., 2008). It was proposed that when cytoplasmic Ca^{2+} levels increase, CaM associates with Ca^{2+} thereby increasing its affinity for STIM1 and STIM2. The interaction with CaM and the STIM proteins may result in the destabilisation and dissociation of STIM1 from plasma membrane Orai1 and act as an effective switch to terminate SOC influx when cytosolic Ca^{2+} levels are high (Bauer et al., 2008). However, an interaction between full length STIM1 and CaM has not been demonstrated. CaM also coimmunoprecipitates with Orai1 and mutational analyses of Orai1 have identified a calmodulin binding domain (AA 68-91) within the membrane proximal N-terminus (Mullins et al., 2009). Mutations in this region that eliminate CaM binding also block Ca^{2+} dependent inactivation of I_{CRAC}, suggesting that CaM binding to Orai1 is required for Ca^{2+} dependent inactivation of SOCE (Mullins et al., 2009). Interestingly, the calmodulin binding domain of Orai1 is also involved in interacting with STIM1 for SOC activation (Park et al., 2009). However the exact mechanism through which STIM1 and CaM act together with Orai1 to regulate Ca^{2+} dependent inactivation of SOCE remains to be determined.

Very recently a novel cytoplasmic protein, CRAC regulator 2A (CRACR2A), was identified by affinity purification as a protein that interacts with both STIM1 and Orai1 and this interaction increases upon store depletion (Srikanth et al., 2010a). CRACR2A knockdown results in a decrease in SOCE and inhibition of IL-2 production in Jurkat T cells (Srikanth et al., 2010a) and severely inhibits STIM1 and Orai1 clustering, suggesting that CRACR2A is important for STIM1-Orai1 clustering (Srikanth et al., 2010a). Expression of an EF-hand CRACR2A mutant results in constitutive STIM1 puncta formation, suggesting that CRACR2A forms a ternary complex with STIM1 and Orai1 at ER-PM junctions when stores are depleted (Srikanth et al., 2010a). It remains to be determined whether CRACR2A facilitates the recruitment of STIM1 and/or Orai1 to ER-PM junctions or whether it is required for the stabilisation of STIM1-Orai1 complexes after clustering but it seems that CRACR2A binding favours SOCE in conditions when intracellular Ca^{2+} levels are low.

Coimmunoprecipitation experiments have determined that STIM1 interacts with the sacroplasmic/endoplasmic reticulum Ca^{2+}-ATPase subtype 3 (SERCA3) in human platelets (Lopez et al., 2008). SERCA3 is involved in the regulation of Ca^{2+} reuptake into acidic stores. Although STIM1 and SERCA3 interact in resting cells, store depletion was found to transiently increase their association and treatment of platelets with a STIM1 antibody reduced acidic store refilling (Lopez et al., 2008). STIM1 therefore may regulate Ca^{2+} uptake by SERCA3 to modulate the refilling of acidic stores. However, the specific SERCA3 isoforms involved in this interaction have not been elucidated.

STIM1 has also been implicated in mediating Ca^{2+} entry through voltage gated Ca^{2+} channels as well as Orai1. It has recently been established that expression of the constitutively active STIM1-D76A mutant activates Orai1-mediated Ca^{2+} entry in vascular smooth muscle cells (VSMCs) (Park et al., 2010). Expression of the dominant negative Orai1 mutant inhibits both receptor-induced and thapsigargin-induced Ca^{2+} entry in VSMCs but these mutants had no effect on TRPC3/6-mediated currents (Park et al., 2010). Moreover, depletion of stores with thapsigargin induces an interaction between STIM1 and the $Ca_v1.2$ channel, inhibiting their function (Wang et al., 2010). *In vitro* and *in vivo* studies have determined that the STIM1 CAD domain binds directly to a coiled coil in the II-III loop of $Ca_v1.2$ (Park et al., 2010). These studies suggest that STIM1 regulates the relative distributions of both Orai1 and $Ca_v1.2$ to coordinate Ca^{2+} entry in excitable cells and argue against a role for TRPCs as mediators of store- or receptor-induced Ca^{2+} entry in VSMCs.

1.14 STIM2

While it seems that worms, flies and zebrafish possess only one STIM protein, vertebrates have adapted two STIM proteins, STIM1 and STIM2. It has been suggested that STIM2 arose through a gene duplication event in vertebrates (Brandman et al., 2007). The structure of STIM2 is overall very similar to that of STIM1, with 61% homology between the two proteins. The protein sequences diverge at the extreme N-terminus and also within the C-terminus, suggesting that the STIM2 may carry out functions which are distinct from STIM1.

Unlike STIM1, which is expressed in the ER and the plasma membrane, STIM2 is localised exclusively in the ER (Soboloff et al., 2006a). Its luminal domain within the ER contains paired canonical and non-functional EF-hands and a SAM domain. Recombinant monomeric STIM2 EF-SAM has a low Ca^{2+}-binding affinity, similar to that of STIM1, with a K_d of ~ 0.5 mM (Stathopulos et al., 2009; Zheng et al., 2008). However, the STIM2 EF-SAM domain in the absence of Ca^{2+} is well-folded and structurally more stable than that of STIM1 in the absence of Ca^{2+} and does not readily aggregate (Zheng et al., 2008). Nonetheless, circular dichroism data demonstrated the existence of STIM2 EF-SAM aggregates in the absence of Ca^{2+}, suggesting that the EF-SAM domain of STIM2 undergoes a conformational change and oligomerises on Ca^{2+} depletion (Stathopulos et al., 2009; Zheng et al., 2008). Consistent with this, overexpressed STIM2 translocates from a uniform localisation in bulk ER to ER-PM junctions upon store depletion, similar to the behaviour of STIM1 (Brandman et al., 2007; Soboloff et al., 2006a). Like STIM1, STIM2 may be recruited to puncta via plasma membrane phosphoinositides since the C-terminus of STIM2 binds phosphoinositides in liposomes (Ercan et al., 2009). Interestingly, STIM2 immunoprecipitates with STIM1 (Williams et al., 2001) and both have been shown to colocalise within puncta at ER-PM junctions (Brandman et al., 2007; Soboloff et al., 2006a), suggesting that STIM2 may functionally interact with STIM1 to regulate SOCE. However, the role of STIM2 in Ca^{2+} signalling is a controversial issue. Some studies have shown that overexpression of STIM2 strongly inhibits SOCE in a variety of cell types including HEK293, PC12, A7r5, and Jurkat T cells (Soboloff et al., 2006a; Soboloff et al., 2006b). However, coexpression of STIM2 and Orai1 results in large increases in SOCE in HEK293 RBL mast cells (Brandman et al.,

2007; Parvez et al., 2008; Soboloff et al., 2006b). T cells from STIM2 knockout mice exhibit reduced sustained Ca^{2+} influx, nuclear translocation of NFAT and cytokine production but this reduction is more pronounced in $STIM1^{-/-}$ T cells (Oh-Hora et al., 2008). These results suggest that both STIM1 and STIM2 play a role in the same Ca^{2+} signalling pathways but indicate that STIM1 is the key STIM protein required for SOC influx.

Consistent with this hypothesis, it appears that the major function for STIM2 is in the maintenance of basal cytoplasmic Ca^{2+} levels. STIM2 knockdown, but not STIM1 knockdown, lowers basal cytosolic and ER luminal Ca^{2+} levels in HeLa, HUVEC and HEK293 cells (Brandman et al., 2007). Unlike STIM1, a portion of STIM2 is also punctate and active in resting cells when the stores are replete (Brandman et al., 2007). This led to the proposal that STIM2 may act as a feedback regulator to stabilise both cytosolic and ER Ca^{2+} levels independent of store depletion. When stores are gradually depleted with external EGTA, YFP-STIM2 forms puncta before CFP-STIM1 in the same cell, suggesting that STIM2 translocation occurs with minimal store release, whereas STIM1 puncta formation requires more extensive store depletion (Brandman et al., 2007). However, extensive store depletion induces translocation of STIM2 to puncta, where it may act synergistically with STIM1 to induce extensive Ca^{2+} influx via Orai1 (Brandman et al., 2007). It seems therefore that STIM2 is involved in the constitutive regulation of basal cytosolic and ER Ca^{2+} levels, independent of store depletion and of STIM1, but that it can also participate in SOCE, independently of or along with STIM1, when stores are

depleted to selectively open SOCs in response to receptor stimuli (Brandman et al., 2007).

The increased sensitivity of STIM2 over STIM1 to small decreases in luminal Ca^{2+} may be attributable to differences in the EF-hand structure of the two proteins. Mutation of three residues in the cEF-hand of STIM1 results in a protein with similar sensitivity to luminal Ca^{2+} as STIM2, although the reciprocal mutations in STIM2 to STIM1 residues had no apparent effect on STIM2 function (Brandman et al., 2007). However, the STIM2 EF-SAM region is more stable than STIM1 EF-SAM, with a 3-fold slower unfolding rate and a 70-fold slower oligomerisation rate upon Ca^{2+} depletion when compared with STIM1 (Stathopulos et al., 2009). Additionally, an isoform-specific sequence N-terminal to the EF-SAM domain can influence the stability of the entire luminal domain interaction which is critical for Ca^{2+} sensing (Stathopulos et al., 2009). It has been proposed that the slower rate of STIM2 unfolding and oligomerisation in response to Ca^{2+} dissociation may result in the slower I_{CRAC} activation kinetics displayed by STIM2 compared with STIM1 (Deng et al., 2009; Parvez et al., 2008).

1.15 Orai proteins

The Orai1 family consists of three closely conserved cell surface proteins, termed Orai1-3. All three homologs are plasma membrane proteins with four predicted transmembrane segments which are all highly conserved, with N- and C-termini facing the cytosol. The N-terminus of Orai1 contains proline/arginine-rich regions and a conserved polybasic domain immediately before the first transmembrane

helix (Takahashi et al., 2007). See Figure 1.3 for a schematic of the structure of Orai1. The C-terminal domain of all three proteins includes a putative coiled-coil domain which may be required for protein interactions. Although all three proteins form Ca^{2+} selective channels (Lis et al., 2007), only Orai1 has been identified as the pore forming subunit of the SOC channel (Feske et al., 2006; Vig et al., 2006a; Zhang et al., 2005). The Orai1 monomer is ~33 kD in size but it has been suggested that the channel forms tetramers through an interaction with STIM1 and that these tetramers are the functional Ca^{2+} conducting channels (Ji et al., 2008; Mignen et al., 2008b; Penna et al., 2008).

1.16 Membrane topology of Orai1

Several studies have helped to elucidate the topology of Orai1 in the plasma membrane. Firstly, the surface localisation of Orai1 was determined by extracellular staining of a HA tag inserted into the TM3-TM4 loop (Prakriya et al., 2006). Additionally, the TM3-TM4 loop contains a consensus N-linked glycosylation site at an asparagine residue (N223). SDS-PAGE analysis revealed that mature Orai1 migrates at ~45 kD which is significantly larger than its predicted molecular weight of 33kD and that tunicamycin treatment, which blocks glycosylation in the ER, causes the Orai1 band to migrate close to 33kD (Gwack et al., 2007). These results implied that Orai1 is indeed glycosylated during protein maturation in the ER lumen and therefore becomes extracellular following the insertion of Orai1 into the plasma membrane (Gwack et al., 2007; Prakriya et al., 2006). The TM1-TM2 loop was also found to be extracellular since substitution mutations in this region alter the sensitivity of Orai1 to the extracellular channel blocker, Gd^{3+}. Finally, it was

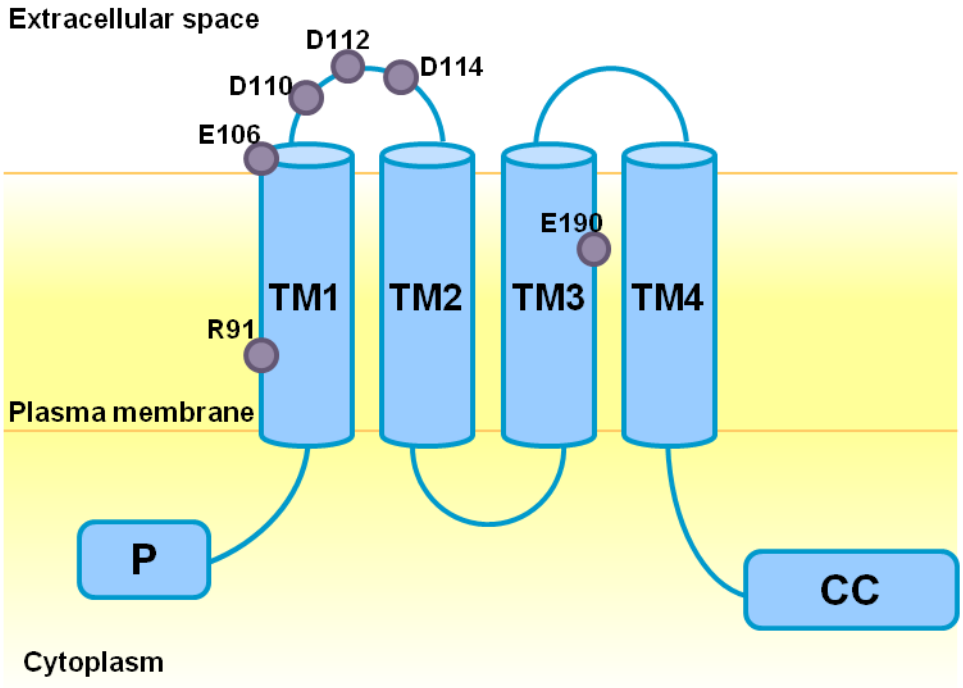

Figure 1.3 Schematic structure of Orai1. The Orai1 protein has four transmembrane domains (TM1-4), with extracellular loops between TM1-TM2 and TM3-TM4. The N- and C-termini of Orai1 are intracellular. The N-terminus contains proline/arginine rich and polybasic regions, while the C-terminus contains a putative coiled-coil domain. Residues E106 and E 190 in TM1 and TM3 as well as D110, D112 and D114 which have all been implicated in controlling the selectivity filter or Orai1 are highlighted in purple. The residue R91 in TM1 which is mutated in many SCID patients is highlighted in purple.

established that the N- and C-termini of Orai1 are intracellular since epitope tags located at either end of the protein are detected only following cell permeabilisation (Prakriya et al., 2006).

1.17 Orai1 functions as a tetramer

Since many ion channels require oligomerisation of individual subunits, it was initially proposed that Orai1 may function as a multimer (Frischauf et al., 2008; Vig et al., 2006a). Coimmunoprecipitation experiments have demonstrated that Drosophila and mammalian Orai1 can form dimers or higher order homomultimers (Gwack et al., 2007) and this was confirmed in reciprocal coimmunoprecipitation experiments using two differently tagged Orai1 proteins in HEK293 cells (Vig et al., 2006a). Size exclusion chromatography experiments using purified Orai1 complexes confirmed that Orai1 forms multimers (Maruyama et al., 2009; Park et al., 2009). Additionally, it seems that Orai homologs can form heteromeric channel complexes (Gwack et al., 2007; Lis et al., 2007; Zhang et al., 2008). In order to determine the exact architecture of the SOC channel pore, Mignen *et al* constructed and expressed preassembled Orai1 tandem multimers containing different numbers of Orai1 subunits (monomers, dimers, trimers and tetramers) into cells stably expressing STIM1 and evaluated their maximal abilities to activate I_{CRAC} (Mignen et al., 2008b). CRAC currents in cells expressing Orai1 tetramers were unaffected by coexpression of a dominant negative Orai1 (E106Q) mutant monomer, indicating that recruitment of additional Orai1 subunits is not necessary in cells expressing tandem tetramers, whereas a large reduction in I_{CRAC} was observed in cells co-expressing monomers, dimers or trimers along with the mutant monomer (Mignen

et al., 2008b). It is likely therefore that the tandem tetramer is sufficient to activate I_{CRAC} and may form a closed functional unit which is unable to recruit further Orai1 molecules. This was confirmed in a separate study which used single molecule photobleaching of Orai1-GFP to calculate the stoichiometry of Orai1 molecules in the CRAC channel pore (Ji et al., 2008). These experiments revealed that four Orai1 subunits and two STIM1 molecules form an active CRAC channel. Additionally, FRET experiments demonstrated that Orai1-mKO monomers could interact with dimers and trimers of Orai1-EGFP but not with Orai1-EGFP tetramers, supporting the conclusion that the Orai1 channel functions as a tetramer (Ji et al., 2008). Furthermore, crosslinking and photobleaching experiments determined that Orai1 exists as a dimer in resting cells which assemble into tetramers when coexpressed with the C-terminal domain of STIM1 (Penna et al., 2008). Limited work has been carried out on the domains responsible for Orai1 channel assembly. Orai1 oligomerisation may require the transmembrane domains since deletion of either or both of the N- and C-terminal cytosolic domains of Orai1 does not prevent its oligomerisation (Li et al., 2007; Muik et al., 2008). However, the exact domains required for Orai1 multimerisation remain to be characterised.

1.18 Orai1 is the store-operated Ca^{2+} channel

A wealth of experimental evidence has implicated Orai1 as the functional CRAC channel subunit. Firstly, the naturally occurring R91W mutation found in several patients with severe combined immunodeficiency abrogates I_{CRAC} (Feske et al., 2006). Orai1 contains several acidic residues which are important for maintaining the Ca^{2+} selectivity of the CRAC channel. Such acidic residues are contained in

selectivity filters of Ca_v channels and confer high Ca^{2+} selectivity to these channels (Yamashita et al., 2007). Mutational analysis has determined that amino acid residues including glutamates at positions 106 in the first transmembrane helix and 190 in the third transmembrane helix are required to maintain the Ca^{2+} selectivity of the pore since the E106D and E190Q mutations result in largely diminished Ca^{2+} influx and an increase in currents carried by monovalent cations such as Na^+ and Cs^+ (Lis et al., 2007; Prakriya et al., 2006; Vig et al., 2006a; Yeromin et al., 2006). In an Orai1 tetramer, it is believed that four negative E106 side chains coordinate Ca^{2+} within the pore. Mutation of this residue to a neutral alanine results in a loss of Ca^{2+} conductance (Prakriya et al., 2006; Yeromin et al., 2006). Overexpression of a E106D mutant Orai1 has a dominant negative effect on I_{CRAC} current, resulting in an outwardly rectifying channel and a shift in the reversal potential (Peinelt et al., 2006; Prakriya et al., 2006; Vig et al., 2006a; Yeromin et al., 2006), which is possibly caused by heteromultimerisation of the Orai1 mutant with wild type Orai1 subunits (Mignen et al., 2008b). Similarly, an E106Q mutation blocks native SOCE in T-cells (Gwack et al., 2007; Prakriya et al., 2006). Interestingly, the point mutations V102I and V105I which are close to E106 in the TM1-TM2 loop alter the voltage sensitivity of Orai1, suggesting that this extracellular loop does form part of the selectivity filter (Spassova et al., 2008). The E190Q and E190A mutations in the TM3-TM4 loop result in severely impaired SOCE (Gwack et al., 2007; Peinelt et al., 2006; Schindl et al., 2008).

Three closely spaced aspartate residues, D110, D112 and D114, which are all located in the TM1-TM2 loop and believed to comprise a putative Ca^{2+} binding site,

may also form major elements of the Orai1 selectivity filter. Mutation of each of these residues to an alanine results in widening of the CRAC channel pore and a consequent increase in the channel's permeability to monovalent cations (Vig et al., 2006a; Yamashita et al., 2007). Moreover, the D110/112/114A mutations reduced the Ca^{2+}-dependent fast inactivation of the channels, which is key to the modulation of CRAC channel gating (Yamashita et al., 2007).

In contrast to the results described above, other groups have different findings. In several studies an E190D mutant had no effect on the Ca^{2+} selectivity of the channel and its permeation to monovalent cations such as Cs^{+} (Prakriya et al., 2006; Schindl et al., 2008) and an E190A mutation failed to inhibit SOCE (Prakriya et al., 2006). In a separate study, McNally *et al* used a substituted cysteine accessibility method whereby cysteines were introduced into the Orai1 subunit pore and their accessibility to thio-reactive agents was investigated. Using this method, the authors determined that the effects of the E190Q and the D110/112/114A mutations do not affect the selectivity filter and that the altered ion permeability observed by these mutations is due to allosteric effects (McNally et al., 2009). However, the same study suggested that binding of a single Ca^{2+} ion to the channel pore is sufficient to block monovalent CRAC currents and that Ca^{2+} selectivity is solely coordinated by the E106 residue which encodes a high affinity Ca^{2+} binding site (McNally et al., 2009). It is clear therefore, that further structural and mutational studies are required in order to determine the exact geometry of the Orai1 channel pore and to uncover the mechanism by which it coordinates Ca^{2+}.

1.19 Orai2 and Orai3

Orai1, Orai2 and Orai3 are present at the mRNA level in a wide range of tissues and cell types and are expressed at the plasma membrane (Gwack et al., 2007). Orai2 and Orai3 share the same membrane spanning topology as the Orai1 channel and all three proteins have a high degree of sequence similarity (60.3% for Orai1 and Orai2, 63.2% for Orai1 and Orai3 and 66.4% for Orai2 and Orai3) (Feske, 2009). Sequence comparison of the transmembrane domains alone demonstrates that the transmembrane segments are nearly completely conserved between all three proteins (92.5%, 93.8% and 93.8%, respectively) (Feske, 2009). Both Orai2 and Orai3 contain glutamate residues which correspond to the E106 and E190 residues within Orai1 and can potentiate I_{CRAC} to levels 15-20 fold higher than endogenous I_{CRAC} when overexpressed with STIM1 (DeHaven et al., 2009; Lis et al., 2007), although the current amplitudes for Orai2 and Orai3 are 2-3 times smaller when compared with Orai1 (Lis et al., 2007). Orai3 currents in particular are more stable than Orai1 or Orai2, suggesting that Orai3 has the weakest potentiating current of the three proteins (Lis et al., 2007). The biophysical properties of these currents are similar to endogenous I_{CRAC} and also to currents produced by Orai1 and STIM1 overexpression (DeHaven et al., 2009; Lis et al., 2007). However, they differ in their permeabilities to Ca^{2+} and monovalent cations, exhibit different pharmacological properties and vary in their Ca^{2+}-dependent inactivation of I_{CRAC}. Na^{+} currents through all three Orai subtypes are blocked to similar extents by extracellular Ca^{2+}, suggesting that they have similarly high affinities for Ca^{2+} in HEK293 cells (DeHaven et al., 2009; Lis et al., 2007). However, Orai3 is more resistant to depotentiation from Ca^{2+}, Ba^{2+} or Mg^{2+} than Orai1 or Orai2 (DeHaven et al., 2009). Additionally,

Orai3 displays increased permeability to monovalent cations such as Na^+ than Orai1 or Orai2 (Lis et al., 2007). It has been suggested that differences in selectivity to monovalent cations may be due to differences in the 110/112/114 residues in the TM1-TM2 loop, since this region has been shown to contribute to monovalent permeation (Lis et al., 2007; Vig et al., 2006a). The three Orais also exhibit distinct responses to the pharmacological agent 2-aminoethoxydiphenyl-borate (2-APB). 2-APB stimulates I_{CRAC} at low concentrations (≤ 5 μM) but higher concentrations of 2-APB (10-50 μM) completely inhibit Orai1-dependent I_{CRAC} and partially suppress Orai2-dependent currents (DeHaven et al., 2009; Lis et al., 2007; Peinelt et al., 2008; Schindl et al., 2008; Zhang et al., 2008). However, 2-APB activates Orai3 currents at all concentrations tested, even in the absence of store depletion and STIM1 (Lis et al., 2007; Peinelt et al., 2008; Schindl et al., 2008; Zhang et al., 2008). Replacing the 2nd and 3rd transmembrane regions of Orai1 with those from Orai3 resulted in full 2-APB induced Ca^{2+} influx through Orai1 which was comparable to that of Orai3 (Zhang et al., 2008). The altered selectivity of Orai3 to 2-APB is associated with a widening of the Orai3 pore size, leading to an increased conductance for monovalent cations (Peinelt et al., 2008; Schindl et al., 2008; Zhang et al., 2008). Orai3 proteins containing single point mutations in the channel pore exhibited similar ion permeation properties to 2-APB stimulated Orai3 (Schindl et al., 2008). Additionally, single point mutations in the Orai1 selectivity filer enable 2-APB to activate Orai1 independently of STIM1 (Peinelt et al., 2008), suggesting that 2-APB regulates the Orai channels by altering the size of the channel pores. The distinct features of the Orai proteins and their ability to heteromultimerise may provide flexibility to fine-tune the regulation of Ca^{2+} signalling, although specific

functions for Orai2 and Orai3 in the various tissues and cell types in which they are expressed remains to be addressed.

1.20 STIM1 and Orai1 coupling

It is now well established that store depletion is coupled to SOC activation via a direct interaction between STIM1 and Orai1 within puncta at ER-PM junctions. Numerous biochemical assays including GST-pulldown and coimmunoprecipitation studies have demonstrated direct binding between STIM1 and Orai1 *in vitro* (Muik et al., 2008; Park et al., 2009; Vig et al., 2006a; Yeromin et al., 2006). An association between the two proteins within puncta has also been demonstrated *in vivo* by a number of groups by use of FRET between appropriately tagged donor/acceptor derivatives of STIM1 and Orai1 (Calloway et al., 2009; Muik et al., 2008; Navarro-Borelly et al., 2008; Wang et al., 2009). These interaction studies are supported by independent reports that overexpressed STIM1 and Orai1 colocalise within puncta following store depletion (Chvanov et al., 2008; Ji et al., 2008; Li et al., 2007; Park et al., 2009; Penna et al., 2008; Varnai et al., 2007; Xu et al., 2006). Additionally, in ER-PM junctions, the distance between the ER and the plasma membrane is ~10-25 nm which is close enough to allow for an interaction to occur between STIM1 in the ER and Orai1 in the plasma membrane (Wu et al., 2006a). However, FRET studies imply a distance of less than 10 nm between STIM1 and Orai1 within puncta (Barr et al., 2008; Muik et al., 2008).

1.21 Molecular interactions mediating STIM-Orai1 coupling

Full length STIM1 requires oligomerisation before it can translocate to ER-PM junctions to interact with and activate Orai1 channels. However, expression of the C-terminal domain of STIM1 alone constitutively activates SOCs independently of store depletion (Baba et al., 2006; Li et al., 2007; Park et al., 2009; Williams et al., 2002). Additionally, overexpression of Orai1 is required to recruit the C-terminus of STIM1 to the plasma membrane (Muik et al., 2008), suggesting that a domain within the STIM1 C-terminus mediates the interaction with Orai1. Coupling of STIM1 to Orai1 is reversible, since store refilling stimulates the dissociation of STIM1 oligomers and the redistribution of STIM1 back to bulk ER, resulting in attenuation of SOCE (Chvanov et al., 2008; Liou et al., 2005; Muik et al., 2008).

In recent years, many groups have sought to uncover the molecular mechanism controlling the coupling between STIM1 and Orai1. Five groups have independently identified a minimal region within the STIM1 C-terminus which is essential for binding to and activating Orai1 (Huang et al., 2006; Kawasaki et al., 2009; Muik et al., 2009; Park et al., 2009; Wang et al., 2009). Systematic truncation of the STIM1 C-terminus, starting from immediately downstream of the transmembrane region (aa 233), have demonstrated that STIM1 fragments beginning with aa 344 within the first coiled-coil domain retain the ability to fully activate SOCE without store depletion (Huang et al., 2006) but deleting up to aa 350 results in the complete removal of the first coiled-coil domain and produces a non-functional truncation mutant (Park et al., 2009; Yuan et al., 2009).

Serial deletions from the C-terminal end of STIM1 has produced functionally active fragments ending in from aa 505 (S1ctCC) (Wang et al., 2009), aa 448 (CAD) (Park et al., 2009), 444 (CCb9) and down to aa 442 (SOAR) (Yuan et al., 2009). These studies have revealed that just over 100 amino acids within the C-terminus of STIM1 including the second coiled-coil domain is sufficient for I_{CRAC} activation (Park et al., 2009; Yuan et al., 2009). This has been demonstrated independently by two groups. Park *et al* produced the Ca^{2+}-activating domain (CAD; aa 340-448) (Park et al., 2009) and Yuan *et al* produced the STIM1 Orai1 activating region (SOAR; aa 344-442) (Yuan et al., 2009). Further deletions from this minimal region results in STIM1 fragments that fail to interact with and activate Orai1 (Kawasaki et al., 2009; Muik et al., 2009; Park et al., 2009; Yuan et al., 2009).

The STIM1 C-terminus induces both the clustering and the activation of Orai1 channels (Ji et al., 2008; Park et al., 2009; Penna et al., 2008; Wang et al., 2009). CAD has been shown to bind to both the C-terminus of Orai1, which has previously been demonstrated for the full STIM1 C-terminus (Muik et al., 2008), but also binds to the Orai1 N-terminus (aa 70-91), a region which is required for I_{CRAC} activation (Park et al., 2009). Deletion of the Orai1 N-terminus does not affect clustering but abolishes Orai1 activation, suggesting that Orai1 clustering and activation are separate processes (Li et al., 2007; Muik et al., 2008; Takahashi et al., 2007). A truncated version of CAD which lacks 8 C-terminal amino acids (aa 441-448), induces Orai1 clustering but fails to activate I_{CRAC}, indicating that CAD is involved in both the clustering and gating of Orai1 (Park et al., 2009). The ability of CAD to gate Orai1 was confirmed in a recent study which identified a basic sequence within the

CAD domain (residues 384-286 in human STIM1) which associates physically with the C-terminal acidic coiled coil domain of Orai1 to transmit the Ca^{2+} gating signal to Orai1 following store depletion (Calloway et al., 2010). Two STIM1 constructs, aa 1-488 and aa 1-440 both translocate to puncta in response to store depletion but only that the aa 1-488 fragment can activate Orai1 (Park et al., 2009). Since SOAR (aa 344-442) can activate Orai1 (Yuan et al., 2009), it is possible that the 441 and 442 residues are critical for Orai1 gating.

Although CAD and SOAR constitutively bind to and fully activate Orai1, the full C-terminus of STIM1 interacts less efficiently with Orai1 and remains largely cytosolic (Park et al., 2009; Wang et al., 2009). The C-terminus may therefore require partial unfolding in order to expose CAD/SOAR to Orai1. It is possible that during STIM1 recruitment to the plasma membrane, the STIM1 polybasic domain may bind to plasma membrane components, e.g. phosphoinositides, resulting in partial unfolding of the C-terminus and the consequent exposure of CAD/SOAR to the Orai1 channel.

Muik *et al* have identified a minimal region (aa 400-474) within CAD/SOAR, termed the STIM1 homomerisation domain (SHD) which is essential for STIM1 C-terminus homomerisation required for interacting with and activating Orai1 (Muik et al., 2009). C-terminal STIM1 fragments lacking this domain are monomeric and fail to interact with Orai1 (Muik et al., 2009). The stoichiometry of these C-terminal STIM1 fragments alone and clustered with Orai1 is unclear. Purified CAD is tetrameric in solution (Park et al., 2009) whereas the C-terminal STIM1 fragments comprising aa

233-485, aa 336-485 and aa 233-450, exist as dimers in solution (Muik et al., 2009; Yuan et al., 2009). CAD tetramers bind to and link Orai1 channels together causing them to cluster in large multimeric arrays (Park et al., 2009). However the stoichiometry of Orai1 multimers complexed with CAD is not consistent with the hypothesis that Orai1 dimers join to form a tetrameric channel, since Orai1 multimers are of a similar size in the absence as in the presence of CAD (Park et al., 2009). It seems, therefore, that further work is required to clarify the stoichiometry of Orai1 coupling with the STIM1 C-terminus.

A modulatory domain within the STIM1 C-terminus has also been implicated in the coupling of STIM1 to Orai1. This domain includes a cluster of negatively charged amino acids (aa 474-485) located C-terminal to CAD/SOAR (Derler et al., 2009). Addition of these residues to CAD restored Ca^{2+}-dependent inactivation of SOCE (Park et al., 2009). Similarly, extension of OASF up to aa 485, resulted in reduced I_{CRAC} currents and coupling efficiency, suggesting that this domain regulates the affinity of STIM1 C-terminal fragments for Orai and SOCE in a negative manner (Muik et al., 2009). Furthermore, mutation or deletion of these residues results in Orai1 currents that display reduced inactivation when compared with STIM1 proteins containing these residues (Derler et al., 2009). This domain has hence been termed the CRAC modulatory domain (CMD) and has been suggested to play a role in fast Ca^{2+}-dependent inactivation, a negative feedback mechanism regulating SOCE (Derler et al., 2009).

The cytosolic C-terminus of Orai1, that includes a conserved putative coiled-coil domain, has been shown to physically interact with STIM1 (Muik et al., 2008). Orai1 proteins lacking the C-terminal domain fail form puncta with STIM1 after store depletion and therefore do not activate SOCE (Li et al., 2007; Muik et al., 2008). Moreover, a point mutation (L273S) within the coiled-coil domain of Orai1 does not interact with or couple to the OASF fragment of STIM1 (Muik et al., 2009), suggesting that Orai1 couples with STIM1 via its C-terminus. However, it seems that the N-terminus of Orai1 is required for channel gating (Li et al., 2007; Muik et al., 2008; Varnai et al., 2007). Additionally, the N-terminal proline-rich region of Orai1 is required for the inward rectification of the I_{CRAC} current, possibly via an interaction with the STIM1 polybasic domain (Yuan et al., 2009). Since the STIM1 CAD domain has been shown to interact with both the C-terminus and N-terminus of Orai1, it has been suggested that CAD provides the energy for Orai1 gating by bridging the N- and C-termini of Orai1 (Park et al., 2009), although this remains to be demonstrated.

The intracellular loop of Orai1 has recently been shown to be required for the fast inactivation of SOCE. Mutation of four residues within the intracellular loop linking transmembrane segments II and III, inhibited fast inactivation, leading to increased SOCE and higher CRAC currents (Srikanth et al., 2010b). Five key amino acids, N(153)VHNL(157), seem to act as an inactivation particle to promote Ca^{2+}-dependent inactivation of SOCE (Srikanth et al., 2010b).

1.22 Summary of STIM1-Orai1 coupling

An overview of STIM1-Orai1 coupling is outlined in Figure 1.4. Store depletion leads to the dissociation of Ca^{2+} and partial unfolding of the STIM1 EF-SAM domain, stimulating STIM1 oligomerisation within the ER via the EF-SAM domain and a homomultimerisation domain (SHD) within the STIM1 C-terminus. STIM1 oligomers then diffuse through the ER and become trapped in ER-PM junctions, possibly via electrostatic interactions between the polybasic domain of STIM1 and plasma membrane phosphoinositides. Orai1 multimers (dimers or tetramers) within the plasma membrane become trapped in clusters at ER-PM junctions via a direct interaction between the C-terminal domain of Orai1 and the CAD/SOAR domain of STIM1. The CAD/SOAR domain may also interact with the Orai1 N-terminus. These STIM1-Orai1 interactions result in the gating of the Orai1 channels to an open state by a currently unknown mechanism. The coupling of Orai1 to STIM1 may be further modulated by the negatively charged CMD domain within the C-terminus of STIM1 which may contribute to fast Ca^{2+}-dependent inactivation of I_{CRAC}.

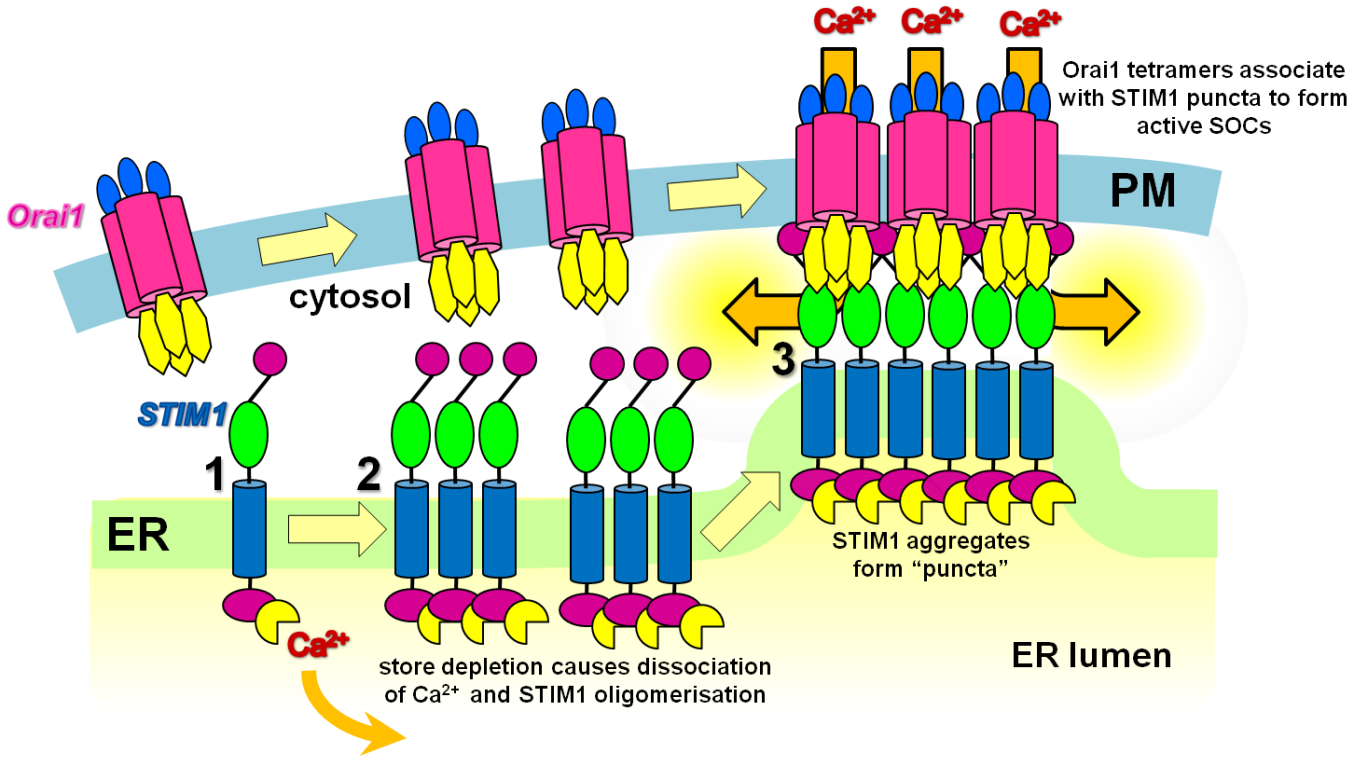

Figure 1.4 Molecular coupling between STIM1 and Orai1 within ER-PM junctions. **(1)** Depletion of Ca^{2+} from the ER triggers the dissociation of Ca^{2+} from the cEF hand of STIM1 in the ER lumen. **(2)** This leads to the unfolding of the EF-SAM domain and the subsequent oligomerisation of STIM1 molecules within the ER. **(3)** Interactions between the C-terminal polybasic domain of STIM1 and the plasma membrane anchor STIM1 aggregates called "puncta" in ER-PM junctions. Diffusing Orai1 tetramers in the plasma membrane become trapped in ER-PM junctions through an interaction with the C-terminal CAD/SOAR domain of STIM1, which binds the N- and C-termini of Orai1 molecules to gate the opening of Orai1 channels, thereby allowing Ca2+ influx into the cytosol. *Adapted from (Deng et al., 2009).*

1.23 Aims and Objectives

The aim of this study was to uncover the mechanisms controlling the physical translocation of STIM1 to puncta at ER-PM junctions. Four main research questions were investigated:

- Firstly, it was of interest to determine whether STIM1 translocation was an active process which requires ATP or whether STIM1 molecules simply diffuse to ER-PM junctions following store depletion.
- The second aim was to ascertain whether or not STIM1 inserts into the plasma membrane following store depletion and if so, to uncover the mechanism required for inserting STIM1 into the plasma membrane.
- Thirdly, this study aimed to define the plasma membrane components required for recruiting STIM1 aggregates to ER-PM junctions following translocation.
- There is evidence to suggest that STIM1 and Orai1 function as part of a macromolecular complex which may involve other, as of yet, unidentified proteins. Therefore the final aim of this project was to identify novel proteins that interact with STIM1 and Orai1 to mediate store operated Ca^{2+} entry.

CHAPTER TWO

Materials and Methods

2.1 Molecular Biology

2.1.1 PCR

DNA sequences for cloning were prepared from cDNA which was made previously in the lab, or subcloned from existing plasmids. pHusion DNA polymerase (New England Biolabs, Herts, UK) was used for the amplification of specific sequences by PCR. Each 100 µl reaction mixture contained 20 µl 5x PCR reaction buffer, 5% (v/v) DMSO, 0.2 mM dNTPs, 0.5 µM forward and reverse primers and 1U pHusion polymerase in distilled water. Approximately 0.5 µl HeLa cell DNA or 0.5 µg plasmid DNA were used as template. The PCR conditions were as follows:

1 cycle:	98^{o}C	1 minute
35 cycles:	98^{o}C	30 seconds
	55-65^{o}C	30 seconds
	72^{o}C	15 seconds per kilobase
1 cycle:	72^{o}C	5 minutes
	30^{o}C	1 minute

2.1.2 Restriction Endonuclease Digestion

The following conditions were used for digestion of PCR products and vectors prior to ligation, or for restriction analysis of recombinant plasmids. Digestion reactions containing 2 µl of the appropriate 10x buffer (New England Biolabs), 0.5 U of each required enzyme (New England Biolabs) and 0.5 – 1 µg of DNA in a total of 20 µl distilled water, were made up and incubated at 37^{o}C for 60 minutes. Digested

products were separated by agarose gel electrophoresis and purified by gel extraction where necessary.

2.1.3 Agarose gel electrophoresis and gel extraction

DNA fragments were separated by agarose gel electrophoresis for further analysis or purification of DNA fragments for subsequent cloning experiments. Gels consisted of 1% (v/w) agarose in TAE buffer (40 mM Tris base pH8, 20 mM acetic acid, 1 mM EDTA). 0.5 µg/µl ethidium bromide or Sybr Safe (Invitrogen, Paisley, UK) was added to the gels to stain the DNA. DNA samples of up to 40 µl combined with a 1:5 dilution of 5x DNA Loading Buffer (Bioline, Sheffield, UK) were loaded on to the gels and run against the Hyperladder I DNA molecular weight marker (Bioline) at 80-90 mV. For purification of DNA fragments from agarose gels, specific DNA bands were viewed on a transilluminator and cut from the gels and purified using the QIAquick DNA gel extraction kit (Qiagen, Crawley, UK). Briefly, excised bands were dissolved to release the DNA fragments and DNA was bound to an ion exchange column, washed and eluted in 30 µl Elution Buffer (Qiagen).

2.1.4 Ligation

Ligation reactions were carried out to generate circular plasmid DNAs from linear fragments, for cloning or subcloning through the insertion of a linear coding DNA sequence into a given vector. Reactions were carried out using 50 ng DNA, with a 1:3 molar ratio of vector:insert DNA. In addition to the DNA fragments, the ligation reaction mixture contained 1 µl 10x ligase reaction buffer (New England Biolabs) and 1,000U T4 DNA ligase (New England Biolabs) made up to a final volume of 10 µl

with distilled water. The reaction was incubated at room temperature for 15 – 30 minutes after which 5 µl was then used to transform chemically competent *E. coli*.

2.1.5 Transformation of chemically competent *E. coli*

XL-1 blue chemically competent cells (Bioline) were used for transformation with the products of a ligation reaction. Competent *E. coli* prepared in-house were used for transformation with routine plasmid DNA. For each transformation, 100 µl of cells were thawed on ice. 5 µl of the ligation reaction or 50-100 ng of purified plasmid DNA was added to the cells and incubate on ice for 20 minutes. The cells were then subjected to a 42^{o}C heat shock for 45 seconds, returned to ice for a further 2 minutes and then added to 900 µl sterile SOC medium (20 g/L tryptone, 5 g/L yeast extract and 500 mg/L NaCl in distilled water), prewarmed to 42^{o}C. The cell suspension was then incubated at 37^{o}C for 1 hour with continuous shaking at 250 rpm. 50 µl – 100 µl of each transformation was then spread on sterile LB-Agar plates (15 g/L Agar, 10 g/L tryptone, 10 g/L NaCl and 5 g/L yeast extract in distilled water), containing an appropriate antibiotic for selection of transformants (100 µg/ml ampicillin or 30 µg/ml kanamycin). Transformed colonies were picked for further analysis following overnight incubation at 37^{o}C.

2.1.6 Purification of plasmid DNA

For the analysis of *E. coli* transformed with ligated DNA clones, single colonies were used to inoculate 5 ml LB broth (10 g/L tryptone, 10 g/L NaCl and 5 g/l yeast extract in distilled water) containing an appropriate antibiotic (100 µg/ml ampicillin or 30 µg/ml kanamycin) and these cultures were incubated overnight at 37^{o}C with

shaking at 250 rpm. The cultures were then pelleted by centrifugation (12000 x g, 10 minutes) and plasmid DNA was extracted using the QIAprep Spin Miniprep Kit (Qiagen) according to the manufacturer's protocol. Briefly, cells were lysed in an alkaline sodium dodecyl sulphate (SDS) solution for 5 minutes and any unwanted material was precipitated by adding an acid solution. This waste material was pelleted by centrifugation (13000 x g, 10 minutes) and the supernatant containing the plasmid DNA was bound to an anion exchange column, washed and eluted in 30 µl Elution Buffer (Qiagen). Purified plasmid DNA was analysed by restriction endonuclease digestion and agarose gel electrophoresis (see above).

For large scale plasmid preparations required for the transfection of HeLa cells, single colonies were used to inoculate 5 ml LB broth containing an appropriate antibiotic and grown for 8 hours at 37^{o}C with shaking at 250 rpm. These cultures were then added to 150 ml LB broth containing an appropriate antibiotic and incubated overnight using the same conditions. Plasmid DNA was extracted from the cultures using the QIAfilter HiSpeed Plasmid Maxi Kit (Qiagen) according to the manufacturer's instructions. The concentration of purified plasmid DNA obtained was determined through spectrophotometry.

2.2 Plasmids

2.2.1 GST-STIM1-CT

The sequence of the human STIM1 C-terminal domain (STIM-CT) comprising amino acids M241-K685 of the STIM1 sequence (PubMed accession no. NM_003156) was amplified from an existing STIM1-EYFP vector (Chvanov et al., 2008) by PCR and

inserted in frame into the pGEX-6-P1 vector (Clontech, Basingstoke, UK) to generate a mammalian expression construct for STIM1-CT, N-terminally tagged with GST. The PCR primers contained restriction endonuclease sites (underlined) to facilitate insertion of the STIM1-CT sequence into the vector. The forward primer used was 5'-ATATGGACTTATCCAGAACCGTTACTCCGAG-3'; BamHI, and the reverse primer was 5'-ATATCCGCGGCTACTTCTTAAGAGGCTT-3'; SacII. The amplified PCR product and the vector were digested with BamHI/SacII and the digested products were ligated using standard methods.

2.2.2 GST-Orai1-CT

The sequence of the human Orai1 C-terminal domain (Orai1-CT) comprising amino acids A267-A315 of the Orai1 sequence (PubMed accession no. BC015369) was amplified from an existing mCherry-Orai1 vector (Chvanov et al., 2008) by PCR and inserted in frame into the pGEX-6-P1 vector to generate a mammalian expression construct for Orai1-CT, N-terminally tagged with GST. The PCR primers contained restriction endonuclease sites (underlined) to facilitate insertion of the Orai1-CT sequence into the vector. The forward primer used was 5'-ATATGGATCCGCCGTCCACTTCTAC-3'; BamHI, and the reverse primer was 5'-ATATCTCGAGCTAGGCATAGTGGCT-3'; XhoI. The amplified PCR fragment and the cut vector were generated through digestion with BamHI/XhoI and the fragments were ligated using standard methods.

2.2.3 GST-Orai1-NT

The sequence of the human Orai1 N-terminus (Orai1-NT) comprising amino acids M1-L86 of the Orai1 sequence (PubMed accession no. BC015369) was amplified from an existing mCherry-Orai1 vector by PCR and inserted in frame as per GST-Orai1-CT. The forward primer used was 5'- ATATGGATCCATGCATCCGGAGCCCGCC-3'; BamHI, and the reverse primer was 5'-ATATCTCGAGAAGCTTGGCGCGGCTCTTGTA-3'. The coding DNA sequence and the vector were cut with BamHI/XhoI and ligated using standard methods.

2.2.4 GST-Golli

The Golli sequence was amplified from Golli-mCherry by PCR and inserted in frame into the pGEX-6-P1 vector to generate a mammalian expression construct for Golli, N-terminally tagged with GST. The PCR primers contained restriction endonuclease sites (underlined) to facilitate insertion of the Golli sequence into the vector. The forward primer used was 5'- ATATGGATCCATGGGAAACCACTCTGGA-3'; BamHI, and the reverse primer was 5'- ATATCTCGAGCTACGGCTCGGAGCTCACCTT-3'; XhoI. The amplified PCR fragment and the cut vector were generated through digestion with BamHI/XhoI and the resulting fragments were ligated using standard methods.

2.2.5 His_6-STIM1-EYFP

The His_6-STIM1-EYFP construct was made using two sequential cloning steps. Firstly, the STIM1 signal peptide comprising 22 amino acids was amplified from STIM1-EYFP by PCR and inserted in frame into the pEYFP-N1 vector (Clontech) to generate a mammalian expression construct containing the STIM1 signal peptide,

N-terminally tagged with EYFP (SP-EYFP). The forward primer was 5'ACTGAAGCTTATGGATGTATGCGTCCGTCTTGCC-3'; HindIII, and the reverse primer was 5'-ATATCCGCGGGAGGCTCTGGCCCTGGTG-3'; SacII. BamHI/SacII were used to digest the signal peptide and the vector, which were then ligated using standard methods to make SP-EYFP.

The His_6-STIM1 sequence was amplified from STIM1-EYFP and N-terminally tagged with 6 histidine residues by PCR and inserted in frame into the SP-EYFP vector to generate a mammalian expression construct containing the STIM1 sequence, N-terminally tagged with a poly-His sequence and C-terminally tagged with EYFP. The PCR primers contained restriction endonuclease sites (underlined) to facilitate insertion of the STIM1 sequence into the vector between the signal peptide and the EYFP sequence. The forward primer also contained the sequence for 6 histidine residues directly downstream of the restriction site in order to label the N-terminus of the STIM1 sequence with a poly-His tag (in italics). The forward primer was 5'-ATATCCGCGG*CATCATCATCATCATCAT*AGCCATAGTCAC-3'; SacII, and the reverse primer was 5'-ATATGGATCCGGCTTCTTAAGAGGCTT-3'; BamHI. The digested PCR fragment and the vector were generated through digested with SacII/BamHI and the resulting fragments were ligated using standard methods.

2.2.6 STIM1-CT-EYFP

The sequence of the human STIM1 C-terminal domain (STIM-CT) was amplified from STIM1-EYFP and inserted in frame into pEYFP-N1 to generate a mammalian expression construct for STIM1-CT, N-terminally tagged with EYFP. The PCR primers

contained restriction endonuclease sites (underlined) to facilitate insertion of the STIM1-CT sequence into the vector. The forward primer was 5'-ATATAAGCTTATCCAGAACCGTTACTCCAAG-3'; HindIII, and the reverse primer was 5'-ATATCCGCGGCTTCTTAAGAGGCTT-3'; SacII. The DNA insert and the vector were digested using HindIII/SacII and ligated using standard methods.

2.2.7 Cerulean-Orai1

The pCerulean-C1 vector (a kind gift from David W Piston, Vanderbilt University Medical Centre, Tennessee) was digested with AgeI/BsrI to excise the Cerulean sequence. mCherry-Orai1 was digested with AgeI/BsrI to excise the mCherry tag. The digested Cerulean sequence and vector were ligated using standard methods.

2.2.8 pcDNA-Orai1

The full length human Orai1 sequence was amplified from mCherry-Orai1 and inserted in frame into pcDNA3.1(-) (Invitrogen) to generate an untagged Orai1 construct for mammalian expression. The PCR primers used contained restriction sites to facilitate insertion of the Orai1 sequence into the vector. The forward primer used was 5'-ATATCTCGAGACCATGCATCCG-3'; XhoI, and the reverse primer was 5'-ATATGGATCCCTAGGCATAGTGGCTGCCGGG-3'BamHI. The amplified PCR fragment and the cut vector were generated through digested with XhoI/BamHI and the fragments were ligated using standard methods.

2.2.9 Orai1-YC and Orai1-YN

The Orai1 sequence was amplified from mCherry-Orai1 by PCR and inserted in frame into the YFP-YC or YFP-YN vectors (Haynes et al., 2007) to generate mammalian expression constructs for Orai1, N-terminally tagged with the C-terminal or N-terminal fragments of the EYFP protein. The PCR primers contained restriction endonuclease sites (underlined) to facilitate insertion of the Orai1 sequence into the vectors. The forward primer used was 5'-ATATCTCGAGATGCATCCGGAGCCCGCC-3'; XhoI, and the reverse primer was 5'-ATATCCGCGGGGCATAGTGGCTGCC-3'; SacII. The amplified PCR product and the vector were digested with XhoI/SacII and the digested products were ligated using standard methods.

2.2.10 STIM1-YN

The full length STIM1 sequence was amplified from STIM1-EYFP by PCR and inserted in frame into the YFP-YN vector to generate a mammalian expression construct for STIM1, N-terminally tagged with the N-terminal fragment of the EYFP protein. The PCR primers contained restriction endonuclease sites (underlined) to facilitate insertion of the STIM1 sequence into the vector. The forward primer used was that described in section 2.2.5 (HindIII) and the reverse primer was 5'-ATATCCGCGGCTTCTTAAGAGGCTT-3'; SacII. The amplified PCR sequence and vector were digested with HindIII/SacII and ligated using standard methods.

2.2.11 STIM1-CT-YN

The C-terminal domain sequence of STIM1 was amplified from STIM1-EYFP by PCR and inserted in frame into the YFP-YN vector to generate a mammalian expression construct for STIM1-CT, N-terminally tagged with the N-terminal fragment of the EYFP protein. The PCR primers used are those described in section 2.2.6. The resulting PCR product and vector were digested with HindIII/SacII and ligated using standard methods.

2.2.12 Golli-BG21-mCherry

The Golli sequence was amplified from a Golli-BG21 sequence-verified cDNA clone (Origene, Cambridge, UK; Cat No. MC205552) by PCR and inserted in frame into the pmCherry-N1 vector to generate a mammalian expression construct for Golli, C-terminally tagged with mCherry. The PCR primers contained restriction endonuclease sites (underlined) to facilitate insertion of the Golli sequence into the vector. The forward primer used was 5'- ATAT<u>CTCGAG</u>ATGGGAAACCACTCTGGA -3'; XhoI, and the reverse primer was 5'- ATAT<u>CCGCGG</u>CGGCTCGGAGCTCACCTT-3'; SacII. The amplified PCR fragment and the cut vector were generated through digestion with XhoI/SacII and the resulting fragments were ligated using standard methods.

2.2.13 Golli-BG21-YC

The Golli sequence was amplified from Golli-mCherry by PCR and inserted in frame into the YFP-YC vector to generate a mammalian expression construct for Golli, N-terminally tagged with the C-terminal fragment of EYFP. The PCR primers contained

restriction endonuclease sites (underlined) to facilitate insertion of the Golli sequence into the vector. The forward primer used was 5'-ATATCTCGAGATGGGAAACCACTCTGGA-3'; XhoI, and the reverse primer was 5'-ATATCCGCGGCGGCTCGGAGCTCACCTT-3'; SacII. The amplified PCR fragment and the cut vector were generated through digestion with XhoI/SacII and the resulting fragments were ligated using standard methods.

2.2.14 mCherry-Rit1

The C-terminal polybasic tail of the Rit1 protein (nucleotides 770 – 847) was amplified from the Rit1-EYFP construct (Walsh et al., 2010) by PCR and inserted in frame into the pmCherry-C1 vector to generate a mammalian expression construct for Rit1, N-terminally tagged with mCherry. The PCR primers contained restriction endonuclease sites (underlined) to facilitate insertion of the Rit1 tail sequence into the vector. The forward primer used was 5'-ATATAAGCTTTAAAAAAATCTAAGCCCAAAAAC-3'; HindIII, and the reverse primer was 5'-ATATCCGCGGTCAAGTTACTGAATCTTTCTTCTTC-3'; SacII. The amplified PCR fragment and the cut vector were generated through digestion with HindIII/SacII and the resulting fragments were ligated using standard methods.

2.2.15 STIM2-EYFP

The human STIM2 sequence was amplified from a sequence verified EST clone (clone ID: HU4 p940D1212D; ImaGenes GmbH, Berlin, Germany) by PCR and inserted in frame into the pEYFP-N1 vector to generate a mammalian expression construct for STIM2, C-terminally tagged with EYFP. The PCR primers contained

restriction endonuclease sites (underlined) to facilitate insertion of the STIM2 sequence into the vector. The forward primer used was 5'-ATATGTCGACCATGTTGCTGGTGCTCGGGCTGCTGGTA-3'; SalI, and the reverse primer was 5'-ATATACCGGTACTTAGATTTCTTCTTAAAAAGGCT-3'; AgeI. The digested PCR fragment and vector were generated through digestion with SalI/AgeI and the resulting fragments were ligated using standard methods.

2.2.16 STIM2-mCherry

The STIM2 sequence was amplified using the template and primers described in section 2.2.14 to facilitate insertion of the STIM2 sequence into the pmCherry-N1 vector to create a mammalian expression construct for STIM2, C-terminally tagged with mCherry. The PCR fragment and vector were digested with SalI/AgeI and ligated using standard methods.

2.2.17 DNA sequencing

Sequences which had been cloned into plasmids were verified by automatic sequencing carried out by "The Sequencing Service" (Dundee, UK).

2.2.18 Other plasmids

Plasmid	Reference
pGEX-6-P1	Clontech, Basingstoke, UK
pEYFP-N1	Clontech, Basingstoke, UK
pmCherry-C1	Clontech, Basingstoke, UK
pmCherry-N1	Clontech, Basingstoke, UK
pcDNA3.1 (-)	Invitrogen, Paisley, UK
YFP-YC	(Haynes et al., 2007)
YFP-YN	(Haynes et al., 2007)
STIM1-EYFP	(Chvanov et al., 2008)
STIM1-mCherry	As STIM1-EYFP in (Chvanov et al., 2008)
STIM1-CFP	
mCherry-Orai1	As STIM1-EYFP in (Chvanov et al., 2008)
GFP-PH-FAPPI	(Chvanov et al., 2008)
Golli peptide AA 1-133-GFP	(Levine and Munro, 2002)
Golli-J37-GFP	Kind gift from Prof A. Campagnoni, LA
Golli-BG21-GFP	Kind gift from Prof A. Campagnoni, LA
EYFP-Rit1	Kind gift from Dr T. Balla, Bethesda, MD
PM-FRB-CFP	(Walsh et al., 2010)
PM-FRB-RFP	Kind gift from Dr T Balla, Bethesda, MD
RFP-5-Ptase-domain	Kind gift from Dr T Balla, Bethesda, MD
GFP-PH-PLC$_\delta$	Clontech, Basingstoke, UK
pGADT7	Clontech, Basingstoke, UK
pGBKT7	Clontech, Basingstoke, UK

Table 2.1 Other plasmids used in this study. The source of each plasmid is listed in the right hand panel.

2.3 Cell culture and transfection

Cell culture reagents were purchased from Invitrogen, except for RPMI-1640 which was purchased from Cambrex (Nottingham, UK) and GeneJuice which was purchased from Merck Biosciences (Darmstadt, Germany). All cell lines were grown in suspension in 75 cm^2 culture flasks at 37^oC in 5% CO_2. The RAMA37 cell line was maintained in Dulbecco's modified Eagle's medium (DMEM) supplemented with 10% Foetal Bovine Serum (FBS), 1% Penicillin and Streptomycin, L-Glutamine, Hydrocortisone (50 ng/ml) and Insulin (50 ng/ml). PANC1 cells were maintained in RPMI-1640 containing 10% Foetal Bovine Serum and 1% Penicillin and Streptomycin. HeLa cells were grown in DMEM containing 5% FBS, 1% non-essential amino acids and 1% Penicillin and Streptomycin.

24 hours prior to transfection, HeLa cells for immunocytochemistry were seeded onto glass coverslips in a 24-well plate at ~50,000 cells per well in 1 ml supplemented media (as above). For live cell imaging, ~100,000 cells were plated onto glass bottom dishes (MatTek Corporation, Massachusetts, USA) in a total of 2 ml supplemented media. In each case, cells became adherent following overnight incubation at 37^oC, 5% CO_2. Transfection of all cell lines was carried out using the same protocol. For the transfection of HeLa cells in 24-well plates, the transfection mixture contained 1 µg of plasmid(s) of interest supplemented with 3 µl GeneJuice and made up to 50 µl/well with DMEM. The reaction mixture was incubated at room temperature for 20 minutes in order for the lipid and DNA complexes to associate, before being added drop-wise to the cells. Cells were maintained for 24 hours following transfection before fixation and staining. For the transfection of live

cells, 3 µg of plasmid(s) of interest was supplemented with 8µl Genejuice in a total of 100 µl/dish with the appropriate unsupplemented media. The reaction mixture was incubated for 20 minutes at room temperature following which it was added drop-wise to the cells. Cells were incubated for a further 24 – 48 hours before imaging.

2.4 Immunocytochemistry

HeLa cells on coverslips were washed twice in phosphate buffered saline (PBS; 137 mM NaCl, 2.7 mM KCl, 10 mM Na_2HPO_4, 2 mM NaH_2PO_4) and fixed in 0.5 ml 4% paraformaldehyde in PBS for 30 minutes at room temperature. For anti-His_6 staining, cells were blocked in PBS containing 3% (w/v) BSA for 30 minutes prior to the addition of primary antibody. For all other antibodies, cells were blocked and permeabilised in PBT (PBS, 0.1% Triton X-100, 0.3% BSA) at room temperature for 30 minutes prior to immunostaining. Cells were then immunostained by incubation with primary antibody in PBT at room temperature for 2 hours. Unbound antibody was removed by washing three times with PBT and the coverslips were then exposed to an appropriate DyLight649 secondary antibody (Pierce Biotechnology, Northumberland, UK) diluted to 1 in 250 with PBT. Cells were washed a further three times in PBT. The coverslips were dried, mounted onto glass slides using Prolong gold antifade mounting reagent (Invitrogen) and left to set for at least 24 hours before imaging. The following table shows the specific primary and secondary antibodies used for experiments in the figures in this study:

Figure	Primary Antibody	Dilution	Secondary Antibody
3.8	anti-αtubulin	1:1000	Dylight649 anti-mouse
3.9	anti-αSNAP	1:500	Dylight649 anti-mouse
3.11; 3.12	anti-His_6	1:1000	DyLight649 anti-mouse

Table 2.2 Antibodies used for immunocytochemistry

The anti-α-tubulin and anti-His_6 antibodies were purchased from Sigma (Dorset, England), and the anti-αSNAP antibody was from Synaptic Systems (Clone C1 77.2; Gothingen, Germany).

2.5 Confocal Microscopy

2.5.1 Fixed cell imaging

Imaging of fixed cells was carried out on a Leica AOBS SP2 microscope (Leica Microsystems AG, Wetzlar, Germany) equipped with a 63x oil immersion objective with a 1.4 numerical aperture and in most cases the pinhole was set to airy1. Images of STIM1-EYFP were obtained with 514 nm excitation light and emission fluorescence selected with a 520-595 nm bandpass filter. For excitation of DyLight 649, a 633 nm excitation laser line was used and light was collected at 660 – 800 nm.

2.5.2 Live cell imaging

Live cell imaging was performed using a Leica AOBS SP2 microscope equipped with a 63x oil immersion objective with a 1.4 numerical aperture and a 63x water objective with a 1.2 numerical aperture. Cells were maintained at room

temperature throughout each experiment. The wavelengths used for excitation of fluorophores and the emission ranges collected are listed for different combinations of fluorophores in Table 2.3 below.

Fluorophores	Excitation wavelengths (nm)	Emission specta (nm)
Cerulean alone	405	460-492
ECFP alone	405	450-500
EGFP alone	488	490-525
EYFP alone	514	520-580
Fluo4 alone	488	495-545
mRFP or mCherry alone	594	610-730
ECFP & RFP/mCherry	405 594	450-530 610-730
EGFP & EYFP	476 514	490-505 580-615
EGFP & RFP/mCherry	488 594	490-510 610-730
EYFP & RFP/mCherry	514 594	520-560 610-730
Fluo4 & RFP/mCherry	488 594	495-545 710-730
Cerulean & EYFP & RFP/mCherry	405 514 594	460-490 520-560 610-730
EYFP & Dylight649	514 633	520-595 660-800

Table 2.3 Fluorophores used in live cell imaging and the excitation and emission wavelengths used.

2.5.3 Anti-His_6 antibody staining of live cells

In order to determine whether STIM1 inserts into the plasma membrane following translocation, thereby exposing its N-terminus at the cell surface, HeLa cells were

transfected with a STIM1-EYFP containing an N-terminal tag of 6 consecutive histidine residues (His_6). Antibody staining was carried out to determine whether this tag became exposed on the cell surface following store-depletion induced translocation of His_6-STIM1-EYFP. Cells were maintained in sodium hepes (NaCl 140 mM, KCl 4.7 mM, $MgCl_2$ 1.13 mM, Hepes 10 mM, glucose 10 mM) containing 2 mM Ca^{2+}. To deplete intracellular stores, cells were treated with 2 µM thapsigargin (Calbiochem, San Diego, California, USA) for 10 minutes. Control cells were kept in sodium hepes only for 10 minutes. Cells were then incubated with 500 µl of a 1 in 40 dilution of mouse monoclonal anti-His_6 primary antibody (Sigma) for 15 minutes, washed with 6 ml of Sodium Hepes and incubated with a 1 in 200 dilution of DyLight649 secondary antibody for 15 minutes. Cells were washed with a further 6 ml Sodium Hepes before being imaged.

2.5.4 ATP depletion of live cells

To examine whether ATP depletion inhibits the translocation of STIM1 to the plasma membrane, HeLa Cells overexpressing STIM1-EYFP alone or in combination with mCherry-Orai1 or GFP-PH-PLC_δ, were washed three times in Sodium Hepes and mounted in a perfusion chamber on the stage of an inverted microscope. During experiments a gravity-fed perfusion system was used to exchange extracellular solutions. To induce ATP depletion cells were perfused with a combination of 5µM Oligomycin (Calbiochem) and 2mM Iodoacetate (Sigma) or 5µM Oligomycin and 10mM 2-Deoxy-D-glucose (Sigma). In experiments using 2-Deoxy-D-glucose, normal glucose was omitted from the extracellular solution. In

some cases in cells expressing GFP-PH-PLC$_\delta$, cells were pretreated with 20 µM wortmannin before perfusion with ATP inhibitors.

2.5.5 Lipid Kinase Inhibition

Several methods were used to inhibit lipid kinases for the depletion of various phosphoinositide species in this study. To inhibit PI3 kinase alone, cells were treated with 50 µM LY294002 (Calbiochem) for 10 minutes. To simultaneously inhibit PI3 kinase and PI4 kinase, cells were treated with either 300 µM LY294002 for 10 minutes or with 20 µM wortmannin (Calbiochem) for 30 minutes. To specifically deplete PtdIns(4,5)P_2 a previously described rapamycin inducible 5-phosphatase system was used (Korzeniowski et al., 2009). For this, cells were cotransfected with PM-FRB-CFP or PM-FRB-RFP and the cytosolic 5-ptase-RFP. Cells were treated with 1 µM rapamycin (Calbiochem) for 2 minutes to activate the 5-phosphatase.

2.5.6 Quantification of fluorescence distribution

In order to quantify the effects of phosphoinositide depletion on the peripheral distribution of mCherry-Rit1 or GFP-PH-PLC$_\delta$ fluorescence, the following means of quantification was used. Regions of interest were drawn around the outside of each cell, immediately beneath the cell periphery (~1 µm in from the cell periphery), and also around the nucleus in cells where nuclear fluorescence was observed. Peripheral fluorescence was calculated by subtraction of the cytoplasmic fluorescence from the outer region of interest. In cases where nuclear fluorescence was observed, cytosolic fluorescence was calculated by subtraction of nuclear

fluorescence. Ratios of peripheral to cytosolic fluorescence were calculated on the basis of the mean fluorescence per pixel in the respective regions rather than total fluorescence to eliminate any variations in the data arising from the size of the selected regions of interest. In cells expressing GFP-FAPPI, regions of interest around the fluorescence observed at the Golgi were drawn and quantified as average fluorescence intensity per pixel.

2.5.7 Quantification of STIM1 puncta

STIM1 puncta, induced by store depletion, were counted under various conditions where phosphatidyl inositide species were depleted. Cells were cotransfected with STIM1-EYFP and PM-FRB-RFP/RFP-5-ptase-domain or with STIM1-EYFP, PM-FRB-RFP/RFP-5-ptase-domain and Cerulean-Orai1, and preincubated with various combinations of lipid kinase inhibitors as described in section 2.5.5. Cells were then treated with 2 µM thapsigargin for 10 minutes. Control cells overexpressing STIM1-EYFP alone were treated with thapsigargin alone for 10 minutes. For quantification of STIM1-EYFP puncta formation, the puncta were selected as spots of high fluorescence intensity ranging from approximately 0.5 – 1.0 µm in diameter and counted blindly. Accuracy of puncta quantification was verified by independent blind counting.

2.5.8 Image analysis

All Images were processed using the CorelDraw software package (Corel Corporation, Ottawa, Canada) or ImageJ Java-based imaging software (NIH, USA).

2.5.9 Calcium influx measurements

To measure changes in intracellular Ca^{2+} ($[Ca^{2+}]_i$), HeLa cells were loaded with 5 µM of the cytosolic Ca^{2+} indicator, Fluo-4 AM (Molecular Probes, Paisley UK) for 30 minutes at room temperature. Cells were was three times in Calcium free Sodium Hepes buffer and mounted in a perfusion chamber on the stage of an inverted Leica AOBS SP2 confocal microscope. During experiments a gravity-fed perfusion system was used to exchange extracellular solutions. Fluo-4 was excited using a 488 nm laser and emission fluorescence was collected between 495-545 nm. To allow for comparison between different cells from different experiments, Fluo-4 fluorescence measurements for each cell were calculated as the ratio of the fluorescence at the first time point and to eliminate variability between experiments in the resting fluorescence level these values are shown as F/F0 normalised to the peak ratio for the control cells in each experiment.

2.5.10 Bimolecular fluorescence complementation (BiFC) Assays

HeLa cells were transfected with Golli-YC, STIM1-CT-YN, full length STIM1-YN and Orai1-YC or Orai1-YN BiFC constructs either alone or in complementary combinations. For further control experiments, each of these constructs was transfected in HeLa cells along with the complementary empty BiFC vector (YFP-YC and YFP-YN), or with both YFP-YC and YFP-YN alone. Cells were treated with thapsigargin (2 µM) or histamine (100 µM) in the presence of 2 mM external Ca^{2+} for 60-90 minutes at room temperature before imaging. The EYFP emission spectra profiles were generated by performing Lambda scans in transfected cells between 510-580 nm, and each scan collected emitted light from within a 10 nm range.

Emission fluorescence values were calculated as the ratio of the fluorescence to the peak fluorescence value in each experiment.

2.6 Production of GST-fusion proteins

GST, GST-Orai1-CT, GST-Orai1-NT, GST-Golli and GST-STIM1-CT proteins were expressed and purified according to standard procedures. Briefly, BL21 *E. coli* (Stratagene, Cheshire, UK) were transformed with the GST construct of interest. A single transformed colony was picked and grown overnight in 100 ml superbroth (0.5% NaCl, 1.5% w/v Tryptone, 2.5% w/v Yeast Extract) containing ampicillin (100 μg/ml). This culture was added to a further 900 ml superbroth plus ampicillin and grown for 1.5 hours. GST-fusion protein expression was induced with 1 mM isopropyl-1-thio-β-D-galactopyranoside (IPTG) for 3 hours. Bacteria were harvested by centrifugation at 4000 g at 4^{o}C for 20 minutes. Pellets were resuspended in ice cold breaking buffer (KCl 500 mM, Hepes 100 mM,. ATP 5 mM, $MgCl_2$ 5 mM, β-mercaptoethanol 2 mM, pH 7.0) containing protease inhibitors (PMSF 1mM, Leupeptin 50 μM, Pepstatin A 1 μM) and frozen at -80^{o}C overnight. Cell suspensions were thawed and incubated with 1 mg/ml Lysozyme on ice for 30 minutes. Cells were disrupted further by sonication and incubated for 15 minutes on ice with DNaseI (2 μg/ml). The lysed samples were then passed through a sterile needle several times to reduce viscosity and subjected to centrifugation at 30,000 rpm and 4^{o}C for 1 hour. The supernatant containing GST-fusion protein was added to washed glutathione cellulose beads (Bioline, London, UK) and incubated at 4^{o}C for 1 hour with agitation. The beads were pelleted by centrifugation at 1000 rpm for 1 minute and the supernatant containing unbound proteins was removed. The beads

were washed three times in ice cold breaking buffer. The GST-fusion protein was eluted in three 1 ml volumes of GST-elution buffer (65 mM Tris base (Sigma) and 10 mM reduced glutathione (Sigma), pH 8.0). For each elution, 1 ml elution buffer was added to the beads and incubated for 10 minutes at 4^{o}C with agitation, after which the beads were sedimented by centrifugation at 1000 rpm for 1 minute. The purified GST-fusion protein in the supernatant was kept and stored at -80^{o}C.

2.7 SDS-PAGE and Western Blotting

Proteins samples were lysed in 2x SDS laemmli buffer (Sigma), boiled for 5 minutes and loaded onto a 12.5% SDS-PAGE gel or a 4-12% Novex pre-cast gel (Invitrogen). 10 µl SeeBlue Plus 2 Prestained Standard molecular weight protein markers (Invitrogen) was loaded alongside each set of protein samples. Protein gels were run at 140 mV for approx 90 minutes using the Mini-Protean 3 electrophoresis system (BioRad, Hertfordshire, UK). Gels were then stained with Coomassie blue protein stain for 30 minutes, or transferred to nitrocellulose membranes. Membranes were stained in Ponceau-S solution (Sigma) for 1 minute to visualise successful protein transfer and subsequently washed with distilled water and twice with PBS to remove the stain. Membranes were placed in blocking buffer (PBS containing 3% milk powder) for 1 hour, followed by incubation in primary antibody for 1 – 2 hours. Primary antibodies were made up in PBS containing 3% milk powder to the following concentrations: anti-Myelin basic protein (rat) 1 in 100 (Santa Cruz Biotechnology, Middlesex, UK) or anti-STIM1-CT (rabbit) 1 in 1000 (ProSci Incorporated, Poway, California,USA). The membranes were washed three times in PBS and incubated with the appropriate secondary antibody conjugated to

horseradish peroxidise (HRP; Sigma) at a concentration of 1 in 400 in PBS containing 5% milk powder and 0.05% Tween-20. Membranes were subsequently washed once in PBS containing 0.05% Tween-20 and twice in PBS. The membranes were incubated in ECL Plus Western Blotting Detection Reagents (GE Healthcare, Buckinghamshire, UK) for ~2 minutes before being imaged on a ChemiDoc XRS System (BioRad).

2.8 Pull Down Assays

1 µM of each of the GST, GST-Orai1-CT, GST-Orai1-NT and GST-STIM1-CT proteins was bound to 250 µl washed glutathione cellulose beads in breaking buffer for 1 hour at 4^{o}C. The bound proteins were washed with breaking buffer and incubated with 1 ml cytosolic bovine brain extract (a kind gift from Dr. Lee Haynes, Liverpool, UK) for 2 hours. The cytosolic extract had been previously dialysed against Binding Buffer (20 mM Hepes, 150 mM NaCl, 1 mM DTT, 1 mM $MgCl_2$, 1 mM ATP, 0.05% Triton, pH 7.4) overnight at 4^{o}C. The beads were then washed three times in binding buffer and boiled at 95-100^{o}C in 250 µl SDS lysis buffer for 5 minutes. These samples were then separated on SDS-PAGE gels and stained with Coomassie Brilliant blue for Mass Spec processing or transferred to nitrocellulose membrane for Western blotting to visualise the proteins present in the samples.

2.9 Maldi-ToF Mass Spectrometry (MS)

Bands for analysis by mass spectrometry were excised from the gel and subjected to standard in-gel de-staining, reduction, alkylation, trypsinolysis and de-salting procedures. Briefly, gel slices were de-stained in 50 mM Ambic/50% Acetonitrile at

37°C for 10 minutes. Slices were reduced in 10 M DTT in 100 mM Ambic at 37°C for 30 minutes, and alkylated by incubation with 5 mM Iodoacetamide in 100mM Ambic at 37°C for 30 minutes. Slices were dehydrated in 100% Acetonitrile at 37°C for 15 minutes. The solvent was removed and slices were left at 37°C for 10 minutes to dry. Proteins were digested by incubation with sequencing grade Trypsin (0.01 µg/ul; Roche, West Sussex, UK) in 50 mM Ambic at 37°C overnight. The reaction was stopped by addition of formic acid. Samples were then desalted using ZipTips (Millipore, Massachusetts, USA). The resulting digested proteins were analysed by MALDI-ToF Mass Spectrometry. The spectra generated were mass-calibrated using known standards and the peaks de-isotoped. Databases were searched with the masses obtained using the MASCOT search database and a 150 ppm mass tolerance window.

2.10 PreScission cleavage of GST-STIM1-CT

It was necessary to remove the GST tag from GST-STIM1-CT for use in binding assays. In order to do this, 2 mg purified GST-STIM1-CT was diluted into 6 ml PreScission buffer (50 mM Tris-HCl, 150 mM NaCl, 1 mM EDTA, 1 mM DTT) and centrifuged at 4000 x g for approximately 1 hour in a vivaspin protein concentrator to concentrate the protein into a total of 1 ml PreScission buffer. All of the concentrated protein was incubated with 500 µl glutathione cellulose beads and 50 µl PreScission protease overnight at 4^{o}C with agitation to allow for the cleavage of the GST tag by the protease. The beads were then pelleted by centrifugation at 13000 rpm for 1 minute and the supernatant containing the cleaved STIM1-CT protein was taken and stored at -80^{o}C.

2.11 Recombinant GST-Golli/STIM1-CT Binding Assays

2 µM GST control protein in breaking buffer or 500 µl protein supernatant containing GST-Golli was incubated with 200 µl glutathione cellulose beads at 4^{o}C for 1 hour with agitation. The beads were washed three times with breaking buffer and incubated with 2 µM PreScission-cleaved STIM1-CT protein (2 µM) in a total volume of 500 µl breaking buffer for 1 hour at 4^{o}C with agitation. The beads were washed three times with breaking buffer and lysed in 200 µl 2x SDS laemmli buffer.

2.12 Yeast 2-Hybrid Screens

1.12.1 Yeast strains

All yeast strains and the Yeast 2-hybrid Matchmaker™ Pretransformed normalised cDNA library were purchased from Clontech. The yeast strain AH109 (Mata, trp1-901, leu2-3, 112, ura3-52, his3-200, gal4Δ, gal80Δ, LYS2::GAL1-HIS3 GAL2-ADE2 URA3::MEL1-LacZ) was used as the bait strain for all yeast 2-hybrid experiments. AH109 carries 4 independent reporter genes which are recognised and bound by the GAL4 binding domain (GAL1-HIS3, GAL2-ADE2, MEL1-LacZ and MEL1). The yeast strain Y187 (Matα, ura3-52, his3-200, ade2-101, trp1-901, leu2-3, 112, gal4Δ, gal80Δ, URA3::GAL1-LacZ, MEL1) was used as the prey strain for all yeast 2-hybrid experiments and carries 2 independent GAL4-responsive reporter genes (GAL1-LacZ and MEL1).

1.12.2 Yeast plasmids

In vivo gap repair recombination cloning (Oldenburg et al., 1997) was used to insert the gene of interest into the Clontech pGADT7 (prey) or pGBKT7 (bait) reporter

vectors (a gift from Prof Chris Sanderson, University of Liverpool, UK) for use in yeast 2-hybrid screens or directed mating experiments. In this method, bait or prey sequences amplified by PCR contain 3'- and 5'-flanking regions which are homologous to the sequences in the reporter vector and the PCR products are used as a template to repair the double strand break in a BamHI-linearised vector via the yeast homologous recombination pathway. The primers for the construction of recombinant yeast plasmids are listed in Table 2.4.

Bait constructs	**Primers**
pGBKT7-STIM1-CT	Fwd: 5'-CTGCATATGGCCATGGAGGCCGAATTCCCGGGGATCCAGAACCGTTACTCCAAGGAG-3' Rev: 5'-GGTTATGCTAGTTATGCGGCCGCTGCAGGTCGAGCCTACTTCTTAAGAGGCTTCTTAAAG-3'
pGBKT7-Orai1-CT	Fwd: 5'-CTGCATATGGCCATGGAGGCCGAATTCCCGGGGGCCGTCCACTTCTACCGCTCACTG-3' Rev: 5'-GGTTATGCTAGTTATGCGGCCGCTGCAGGTCGAGCATGGGCCTAGGCATAGTGGCT-3'
pGBKT7-Orai1-NT	Fwd: 5'-CTGCATATGGCCATGGAGGCCGAATTCCCGGGGATGCATCCGGAGCCCGCCCCGCCCCCGA-3' Rev: 5'-GGTTATGCTAGTTATGCGGCCGCTGCAGGTCGAGCAAGCTTGGCGCGGCTCTTGTA-3'
Prey constructs	
pGADT7-Golli	Fwd: 5'-GAATTCCACCCGGGTGGGCATCGATACGGGATGGGAAACCACTCTGGA-3' Rev: 5'-CTACGATTCATCTGCAGCTCGAGCTCGATGCGGCTCGGAGCTCACCTT-3'
pGADT7-Orai1-CT	Fwd: 5'-GAATTCCACCCGGGTGGGCATCGATACGGGGCCGTCCACTTCTACCGCTCCTG-3' Rev: 5'-CTACGATTCATCTGCAGCTCGAGCTCGATGATGGGCCTAGGCATAGTGGCT-3'
pGADT7-Orai1-NT	Fwd: 5'-GAATTCCACCCGGGTGGGCATCGATACGGGATGCATCCGGAGCCCGCCCCGCCCCCGA-3' Rev: 5'-CTACGATTCATCTGCAGCTCGAGCTCGATGAAGCTTGGCGCGGCTCTTGTA-3'

Table 2.4 Yeast 2-Hybrid plasmids. The plasmid constructs and primers used for yeast 2-hybrid studies are listed. The flanking sequences within the primers required for homologous recombination are underlined. These sequences flank the BamHI restriction site within each of the vectors.

1.12.3 Yeast media

The various selective media used for yeast 2-hybrid studies will be discussed in detail in Chapter 6. A brief description of the media used along with the media recipes are listed in the tables below. For all recipes, 15 g/L agar could be added to make solid media.

YPAD (L)	Synthetic Defined (SD)-X (L)
20 g D-glucose 20 g Peptone 10 g Yeast Extract 100 mg Adenine Hemisulfate 15 g Agar (for solid medium)	10 g D-glucose 6.7 g Yeast Nitrogen Base (without amino acids) Appropriate amount of amino acid mix (Table 2.6) 10 g Agar (for solid medium)

Table 2.5 Recipes for yeast media. Media was autoclaved before use.

A/H/L/W/U Dropout (DO)	
	Grams
Arginine	2
Isoleucine	3
Lysine	3
Methionine	2
Phenylainine	5
Threonine	20
Tyrosine	3
Valine	15

Table 2.6 Dropout (DO) amino acid mix. This was added to SD-X media and then supplemented with the appropriate amino acids to make the selective media required.

	SD-X						
	-W	**-L**	**-WL**	**-WLA**	**-WLH**	**-WAH**	**-LAH**
Adenine hemisulfate	0.2	0.2	0.2		0.2		
Histidine	0.2	0.2	0.2	0.2			
Leucine	1.0					1.0	
Tryptophan	-	0.2					0.2
Uracil	0.2	0.2	0.2	0.2	0.2	0.2	0.2
A/H/L/W/U DO	5.3	5.3	5.3	5.3	5.3	5.3	5.3
Total (g/L of SD)	**0.69**	**0.61**	**0.59**	**0.57**	**0.57**	**0.57**	**0.57**

Table 2.7 SD-X amino acid supplement mixes for selective yeast media.

Media	Description	Application
YPAD	Nutrient rich media	Routine growth of yeast
SD-U	SD media deficient in tryptophan	Bait pGBKT7 selection
SD-L	SD media deficient in leucine	Prey and Library pGADT7 selection
SD-WL	Deficient in tryptophan and leucine	Double selection to select diploid yeast after mating
SD-WAH(AT)	Deficient in tryptophan, adenine and histidine and supplemented with 3-AT	To test for autoactivation of bait constructs
SD-LAH(AT)	Deficient in leucine, adenine and histidine and supplemented with 3-AT	To test for autoactivation of prey constructs
SD-WLA	Deficient in tryptophan, leucine and adenine	Highly stringent selection for interacting partners
SD-WLH(AT)	Deficient in tryptophan, leucine and histidine and supplemented with 3-AT	Triple selection for interacting partners

Table 2.8 Description of yeast media used and their applications in this study

2.12.4 Yeast transformations and gap repair of bait and prey constructs

2 ml YPAD was inoculated with a single colony of haploid AH109 or Y187 yeast strains and incubated at 30^{o}C overnight with shaking at 220 rpm. The following morning, 8 ml YPAD media was added to the culture and incubated at 30^{o}C for a further 5 hours after which cells were sedimented by centrifugation at 2300 rpm for 5 minutes and resuspended in 5 ml 100 mM lithium acetate. 1.5 ml resuspended cells was pelleted by centrifugation at 2300rpm. The supernatant was discarded

and cells were resuspended in Transformation buffer (230 µl 50% PEG-3350, 1M lithium acetate and 55 µl distilled water). For each transformation, 32 µl transformation mixture was added to a PCR tube along with ~100 ng linearised vector and 4 µl PCR product. The transformation mixtures were incubated at 30^{o}C for 30 minutes before subjection to a 42^{o}C heat shock for 25 minutes. Cells were incubated at 30^{o}C for a further minute. The mixtures were spead onto synthetic defined (SD) agar plates and lacking tryptophan (for baits in pGBKT7) or leucine (for preys in pGADT7) and incubated at 30^{o}C for 3 days after which selected colonies were checked for the presence of the appropriate bait or prey construct by PCR. The selected colonies were resuspended in 15 µl sterile distilled water and 3 µl of each suspension was spotted onto selective agar plates to test for autoactivation of the bait and prey constructs (see Table 2.6 for a description of media for autoactivation) and incubated at 30^{o}C for 10 days. If haploid yeast colonies grew on the triple dropout selective plates, these colonies were considered as autoactivators. Only non-autoactivating colonies were used in further mating experiments.

2.12.5 Yeast 2-Hybrid Library Screens

For each library screen, two colonies of AH109 yeast pretransformed with the bait construct of interest were each used to inoculate SD-W media and grown overnight at 30^{o}C and 220 rpm to an OD_{600} of 0.8. The cultures were pelleted by centrifugation at 2300 rpm for 5 minutes and the pellets were pooled in a total of 1 ml YPAD broth. For each bait construct, 1 ml of the Matchmaker™ pretransformed library was thawed on ice and added directly to the bait suspension. The mixture

was vortexed very well and the whole suspension was spread onto a 15 cm^2 YPAD agar plate for 7 hours. Following this, 5 ml sterile distilled water was added to the plate and the mated yeast were detached using a spreader and collected. 400 µl mated yeast suspension was spread onto 14-16 SD-WLA agar plates and incubated for 7 days at 30^oC to select for interacting partners. 10 µl of the mated suspension was diluted 1 in 1000 in a total of 1 ml sterile distilled water and 100 µl of this was spread onto a 90 mm SD-WL agar plate and incubated at 30^oC for 3 days after which time diploid yeast colonies which grew were counted to determine the mating efficiency. After 7 days, up to 96 yeast colonies were picked from the SD-WLA plates onto a fresh SD-WLA agar plate in an 8 x 12 format and incubated at 30^oC for 3 days. Prey inserts from the resulting colonies were amplified by PCR using the *Matchmaker* AD LD-Insert Screening Amplimer Set (Clontech).

2.12.6 Reconfirmation of library screens

To reconfirm that preys interacted with the bait and did not autoactivate in diploid yeast, the PCR products from the library prey constructs described in section 2.13.4 were cloned by *in vivo* gap repair recombination back into the pGADT7 prey vector into Matα yeast. These "rescued" preys were then mated with the bait construct of interest or an empty pGBKT7 bait vector. Rescued prey were spotted onto SD-L agar plates and incubated at 30^oC for 3 days. The yeast spots were replicated onto two YPAD plates using a sterilised velvet cloth. A bait colony was resuspended in 250 µl sterile distilled water and 2 µl was spotted on top of each prey spot on one YPAD plate. On the second YPAD plate, 2 µl yeast suspension transformed with empty bait vector was spotted onto the preys. The YPAD plates were incubated at 30^oC for

24 hours after which each plate was replicated onto both an SD-WLA and an SD-WLH plate and incubated at 30^{o}C for up to 2 weeks. After this time, colonies that produced a growth phenotype on the triple selection plates that do not grow on the mated control triple selection plates were considered as real interacting partners and the prey constructs were sent for DNA sequencing as described in section 2.2.16.

2.12.7 Directed Yeast Mating

Prey transformed Matα yeast colonies were resuspended in 50 µl sterile distilled water and 2 µl was spotted onto a YPAD plate in triplicate. Bait transformed yeast colonies were resuspended in 50 µl sterile distilled water and 2 µl was spotted onto the prey colonies so that each mating was carried out in triplicate. YPAD plates were left to dry at room temperature and incubated at 30^{o}C for 24 hours. The following day, YPAD plates were replicated onto SD-WL plates using a sterilised velvet cloth to select for diploid yeast. Plates were incubated at 30^{o}C for 4 days following which the diploid yeast colonies were replicated onto SD-WLA and SD-WLH(AT) plates containing 4 mg/ml X-α-GAL (Clontech) using a sterile velvet cloth. These plates were incubated for 5-7 days. A blue growth phenotype indicated positive interactions.

CHAPTER THREE

Characterisation of STIM1 translocation

3.1 Introduction

STIM1 is an ER Ca^{2+} sensing protein that is essential for the activation of SOCs following Ca^{2+} release from the ER. In resting cells, STIM1 resides in the ER but upon store depletion translocates in aggregates called "puncta" to ER-PM junctions to activate SOCs. It is possible that STIM1 may either associate with the plasma membrane in ER-PM junctions or insert into the plasma membrane following translocation. Experiments using an N-terminally YFP-labelled STIM1 failed to detect fluorescence at the cell surface and TIRF microscopy revealed that STIM1 puncta are not within the plasma membrane but are in close proximity, within 100 nm, of the membrane (Liou et al., 2005). A study using fluorescence quenching and electron microscopy (EM) analysis demonstrated that STIM1 accumulates in distinct subregions of junctional ER within 10-25 nm of the plasma membrane (Wu et al., 2006a). Furthermore, STIM1 constructs which fail to insert into the plasma membrane can still activate SOCs (Hauser and Tsien, 2007; Liou et al., 2005; Mercer et al., 2006; Wu et al., 2006a). These observations suggest that STIM1 puncta are subplasmalemmal and support the hypothesis that STIM1 does not insert into the plasma membrane to activate SOCs but rather associates with some unidentified component(s) of the plasma membrane to anchor puncta to ER-PM junctions. In contrast, immuno-EM and biotinylation studies have demonstrated that STIM1 inserts into the plasma membrane (Zhang et al., 2005). It has also been suggested that STIM1 may be inserted into the plasma membrane via a mechanism of

exocytosis involving the fusion of the ER with the plasma membrane (Hauser and Tsien, 2007) and that SOC activity is dependent on proteins involved in exocytosis (Yao et al., 1999; Zhang et al., 2006). Furthermore, several groups have shown that plasma membrane STIM1 plays a role in the activation of SOCE (Hewavitharana et al., 2008; Spassova et al., 2006). It is therefore possible that STIM1 is inserted into the plasma membrane at ER-PM junctions following translocation to regulate SOCs.

Since little is known regarding the mechanism of translocation and membrane insertion of STIM1, the present study aimed to define the localization of STIM1 following translocation and the energy requirements for translocation to occur. The possible insertion of STIM1 into the plasma membrane from bulk ER to ER-PM junctions was tested using a His_6-STIM1-EYFP construct similar to that used by Hauser and Tsien (Hauser and Tsien, 2007). The role of exocytosis in the formation of STIM1 puncta was also determined. The bioenergetics of STIM1 translocation was examined to investigate the dependence of puncta formation on ATP. This works confirms that store depletion does in fact stimulate STIM1 translocation to the plasma membrane where it colocalises with Orai1 but also provides results concerning the plasma membrane insertion of STIM1 following store depletion and novel findings regarding the bioenergetics of STIM1 translocation.

The means by which STIM1 moves to the plasma membrane from bulk ER is a controversial issue. STIM1 may diffuse to ER-PM junctions following store depletion or may be actively transported from bulk ER to ER-PM junctions via an ATP-dependent process. Respiring mitochondria are essential for the activation of SOC

channels and play a crucial role in all stages of SOC influx (Parekh, 2003). Previous studies have shown that inositol trisphosphate (IP_3) fails to activate SOCE unless mitochondria are in an energized state and that SOCE is suppressed when mitochondria are depolarized (Glitsch et al., 2002). In fact, it has been reported that a reduction in as little as 5% in ATP levels is sufficient to cause a 50% drop in Ca^{2+} influx (Gamberucci et al., 1994), suggesting a role for mitochondrial ATP in the activity of SOCE. One recent report has shown that STIM1 binds to the microtubule plus-end-binding protein, EB1 (Grigoriev et al., 2008). Since the movement of many proteins along microtubules requires ATP-dependent molecular motors, it is possible that ATP may be required for the movement and translocation of STIM1 to the plasma membrane.

3.2 Results

3.2.1 Store depletion stimulates STIM1 translocation and the formation of STIM1-Orai1 complexes

Previous work has shown that STIM1 is a transmembrane Ca^{2+} sensor within the endoplasmic reticulum (ER), which, upon depletion of the Ca^{2+} stores of the ER, translocates to the plasma membrane and activates SOC influx (Liou et al., 2005; Zhang et al., 2005). This was confirmed in this study by monitoring the localisation of a C-terminally EYFP-tagged STIM1 (STIM1-EYFP) construct in live HeLa cells using confocal microscopy. HeLa cells transfected with STIM1-EYFP were perfused with the sarco/endoplasmic reticulum (Ca^{2+} and Mg^{2+}) ATPase (SERCA) pump inhibitor, thapsigargin, to deplete the ER Ca^{2+} store. In the resting cell, STIM1-EYFP was

distributed throughout the ER and redistributed to plasmalemmal puncta following the application of thapsigargin (Figure 3.1, n = 10).

The plasma membrane protein, Orai1, has recently been identified as the functional SOC channel (Feske et al., 2006; Prakriya et al., 2006; Vig et al., 2006b; Zhang et al., 2006). Coexpression of STIM1 and Orai1 in HEK293 cells results in a 100-fold increase in SOC influx (Spassova et al., 2006), indicating that these two proteins are sufficient to mediate the activity of SOC channels. Studies using approaches such as affinity chromatography and FRET showed that the two proteins interact at the plasma membrane (Muik et al., 2008). In order to confirm this, HeLa cells over-expressing STIM1-EYFP and mCherry-Orai1 were perfused with thapsigargin to induce STIM1 translocation. Before store depletion, both proteins exhibited different cellular localisations. Prior to store depletion, STIM1-EYFP was distributed throughout the ER (Figure 3.2, 1A), whereas Orai1 was expressed diffusely throughout the plasma membrane (Figure 3.2, B) and there was very little overlap in the expression of both proteins (Figure 3.2, C). Following perfusion with thapsigargin, both STIM1-EYFP and mCherry-Orai1 proteins underwent a dynamic redistribution into coincidental puncta within 600 seconds of store depletion, resulting in the extensive localisation of both proteins within puncta (Figure 3.2, F; n = 9). Figure 3.3 shows a series of images taken over the 600 seconds of thapsigargin treatment, focussing specifically around the times when puncta formation begins and develops.

Figure 3.1

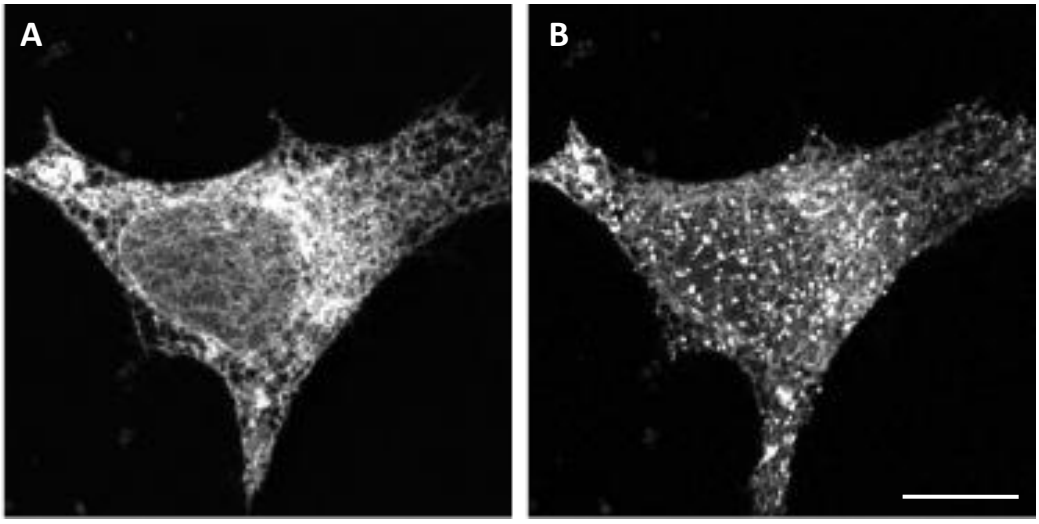

Figure 3.1. STIM1-EYFP accumulates in subplasmalemmal puncta in store-depleted HeLa cells. HeLa cells were transfected with STIM1-EYFP. 24 hours post-transfection the cells were washed in standard buffer and perfused with a supramaximal concentration of thapsigargin (2 μM). Cells were imaged before (**A**) and 300 s after (**B**) application of thapsigargin. STIM1-EYFP accumulated in puncta near the plasma membrane within 300 seconds of store depletion. Scale bar = 10 μm.

Figure 3.2

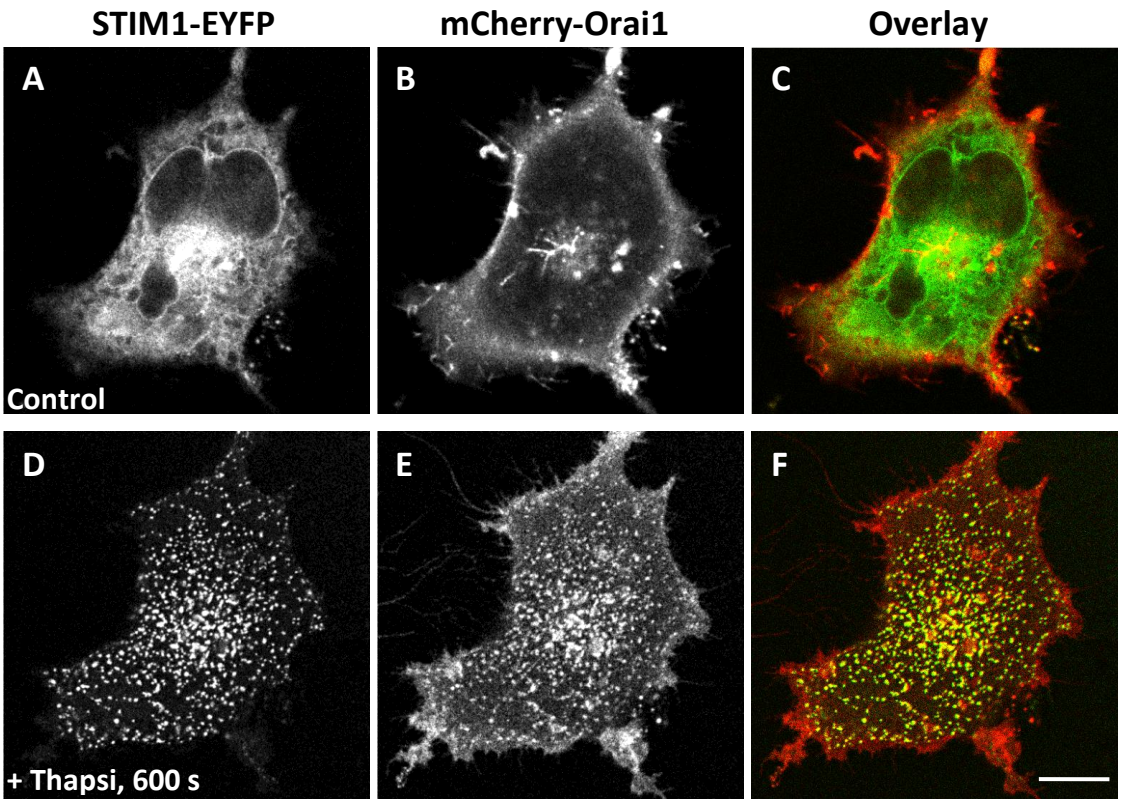

Figure 3.2 Store depletion induces the formation of STIM1-ORAI1 complexes. HeLa cells were cotransfected with STIM1-EYFP and mCherry-ORAI1. 24 hours post-transfection cells were perfused with thapsigargin (2 µM) for 600 seconds. Images in the upper panel (**A – C**) show the relative localisation of STIM1-EYFP (**A**), mCherry-Orai1 (**B**) and an overlay of both images (**C**) within a cell before store depletion. The images in the lower panel (**D – F**) show the corresponding images of both proteins and their overlay after thapsigargin treatment. STIM1-EYFP and mCherry-Orai1 colocalise in the same punctate structures after store depletion. Scale bar = 10 µm.

In this experiment, the appearance of puncta was initially apparent at around 360 seconds after the addition of thapsigargin and continued to develop over the course of approximately 140 seconds (Figure 3.3). If STIM1-EYFP is recruited to puncta first, one would expect puncta to initially appear green and subsequently turn yellow as mCherry-Orai1 is recruited. However, it was seen that puncta were yellow as they formed (Figure 3.3), suggesting that STIM1 and Orai1 entered puncta simultaneously.

The redistribution of STIM1-EYFP and mCherry-Orai1 to the same puncta was also observed using the membrane-permeable low affinity calcium buffer N,N,N,N-Tetrakis(2-pyridylmethyl)ethylenediamine (TPEN; 500 μM). Buffering the intracellular Ca^{2+} stores in this manner stimulated the translocation of STIM1 from bulk ER (Figure 3.4, A) to puncta (Figure 3.4, D) and the clustering of Orai1 at the sites of puncta formation (Figure 3.4, E). The formation of STIM1-Orai1 complexes occurred over a similar timecourse as that observed with thapsigargin treatment (Figure 3.4, F; n = 4), confirming that depletion of the intracellular Ca^{2+} stores is the stimulus responsible for inducing STIM1 translocation and the subsequent formation of STIM1-Orai1 puncta.

Since STIM1 and Orai1 colocalise at the plasma membrane following store depletion, a previously described Bimolecular Fluorescence Assay (Robida and Kerppola, 2009) was used to try and determine whether their direct interaction could be detected within puncta. The interaction between STIM1 and Orai1 was investigated in live HeLa cells using a previously described experimental

Figure 3.3

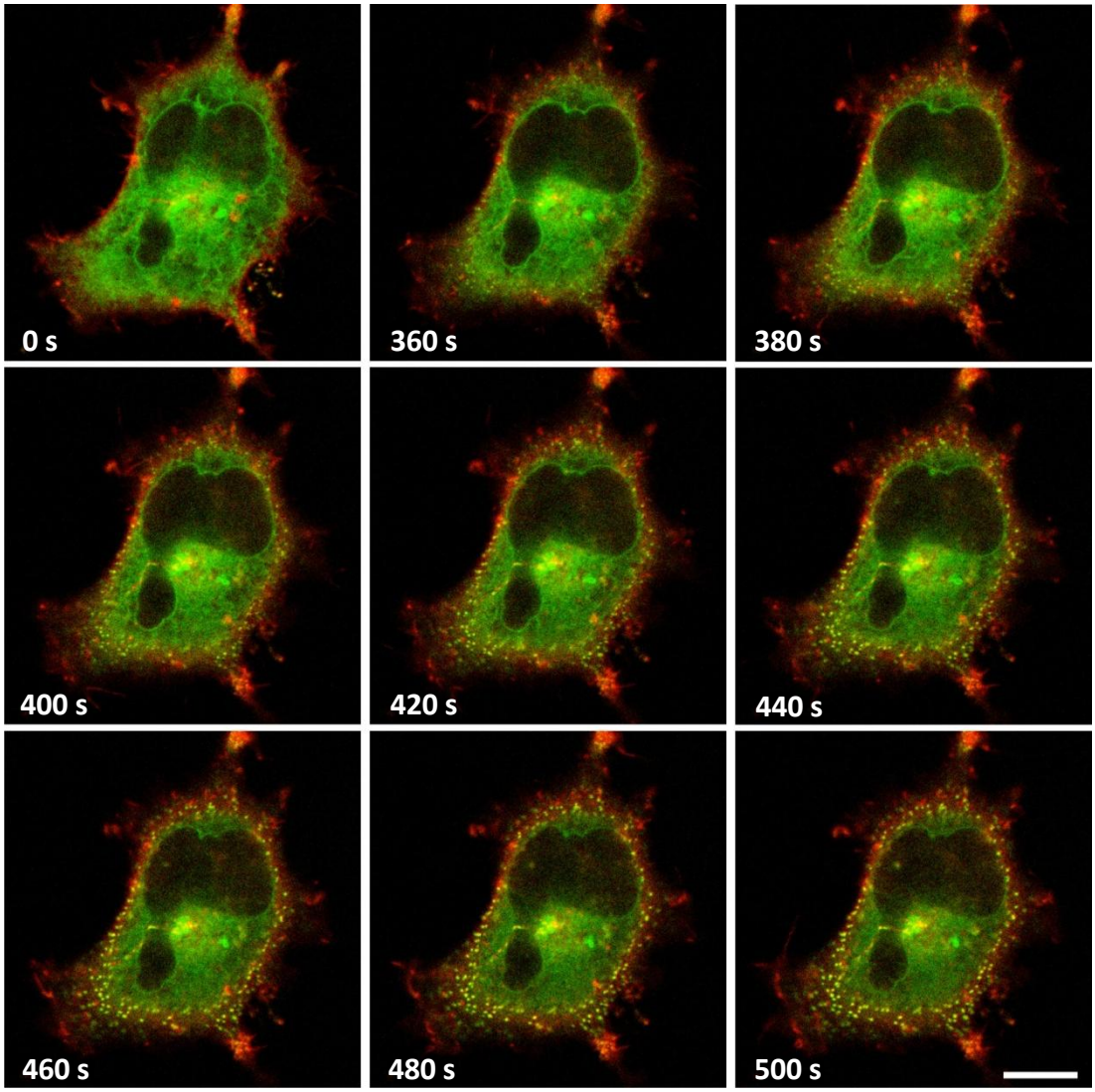

Figure 3.3 Timecourse of STIM1-EYFP and Orai1 puncta formation. HeLa cells were transfected with STIM1-EYFP (green) and mCherry-Orai1 (red) and treated with thapsigargin over a period of 600 seconds. Images were taken every 20 seconds during treatment. No puncta are visible at 0 seconds of treatment. Puncta formation begins ~360 seconds after the addition of thapsigargin with full puncta formation observed at ~480 seconds. These puncta appear yellow as they form, suggesting that both STIM1-EYFP and Orai1-mCherry are recruited to puncta coincidentally. Scale bar = 10 μm.

Figure 3.4

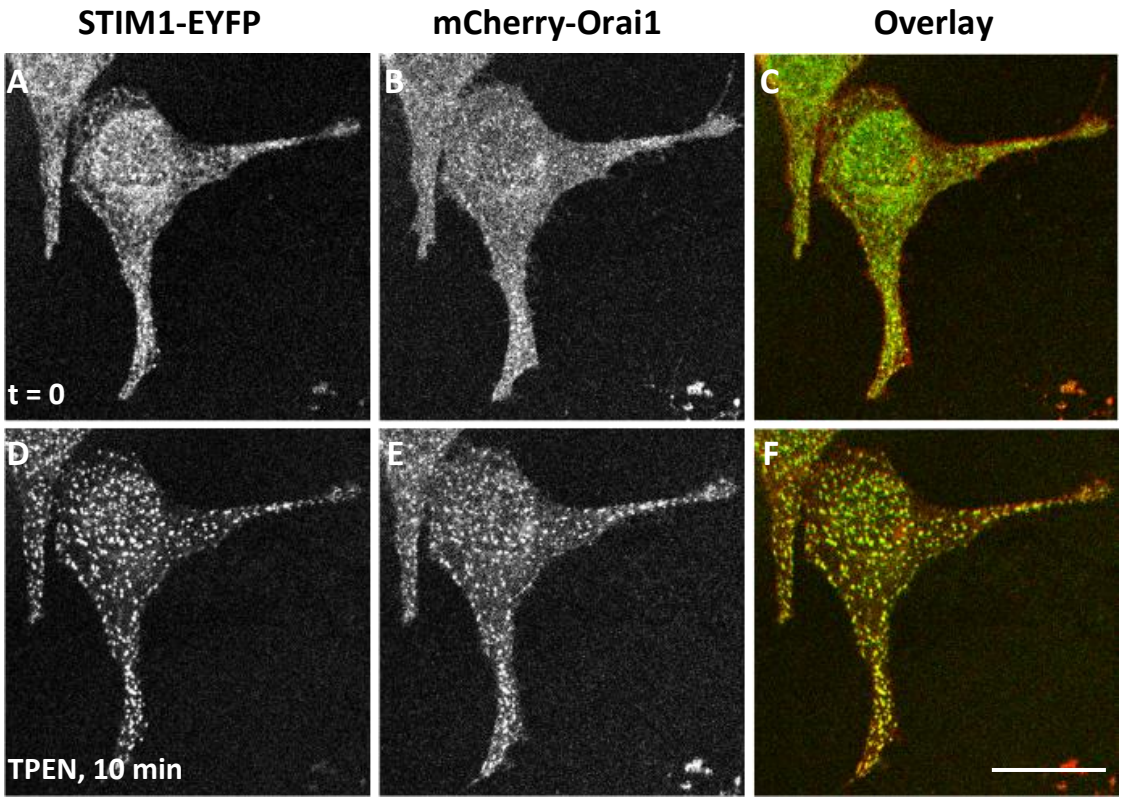

Figure 3.4 Depletion of store with TPEN induces the formation of STIM1-ORAI1 complexes. HeLa cells were cotransfected with STIM1-EYFP and mCherry-Orai1. 24 hours post-transfection cells were perfused with TPEN (500 µM) for 10 minutes. Images in the upper panel (**A – C**) show the relative localisation of STIM1-YFP (**A**), mCherry-Orai1 (**B**) and an overlay of both images (**C**) within a cell before TPEN treatment (500 µM). The images in the lower panel (**D – F**) show the corresponding images of both proteins after perfusion with TPEN. Scale bar = 10 µm.

approach (Haynes et al., 2007). In these experiments, the cytosolic C-terminal domain of STIM1 (STIM1-CT) and the full length Orai1 protein were tagged with the N-terminal and C-terminal fragments of the EYFP protein, respectively, and co-transfected into HeLa cells. The cells were then imaged using confocal microscopy. The STIM1-CT fragment should not retain its ER distribution since it is lacking the N-terminal and transmembrane regions which anchor it to the ER. It was expected that this truncated STIM1 protein should interact with plasmalemmal Orai1, thus enabling the reconstitution of the full length EYFP protein. Sites of EYFP fluorescence should represent site of functional SOCs. However, restoration of EYFP fluorescence was not observed under these conditions (Figure 3.5, left image; n = 16).

3.2.2 ATP depletion induces the translocation of STIM1 and formation of punctate STIM1-Orai1 complexes

Some studies have implicated mitochondrial ATP in the activity of SOCE (Gamberucci et al., 1994). Since the movement of many proteins along microtubules requires ATP-dependent molecular motors, it is possible that ATP may be required for the movement and translocation of STIM1 to the plasma membrane. To investigate this possibility, STIM1 translocation was monitored following depletion of cytosolic ATP. For this, HeLa, Rama37 and PANC1 cell lines were transfected with STIM1-EYFP. After transfection, cells were simultaneously perfused with the ATP synthase inhibitor, Oligomycin (Olig; 5 µM), to prevent mitochondrial ATP production, in combination with the glucose-3-phosphate dehydrogenase inhibitor, Iodoacetate (IA; 2 mM), or the glucose analog, 2-

Figure 3.5

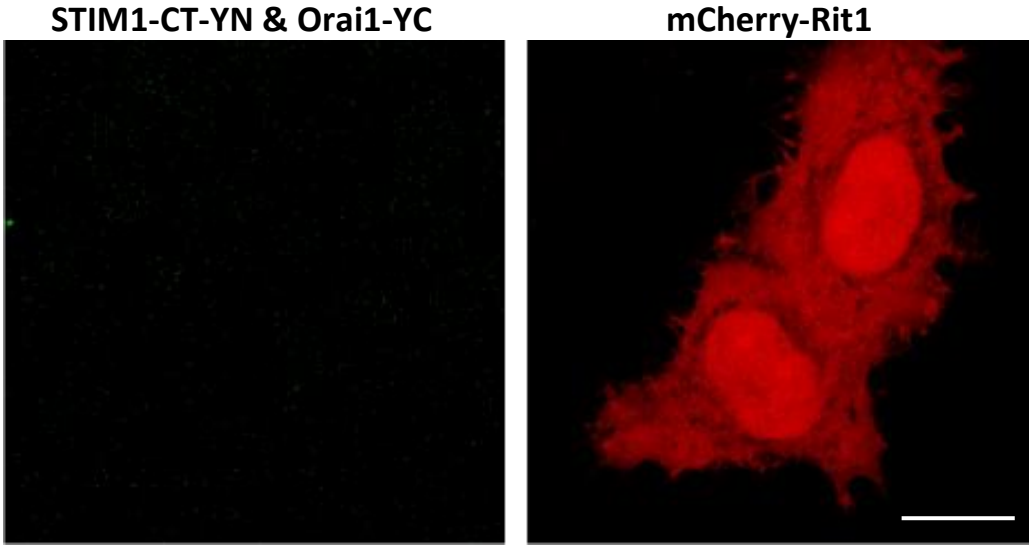

Figure 3.5 STIM1-CT-YN and Orai1-YC Bimolecular Fluorescence Complementation Assay. HeLa cells were transfected with STIM1-CT-YN and Orai1-YC constructs (**left image**) along with an mCherry-Rit1 transfection marker (**right image**) and imaged after 24 hours. Co-expression of STIM1-CT-YN and Orai1-YC failed to reconstitute EYFP fluorescence at the plasma membrane. Scale bare = 10 μm.

Deoxy-D-Glucose (2DG), to inhibit glycolysis. We expected that if STIM1 translocation is dependent on ATP, puncta formation would be inhibited by suppressing ATP production. Surprisingly, ATP depletion strongly induced STIM1 translocation in the three cell types tested (Figure 3.6; A-L: n = 40 for RAMA37; n = 6 for PANC1; n = 24 for HeLa). These data suggest that not only is ATP not essential for STIM1 translocation but that its translocation is in fact stimulated in conditions of ATP depletion. The formation of STIM1 puncta was also triggered by Rotenone, an inhibitor of Complex I of the mitochondrial electron transport chain (Figure 3.6, M & N; n = 5).

Many previous studies, including work from our own lab (Chvanov et al., 2008), have revealed that ATP depletion inhibits SOC influx, suggesting that ATP positively modulates SOC channels. Since STIM1 puncta formation can occur in an ATP independent manner, we sought to determine whether ATP is perhaps required downstream of STIM1 translocation during the assembly of STIM1-Orai1 complexes. To investigate this, STIM1-EYFP and mCherry-Orai1 were coexpressed in HeLa cells and treated with Olig/IA as described above. Under these conditions the translocation of both STIM1-EYFP and mCherry-Orai1 proteins to the same plasmalemmal puncta was induced within 900 seconds (Figure 3.7, n=5), suggesting that ATP is not required for the formation of these complexes and in fact the interaction between the two proteins is stimulated as a consequence of ATP depletion.

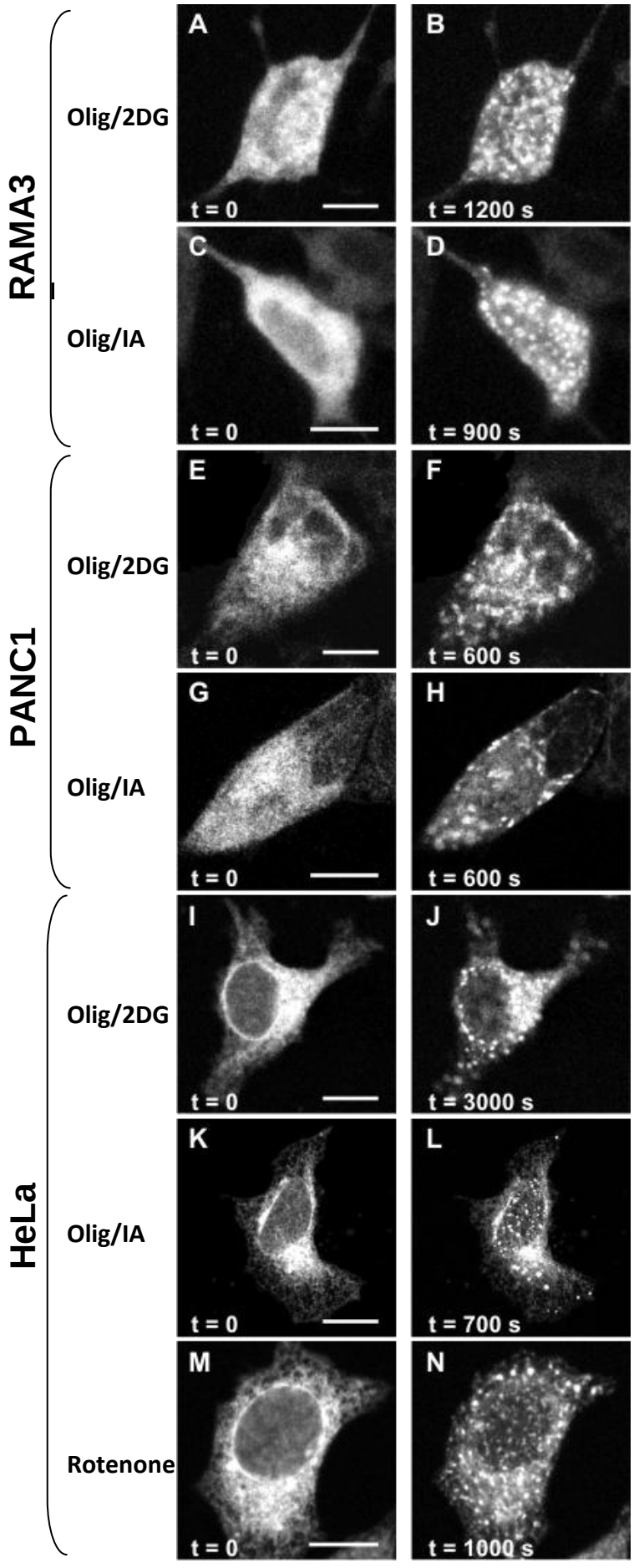

Figure 3.6 STIM1 translocation is induced by ATP depletion. RAMA37, PANC1 and HeLa cells were transfected with STIM1-EYFP. Images in the left column were taken immediately before the application of inhibitors of ATP production (**left panel**; t = 0). Depleting ATP with a combination of Oligomycin and 2-deoxy-d-glucose or Oligomycin and Iodoacetate stimulated STIM1 translocation in RAMA37 (**A - D**), PANC1 (**E – H**) and HeLa cells (**I – L**). STIM1 translocation was also induced by depleting ATP with rotenone (**M and N**). Times for which each cell was perfused with inhibitors is indicated on individual images. Scale bars = 10 µm.

Figure 3.7

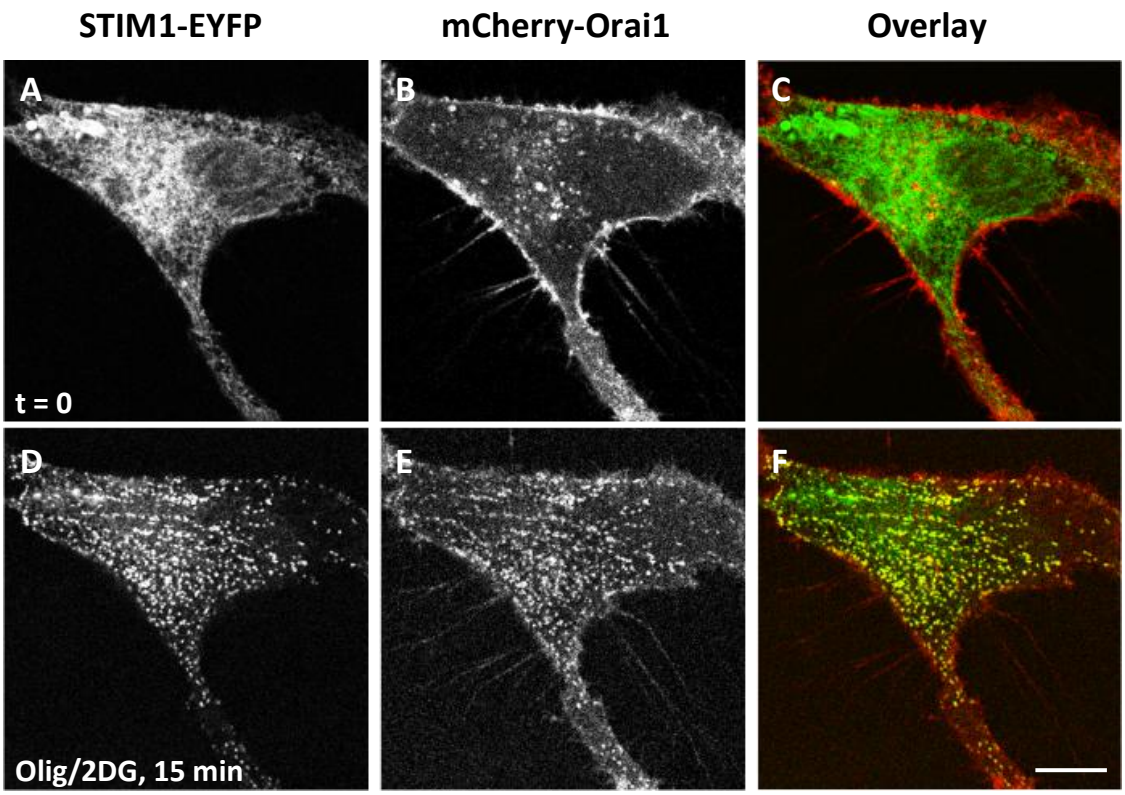

Figure 3.7 ATP depletion induces the formation of STIM1-Orai1 complexes. HeLa cells were cotransfected with STIM1-EYFP and mCherry-Orai1. Images in the upper panel (**A – C**) show the relative localisation of STIM1-EYFP (**A**), mCherry-Orai1 (**B**) and an overlay of both images (**C**) within a transfected cell before ATP depletion. The images in the lower panel (**D – F**) show the corresponding images of both proteins after perfusion with Olig/2DG for 15 min. STIM1-EYFP and mCherry-Orai1 colocalise in the same puncta following ATP depletion. Scale bar = 10 µm.

The microtubule cytoskeleton is important in maintaining Ca^{2+} influx in a variety of cell types (Oka et al., 2005; Smyth et al., 2007). It has been demonstrated that disruption of microtubules with agents such as nocodazole or colchicine results in the inhibition of SOC influx (Oka et al., 2005). Others have shown that STIM1 localisation is related to that of microtubules (Smyth et al., 2007) and STIM1 has recently been found to interact with EB1, a plus end microtubule tracking protein (Grigoriev et al., 2008). One study claimed that STIM1 translocation is stimulated by the disruption of microtubules, indicating a possible role for the microtubule cytoskeleton in blocking SOC function (Smyth et al., 2007). It was possible, therefore, that inhibiting ATP production could result in a loss of microtubule structure and lead to STIM1 translocation to the membrane by diffusion. To determine whether ATP depletion disrupts microtubules in HeLa cells, the cells were transfected with STIM1-EYFP and treated with Olig/2DOG for 30 minutes. The cells were then fixed and stained with an antibody directed against the microtubule marker, α-tubulin. Confocal imaging revealed that microtubules remain intact in ATP-depleted cells in which STIM1 puncta had formed (Figure 3.8, D-F; n = 4) with no differences to control cells (Figure 3.8, A-C; n = 4), suggesting that ATP does not stimulate STIM1 translocation through the destruction of the microtubule network.

3.2.3 STIM1 insertion into the plasma membrane is not required for puncta formation

A recent study demonstrated that STIM1 does not remain subplasmalemmal but rather inserts into the membrane following translocation (Hauser and Tsien, 2007). Other reports have pointed towards a role for exocytosis in this process, where

Figure 3.8

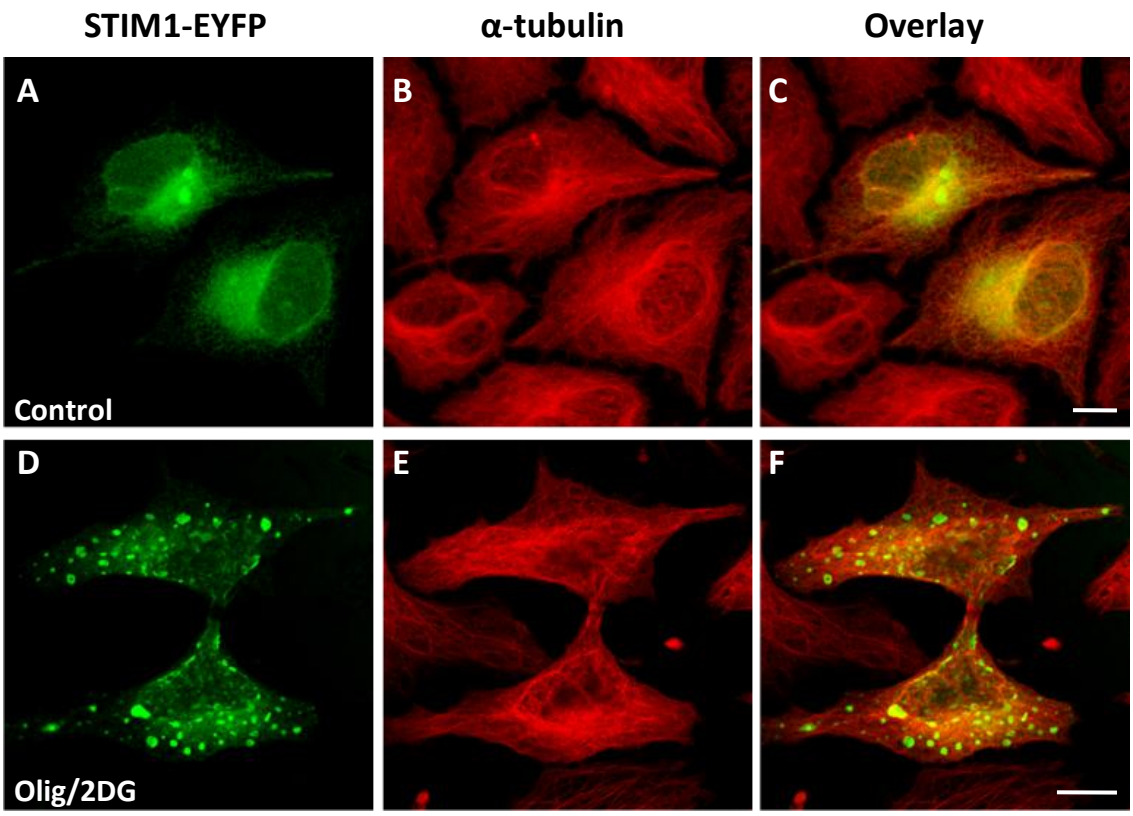

Figure 3.8 ATP depletion does not disrupt the microtubule cytoskeleton. HeLa cells were transfected with STIM1-EYFP (**A and D**).24 hours post-transfection cells were treated with Olig/2DG or left in sodium hepes solution for 30 minutes. Cells were fixed and stained with an antibody directed against α-tubulin to stain for microtubules (**B and E**). Overlays are also shown (**C and F**). STIM1-EYFP retains a reticular pattern in control cells (**A**) but translocates to subplasmalemmal puncta after ATP depletion by Olig/2DG (**D**). The structure of the microtubule cytoskeleton remains intact in both control cells (**B**) and in ATP-depleted cells (**E**). Scale bars = 10 μm.

STIM1 is secreted via ER fusion with the plasma membrane (Rosado et al., 2005). This hypothesis is supported by two studies which independently demonstrate that SOC activity can be inhibited by suppressing or mutating proteins involved in exocytosis (Yao et al., 1999; Zhang et al., 2006). Indeed, ER fusion with the plasma membrane has previously been observed during phagocytosis, where it has been suggested that the ER directly associates and fuses with the plasma membrane for phagosome formation (Gagnon et al., 2002; Guermonprez et al., 2003; Touret et al., 2005). It is possible that a similar mechanism is required for the insertion of STIM1 into the plasma membrane. This was tested by doubly transfecting HeLa cells with STIM1-EYFP and the previously described αSNAP (L294A) mutant (Barnard et al., 1997) which acts as a general inhibitor of all fusion steps through the inhibition of SNARE protein function. 24 hours after transfection, cells were treated with thapsigargin (2 μM) for 15 minutes or with sodium hepes as a control. Cells were then fixed and stained with a previously described antibody directed against wild-type αSNAP (Graham et al., 2001) but which will also recognise the αSNAP mutant protein, and counterstained with a fluorescently conjugated secondary antibody. Thapsigargin-induced STIM1-EYFP puncta formation was observed even in the presence of the αSNAP mutant (Figure 3.9; n = 8). The effectiveness of αSNAP(L294A) was confirmed below (see Figure 3.11). These results, therefore, suggest that SNARE-dependent exocytotic events are not required for the aggregation and translocation of STIM1 to the plasma membrane but do not rule out whether plasma membrane STIM1 is required for the activity of SOCs.

Figure 3.9

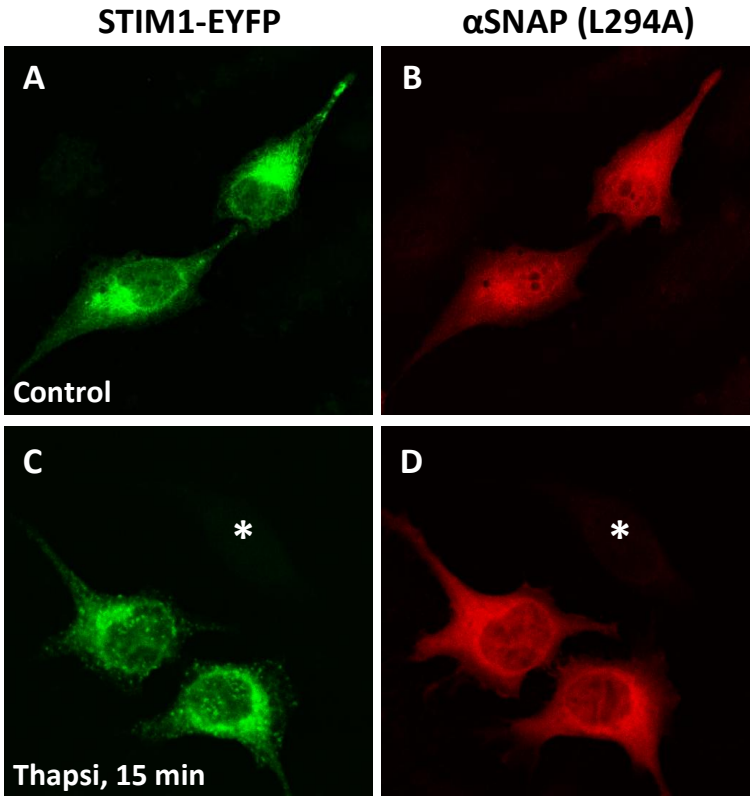

Figure 3.9 Inhibition of exocytosis does not prevent STIM1 translocation. HeLa cells were transfected with STIM1-EYFP and a non-fluorescent αSNAP(L294A) mutant. Cells were treated either with thapsigargin (2 µM) for 15 minutes or left in control media, fixed and stained with an antibody directed against αSNAP. In control cells expressing both STIM1-EYFP and the αSNAP mutant (**A and B**), STIM1-EYFP expression is distributed throughout the ER. STIM1-EYFP translocation is observed in thapsigargin treated cells expressing both STIM1-EYFP and αSNAP(L294A) (**C and D**). The asterix marks an untransfected control cell, showing that the antibody is specific for αSNAP(L294A) and does not pick up wild type αSNAP. Scale bar = 10 µm.

3.2.4 The use of a His_6-STIM1-EYFP protein to monitor STIM1 insertion into the plasma membrane

Whether or not STIM1 inserts into the plasma membrane following translocation and the role of plasma membrane STIM1 is currently uncertain. It was believed that this controversy may have been resolved by Hauser and Tsien who demonstrated that the addition of some bulky N-terminal tags such as HA tags, horseradish peroxidase and fluorescent proteins such as CFP prevent the plasma membrane insertion of STIM1 but that externalisation of the N-terminus is permitted using N-terminal His_6 and C-terminal fluorescent protein tags, thereby conclusively demonstrating that STIM1 can insert into in the plasma membrane (Hauser and Tsien, 2007). However, constructs of STIM1 with N-terminal tags that prevent plasma membrane insertion still retain the ability to stimulate SOCE (Hauser and Tsien, 2007; Liou et al., 2005; Mercer et al., 2006; Wu et al., 2006a), so the significance of STIM1 in the plasma membrane is unclear. The present study aimed to make a similar construct to that used by Hauser & Tsien to explore the mechanism of STIM1 insertion into the plasma membrane and the role of plasma membrane STIM1 in the regulation of SOCs. There were several small differences in the sequences of Hauser and Tsien's His_6-STIM1-ECFP construct and the His_6-STIM1-EYFP construct created in this study. A schematic representation of both Hauser and Tsien's His_6-STIM1-ECFP protein (Figure 3.10, A) and the His_6-STIM1-EYFP protein used in this study (Figure 3.10, B) are outlined in Figure 3.9. Both proteins contain the STIM1 signal peptide at the N-terminus of the protein, followed by the insertion of 6 histidine residues directly before the STIM1 coding sequence and a

fluorescent tag at the very C-terminus of the protein. This study used a C-terminal EYFP tag in place of Hauser and Tsien's ECFP tag. Apart from that, the constructs differ only in the 3 or 4 amino acids inserted between the signal peptide and the poly-histidine tag (which in our construct is a restriction site introduced to allow the insertion of the His_6 tag) and in the multiple cloning site within the plasmid itself (differences are highlighted in red boxes in Figure 3.10).

To study the plasma membrane insertion of STIM1 following translocation, HeLa cells were transfected with His_6-STIM1-EYFP. 24 hours post-transfection cells were treated with thapsigargin (2 μM) or sodium hepes for 10 minutes, fixed without permeabilisation and probed with an antibody directed against His_6. It was expected that STIM1 insertion into the plasma membrane should occur following thapsigargin treatment only, resulting in the subsequent externalisation of the N-terminal His_6 tag at the cell surface following STIM1 translocation, which should be detectable by staining with the anti-His_6 antibody. If this was the case, there should be a large increase in the amount of His_6 detected at the cell surface following thapsigargin treatment when compared with control cells. Surprisingly, there was no qualitative difference in the extent of cell surface His_6 staining in control cells (Figure 3.11,A; n = 8) versus thapsigargin treated cells (Figure 3.11, B; n = 11), suggesting that His_6-STIM1-EYFP is already present in the plasma membrane before store depletion and also that store depletion has little effect on the amount of His_6-STIM1-EYFP in the plasma membrane. In Figure 3.11A, the His_6 stain does not completely overlap the distribution of EYFP, possibly due to bleed-through from another confocal plane of the cell where staining was particularly intense.

Figure 3.10

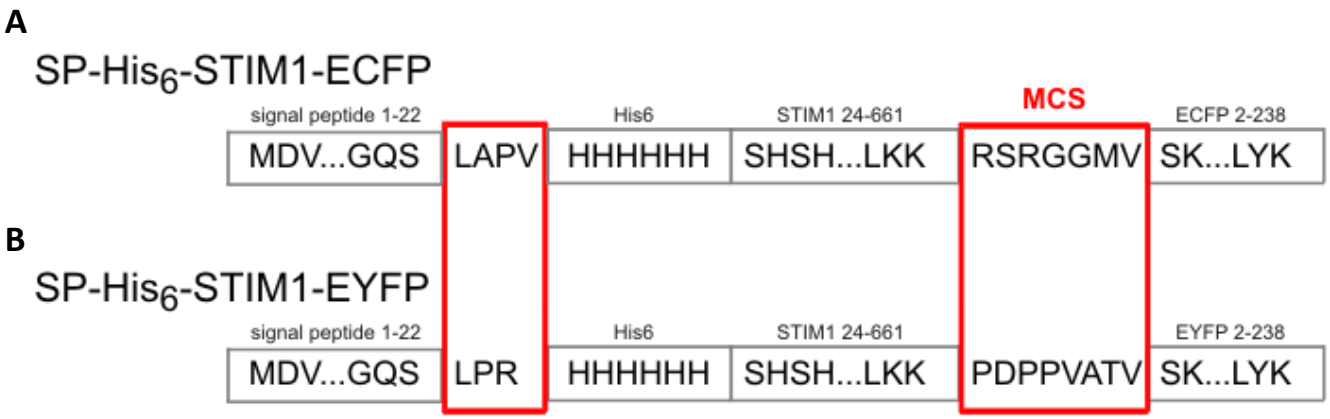

Figure 3.10 Schematic representation of His_6-STIM1-ECFP/EYFP constructs. The structures of Hauser and Tsien's His_6-STIM1-ECFP protein (**A**) and the His_6-STIM-EYFP protein used in this study (**B**) are outlined above. Both constructs contain the STIM1 signal peptide on the N-terminus of the protein, followed by the insertion of 6 histidine residues directly before the STIM1 protein sequence and a C-terminal fluorescent tag. Differences between the constructs lie in the restriction endonuclease recognition site and the multiple cloning site (MCS) and are highlighted in red boxes.

It was possible that plasma membrane staining was caused by the His_6 antibody binding non-specifically to some other cell surface protein, which was masking changes in the extent His_6-STIM1-EYFP staining. To examine the specificity of the antibody, fixed HeLa cells transfected with His_6-STIM1-EYFP were permeabilised prior to staining to reveal all of the His_6-STIM1-EYFP and the distribution of His_6 antibody staining was compared with EYFP fluorescence in these cells. There was nearly complete overlap between antibody staining and EYFP fluorescence (Figure 3.11, C; n = 16), demonstrating that the antibody was specifically recognising the His_6-STIM1-EYFP protein.

It seemed likely that the N-terminal His_6 tag resulted in the mislocalisation of STIM1 from the ER to the plasma membrane. To examine this, HeLa cells were cotransfected with His6-STIM1-EYFP and a mutant αSNAP(L294A) protein in an attempt to inhibit protein trafficking to the plasma membrane and fixed and stained as described above. Under these conditions, EYFP fluorescence was detected in a reticular ER-like lcoalisation pattern but no antibody staining was detected at the cell surface (Figure 3.11, D; n = 11), suggesting that in the absence of the αSNAP mutant, His_6-STIM1-EYFP is unexpectedly trafficked constitutively to the plasma membrane. This effect of αSNAP(L294A) demonstrates the effectiveness of the mutant αSNAP construct that had been used earlier in an attempt to block exocytosis (Figure 3.9).

The EYFP fluorescence observed in His_6-STIM1-EYFP transfected HeLa cells did not exhibit a reticular pattern in control cells (Figure 3.11, A) nor a punctate pattern in

Figure 3.11

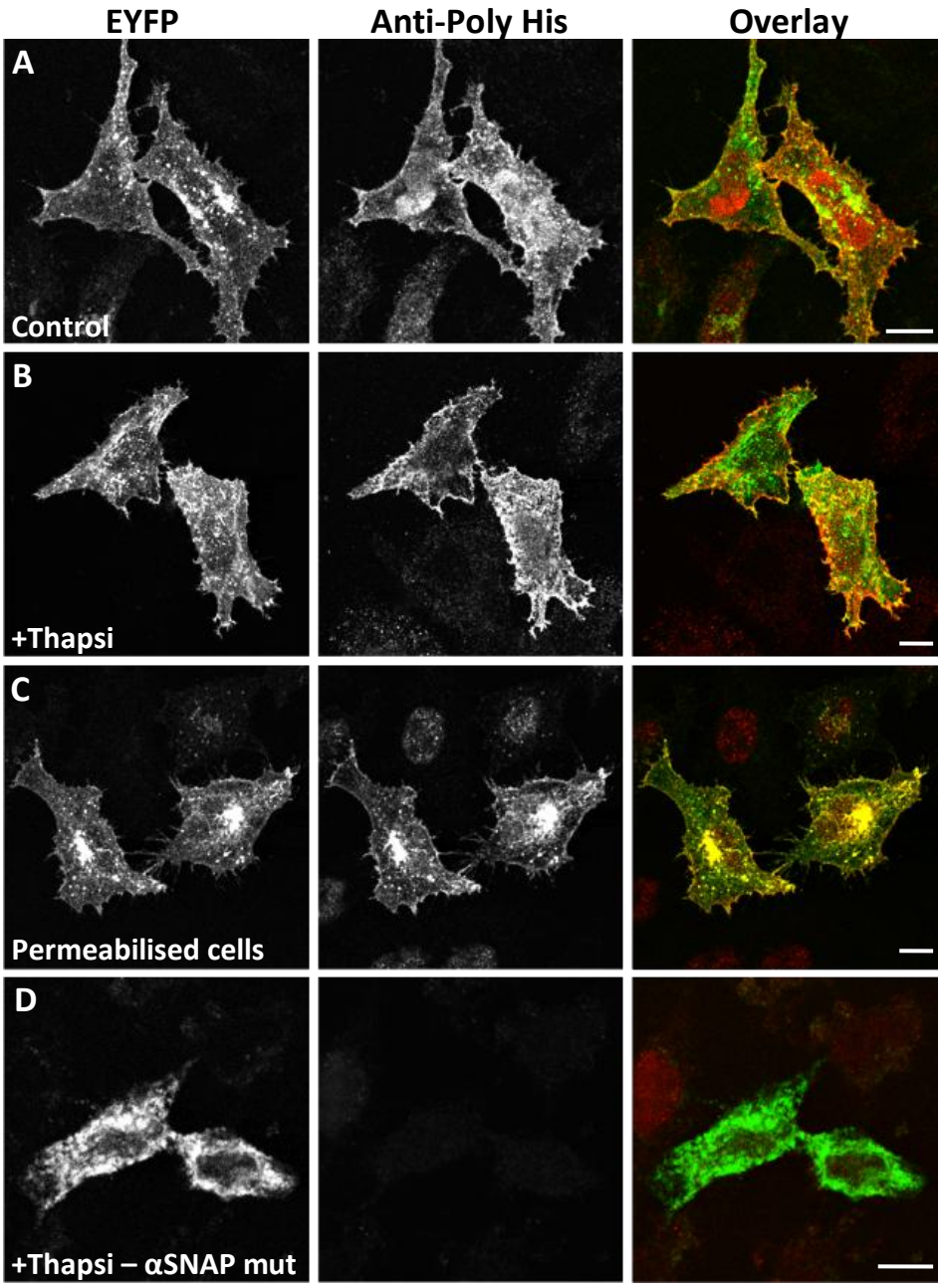

Figure 3.11 His_6-STIM1-EYFP is constitutively localised at the plasma membrane. HeLa cells were transfected with His_6-STIM1-EYFP alone (**A - C**) or in combination with αSNAP (L294A) (**D**) and treated with or without thapsigargin for 15 min before they were fixed and stained with an antibody against the poly-His tag. His_6-STIM1-EYFP was constitutively localised in the plasma membrane before and after thapsigargin treatment (**A and B**) Permeabilising cells before fixation confirmed that the antibody specifically recognised the His_6-STIM1-EYFP protein (**C**). His_6-STIM1-EYFP failed to localise to the plasma membrane in the presence of the αSNAP mutant (**D**). Scale bars = 10 µm.

Figure 3.12

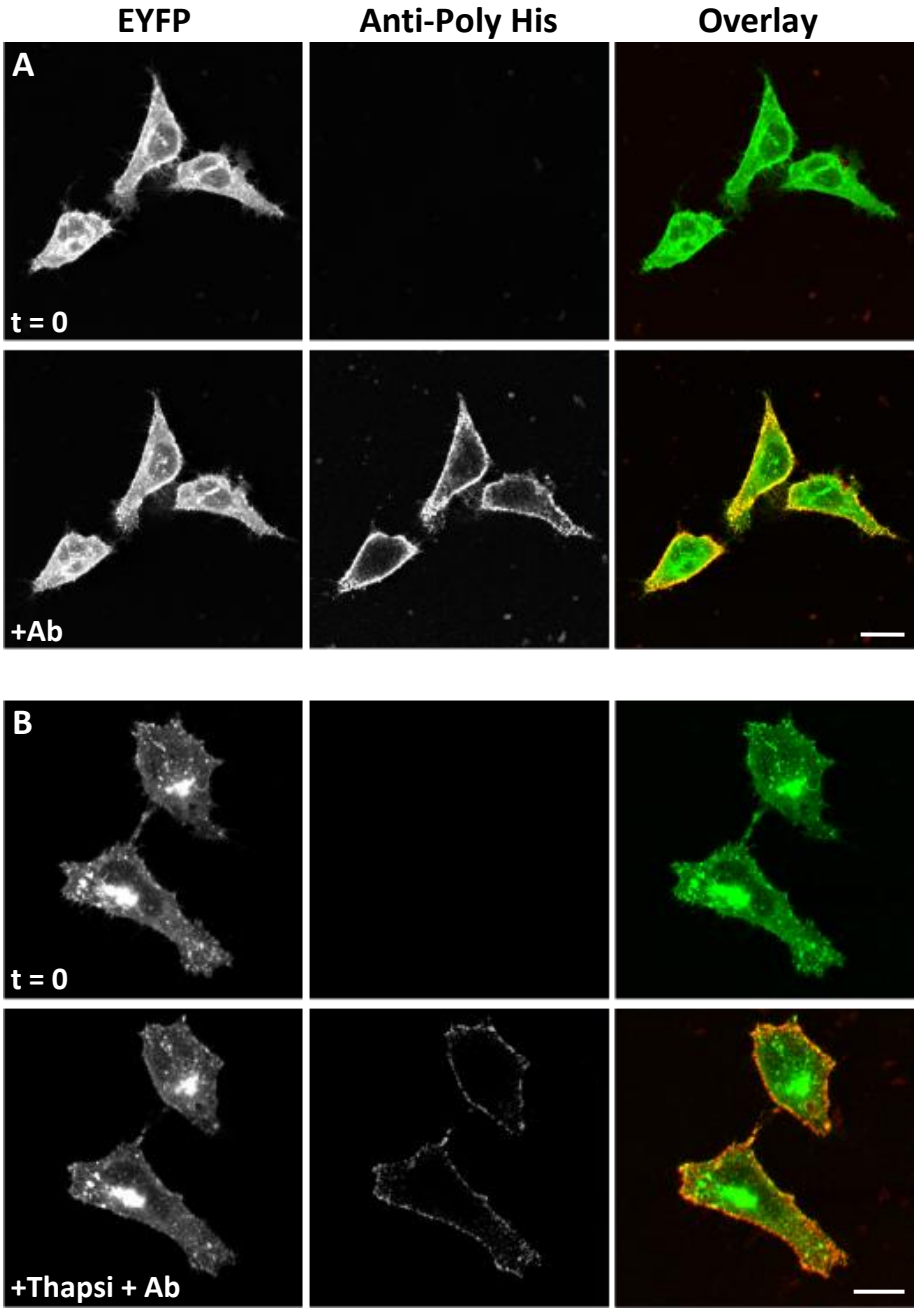

Figure 3.12 His_6-STIM1-EYFP is constitutively targeted to the plasma membrane in live HeLa cells. (**A**) HeLa cells were transfected with His_6-STIM1-EYFP. 24 hours post-transfection cells were treated with thapsigargin (2 µM; **B**) or sodium hepes solution (**A**) for 10 minutes, after which cells were treated with anti-poly-his antibody for 15 minutes, washed, and incubated in Dylight649 secondary antibody for a further 15 minutes. Ce; aalls were then washed and imaged. There was no qualitative change in cell surface antibody staining in control cells (**A**) versus thapsigargin treated cells (**B**), suggesting that the His_6-STIM1-EYFP protein is constitutively localised at the plasma membrane.

thapsigargin-treated cells (Figure 3.11, B). This, in addition to the constitutive plasma membrane localisation observed could possibly be a result of the fixation process. To determine whether this is the case, HeLa cells were seeded onto glass bottomed dishes and transfected with His_6-STIM1-EYFP and imaged using live confocal microscopy. Cells were perfused with thapsigargin (2 μM) or sodium hepes for 10 minutes, after which cells were incubated with the anti-His_6 antibody and subsequently with a fluorescent-conjugated secondary antibody to probe for externalisation of the N-terminal His_6 tag in live cells. His_6 staining was observed in both control (Figure 3.12, A; n = 10) and thapsigargin treated cells (Figure 3.12, B; n = 9), indicating that the plasma membrane localisation of His_6-STIM1-EYFP, and the lack of reticular and punctate expression, was not a result of paraformaldehyde fixation but may rather be an artefact produced by the addition of the N-terminal His_6 tag.

3.3 Discussion

Previous studies have established that STIM1 regulates the activity of SOC channels by translocating to punctate structures at the plasma membrane following intracellular store depletion (Zhang et al., 2005). This study confirms that STIM1 translocation is induced by store depletion but also reports that STIM1 translocation is stimulated by the depletion of ATP. Other work from this lab has demonstrated that the re-translocation of STIM1 back into bulk ER can also occur in ATP depleted cells (Chvanov et al., 2008). ATP depletion also induced the formation of STIM1-Orai1 complexes at the plasma membrane based on colocalisation of the two proteins. Co-expression of these two proteins was previously shown to greatly

enhance SOC influx by a magnitude of over 100 (Soboloff et al., 2006b), suggesting that they are sufficient for the activation of SOC channels. However, data from this lab has shown that the increase in Ca^{2+} influx following store depletion is inhibited by depleting ATP (Chvanov et al., 2008). These data support previous studies which have reported that an inhibition of ATP production suppresses SOC influx (Gamberucci et al., 1994; Glitsch et al., 2002; Parekh, 2003) . It is interesting that even though the molecular machinery required for SOCE is assembled upon ATP depletion, the activity of the channels is markedly reduced. This would suggest that there are other unknown factors involved in the activation of the channels. Indeed, a recent report by Varnai *et al*, in which they used a chemically inducible bridge formation to link the plasma membrane and the ER, suggested that Orai1 exists as part of a large molecular complex (Varnai et al., 2007). It is possible therefore that an ATP-dependent process such as the trafficking or phosphorylation of a protein within this complex is required to activate SOCE.

The microtubule network has been suggested to play a regulatory role in the movement of STIM1 to the membrane. Interestingly, an EYFP-tagged STIM1 protein was observed to colocalise with microtubules in HEK293 cells (Liou et al., 2007; Smyth et al., 2007) and more recently STIM1 was found to track growing microtubule ends through its interaction with the microtubule plus-end protein, EB-1 (Grigoriev et al., 2008). Furthermore, depolymerisation of the microtubule cytoskeleton results in the inhibition of SOC influx while causing STIM1 translocation, possibly by diffusion to the plasma membrane (Smyth et al., 2007). It was possible that STIM1 puncta formation during ATP depletion is the direct result

of depolymerisation of microtubules. However, the finding that the microtubule cytoskeleton remains intact in conditions of ATP depletion argues against this hypothesis. The microtubule cytoskeleton plays a role in the organisation of the ER (Terasaki et al., 1986), and recent studies have shown that STIM1 oligomerisation in the ER precedes its translocation to the plasma membrane (Luik et al., 2008; Stathopulos et al., 2006), suggesting that STIM1 puncta are preformed within the ER membrane. In the present study, however, STIM1 puncta formation seems to coincide with Orai1 puncta formation (Figure 3.3), suggesting that although STIM1 oligomers may form within the ER following store depletion, STIM1 puncta are formed at ER-PM junctions and not within the bulk ER itself. It is possible, therefore, that microtubules facilitate ER movement to the plasma membrane during STIM1 translocation. The mechanism for such transport remains to be determined but this might involve an ATP-independent transport process, for example, one that depends on GTP-based motors, or a diffusional model whereby STIM1 oligomers are anchored to the plasma membrane by some plasma membrane constituents. The membrane targeting of STIM1 will be discussed in further detail in Chapter 4.

It is intriguing that ATP depletion induces STIM1 formation even though SOC influx is inhibited. One important observation is that the timing of STIM1 translocation during ATP depletion is significantly slower than translocation induced by store depletion. It is possible that ATP depletion may induce a slow Ca^{2+} release from the ER which could in turn trigger the translocation of STIM1. This was demonstrated in experiments that measured Ca^{2+} content of the ER during ATP depletion (Chvanov

et al., 2008) which showed that it induces a slow Ca^{2+} leak which over time may be sufficient to trigger the translocation of STIM1. This would explain the time delay in translocation after ATP depletion compared with that of standard methods of store depletion.

Surprisingly, several studies have shown that SOCE can be inhibited by interfering with proteins which are involved in exocytosis. The SNARE protein Syntaxin 5 was recently identified in a high-throughput RNAi screen as a protein which is required for SOC activation (Zhang et al., 2006) and cleavage of the SNAP-25 and VAMP-2 proteins impairs store-operated Ca^{2+} entry in mouse pancreatic acinar cells (Rosado et al., 2005). In the latter study, Rosado et al proposed that SOCE is mediated via a reversible interaction between the plasma membrane and the ER, a process known as "secretion-like coupling". ER fusion with the plasma membrane has also been observed during phagocytosis (Gagnon et al., 2002; Hatsuzawa et al., 2006; Touret et al., 2005). Despite these discoveries, the link between SOCE and secretion has remained elusive. It is possible that STIM1 may be inserted into the plasma membrane via an exocytotic secretion mechanism involving the fusion of the ER with the plasma membrane (Rosado et al., 2005). However, it was found that STIM1 trafficking to the plasma membrane can still occur in the presence of αSNAP (L294A), which is expected to block all steps of SNARE-dependent exocytosis, arguing against a fusion mechanism for STIM1 insertion into the plasma membrane. It is possible, however, that although STIM1 translocates to the plasma membrane under these conditions, its insertion into the plasma membrane may be inhibited and that this insertion is required for SOCE. The efficacy of αSNAP (L294A) to inhibit

SNARE-dependent exocytosis was tested by assessing the incorporation of a previously described His_6-STIM1-EYFP construct (Hauser and Tsien, 2007) into the plasma membrane in cells where exocytosis is inhibited. As expected, the αSNAP mutant prevented the plasma membrane insertion of the His_6-STIM1-EYFP protein, thereby confirming that exocytosis is inhibited under these conditions. These results argue against a role for exocytosis in the formation of STIM1 puncta. It would be of interest to investigate SOC activation in cells co-expressing this STIM1 construct and the αSNAP(L294A) mutant construct to determine whether SOC activity is suppressed when exocytotic steps are blocked. One report investigated the effects of a similar αSNAP mutant on the activation of the native I_{CRAC} current in rat basophilic leukaemia cells and found that inhibiting exocytosis in this manner had no effect on I_{CRAC} activation (Bakowski et al., 2003).

In the present study, a His_6-STIM1-EYFP protein was constructed in order to study the plasma membrane insertion of STIM1 and how this affects SOCE. Hauser and Tsien showed that a similar His_6-STIM1-CFP construct was inserted into the plasma membrane following STIM1 translocation, thereby exposing the N-terminal His_6 tag on the extracellular surface which they could detect using a hexahistidine-Zn^{2+}-dye (Hauser and Tsien, 2007). However, in the data presented here, the His_6-STIM1-EYFP protein distribution deviated from the expected expression pattern in a number of ways. The hexahistidine staining in cells expressing His_6-STIM1-EYFP displays a uniform plasma membrane pattern, not the expected punctate pattern, both in thapsigargin-treated and untreated cells and this staining is lost in cells where membrane trafficking is inhibited. These results suggest that the His_6-STIM1-

EYFP protein is constitutively mistargeted to the plasma membrane, irrespective of whether stores are replete or depleted. Since the addition of other N-terminal tags to the STIM1 protein actually prevents plasma membrane insertion of the STIM1 protein and C-terminal tags have seemingly no affect on STIM1 distribution, it is probable that the hexahistidine tag is responsible for the constitutive trafficking of STIM1 to the plasma membrane. It is also possible that the presence of the LPR amino acid sequence between the STIM1 signal peptide and the hexahistidine tag, in place of the LAPV sequence present in Hauser and Tsien's construct, results in this continuous plasma membrane targeting. A further explanation for this is that there may be no change in the surface expression of STIM1 following store depletion, as has been previously noted (Soboloff et al., 2006a).

In addition, the His_6-STIM1-EYFP construct before thapsigargin treatment did not exhibit the typical reticular expression in both fixed and live cells which was observed with STIM1-EYFP. Instead, EYFP fluorescence was seen throughout the plasma membrane and in intracellular aggregates, and there was surprisingly little change in the distribution of EYFP fluorescence before and after thapsigargin. Similarly, in the study by Hauser and Tsien, CFP fluorescence was uniformly distributed throughout the plasma membrane with little reticular expression of the His_6-STIM1-CFP construct after thapsigargin treatment. Images of cells expressing His_6-STIM1-CFP were shown after thapsigargin treatment only. Surprisingly, no images were shown of cells before treatment although the authors state that, unlike the His_6-STIM1-EYFP protein used in this study, their His_6-STIM1-CFP fusion protein showed the expected ER distribution before thapsigargin stimulation. Again,

the fusion of the hexahistidine tag to the STIM1 N-terminus may be responsible for the mistrafficking of His_6-STIM1-EYFP to intracellular aggregates and to the plasma membrane. In light of these data, it is apparent that the His_6-STIM1-EYFP protein is not a suitable construct to use for investigating the trafficking and insertion of STIM1 into the plasma membrane following thapsigargin treatment, since it is already present in the plasma membrane prior to store depletion.

In conclusion, this study has identified that ATP depletion stimulates STIM1 translocation, which is not due to the disruption of microtubules, and argues for a diffusional model for STIM1 puncta formation. In addition, it has been convincingly demonstrated that a previously described His_6-STIM1 fusion protein is not suitable for use in studies to investigate the plasma membrane insertion of STIM1. It has been shown here that the plasma membrane insertion of STIM1 is not required for STIM1 puncta formation. This brings into question whether the plasma membrane insertion of STIM1 actually occurs following store depletion and whether plasma membrane STIM1 is required for SOCE.

CHAPTER FOUR

The role of phosphoinositides in STIM1 dynamics and store operated Ca^{2+} entry

4.1 Introduction

The C-terminus of STIM1 contains several distinct domains: an ezrin/radixin/moesin (ERM) domain which is conserved between both STIM1 and STIM2 proteins, a glutamate-rich domain, a serine-proline-rich region and a short lysine-rich region at the very C-terminal end of the protein. Many recent reports have identified a minimal region within the ERM domain to be essential for the clustering of Orai1 and the activation of SOCs (Kawasaki et al., 2009; Muik et al., 2009; Park et al., 2009; Wang et al., 2009; Yuan et al., 2009). A recent study by Huang et al carried out mutational analysis of each of these domains and demonstrated that the ERM and lysine-rich domains of STIM1 are required to bind and gate TRPC channels (Huang et al., 2006).

Numerous studies have also implicated the lysine-rich domain in the regulation of SOCs, since mutation or deletion of this polybasic region inhibits STIM1 puncta formation, resulting in a decrease in SOCE and its associated current, I_{CRAC} in a variety of cell types (Li et al., 2007; Liou et al., 2007; Park et al., 2009; Yuan et al., 2009). It was suggested therefore that the polybasic domain exert its role in SOCE by directing STIM1 oligomers from the bulk ER to ER-PM junctions, possibly through an interaction with some component of the ER-PM junctions which remains to be

identified (Li et al., 2007; Liou et al., 2007; Park et al., 2009). Interestingly, short polybasic regions such as that found in STIM1 are responsible for the plasma membrane targeting of many proteins. For example some small GTPases are anchored to the plasma membrane through binding to phosphorylated inositiol lipid species at the plasma membrane via short C-terminal lysine-rich regions (Heo et al., 2006).

Plasma membrane phosphoinositides have been reported to regulate the activity of a variety of ion channels and transporters (Gamper and Shapiro, 2007). There are several lines of evidence to indicate that phosphoinositides may regulate the activity of store operated calcium channels. Firstly, phosphoinositide depletion blocks both SOCE and I_{CRAC} in several cells types including platelets (Jenner et al., 1996; Rosado and Sage, 2000), rat basophilic leukemia cells (Broad et al., 2001) and COS-7 cells (Korzeniowski et al., 2009). In addition, a recent study uncovered a requirement for both PtdIns(4,5)P_2 and PtdIns(3,4,5)P_3 to regulate the plasma membrane localisation of many proteins which contain a cluster of polybasic amino acids within their C-termini (Heo et al., 2006). The polybasic region of STIM1, therefore, makes it an excellent candidate as a membrane-targeting domain via binding to phosphoinositides. It has been suggested that the phosphoinositides target STIM1 to puncta in the ER-PM junction through its polybasic domain (Liou et al., 2007), although other reports have argued against a role for phosphoinositides in STIM1 translocation (Korzeniowski et al., 2009; Varnai et al., 2007).

The current study aims to investigate the role of the phosphoinositides in the translocation of STIM1 and the activation of SOCE. The data presented in this report show that phosphoinositides may be the plasma membrane components responsible for targeting STIM1 to ER-PM junctions and reveal a role for the phosphoinositides in the regulation of SOC activity.

4.2 Results

4.2.1 Depletion of phosphoinositides using non-specific methods argues against a role for phosphoinositides in STIM1 translocation to the plasma membrane

In Chapter 3 of this study, it was demonstrated that inhibiting ATP production simulates STIM1 translocation to plasmalemmal puncta. Further studies from this lab have revealed that this is probably due to a slow release of Ca^{2+} from the ER in ATP-depleted cells (Chvanov et al., 2008). However, one of the potential effects of ATP depletion would be the depletion of phosphoinositides. To test whether the inhibition of ATP production results in phosphoinositide depletion, Rama37 cells were transfected with a GFP-tagged PH domain of $PLC_{\delta 1}$ (GFP-PH-PLC_{δ}) which associates with the plasma membrane via an interaction with $PI(4,5)P_2$ and can therefore be used as a marker for plasma membrane $PI(4,5)P_2$. 24h post-transfection, cells were treated with the PI3 and PI4 kinase inhibitor, wortmannin (20 μM), alone or with the ATP synthase inhibitor oligomycin (Olig; 5 μM) and iodoacetate (IA; 2 mM), to simultaneously block mitochondrial ATP production and glycolysis, respectively, or with a combination of both wortmannin and oligomycin/iodoacetate.

Perfusion with Olig/IA resulted in the dissociation of PH-PLC$_\delta$-GFP from the plasma membrane to the cytosol (Figure 4.1, A and B). This loss of membrane-bound GFP-PH-PLC$_\delta$ corresponds indirectly to the depletion of plasma membrane PtdIns(4,5)P_2. Quantification of GFP-PH-PLC$_\delta$ fluorescence revealed that the removal of GFP-PH-PLC$_\delta$ from the membrane was complete after 510±87 s (n=10; (Chvanov et al., 2008)). This timing precedes the timing of STIM1-EYFP puncta formation induced by ATP depletion (~600 seconds), suggesting that PtdIns(4,5)P_2 is not essential for anchoring STIM1-EYFP to the plasma membrane following Olig/IA treatment.

To determine whether PtdIns(3,4,5)P_3 is required in order for STIM1 to translocate, high concentrations of PI3 and PI4 kinase inhibitor, wortmannin (20 μM), were used to deplete PtsIns(3,4,5)P_3 in Rama37 cells transfected with GFP-PH-PLC$_\delta$. Wortmannin treatment for 30 minutes did not inhibit thapsigargin-induced translocation of STIM1-EYFP in Rama37 cells (Figure 4.1, C and D; n=2), suggesting that PtdIns(3,4,5)P_3 may not be essential to target STIM1 to the plasma membrane. Wortmannin treatment did not, however, result in the loss of GFP-PH-PLC$_\delta$ from the plasma membrane (Figure 4.1, E and F; n=8), suggesting that although such concentrations of wortmannin may deplete PtdIns(3,4,5)P_3, surprisingly they do not deplete PtdIns(4,5)P_2. In other experiments, PtdIns(3,4,5)P_3 levels were depleted by preincubating cells with wortmannin prior to prolonged combined treatment with Olig/IA and wortmannin to deplete PtdIns(4,5)P_2 levels. It was expected that such treatment would deplete both PtdIns(4,5)P_2 and PtdIns(3,4,5)P_3 at the plasma membrane. STIM1-EYFP puncta can still form even after prolonged combined

Figure 4.1

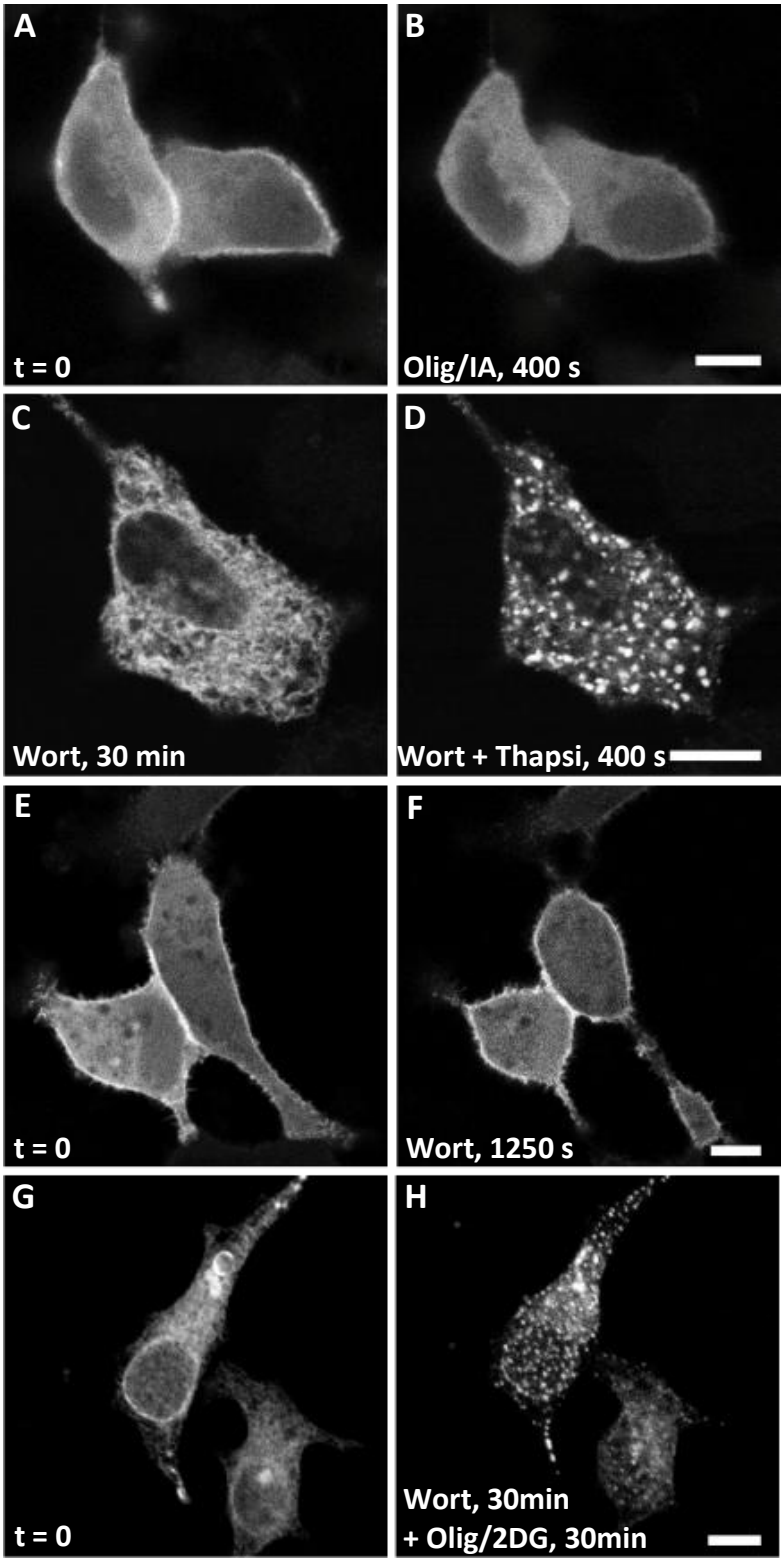

Figure 4.1 Effects of ATP depletion and Wortmannin on STIM1 translocation and PtdIns(4,5)P_2 levels. A & B: Confocal images of Rama37 cells expressing GFP-PH-PLC$_\delta$. Depleting ATP with a combination of Olig and IA results in the removal of GFP-PH-PLC$_\delta$ from the plasma membrane. **C & D:** Prereatment of cells with wortmannin (20 μM; **C**) to deplete PtdIns(3,4.5)P_3 does not prevent thapsigargin induced translocation of STIM1-EYFP (**D**). **E & F:** Confocal images of Rama37 cells expressing GFP-PH-PLC$_\delta$. Inhibition of PI3 Kinase with wortmannin does not deplete PtdIns(4,5)P_2 levels (**E and F**). Pretreatment of cells with wortmannin before ATP depletion with Olig and 2DG does not prevent STIM1 translocation (**G and H**). Times for which cells were treated with inhibitors are indicated on the individual images. Scale bars = 10 μm.

treatment with Olig/IA and wortmannin (Figure 4.1, G and H; n=2). These data could argue against a role for PtdIns(4,5)P_2 and PtdIns(3,4,5)P_3 in the formation and maintenance of STIM1-EYFP puncta.

Wortmannin has been documented as a reliable PI3 and PI4 kinase inhibitor (Downing et al., 1996). However, in the previous experiment no marker was present to indicate the levels of PtdIns(3,4,5)P_3 present at the plasma membrane before and after wortmannin treatment. A previous study by Heo et al demonstrated that the short polybasic tail of the small GTPase, Rit, binds to both PtdIns(4,5)P_2 and PtdIns(3,4,5)P_3 to anchor the protein to the plasma membrane (Heo et al., 2006). It is possible therefore, that this Rit tail may be used to monitor the expression of both phosphoinositides at the plasma membrane. To determine this, HeLa cells were transfected with an N-terminally EYFP-tagged (EYFP-Rit) or mCherry-tagged Rit tail (mCherry-Rit). 24 hours post-transfection, cells were perfused with oligomycin (Olig; 5 µM) and 2-deoxy-D-glucose (2DG; 10 mM), to simultaneously deplete ATP and PtdIns(4,5)P_2, with wortmannin to deplete PtdIns(3,4,5)P_3 or with a combination of wortmannin and Olig/2DG to deplete both phosphoinositides. Olig/2DG treatment resulted in a partial loss of the Rit tail from the plasma membrane (Figure 4.2, A; n = 13), as did wortmannin treatment (Figure 4.2, B; n = 12). This is consistent with the depletion of a single phosphoinositide species with each treatment. However, combined treatment with wortmannin and Olig/2DG resulted in a near complete dissociation of the Rit tail from the plasma membrane (Figure 4.2, C; n = 6), indicating that both PtdIns(4,5)P_2 and PtsIns(3,4,5)P_3 are both depleted under these conditions. These data confirm that the Rit tail is a suitable

marker to monitor changes in PtdIns(4,5)P_2 and PtdIns(3,4,5)P_3 levels at the plasma membrane.

In a separate approach to determine whether these phosphoinositides are required for the recruitment of STIM1 to ER-PM junctions, PtdIns(4,5)P_2 and PtdIns(3,4,5)P_3 levels were depleted by inhibiting PI3-kinase and attenuating ATP production while simultaneously monitoring STIM1 distribution and plasma membrane phosphoinositide levels. For this, HeLa cells were cotransfected with STIM1-EYFP and an mCherry-conjugated polybasic tail from the small-GTPase Rit (mCherry-Rit). 24h post-transfection, cells were treated with wortmannin for 30 min, followed by combined perfusion with the ATP synthase inhibitor oligomycin (Olig; 5 µM) and the glucose analog 2-deoxy-D-glucose (2DG; 10 mM), to simultaneously block mitochondrial ATP production and glycolysis, respectively.

Treatment with wortmannin resulted in the partial redistribution of mCherry-Rit from the plasma membrane to the cytosol, which is expected since PtdIns(3,4,5)P_3, but not PtdIns(4,5)P_2 levels were reduced (Figure 4.3, B). Subsequent perfusion with a combination of wortmannin and Olig/2DG stimulated extensive loss of mCherry-Rit fluorescence from the plasma membrane which was complete within 15 minutes (Figure 4.3, C and E), revealing that levels of both PtdIns(4,5)P_2 and PtdIns(3,4,5)P_3 are substantially depleted within 15min Olig/2DG, at which time STIM1-EYFP puncta had not formed. The qualitative changes in mCherry-Rit distribution are reflected in the quantification of plasma membrane mCherry fluorescence throughout the experiment. Wortmannin treatment results in a

Figure 4.2

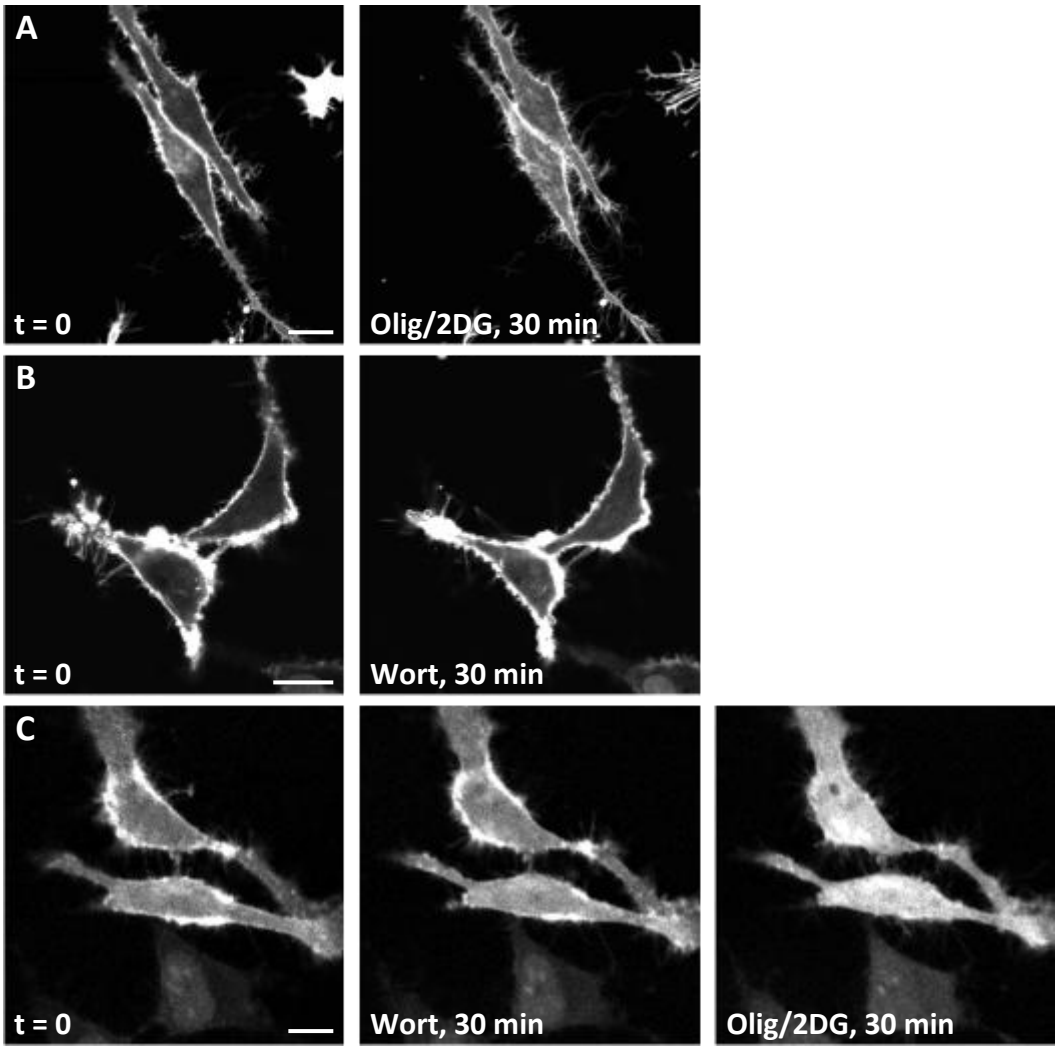

Figure 4.2 Rit tail is a marker for PtdIns(4,5)P_2 and PtdIns(3,4,5)P_3 at the plasma membrane. HeLa cells were transfected with either EYFP-Rit (**A and B**) or mCherry-Rit (**C**). Treatment with either Olig/2DG or Wortmannin alone to deplete PtdIns(4,5)P_2 and PtdIns(3,4,5)P_3, respectively, failed to induce significant redistribution of the Rit tail to the cytosol (**A and B**). However, combined treatment with Wortmannin and Olig/2DG resulted in a near complete redistribution of the Rit tail to the cytoplasm (**C**). Scale bars = 10 µm.

Figure 4.3

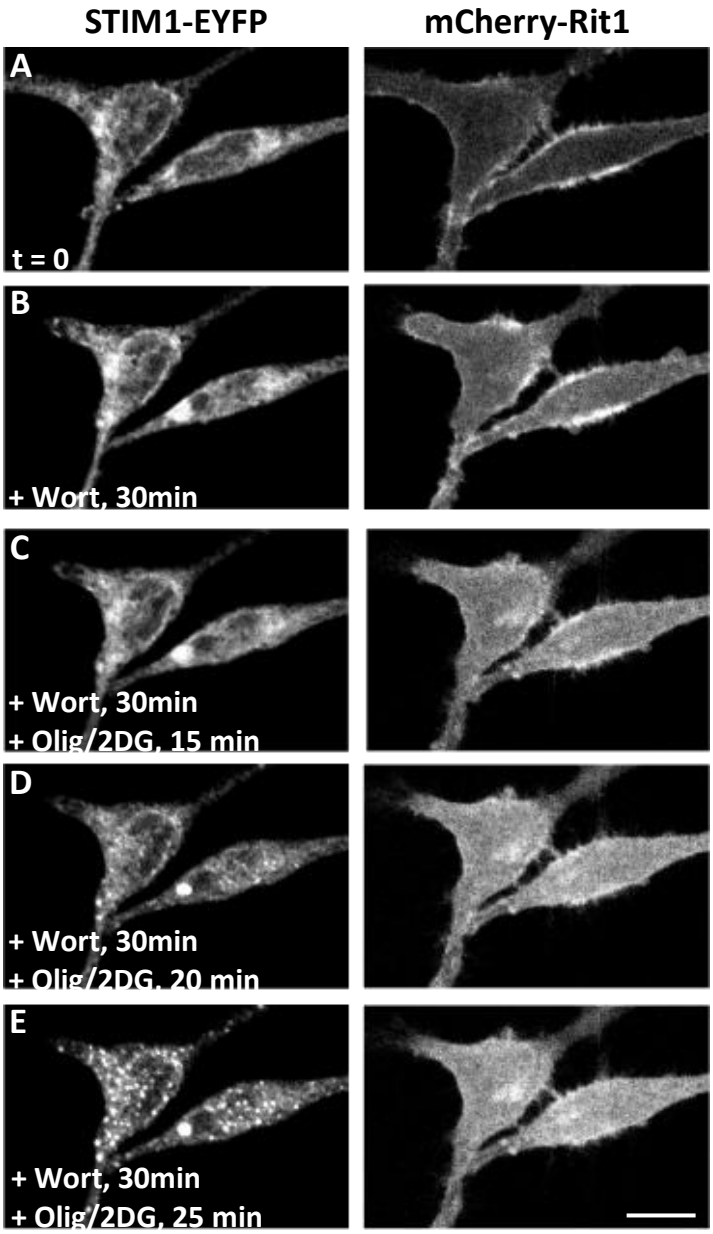

Figure 4.3. Inhibition of ATP production and of PI4 kinase does not affect STIM1-EYFP translocation. HeLa cells were cotransfected with STIM1-EYFP and mCherry-Rit. 24h post-transfection, cells were perfused initially with the PI-4 kinase inhibitor, wortmannin (20 μM) for 30 min to deplete plasma membrane levels of PtdIns(3,4,5)P_3 (**B**), followed by a combination of wortmannin and a combination of Olig/2DG to gradually deplete PtdIns(4,5)P_2 levels (**C**). STIM1 puncta formation begins after ~25 min of Olig/2DG treatment, after which time most of the Rit tail has redistributed from the plasma membrane to the cytosol (**D**). Maximal puncta formation is reached after ~30 min (**E**). Scale bar = 10 μm.

Figure 4.4

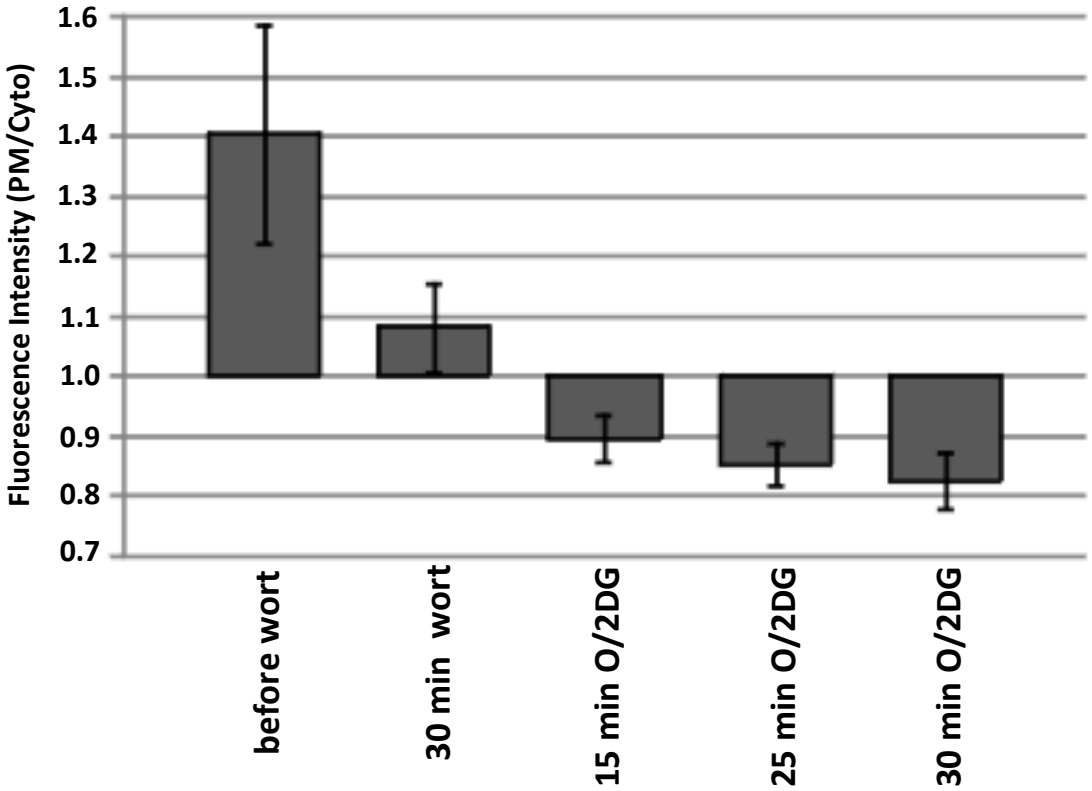

Figure 4.4 Quantification of mCherry-Rit fluorescence at the plasma membrane. HeLa cells were transfected with mCherry-Rit. 24 hours later cells were treated with wortmannin for 30 minutes, followed by a combination of Olig/2DG for 30 minutes. mCherry-Rit fluorescence at the plasma membrane was quantified before, during and after treatment. Plasma membrane fluorescence (calculated as a ratio of peripheral to cytosolic fluorescence) is diminished with a combination of wortmannin and Olig/2DG treatment, suggesting that plasma membrane PtdIns(4)P and PtdIns(4,5)P_2 levels are depleted with this combined treatment.

significant decrease in plasma membrane fluorescence, with a further significant drop after 15 minutes of Olig/2DG which does not change further with prolonged Olig/2DG treatment (Figure 4.4). These data are consistent with the observation that dissociation of mCherry-Rit is complete within 15 min Olig/2DG treatment. However, STIM1-EYFP translocation was observed to begin at approximately 25min Olig/2DG treatment with maximal puncta formation reached within ~30 minutes (Figure 4.3, D; n = 8 of 8 cells). These results suggest that STIM1 translocation can occur in the absence of plasma membrane phosphoinositides. They also question whether phosphoinositides are crucial for the targeting of STIM1 to the plasma membrane. The potential role of both PtdIns(4,5)P_2 and PtdIns(3,4,5)P_3 in STIM1 puncta formation was therefore investigated in more detail.

4.2.2 Activation of the rapamycin-inducible phosphatase results in rapid depletion of plasma membrane PtdIns(4,5)P_2

In the experiment described above, methods were employed which decreased phosphoinositide levels over a prolonged period of time while ATP was coincidentally depleted. While studies have proven that PtdIns(3,4,5)P_3 should be reliably depleted by wortmannin (Downing et al., 1996), less is known about the kinetics of PtdIns(4,5)P_2 depletion as ATP levels drop. In addition, it is probable that inhibiting ATP production will result in changes in the phosphorylation state of a wide variety of proteins within the cell. Based on the previous experiment, therefore, it is not possible to state conclusively that STIM1 translocation is not dependent on plasma membrane phosphoinositides. To overcome this problem, a previously described inducible type IV 5-phosphatase system was utilised which

enables the specific hydrolysis of PtdIns(4,5)P_2 (Suh et al., 2006; Varnai et al., 2006). This system is based on the rapamycin-stimulated heterodimerisation of two proteins: the fragment of mTOR that binds FKBP12 (FRB) and FKBP12 itself. The FRB fusion protein contains an N-terminal plasma membrane localisation signal and a C-terminal CFP (PM-FRB-CFP) or RFP (PM-FRB-RFP) tag to monitor its cellular localisation. The second protein, FKBP12 is fused to a type IV 5-phosphatase and an RFP tag (RFP-ptase-dom). This phosphatase has been modified so that it lacks a plasma membrane localisation signal, and is therefore distributed throughout the cytosol where, in the absence of rapamycin, it remains inactive. Addition of rapamycin allows the RFP-ptase-dom to move to the plasma membrane via an interaction between the FRB and FKBP12 proteins, and the phosphatase then becomes active at the plasma membrane.

In order to test the efficiency of the inducible phosphatase system to alter PtdIns(4,5)P_2 levels, HeLa cells were co-transfected with GFP-PH-PLC$_\delta$ to monitor PtdIns(4,5)P_2 levels at the plasma membrane, along with the PM-FRB-CFP and RFP-ptase-dom phospatase system. Perfusion with rapamycin (1 μm) induced the rapid translocation of the RFP-ptase-dom from the cytosol to the plasma membrane and the consequent removal of GFP-PH-PLC$_\delta$ from the plasma membrane (Figure 4.5, A). Quantification of the ratio of fluorescence intensity at the plasma membrane versus the cytosol showed that dissociation of GFP-PH-PLC$_\delta$ is complete within 2 minutes with no further significant decrease in membrane fluorescence after 2 minutes (Figure 4.5, B; n = 6), indicating that PtdIns(4,5)P_2 depletion is complete within this

Figure 4.5

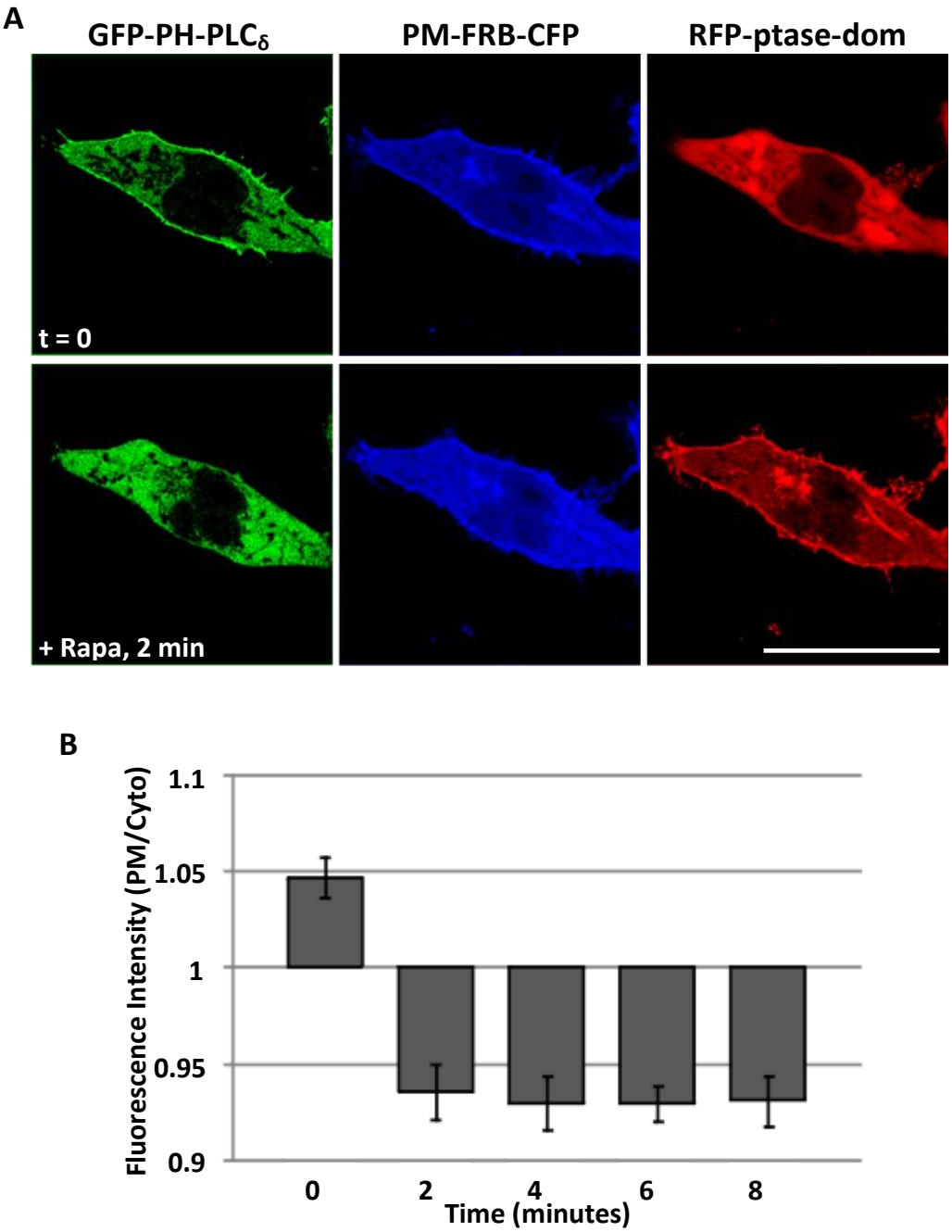

Figure 4.5 Rapid depletion of PtdIns(4,5)P_2 with a rapamycin inducible phosphatase. HeLa cells were transfected with GFP-PH-PLCδ1 and the PM-FRB-CFP/RFP-ptase-dom system. Treatment with 1 µM rapamycin (Rapa) rapidly depleted PtdIns(4,5)P_2 as shown by the removal of GFP-PH-PLC$_{\delta 1}$ from the plasma membrane to the cytosol (**A**). Quantification of fluorescence at the plasma membrane revealed that depletion was complete within 2 minutes (**B**). Scale bar = 10 µm.

timeframe. These results demonstrate that this method can be used for specifically and effectively decreasing PtdIns(4,5)P_2 levels at the plasma membrane.

To demonstrate that PtdIns(4,5)P_2 and PtdIns(3,4,5)P_3 can be rapidly and efficiently depleted by a combination of wortmannin and the inducible phosphatase, HeLa cells were transfected with EYFP-Rit and RFP chimeras of both the PM-FRB-RFP and RFP-ptase-dom constructs. In this case, there is some plasma membrane fluorescence from the RFP-PM-FRB construct prior to the addition of rapamycin but a clear translocation of the RFP-ptase-dom from the cytosol to the plasma membrane is visible following rapamycin treatment (Figure 4.6, A). It was necessary to use RFP fusion chimeras of both the FRB and phosphatase proteins so that in future experiments it was possible simultaneously monitor these proteins along with the distribution of Cerulean-Orai1 (Cer-Orai1) and STIM1-EYFP proteins in the same cell. Cells were treated with wortmannin for 30 minutes to deplete PtdIns(3,4,5)P_3. Wortmannin treatment again resulted in a partial decrease in plasma membrane EYFP fluorescence (Figure 4.6, B). Addition of rapamycin induced the translocation and activation of the RFP-ptase-dom to the plasma membrane and a subsequent rapid loss of plasma membrane EYFP fluorescence (Figure 4.6, C; n = 13).

4.2.3 Neither PtdIns(4,5)P_2 nor PtdIns(3,4,5)P_3 alone is essential for targeting STIM1 to the plasma membrane

With the PtdIns(4,5)P_2-specific inducible phosphatase system, it was possible to test whether either PtdIns(4,5)P_2 or PtdIns(3,4,5)P_3 alone was required to anchor STIM1

Figure 4.6

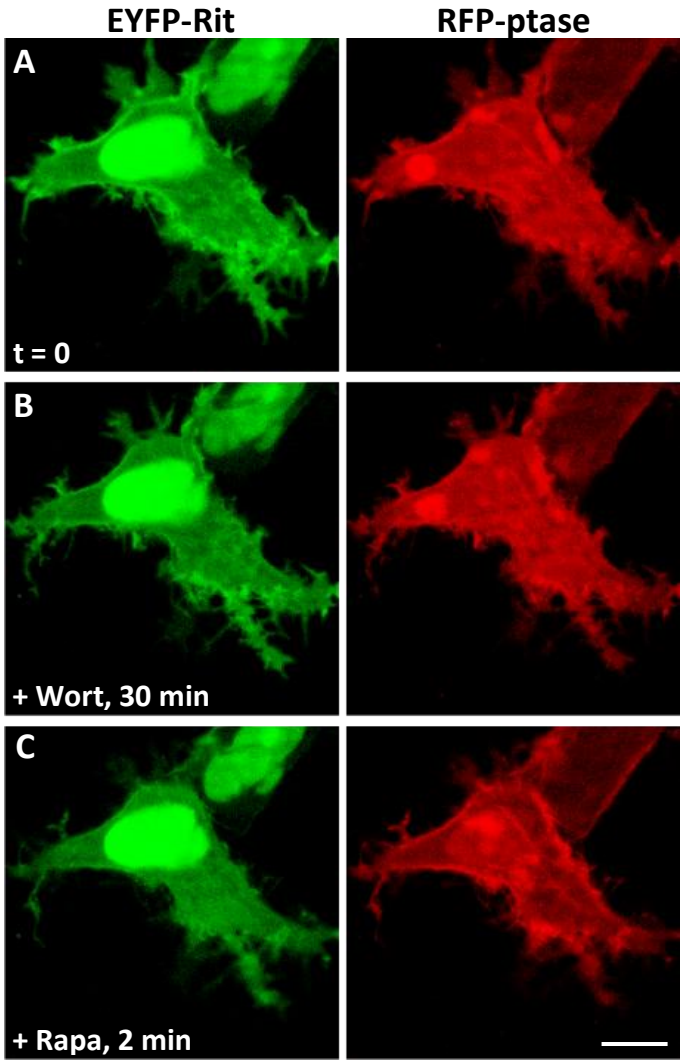

Figure 4.6 Depletion of PtdIns(4,5)P_2 and PtdIns(3,4,5)P_3 using wortmannin and a rapamycin-inducible phosphatase. (**A**) HeLa cells were cotransfected with EYFP-Rit and the PM-FRB-RFP/RFP-ptase-dom (RFP-ptase) system. (**B**) 30 minutes incubation with wortmannin stimulated a partial loss of the EYFP-Rit marker from the plasma membrane. (**C**) Subsequent addition of rapamycin induced the translocation of the phosphatase to the plasma membrane and the complete redistribution of EYFP-Rit from the plasma membrane to the cytosol. Scale bar = 10 µm.

to the plasma membrane. To determine whether STIM1 puncta formation is dependent on PtdIns(4,5)P_2, HeLa cells were transfected with STIM1-EYFP along with the PM-FRB-RFP/RFP-ptase-dom constructs. Cells were initially perfused with rapamycin for 1 minute to activate the phosphatase. Further perfusion with a combination of rapamycin and thapsigargin for 10 minutes, to deplete intracellular stores, failed to inhibit the translocation of STIM1 (Figure 4.7, A-Right panel; n = 8), suggesting that PtdIns(4,5)P_2 alone is not essential for the formation of STIM1 puncta at the plasma membrane. Quantification of the number of puncta per cell indicated, however, a 40% reduction in the mean number of puncta per cell following PtdIns(4,5)P_2 depletion (Figure 4.13) when compared with thapsigargin treated control cells (Figure 4.7A, left) indicating a partial contribution of this PtdIns(4,5)P_2 in STIM1 puncta formation.

Similarly, in cells transfected with STIM1-EYFP alone, thapsigargin-induced STIM1 translocation was still observed after pre-incubation with wortmannin to deplete PtdIns(4)P/PtdIns(3,4,5)P_3 (Figure 4.7B, right; n = 20) but the mean number of puncta was again reduced by approximately 40% (Figure 4.13) compared with thapsigargin treated control cells (Figure 4.7B, left) arguing that PtdIns(4)P and PtdIns(3,4,5)P_3, like PtdIns(4,5)P_2, are not essential but also contribute to STIM1 puncta formation.

4.2.4 Phosphoinositides together regulate STIM1 targeting to the plasma membrane

The experiments described above imply that neither PtdIns(4,5)P_2 nor PtdIns(3,4,5)P_3 alone is a sole mediator for targeting STIM1 clusters to the plasma membrane via its polybasic domain. They do not, however, rule out the possibility that both phosphoinositides are together involved in targeting STIM1 to ER-PM junctions. In order to test this, HeLa cells were transfected with STIM1-EYFP and the RFP-PM-FRB/RFP-ptase-dom phosphatase system and pretreated with wortmannin for 30 minutes (Figure 4.8, A). Perfusion with for 1 minute with rapamycin stimulated the translocation of the phosphatase to the membrane and its subsequent activation (Figure 4.8, B). Remarkably, simultaneously depleting PtdIns(4,5)P_2 and PtdIns(3,4,5)P_3 by this strategy inhibited thapsigargin-induced STIM1 puncta formation (Figure 4.8, C, n = 17), with over a 95% reduction in the numbers of puncta observed (Figure 4.13), suggesting that both PtdIns(3,4)P_2 and PtdIns(3,4,5)P_3 together do in fact mediate the association of STIM1 with the plasma membrane, as is the case for many plasma-membrane localised proteins (Heo et al., 2006).

In a second approach, similar experiments were performed using the LY294002 compound as an alternative lipid kinase inhibitor. LY294002 was used in these experiments at two different concentrations at which it has been reported previously to inhibit either PI3 kinase alone (50 μM) or both PI3 kinase and PI4 kinase (300 μM) (Downing et al., 1996). To confirm the effects of lipid kinase inhibition on STIM1 puncta formation observed with wortmannin, HeLa cells were

Figure 4.7

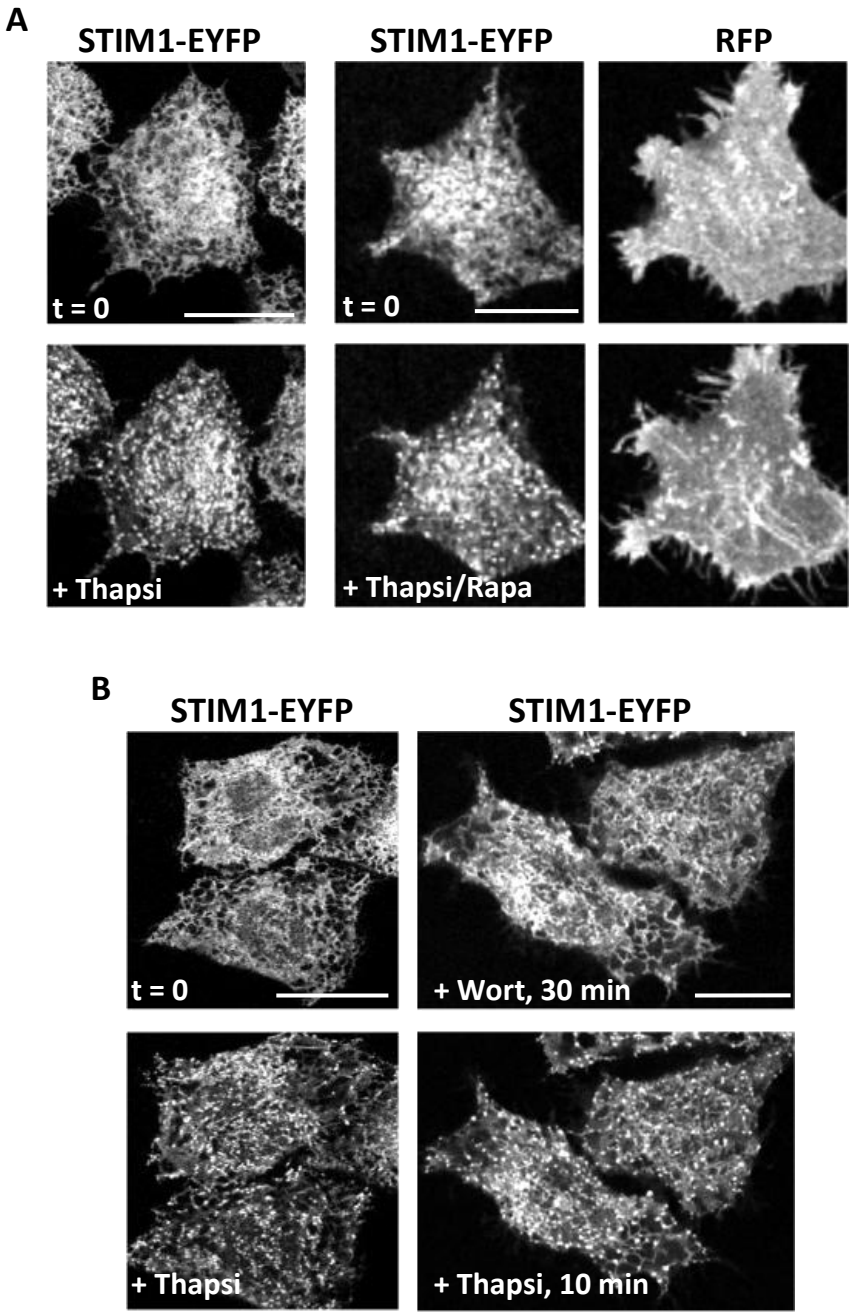

Figure 4.7 STIM1-EYFP translocation occurs in cells following depletion of either PtdIns(4,5)P_2 or PtdIns4P/PtdIns(3,4,5)P_3. HeLa cells were transfected with either STIM1-EYFP alone or cotransfected with the STIM1-EYFP, PM-FRB-RFP and RFP-ptase-dom constructs. (**A**) Control cells treated only with thapsigargin are shown on the left. In cells which overexpress all three proteins, depletion of PtdIns(4,5)P_2 by the rapamycin-inducible phosphatase did not prevent the translocation of STIM1-EYFP stimulated by thapsigargin. (**B**) Control cells treated only with thapsigargin are shown on the left. Inhibition of PI3K and PI4K by wortmannin pre-treatment did not prevent thapsigargin-induced STIM1 translocation in cells expressing STIM1-EYFP alone. Scale bars = 10 µm.

Figure 4.8

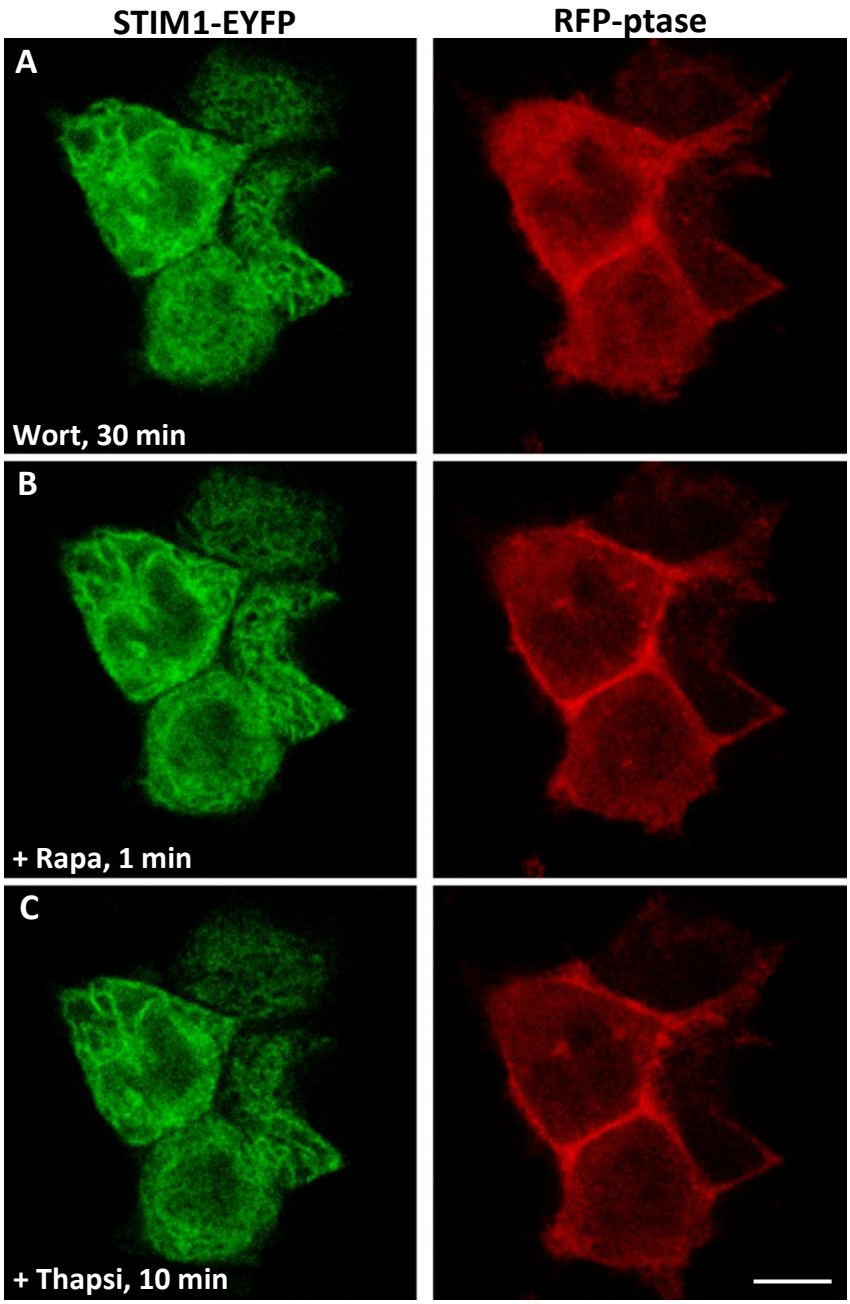

Figure 4.8 Translocation of STIM1-EYFP is inhibited by the depletion of multiple phosphoinositides in cells treated with Wortmannin. HeLa cells were cotransfected with the STIM1-EYFP, PM-FRBP-RFP and RFP-5-ptase-dom constructs. Cells were perfused with wortmannin for 30 minutes (**A**). Addition of rapamycin induces the translocation of the phosphatase domain to the plasma membrane (**B**). Addition of thapsigargin at this point to deplete intracellular Ca^{2+} stores had no effect on the distribution of STIM1, which remained in the ER (**C**). Scale bar = 10 μm.

transfected with STIM1-EYFP and pretreated with 50 µM or 300 µM of the LY294002 inhibitor alone. STIM1-EYFP translocation into puncta was still observed in response to thapsigargin treatment, although the mean number of puncta per cell was reduced. Preincubation with 50 µM inhibitor resulted in nearly a 50% reduction in the number of puncta observed after thapsigargin treatment (Figure 4.9, B; n = 19), when compared with control thapsigargin treated cells (Figure 4.9, A), which is consistent with the results obtained for PtdIns(3,4,5)P_3 inhibition with wortmannin. STIM1 puncta were reduced following incubation with 300 µM LY294002 (Figure 4.9, C; n = 21), with a 70% decrease in the mean number of puncta formed when compared with thapsigargin treated control cells.

When HeLa cells transfected with STIM1-EYFP and RFP-PM-FRB/RFP-ptase-dom were additionally treated with rapamycin to deplete PtdIns(4,5)P_2 levels, STIM1 translocation to plasmalemmal puncta was further inhibited following preincubation with 50 µM LY294002 (Figure 4.10, A; n = 21). Indeed puncta were barely visible at the higher concentration of LY294002 (Figure 4.10, B; n = 16). Quantification of the number of puncta formed per cell (Figure 4.13) indicated a significantly larger effect after rapamycin treatment compared to LY294002 alone. There was a 75% reduction in mean number of puncta per cell at the lower concentration of LY294002 after phosphatase activation with a further reduction at the higher concentration (90% inhibition) (Figure 4.13). The large effect of the low concentration of LY294002 at which PI3 kinase would be inhibited is consistent with major contributory roles for the lipids, PtdIns(4,5)P_2 and PtdIns(3,4,5)P_3 in puncta formation.

Figure 4.9

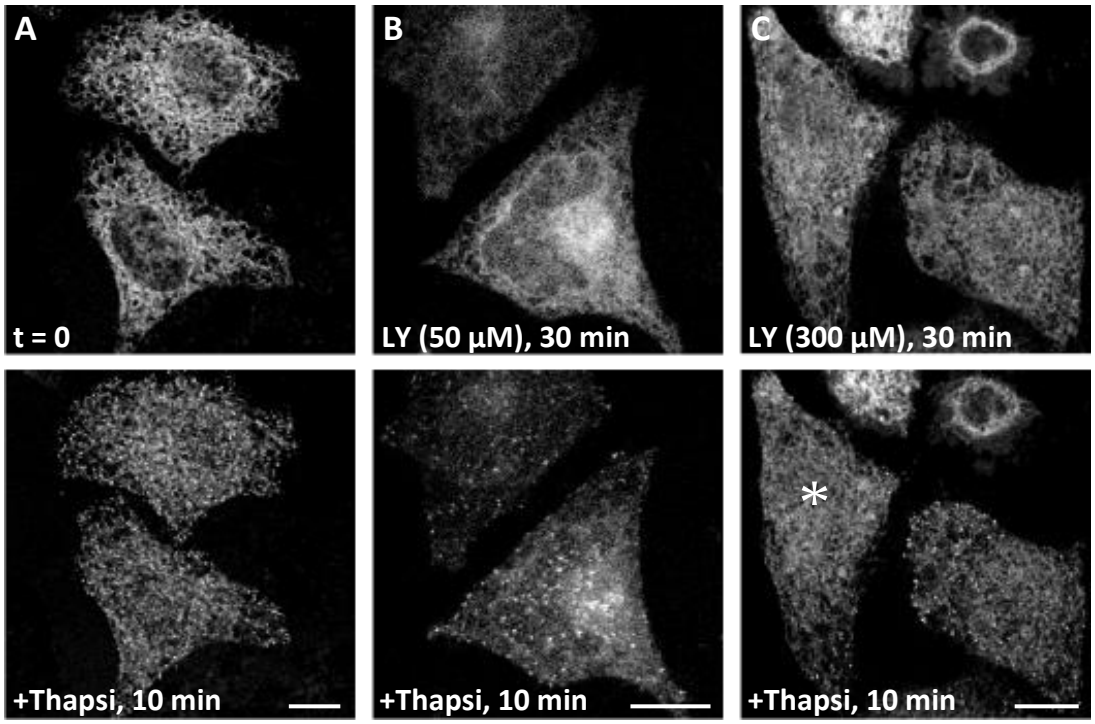

Figure 4.9. Translocation of STIM1-EYFP is partially inhibited by the depletion of multiple phosphoinositides in cells treated with LY294002. HeLa cells were cotransfected with the STIM1-EYFP, PM-FRB-RFP and RFP-ptase-dom constructs. Cells were perfused with no additions (controls) (**A**), 50 µM LY294002 (**B**) or 300 µM LY294002 (**C**) for 30 min followed by addition of thapsigargin which resulted in some STIM1 translocation into puncta under all conditions. Note that after treatment with 300 µM LY294002, few ST1M1 puncta formed in some cells (e.g. the cell marked by an asterisk). Scale bar = 10 µm.

Figure 4.10

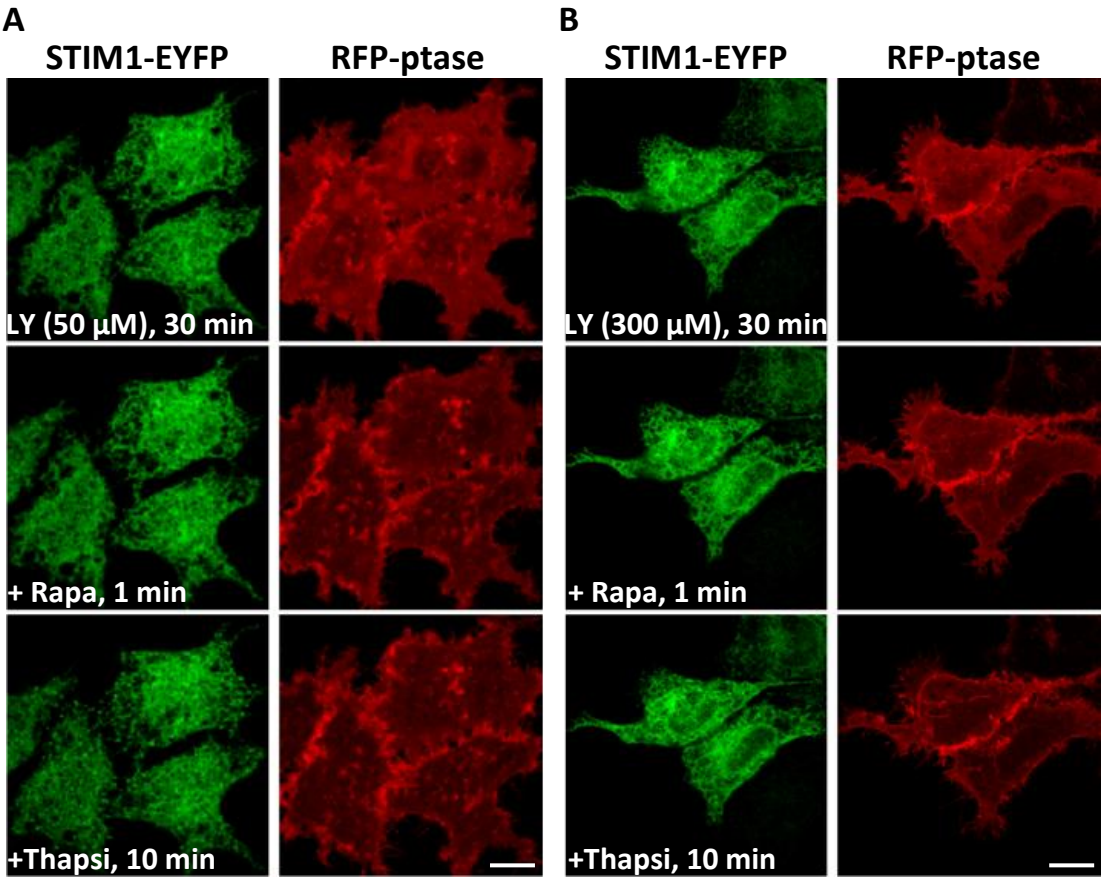

Figure 4.10 Translocation of STIM1-EYFP is inhibited by the depletion of multiple phosphoinositides in cells treated with LY294002. HeLa cells were cotransfected with the STIM1-EYFP, PM-FRB-RFP and RFP-ptase-dom constructs. Cells were perfused with 50 or 300 µM LY294002 for 30 minutes followed by addition of rapamycin for 1 minute. Addition of thapsigargin induced puncta in cells treated with 50 µM LY294002 (**A**) but pretreatment with 300 µM LY294002 resulted in near complete inhibition of STIM1 puncta formation (**B**). Scale bar = 10 µm.

Several studies have demonstrated that changes in PtdIns4P levels affect SOCE (Broad et al., 2001; Rosado and Sage, 2000). A recent report by Korzeniowski *et al* showed that PI4 kinase inhibition alone greatly reduced I_{crac} currents, suggesting that PtdIns4P rather than PtdIns(4,5)P_2 is involved in the activation of SOCE (Korzeniowski et al., 2009). The lower concentration of LY294002 used in this study is reported to have little effect on PI4 kinase activity (Downing et al., 1996) yet this concentration of the compound effectively inhibits STIM1 puncta formation. To determine whether PI4 kinase inhibition correlates with the prevention of STIM1 puncta formation by both LY294002 and wortmannin, HeLa cells were transfected with the PtdIns4P-specific PH domain reporter, GFP-PH-FAPP1 (Levine and Munro, 2002). This reporter protein binds to PI(4)P at both the golgi apparatus and the plasma membrane. Although the plasma membrane localisation of FAPPI is hardly visible using confocal microscopy (Wuttke et al., 2010), it is still a useful marker protein for studying the activity of PI4 kinase. 24 hours post-transfection, cells were treated for 10 minutes with 50 or 300 µM LY294002 or for 30 minutes with 20 µM wortmannin. Treatment with 50 µM LY294002 has little effect on the level of FAPPI fluorescence at the Golgi complex (Figure 4.11, A; n = 6), whereas treatment with either 300 µM LY294002 or wortmannin resulted in a significant loss of FAPPI fluorescence (Figure 4.11, B; n = 6). Quantification of fluorescence pre and post treatment revealed that 50 µM LY29400 caused a 20% drop in fluorescence, whereas 300 µM LY294002 stimulated a greater than 50% reduction in fluorescence (Figure 4.11, D), suggesting that PI4 kinase inhibition by the higher concentration of LY294002 is 2.5 fold greater than the inhibition observed with lower concentration of LY294002. As expected, the extent of PI4 kinase inhibition obtained using

Figure 4.11

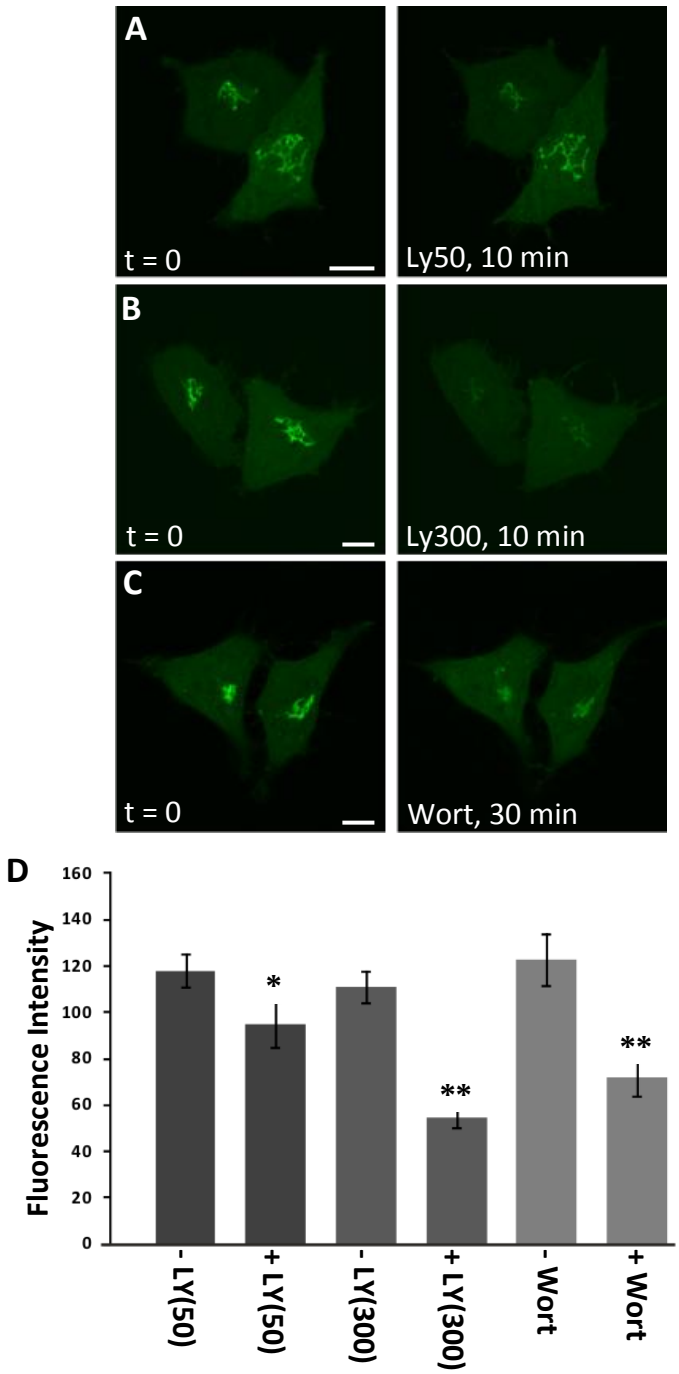

Figure 4.11 Inhibition of PI4 kinase but not PI3 kinase depletes the PtdIns(4)P-specific PH domain reporter, GFP-PH-FAPPI, from the Golgi complex. HeLa cells were transfected with FAPPI-PH-GFP and treated with a low (50 µM; **A**) or high (300 µM; **B**) concentration of LY294002 for 10 min or with wortmannin for 30 min (C). (**D**) Quantification of fluorescence at the Golgi apparatus before and after each treatment. *p<0.01; **p<0.001.

wortmannin was similar to that seen with 300 µM LY294002, with a 41% decrease in FAPP1 fluorescence (Figure 4.11, C & D; n = 6).

4.2.5 Overexpression of Orai1 rescues STIM1 puncta formation in the absence of PtdIns(4,5)P_2 and PtdIns(3,4,5)P_3

Mammalian STIM1 contains a short positively charged polybasic domain in its C-terminus. Interestingly, many small GTPases are targeted to the cell surface by an interaction with phosphoinositides through a similar polybasic tail (Heo et al., 2006). In addition, deletion or mutation of this domain has been reported in several studies to prevent STIM1 puncta formation and SOC activation (Huang et al., 2006; Liou et al., 2007), possibly by preventing its interaction with phosphoinositides. It is possible therefore, that STIM1 is targeted to phospholipids in the plasma membrane via this region. It has recently been shown, however, that overexpression of Orai1 can rescue puncta formation and SOC activation under such conditions due to the direct interaction of a separate domain within the C-terminus of STIM1 with Orai1 (Park et al., 2009). We therefore tested the prediction that STIM1 puncta formation could be restored in cells overexpressing Orai1 in addition to STIM1 under conditions where PtdIns(4,5)P_2 and PtdIns(3,4,5)P_3 are depleted. In order to do this, HeLa cells were cotransfected with STIM1-EYFP, Cer-Orai1, RFP-PM-FRB and RFP-ptase-dom and preincubated with wortmannin (Figure 4.12, A). Translocation of the phosphatase was then stimulated by the addition of rapamycin, followed by the perfusion of cells with a combination of rapamycin and thapsigargin to deplete internal stores. Interestingly, translocation of STIM1-EYFP now occurred despite the depletion of phosphoinositides in cells where Cer-Orai1

Figure 4.12

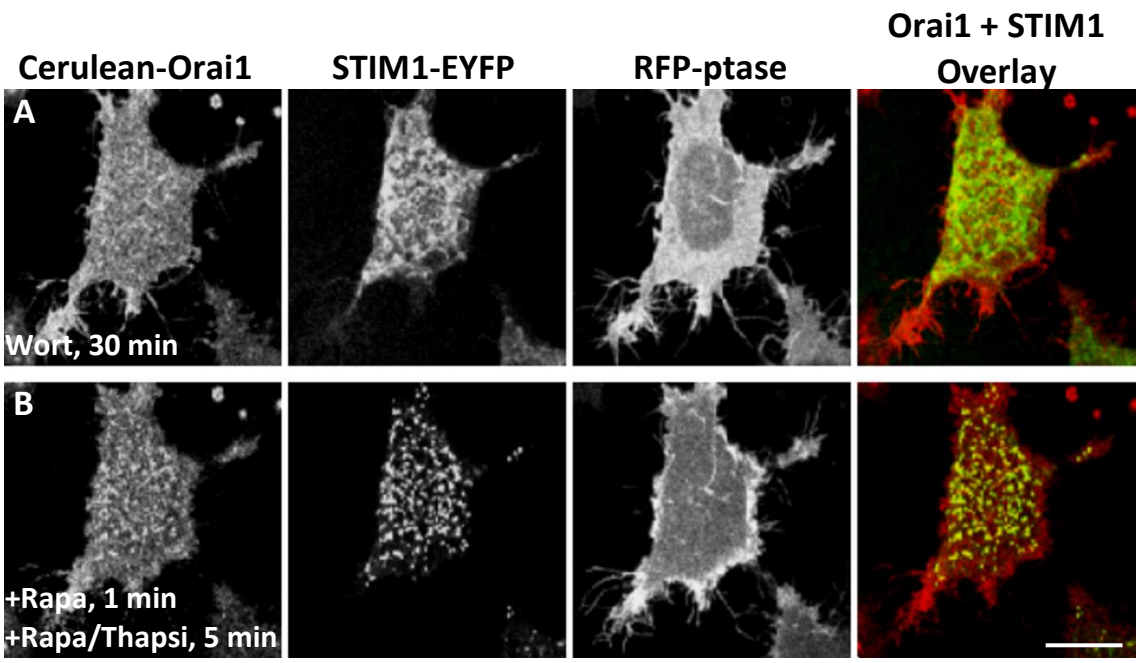

Figure 4.12 Overexpression of Orai1 rescues STIM1 puncta formation following depletion of phosphoinositides. HeLa cells were cotransfected with STIM1-EYFP, PM-FRB-RFP and RFP-5-ptase-dom constructs and Cerulean-Orai1. The cells were treated with wortmannin (A) followed by addition of rapamycin to deplete PtdIns(4,5)P_2. Overexpression of Orai1 rescued thapsigargin-stimulated translocation of STIM1 (B). Scale bar = 10 µm.

Figure 4.13

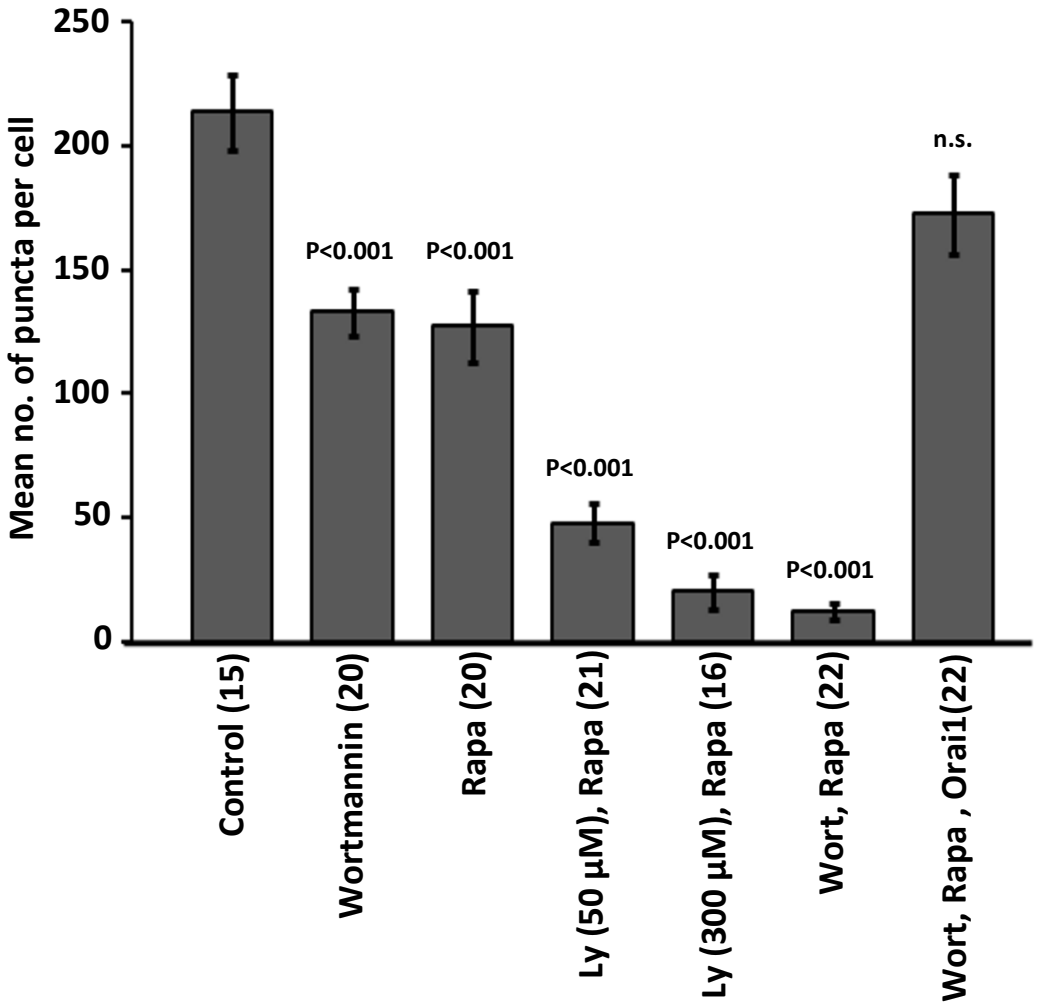

Figure 4.13. Quantification of puncta formed in response to thapsigargin treatment and the effect of depletion of PtdIns(4,5)*P*2 and inhibition of lipid kinases. Cells from the various treatments used in the study were analysed and the number of puncta formed following thapsigargin treatment counted and expressed as mean per cell ±SEM based on the number of cells indicated in the parentheses. The statistical significance of values for all conditions compared to control thapsigargin-treated cells and indicated pairwise comparisons were determined using the two-tailed Student's t-test and statistically significant differences are indicated.

was also overexpressed (Figure 4.12, B; n = 21). The mean number of puncta formed per cell was not significantly different from control cells expressing only STIM1-EYFP treated with thapsigargin (Figure 4.13). These data agree with previous reports which support a role for the polybasic region of STIM1 in targeting STIM1 to the plasma membrane but imply that a second domain within the STIM1 protein can also interact with Orai1 to independently target it to the plasma membrane for SOC activation (Kawasaki et al., 2009; Muik et al., 2009; Park et al., 2009; Wang et al., 2009; Yuan et al., 2009).

4.2.6 Phosphoinositides contribute to STIM1-mediated store operated Ca^{2+} entry

A number of recent investigations point to a crucial role for phosphoinositides in the activity of SOCs (Broad et al., 2001; Jardin et al., 2008b; Trebak et al., 2009). To determine whether the inhibition of STIM1 puncta formation by phosphoinositide depletion affects SOCE, we measured $[Ca^{2+}]_i$ in HeLa cells expressing STIM1-ECFP and the RFP-PM-FRB/RFP-ptase-dom constructs by loading them with the cytosolic Ca^{2+} indicator, Fluo4-AM. Cells were pretreated with wortmannin for 30 minutes before imaging. At the beginning of each recording, cells were perfused with either Ca^{2+}-free solution or Ca^{2+}-free solution containing 1 µM rapamycin. Thapsigargin was subsequently added to deplete intracellular stores. SOCE could be measured by reintroducing Ca^{2+} to the solution and levels of Ca^{2+} entry could then be compared between cells which had been treated with and without rapamycin. Thapsigargin induced efficient SOCE in cells where PtdIns(4,5)P_2 had not been depleted (Figure 4.14, A, red trace; n = 27). However, influx was greatly reduced in cells where phosphoinositides had been depleted (Figure 4.14, A, blue trace, n = 18). This

significant reduction was also indicated by comparison of the peak fluorescence ratio values for each trace (Figure 4.14, B), which showed a 60% reduction in peak fluorescence after phosphoinositide depletion. These data suggest that phosphoinositides at the plasma membrane contribute to SOCE under these conditions.

4.2.7 Overexpression of Orai1 restores Ca^{2+} influx in cells depleted of phosphoinositides

In Figure 4.12 it was shown that overexpression of Orai1 rescues STIM1 puncta formation in cells depleted of phosphoinositides. To investigate whether SOCE is also restored under these conditions, cells were cotransfected with STIM-EYFP and the RFP-PM-FRB/RFP-ptase-dom constructs as before but in this case untagged Orai1 was also overexpressed in the same cells. Cells were loaded with Fluo-4 and $[Ca^{2+}]_i$ was recorded as described above. Surprisingly, the increase in fluorescence intensity due to Ca^{2+} influx in cells depleted of PtdIns(4,5)P_2 and PtdIns(3,4,5)P_3 was not only rescued by Orai1 overexpression (Figure 4.15, A, blue trace, n = 15) but was slightly higher in rapamycin treated cells than control cells which had not been treated with rapamycin (Figure 4.15, A, red trace, n = 18). Comparison of the peak fluorescence ratio values revealed that influx was over 20% greater in Orai1 overexpressing cells than control cells (Figure 4.15, B). These data suggest that although phosphoinositides contribute to SOCE, they are not absolutely essential for Ca^{2+} influx and agree with previous reports which suggest that the interaction between STIM1 and Orai1 is the key for activation of store operated Ca^{2+} influx. In the experiments detailed in this report, Ca^{2+} influx appears to be somewhat larger

Figure 4.14

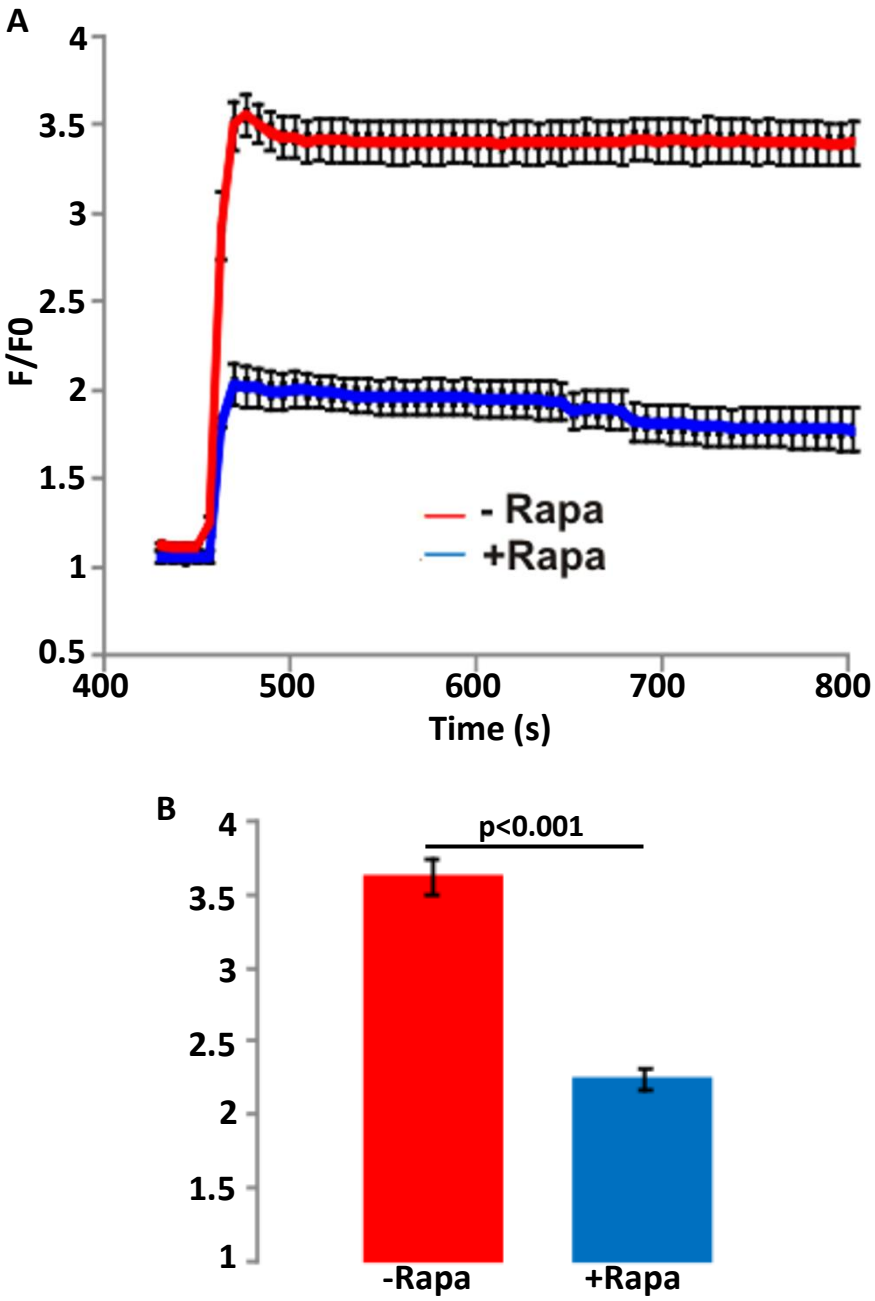

Figure 4.14 Phosphoinositide depletion rescues store operated Ca^{2+} influx in STIM1-EYFP overexpressing cells. (A) HeLa cells were transfected with STIM1-EYFP, RFP-PM-FRBP and RFP-5-ptase-dom, loaded with Fluo-4 and incubated in wortmannin for 30 min. Intracellular stores were depleted with thapsigargin. Re-addition of Ca^{2+} allowed the measurement of Ca^{2+} influx. Rapa treatment resulted in the inhibition of Ca^{2+} influx when compared to cells which had been incubated in the absence of rapa. (B) Quantification of the average peak values of Ca^{2+} influx revealed a significant decrease in peak $[Ca^{2+}]_i$ values in rapa-treated cells.

Figure 4.15

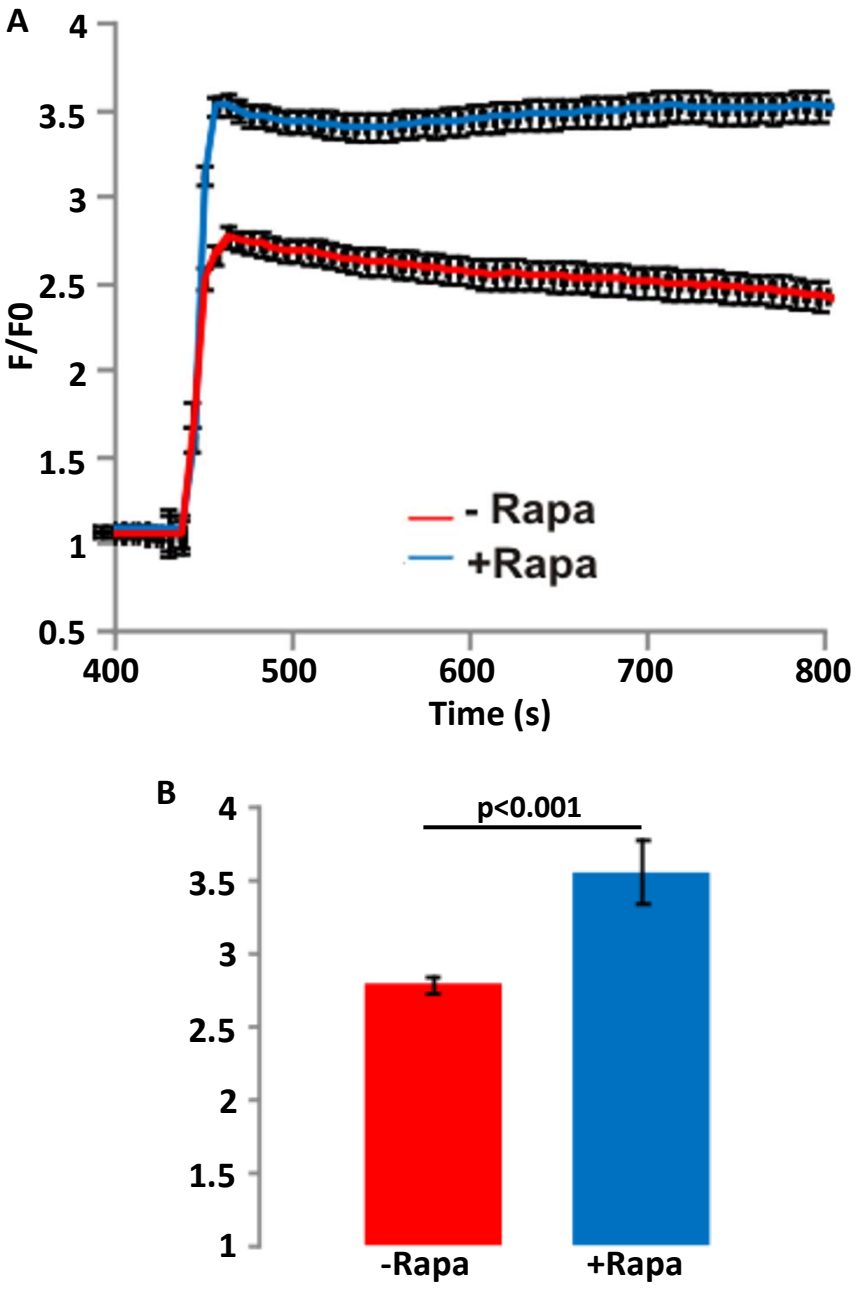

Figure 4.15 Orai1 rescues store operated Ca^{2+} influx in cells in which phosphoinositides have been depleted. HeLa cells were transfected with STIM1-EYFP, pcDNA-Orai1, RFP-PM-FRBP and RFP-5-ptase-dom and loaded with Fluo-4 and incubated in wortmannin for 30 min. Intracellular stores were depleted with thapsigargin. Readdition of Ca^{2+} allowed the measurement of Ca^{2+} influx. Ca^{2+} influx in rapa-treated cells was greater than that of cells which had not been treated with rapa, as shown in the averaged traces (A) and the peak $[Ca^{2+}]_i$ values (B).

following the depletion of phosphoinositides which may suggest that they play an additional negative role in SOCE.

4.2.8 Phosphoinositides contribute to store-operated Ca^{2+} entry mediated by endogenous STIM1

The experiments described above revealed that phosphoinositides are involved in the regulation of SOCE in cells overexpressing STIM1. In order to test whether SOCE mediated by endogenous STIM1 is affected by phosphoinositide levels, cells were transfected with the RFP-PM-FRB/RFP-ptase-dom system alone and pretreated with wortmannin for 30 minutes. Following rapamycin and thapsigargin treatment, the response to Ca^{2+} re-addition was again monitored as described above. It was possible in these experiments to make a direct comparison between non-transfected (-ptase) cells which acted as controls, and transfected (+ptase) cells in the same microscope fields. This experiment also ruled out any potential effects of rapamycin itself since all cells were simultaneously exposed to the drug. In agreement with the experiments above, rapamycin treatment resulted in reduced Ca^{2+} influx in cells expressing the phosphatase system (Figure 4.16, A, blue trace; n = 9) when compared with untransfected cells (Figure 4.16, A, red trace, n = 18). Quantification of the peak fluorescence ratio values indicated a significant 20% reduction in peak fluorescence in cells expressing the phosphatase system versus control cells (Figure 4.16, B). These data suggest that phosphoinositides are involved in the regulation of endogenous STIM1 mediated SOCE.

Figure 4.16

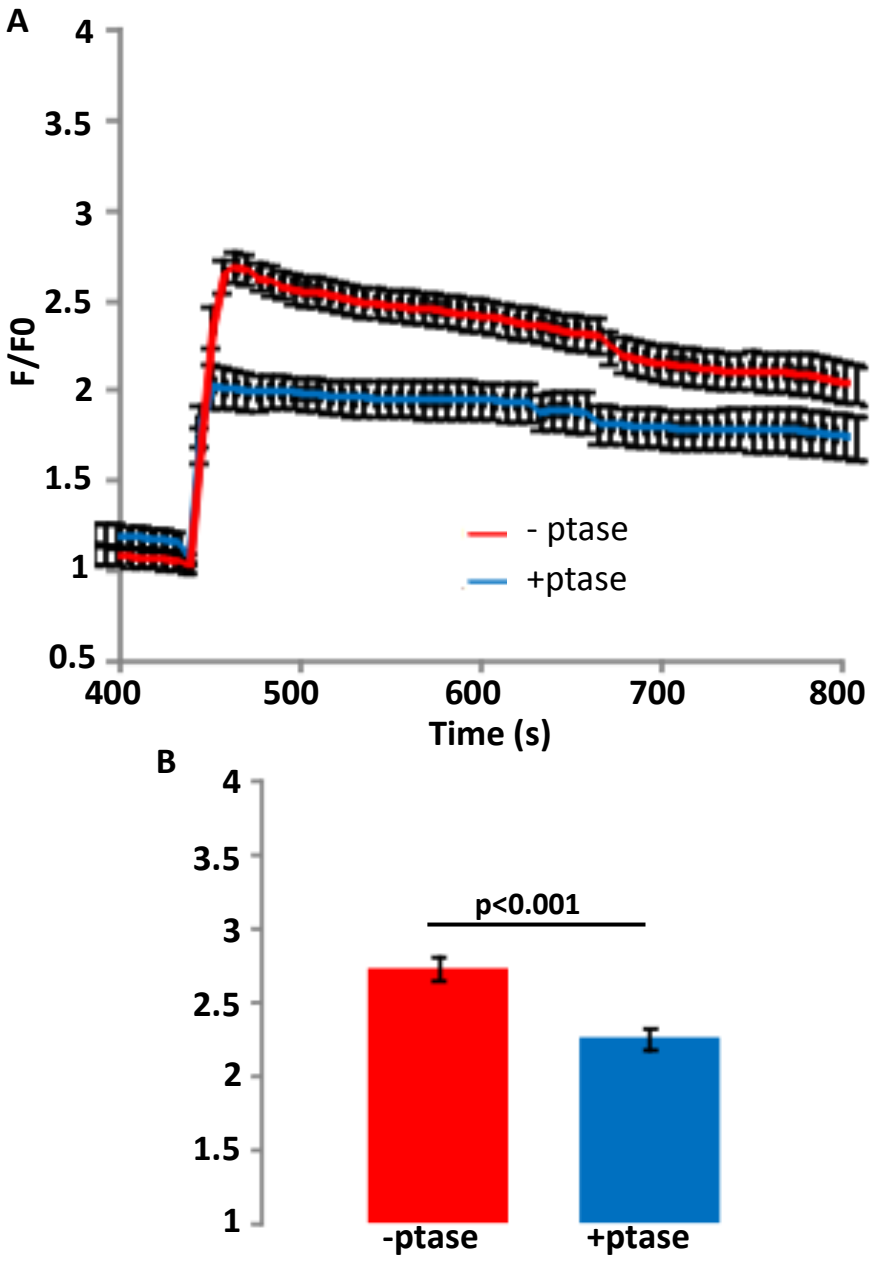

Figure 4.16 Phosphoinositide depletion reduces store-operated Ca^{2+} influx due to endogenous STIM1. Cells were transfected with RFP-PM-FRBP and RFP-ptase-dom. 48h post-transfection, cells were loaded with Fluo-4, incubated with wortmannin for 30 min and treated with rapamycin before thapsigargin treatment and readdition of Ca^{2+} to the external solution after 620s. In this experiment $[Ca^{2+}]_i$ was monitored in transfected and nontransfected cells in the same microscope fields and directly compared so that all cells had been treated with rapamycin.

4.3 DISCUSSION

Recent reports have established that the ER protein, STIM1, regulates SOCE by translocating to ER-PM junctions following intracellular store depletion and that this can be visualised as the formation of STIM1 aggregates known as “puncta” (Wu et al., 2006a; Xu et al., 2006; Zhang et al., 2005). The site of STIM1 puncta at the plasma membrane is critical for SOCE. STIM1 clustering has been suggested to be in part determined by lipid raft domains which anchor it to the plasma membrane (Pani et al., 2008), but the constituent(s) within the plasma membrane responsible for this have not been identified. There are several lines of evidence suggesting that the phosphoinositides might be involved in STIM1 translocation. Firstly, several studies have pointed to a role for plasma membrane phosphoinositides in the activity of store operated Ca^{2+} channels in a variety of cell types (Broad et al., 2001; Jardin et al., 2008b; Rosado and Sage, 2000). In addition, a recent study uncovered a requirement for both PtdIns(4,5)P_2 and PtdIns(3,4,5)P_3 to regulate the plasma membrane localisation of many proteins which contain a cluster of polybasic amino acids within their C-termini (Heo et al., 2006). The polybasic region of STIM1, therefore, makes it an excellent candidate as a membrane-targeting domain through binding to phosphoinositides.

The aim of the present study was to investigate whether the phosphoinositides are required for STIM1 puncta formation. Several methods were used to individually or simultaneously reduce PtdIns4P, PtdIns(4,5)P_2 and PtdIns(3,4,5)P_3 levels and to study the effects of phosphoinositide depletion on the formation of STIM1 puncta

at ER-PM junctions triggered by both ATP depletion and Ca^{2+} store depletion. The consequence of phosphoinositide depletion on STIM1-mediated SOCE was also tested. Initially, depletion of phosphoinositides was carried out using a combination of both high dose wortmannin treatment at levels which have been shown to inhibit both PI3 kinase and PI4 kinase (Broad et al., 2001) and ATP depletion (Chvanov et al., 2008). Under these conditions, STIM1 translocation still occured even though levels of both PtdIns(4,5)P_2 and PtdIns(3,4,5)P_3 were reduced as shown by dissociation of the mCherry-Rit reporter from the plasma membrane before the first signs of puncta formation. Although this argues against a role for the phosphoinositides in the translocation of STIM1, it is possible that since ATP depletion would alter the state of phosphorylation of many proteins, this treatment may have other effects on processes which function in regulating the localisation of STIM1. For example, inhibiting ATP production may be uncovering an inhibitory mechanism which normally prevents the aggregation of STIM1 oligomers in puncta. Alternatively ATP depletion may not deplete the phosphoinositides sufficiently or rapidly enough. It was clear that a more specific and more rapid method for the depletion particularly of PtdIns(4,5)P_2 was required to investigate the specific roles of each of the phosphoinositides in STIM1 translocation. For this reason, we used an inducible phosphatase system, which has recently been reported to specifically and reliably deplete PtdIns(4,5)P_2 levels (Suh et al., 2006; Varnai et al., 2007). The data presented in this study reveal a contribution of phosphoinositides to the recruitment of STIM1 to puncta, since puncta formation was inhibited under conditions that would deplete PtdIns4P, PtdIns(4,5)P_2 and PtdIns(3,4,5)P_3. Interestingly, puncta formation was partially affected by the singular depletion of

either PtdIns(4,5)P_2 or PtdIns4p/PtdIns(3,4,5)P_3 but depletion of all phosphoinositides was required for the near complete inhibition of puncta formation suggesting that STIM1 requires a combination of multiple phosphoinositides for maximal puncta formation.

These data complement previous reports which have shown that the STIM1 polybasic domain plays a role in STIM1 function at the plasma membrane (Li et al., 2007; Liou et al., 2007; Park et al., 2009; Yuan et al., 2009). Several hypotheses have been put forward for the function of the polybasic domain in STIM1. Some have suggested that it interacts directly with Orai1 to regulate the activity of the channel (Yuan et al., 2009), while others have proposed that it is targeted to the plasma membrane by an interaction with some constituent(s) within the plasma membrane itself (Li et al., 2007; Liou et al., 2007; Park et al., 2009). To this end, it has been suggested that the polybasic domain may direct the recruitment of STIM1 to ER-PM junctions by binding directly to phosphoinositides via electrostatic interactions as is the case for small GTPases with polybasic tails (Heo et al., 2006). Our studies are consistent with this hypothesis.

The data presented here also show that the phosphoinositides also contribute to SOCE since depletion of phosphoinositides significantly reduced thapsigargin induced Ca^{2+} entry. Extensive phosphoinositide depletion resulted in a 94% reduction in STIM1 puncta formation but only a 60% overall reduction in the peak of normalised Fluo4 response. It should be noted, however, that the fluorescence ratio is not linearly related to $[Ca^{2+}]_i$ and this will lead to an underestimate of the

degree of inhibition of SOCE, suggesting that phosphoinositides do play a crucial role in SOCE activity under these conditions. The finding that depletion of individual phosphoinositides results in the partial inhibition of STIM1 puncta formation is consistent with previous findings that inhibition of PI3 kinase (Hsu et al., 2000) and PI4 kinase (Nakanishi et al., 1994; Watanabe et al., 1996) affects agonist-induced Ca^{2+} influx. In addition, some studies have reported the inhibition of SOCE and I_{CRAC} by the simultaneous inhibition of both PI3 kinase and PI4 kinase(Broad et al., 2001; Rosado and Sage, 2000). Broad *et al* used high levels of wortmannin to inhibit both PI3 and PI4 kinases and consequently blocked both Ca^{2+} influx and I_{CRAC} in rat basophilic leukemia cells (Broad et al., 2001). The authors noted that this effect was not due to a decrease in IP3 and DAG production but could not determine the precise mechanism for the phosphoinositides in SOC activity. Rosado *et al* used LY294002 to inhibit both PI3 and PI4 kinase activity in platelets and suggested that they are involved in mediating Ca^{2+} entry through a mechanism which involves reorganisation of the actin cytoskeleton following store depletion (Rosado and Sage, 2000). However, our data imply that it is probable that the phosphoinositides contribute to the regulation of Ca^{2+} influx through the recruitment of STIM1 to the plasma membrane following store depletion, since STIM1 puncta formation was substantially inhibited when plasma membrane phosphoinositides were depleted by treatment with either wortmannin or LY294002 and hydrolysis of PtdIns(4,5)P_2 by an inducible phosphatase. The lower concentration of LY294002 that was used in the present study has been reported to have little effect on PI4 kinases (Downing et al., 1996). We established that at the low (50 μM) concentration of LY294002, dissociation of the PtdIns4P-specific PH domain reporter FAPPI (Levine and Munro,

2002) as a marker of PI4 kinase inhibition from the Golgi complex was 2.5 fold less than at the high (300 μM) concentration. The effectiveness of the higher concentration of LY294002 in inhibiting STIM1 puncta formation is consistent with key roles for the two lipids PtdIns(4,5)P_2 and PtdIns(3,4,5)P_3 although based on these experiments an additional contribution of PtdIns4P cannot be ruled out.

A recent study (Park et al., 2009) showed that a truncated STIM1 protein lacking the polybasic domain fails to form puncta when expressed alone in HEK293 or HeLa cells but does redistribute into puncta and activate I_{CRAC} when coexpressed with Orai1 in the same cells, thereby accounting for the different effects reported of deletion of this domain. This led to the proposal of two separate mechanisms for the recruitment of STIM1 to the plasma membrane. STIM1 can be anchored to the plasma membrane via a direct interaction of a region within its C-terminal ERM domain with Orai1 (Kawasaki et al., 2009; Muik et al., 2009; Park et al., 2009; Wang et al., 2009; Yuan et al., 2009). Alternatively, STIM1 can be recruited to ER-PM junctions via an Orai1-independent mechanism involving its polybasic domain (Li et al., 2007; Liou et al., 2007; Park et al., 2009). It has been proposed that under physiological conditions, the polybasic domain may initially direct STIM1 oligomers to ER-PM junctions and thereby facilitate its interaction with and activation of Orai1 (Park et al., 2009). This dual targeting mechanism seems to be a vertebrate adaptation since the polybasic domain is present only in vertebrate STIM homologues. In this study, it was observed that STIM1 can effectively form puncta in cells depleted of plasma membrane phosphoinositides when Orai1 is overexpressed in the same cells, suggesting that the binding of STIM1 to the

phosphoinositides is not essential for puncta formation. This report also investigated whether SOCE was recovered following phosphoinositide depletion by the overexpression of Orai1. Note that in these experiments overexpression of both STIM1 and Orai constructs in control cells did not produce an increase in SOCE above that seen with overexpression of STIM1 alone as described in other studies (Mercer et al., 2006; Peinelt et al., 2006; Soboloff et al., 2006b). These previous observations have however been obtained from studies of HEK293 cells in which there is little endogenous SOCE (Mercer et al., 2006; Peinelt et al., 2006; Soboloff et al., 2006b) and possibly low levels of endogenous Orai1 expression.

The results in this study showed that Orai1 overexpression resulted in a recovery of SOCE in cells depleted of phosphoinositides. These observations support the hypothesis that there are two mechanisms involved in STIM1 targeting to the plasma membrane. In addition, Ca^{2+} influx was restored to above that of control levels in these cells. These data agree with several recent reports which suggest that the interaction between the ERM domain of STIM1 and Orai1 is necessary and sufficient for the activation of SOCs and does not require the polybasic domain (Kawasaki et al., 2009; Muik et al., 2009; Park et al., 2009; Wang et al., 2009; Yuan et al., 2009). These results also suggest two potential functions for the phosphoinositides in SOCE. Under physiological conditions, the phosphoinositides may contribute to the activation of SOCE by increasing the recruitment of STIM1 to ER-PM junctions, thereby increasing the likelihood of an interaction between STIM1 and Orai1 for the activation of Ca^{2+} influx. Additionally, they might regulate the ability of STIM1 to activate SOCs when bound to Orai1, since Ca^{2+} influx is enhanced

in the absence of the phosphoinositides in cells coexpressing Orai1. It is possible that in the absence of the phosphoinositides the ERM domain of STIM1 is exposed, resulting in enhanced binding of the ERM domain to Orai1 and consequently increased Ca^{2+} influx. Enhanced activation of SOCS by a STIM1 protein which lacks a functional polybasic domain has previously been observed in cells coexpressing Orai1 (Yuan et al., 2009). This regulatory mechanism may therefore be required under physiological conditions to prevent over-activation of the channels and may have evolved in vertebrates as an additional mechanism to protect cells against Ca^{2+} toxicity.

A recently publish report investigated the role of the phosphoinositides in STIM1 and Orai1 mediated Ca^{2+} entry and found only a small effect of phosphoinositide depletion on STIM1 puncta formation (Korzeniowski et al., 2009). The experimental approach used in that study differed from that in the present paper since STIM1 translocation and puncta formation were stimulated before subsequently depleting the phosphoinositides using a combination of the PtdIns(4,5)P_2-specific inducible phosphatase system and high concentration of LY294002 which should inhibit both PI3 and PI4 kinase. It is possible that in these experiments, the preformed STIM1 puncta might render PtdIns(4,5)P_2 inaccessible to the phosphatase, thereby preventing its efficient hydrolysis. In the present report, stimulation of STIM1 puncta formation by store depletion was only carried out after the cells were treated with a combination of either wortmannin or LY294002 and the inducible phosphatase. This would, thereby, ensure a reduction in the levels of plasma membrane phosphoinositides prior to puncta formation. This method proved to be

effective in preventing STIM1 puncta formation. Korzeniowski et al (Korzeniowski et al., 2009) showed that PLC activation or PI3 kinase/PI4 kinase inhibition by LY294002 reduced both I_{CRAC} and SOCE in COS-7 cells, even under conditions where PtdIns(4,5)P_2 levels remained unchanged, suggesting that PtdIns(4)P rather than PtdIns(4,5)P_2 is the major phosphoinositide required for activation of SOCs. Similarly, in our experiments we noted a significant difference in peak cytosolic Ca^{2+} influx values in cells depleted of phosphoinositides. These data suggest that PtdIns(4,5)P_2 and PtdIns(3,4,5)P_3 are the key lipids involved in targeting STIM1 to ER-PM junctions.

Although the present study provides evidence for a role for phosphoinositides in STIM1 targeting to the plasma membrane, it has not investigated whether a direct interaction between the STIM1 polybasic domain and phosphoinositides occurs. Since the completion of the present study, a separate report was published which provided evidence for a direct interaction between the STIM proteins and phosphoinositides. In their study, Ercan *et al* used GFP-tagged recombinant C-termini of both STIM1 and STIM2 to show that they bind to phosphoinositides in phosphoinositide-containing liposomes. In addition, they demonstrated that STIM1 requires an intact coiled-coil domain and the polybasic lysine-rich domain for this interaction to occur (Ercan et al., 2009). This suggests that multimerisation of STIM1 is necessary to enable its binding to phosphoinositides at the plasma membrane. This study confirms that STIM1 does in fact interact with phosphoinositides at the plasma membrane and provides additional evidence for the involvement in phosphoinositides in the regulation of SOCE.

In summary, the present study confirms that there are two distinct modes of STIM1 translocation to the plasma membrane. One involves a direct interaction between STIM1 and Orai1, the other occurs through the potential binding of the cationic polybasic tail of STIM1 to anionic phosphoinositides in the plasma membrane. This study proposes two functions for this interaction in the regulation of SOCE. Initially, the phosphoinositides may target STIM1 to ER-PM junctions to facilitate its subsequent interaction with Orai1 at these sites. In addition, the potential binding of the polybasic domain of STIM1 to phosphoinositides may regulate the activity of the Orai1 channel by determining the extent of STIM1-Orai1 binding. Further studies are required to confirm a direct interaction between full length STIM1 and the various phosphoinositides and to determine the extent to which each phosphoinositide species contributes to the activity of store operated Ca^{2+} channels.

CHAPTER FIVE

Evidence for an interaction between Golli and STIM1 in store operated Ca^{2+} entry

5.1 Introduction

A recent paper by Varnai et al suggested that STIM1 and Orai1 form part of a large macromolecular complex which may indicate the presence of other proteins within STIM1-Orai1 clusters (Varnai et al., 2007). One potential candidate for this is Golli protein, encoded by the myelin basic protein (MBP) gene. Golli proteins are alternative splice isoforms of the classic MBP proteins (Feng et al., 2004). The alternative splicing of the MBP and Golli proteins is outlined in Figure 5.1. Unlike MBP, which is a major constituent of myelin in the nervous system, Golli proteins are expressed ubiquitously although their function is not well understood.

The BG21 isoform of Golli (Golli-BG21) is expressed at high levels in T-cells (Campagnoni et al., 1993) where it acts as a negative regulator of T-cell activation (Feng et al., 2004). T-cells from Golli-deficient mice are hyperproliferative and exhibit increased IL-2 production (Feng et al., 2006). It has been shown that this is due to enhanced SOC influx in Golli-deficient cells, suggesting that Golli is a negative regulator of SOCE (Feng et al., 2006). Conversely, overexpression of Golli-BG21 in Jurkat T cells results in decreased SOC influx (Feng et al., 2006). Golli-BG21 also regulates voltage-gated and store-operated calcium channels to mediate the migration and proliferation of oligodendrocyte precursor cells (Paez et al., 2009a; Paez et al., 2009b; Paez et al., 2007).

Figure 5.1

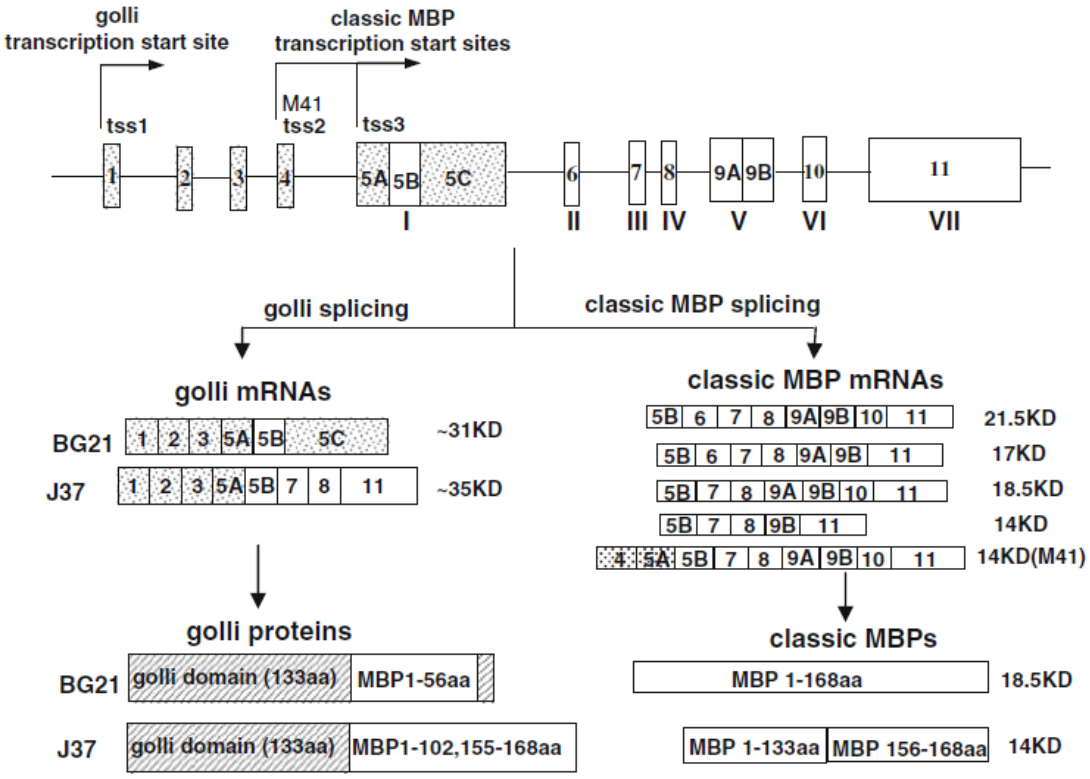

Figure 5.1 Schematic of the MBP gene and its products. There are three transcription sites within the MBP gene. The first transcription start site generates the Golli transcripts, whilst the second and third transcription start sites generate the classical MBPs. Golli specific exons are highlighted in grey. The Golli proteins, BG21 and JL37, share a common N-terminal "golli domain" and their C-termini contain variable epitopes of the MBP sequence. ***Figure taken from (Feng, 2007).***

Interestingly, a fraction of Golli-BG21 is constitutively localised to lipid rafts at the plasma membrane and this plasma membrane association increases following T-cell stimulation (Feng et al., 2006). Mutation of the N-terminal Golli myristoylation site required for plasma membrane association abolishes its ability to regulate Ca^{2+} influx (Feng et al., 2006). Golli-BG21 does not affect the IP_3-dependent release of Ca^{2+} from internal stores but rather regulates store depletion induced Ca^{2+} entry itself (Feng et al., 2006). It is not yet known how Golli-BG21 regulates SOC activity in T-cells, whether it is due to a direct effect on the channel itself or through the regulation of the signalling pathway responsible for SOC activation or inactivation.

The current study aimed to find new interacting proteins for STIM1 and Orai1 using the cytosolic domains of both proteins as baits in yeast 2-hybrid library screening analysis and also as GST-fusion proteins for pulldown assays. The data presented revealed a novel interaction of STIM1 with Golli-BG21. The results also show that STIM1 interacts with Golli-BG21 in puncta and suggest that down-regulation of SOCE is the likely consequence of this interaction.

5.2 Results

5.2.1 Yeast 2-hybrid screening approach to find novel STIM1 and Orai1 binding partners

A recent report suggested that STIM1-Orai1 complexes at the plasma membrane may contain additional molecular components (Varnai *et al.*, 2007), suggesting that STIM1 and Orai1 may interact with other proteins to modulate SOC channel

activity. In spite of this, few interacting partners have been found for the STIM1 and Orai1 proteins. To search for novel interacting partners for STIM1 and Orai1, a high-throughput yeast 2-hybrid (Y2H) screening approach was used. This approach is commonly used to study binary protein-protein interactions. In this study, we employed a Gal-4 based Y2H assay, in which a "bait" protein of interest is fused to the binding domain (BD) of the Gal-4 transcription factor, while a library of "prey proteins" are expressed as fusion proteins containing the activation domain (AD) of Gal-4. When a bait and prey protein pair interact, the binding domain and activation domain come into close proximity to enable transcription of four reporter genes: ADE2, HIS3, MEL1 and LacZ.

For bait protein construction, the genes of interest (i.e the cytosolic domain of STIM1 (STIM1-CT) and the cytosolic domains of Orai1 (Orai1-CT and Orai1–NT)) were PCR amplified with primers containing forward and reverse flanking sequences and used for in vivo recombinant gap repair cloning into the pGBKT7 Y2H bait vector as described previously (Semple et al., 2005) so that the resulting bait proteins were N–terminally fused to the Gal4 binding domain. Since the pGBKT7 bait vector encodes the TRP1 gene, positively transformed Mata (AH109) yeast cells were selected for by growth on synthetic defined agar lacking tryptophan (SD-W). Positive colonies were screened for the presence of the bait of interest by PCR using bait-specific primers to ensure that vector contained the correct sized insert. Occasionally, recombinant bait proteins can alone activate transcription of reporter genes in haploid yeast to generate Y2H false positives, without the need for a prey protein. Such baits are known as autoactivators. To test for autoactivators, positive

Figure 5.2

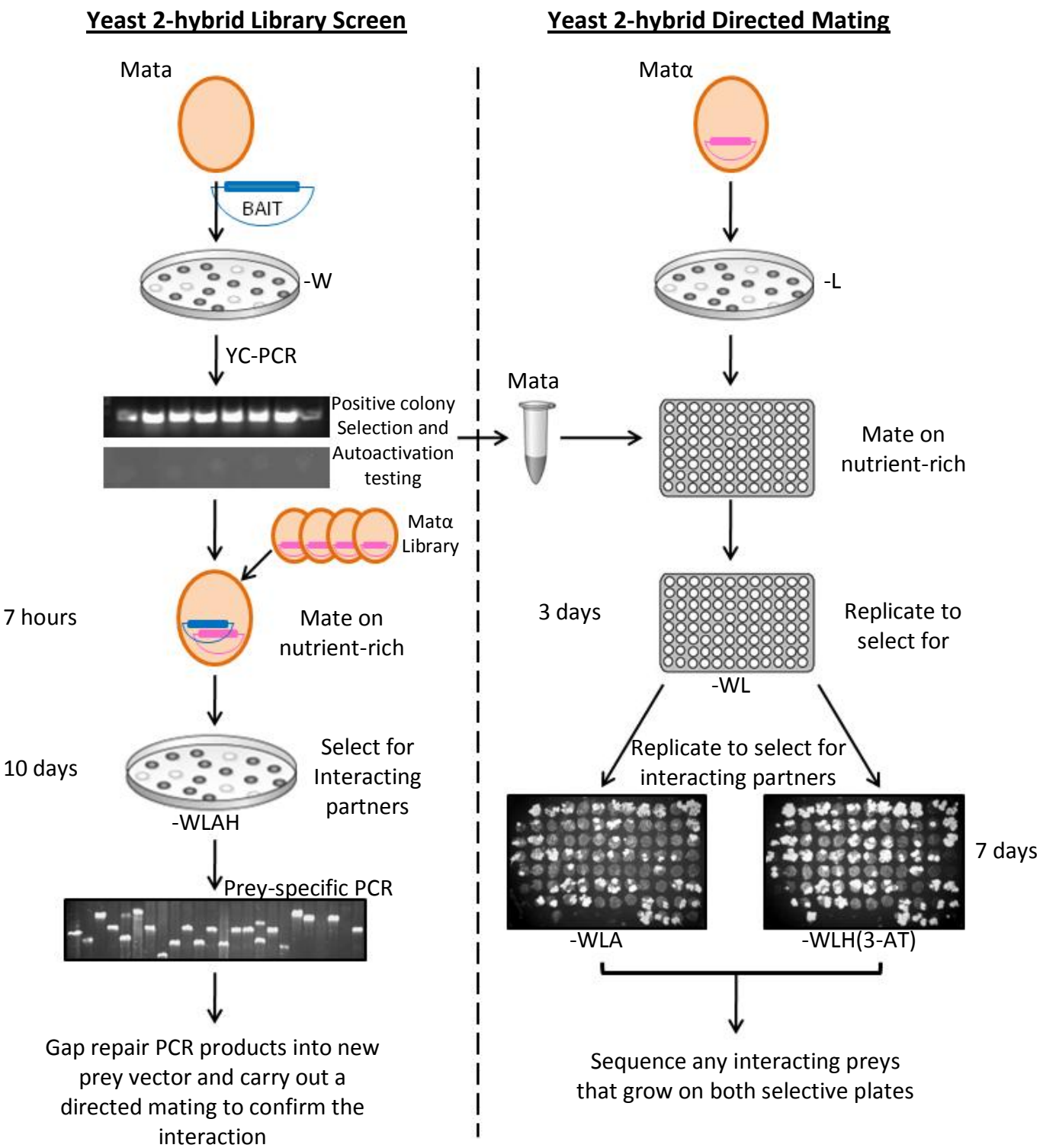
Yeast 2-hybrid Library Screen
Yeast 2-hybrid Directed Mating
Mata
BAIT
-W
YC-PCR
Positive colony Selection and Autoactivation testing
Matα Library
7 hours
Mate on nutrient-rich
10 days
Select for Interacting partners
-WLAH
Prey-specific PCR
Gap repair PCR products into new prey vector and carry out a directed mating to confirm the interaction
Matα
-L
Mata
Mate on nutrient-rich
3 days
Replicate to select for
-WL
Replicate to select for interacting partners
-WLA
-WLH(3-AT)
7 days
Sequence any interacting preys that grow on both selective plates

Figure 5.2 Y2H library screen and directed mating schematics. For library screens, Mata yeast were transformed with pGBKT7 bait constructs and colonies were checked for the presence of baits by PCR and for autoactivation. Positive colonies were mated with a pretransformed pGADT7 prey library on rich medium for 7 hours and spread onto quadruple dropout selection plates (SD-WLAH) that positively select for interacting partners. 7 days later, positive colonies were spotted in a 96 well plate format onto SD-WLAH plates and grown for 3 days. Positive colonies tested by YC-PCR. Prey PCR products were transformed by gap repair into the pGADT7 prey vector in Matα yeast and used to carry out a directed mating with baits of interest to confirm interactions. For directed mating, different preys were spotted into a 96-well plate format on rich medium and yeast transfected with one bait construct was spotted on top of each individual prey spot. Mating on rich medium resulted in diploid yeast formation that were selected for on SD-WL medium (-WL). Yeast on –WL plates were replicated onto triple dropout selection plates (-WLA and -WLH(3-AT)), that positively select for interacting partners. Preys that resulted in colonies were sent off for sequencing.

yeast colonies were grown on agar lacking tryptophan, leucine and histidine (SD-WLH). Yeast which grew on these plates were considered as autoactivators and eliminated from further studies.

The method used for the Y2H interaction screen is outlined in Figure 5.2. Briefly, Mata yeast containing the bait fusion protein of interest were mated with a pretransformed Matα (Y187) Y2H Matchmaker normalised cDNA library onto nutrient rich media. 7 hours later, mated yeast were collected, pooled and spread onto SD-WLAH agar to select for interacting partners. Following 7 days of growth, 96 colonies were picked, replated onto SD-WLAH agar and grown for three days. Prey DNA present in each colony was isolated by PCR using prey vector-specific primers. To confirm the interaction between bait and prey proteins, the prey PCR product was retransformed into the pGADT7 prey yeast vector by in vivo recombinant gap repair and used in a Y2H directed mating assay with the bait of interest and also empty bait vector as a negative control. This involved mating the bait and prey yeast again on nutrient rich media and selecting for growth on SD–WLA and SD-WLH(3-AT) plates. Positive colonies that grew on both of these plates that did not grow on the control plates were considered as true interacting partners and the prey PCR product was sent for sequencing.

Unfortunately, I encountered several problems with this screening approach. Firstly, the STIM1-CT bait protein used failed to produce colonies when mated with the yeast prey library. The STIM1-CT insert was cloned into two different bait vectors (pGBDU-C1 and pGBKT7) and used in screens with two yeast prey libraries (the Matchmaker cDNA library and a library derived from K562 cells)

and in each case very few colonies grew. It was therefore decided that STIM1-CT may not be a suitable bait for use in Y2H studies and the use of this bait protein was not continued. Secondly, although the Orai1-CT and Orai1-NT baits mated successfully with the yeast prey library, each with an efficiency of over 1 million diploid clones formed per screen, fewer than 96 colonies could be picked from the Orai1-NT screen for further evaluation (Figure 5.3, A). Of these colonies, none grew on both selective plates that did not also grow on pGBKT7-mated control plates (Figure 5.3, A) and were therefore not classed as true interacting partners. When the Orai1-CT bait was mated with the prey library, however, it produced a subset of colonies that grew on both of the selective plates that did not grow on the control plates (Figure 5.3, B). These preys were classed as potential Orai1 interacting proteins and were sequenced. Prey sequences were identified using an online BLASTn search. The resulting Orai1 interacting partners identified in this manner are listed in Table 5.1. None of these proteins are known Orai1 binding proteins nor have they been implicated in SOCE. For this reason, we decided not to follow up on these potential interacting partners but carried out a pulldown approach to attempt to find novel interacting partners for STIM1 and Orai1.

5.2.2 Purification and identification of recombinant GST fusion proteins

GST fusion proteins of the cytosolic domains of STIM1 (GST-STIM1-CT) and Orai1 (GST-Orai1-CT and GST-Orai1-NT) were constructed for use in pull down experiments. For protein production, BL21 E. coli were transformed with the plasmid encoding GST-Orai1-CT, GST-Orai1-NT or GST-STIM1-CT. GST protein production was induced with 1 mM IPTG. The GST fusion proteins were then

Figure 5.3

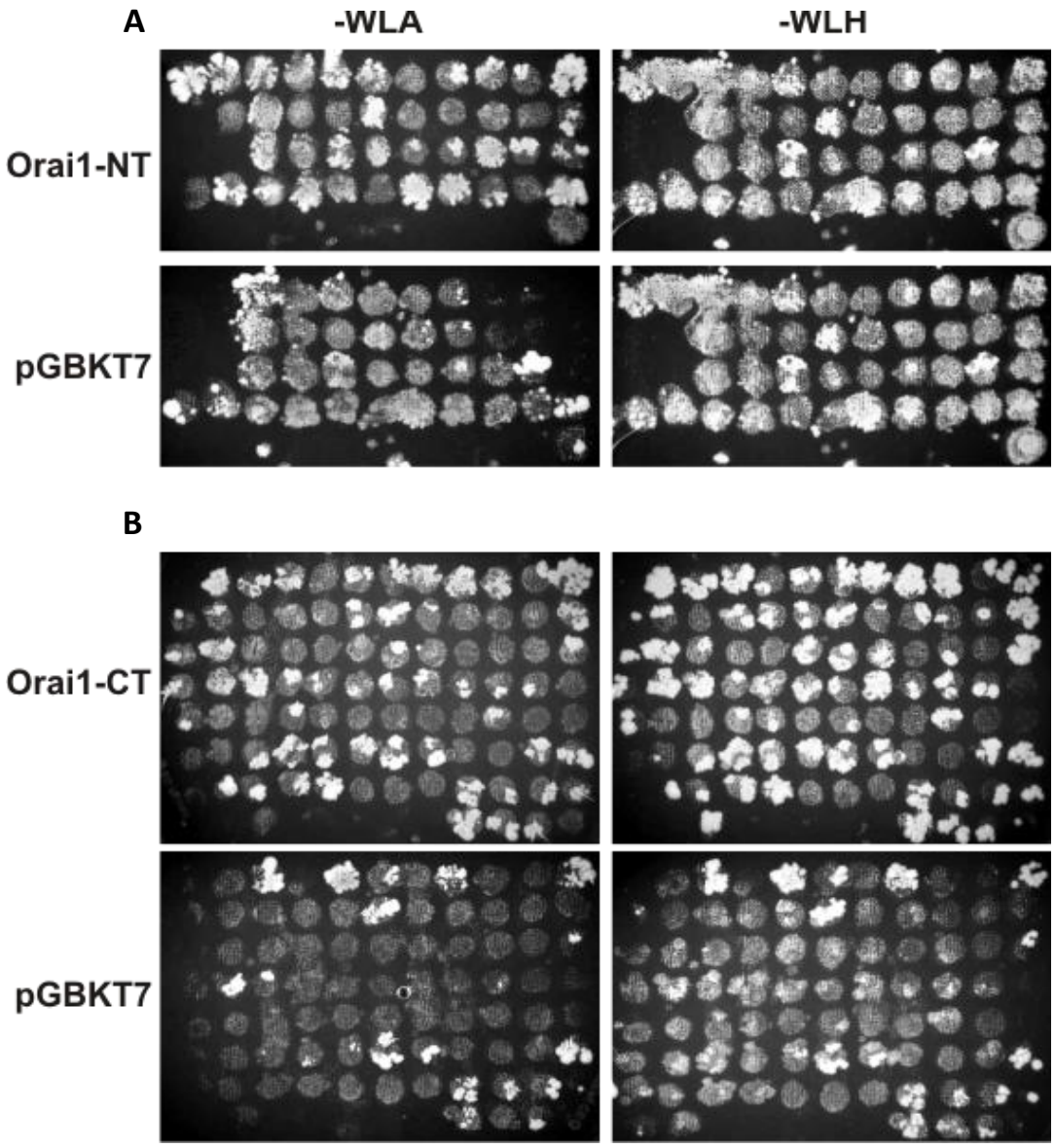

Figure 5.3 Y2H library screening results. pGBKT7-Orai1-CT or pGBKT7-Orai1-NT transformed MATa yeast was mated with Matα yeast transformed with a library of prey proteins. To confirm positive bait and prey interactions, prey proteins were retransformed into Matα yeast and mated with the same bait as before in Mata yeast in a directed mating assay, and also mated with empty pGBKT7 vector as a control. Yeast diploids were allowed to velvet replicate onto SD–WLA and SD–WLH(3-AT) agar plates for 7 days before growth was assessed. Colonies that did grow on both of the selective plates and did not grow on pGBKT7-mated plates were sent for sequencing.

Table 5.1

Protein	Localisation	Known function
Dysbindin domain containing 2	Cytoplasm	Negatively regulates protein kinase activity
Von Willebrand factor C domain-containing protein 2-like protein	Extracellular (secreted)	
Hypothetical protein LOC257177	Unknown	Unknown but protein sequence displays similarities to ubiquitin
Copper metabolism (Murr1) domain containing 1	Nucleus	Inhibits NF-kappaB activity
Translation elongation factor 1	Endoplasmic Reticulum	Binds tRNAs to direct them to the ribosome
Myeloid/lymphoid or mixed lineage leukemia 5	Nucleus	A histone methyltransferase associated with acute leukemias
Zygin 1	Cytoplasm	implicated in axonal outgrowth and kinesin-mediated transport
Carbonic anhydrase VB pseudogene	Unknown	Unknown
cAMP-specific phosphodiesterase 4A	Associates with membranes	cAMP hydrolysis
Proline rich membrane anchor 1 precusor	Cell membrane/synapse	Neurotransmitter degradation
Zinc finger RNA binding protein	Nucleus	Transcription enhancer
Signal recognition particle	Cytoplasm	Targets proteins to the endoplasmic reticulum

Table 5.1 Yeast 2-Hybrid screen Results. Positive prey construct from the yeast 2-hybrid screen using Orai1-CT as bait were sent for sequencing and the sequences were searched against using the nucleotide blast online database. Gene sequences identified from blastn searches are listed in the table above.

extracted from the cells by sonification and centrifugation, and purified using affinity chromatography with glutathione cellulose beads. Purified GST fusion proteins were analysed by SDS-PAGE (Figure 5.4). Each recombinant GST fusion protein band was subsequently excised for analysis by MALDI-ToF to confirm the identity of each protein. For MALDI-ToF analysis, excised protein bands were de-stained in 50% ambic/50% acetonitrile, reduced with DTT and alkylated using iodoacetamide. Samples were incubated overnight with trypsin and de-salted using ZipTips.

Trypsin digestion resulted in the cleavage of each protein sample into a series of smaller peptides. The peptide mixtures were then analysed by MALDI-ToF mass spectrometry which measured the absolute mass of each peptide to produce a unique "peptide mass fingerprint" for each protein. Figure 5.5 shows the peptide mass fingerprints for GST-Orai1-CT (~34.6 kD; Figure 5.5, A), GST-Orai1-NT (~36 kD; Figure 5.5, B) and GST-STIM1-CT (~80 kD; Figure 5.5, C). These were searched against the MASCOT online protein database which confirmed the identities of each protein.

5.2.3 Pulldown assays using recombinant GST fusion proteins

To search for novel binding partners for STIM1 and Orai1, pull-down experiments were performed on immobilised GST, GST-STIM-CT, GST-Orai1-CT and GST-Orai1-NT using solubilised bovine brain cytosol (Figure 5.6, A). Unique protein bands identified in the STIM1 and Orai1 pulldowns that were absent from the GST control pulldown were excised and prepared for MALDI-ToF mass spectrometry analysis as

Figure 5.4

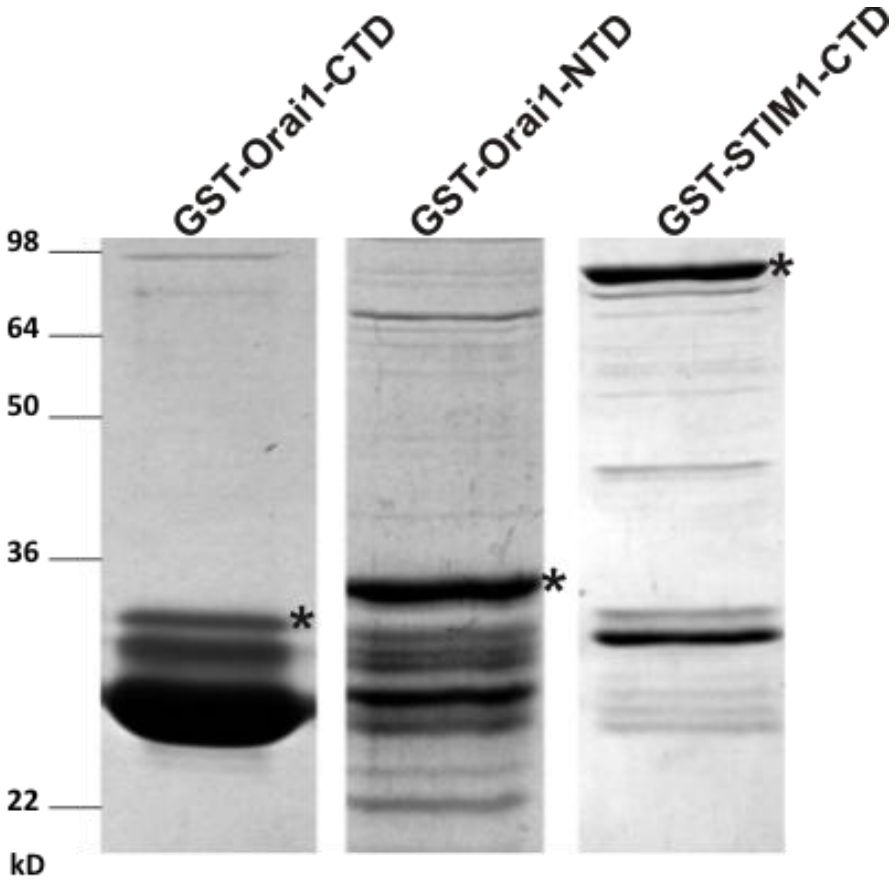

Figure 5.4 SDS-PAGE analysis of recombinant GST-fusion proteins. Coomassie-blue stained gel showing purified recombinant GST-Orai1-CT, GST-Orai1-NT and GST-STIM1 proteins. Asterisks indicate the GST-protein of interest. kD = molecular weight markers in kilodaltons.

Figure 5.5

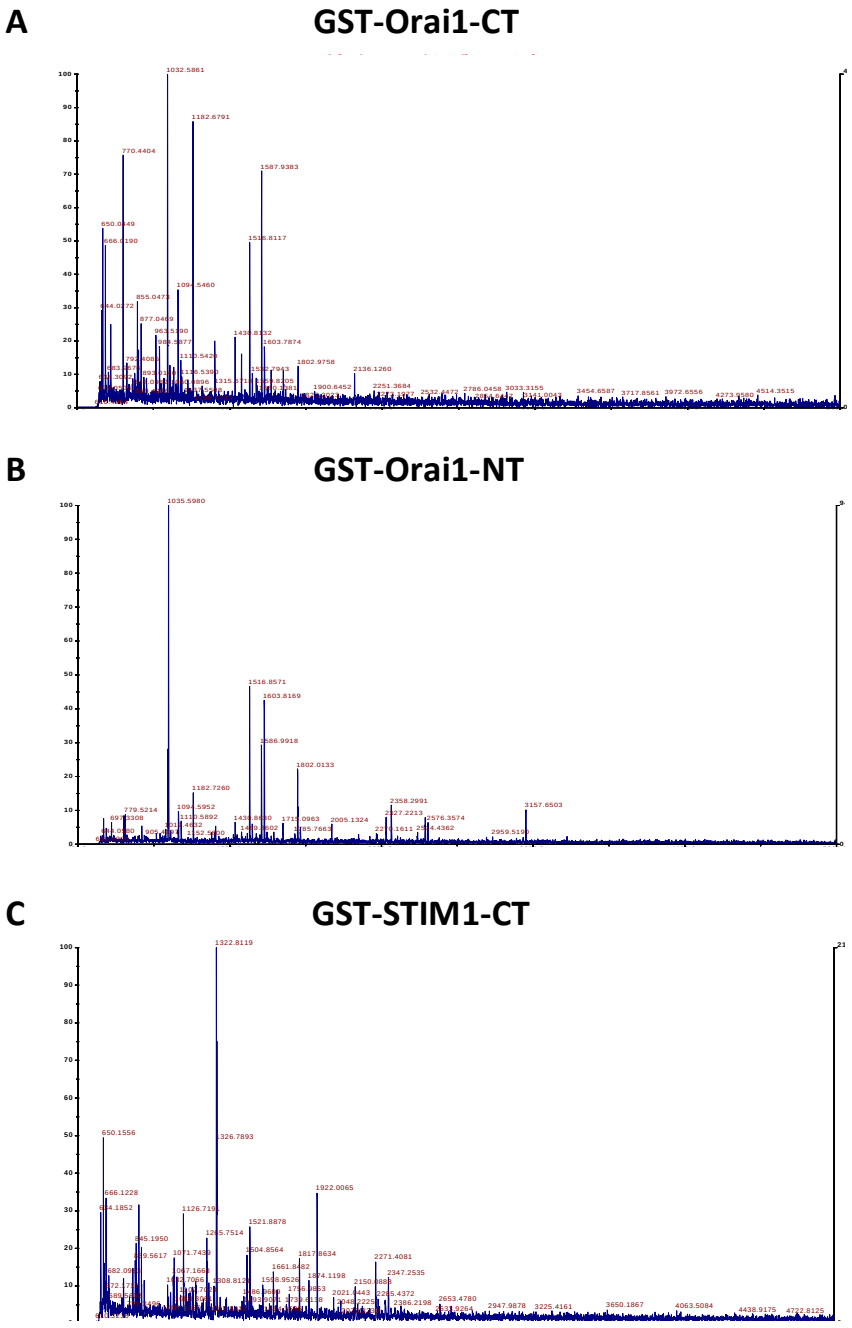

Figure 5.5 MALDI-ToF peptide mass fingerprints of recombinant GST fusion proteins. Recombinant proteins were excised from an SDS-PAGE and subjected to standard in-gel de-staining, reduction, alkylation, trypsinolysis and de-salting procedures. The protein digests were analysed by MALDI-ToF to obtain unique peptide mass fingerprints for each of the proteins to confirm the identities of the recombinant proteins.

described in Section 5.2.1. Excised bands were each assigned numbers as outlined in Figure 5.6, A). MALDI-ToF analysis of the excised protein bands identified a number of potential binding proteins for both STIM1 and Orai1, as outlined in Figure 5.6, B. Of the 8 proteins identified, which included a fragment of the recombinant GST-STIM1-CT protein and a keratin contaminant, myelin basic protein (MBP; 8 matching peptides with 39% sequence coverage) was revealed as a protein which bound to the C-terminus of STIM1 (Figure 5.6, B). Western blotting of the pulldown eluates using an anti-MBP antibody confirmed that MBP bound specifically and efficiently to the C-terminus of STIM1 and also less effectively to the N-terminus of Orai1 but did not bind the GST control protein (Figure 5.7).

5.2.4 Evidence for an interaction between Golli-BG21 and STIM1

Figure 5.7 revealed that the C-terminus of STIM1 binds to MBP from solubilised bovine brain cytosol in pulldown assays. This was surprising, since classic MBP itself is required for central nervous system myelination and has not been implicated in the activity of SOCs. The Golli family of proteins are spliced variants of classical MBPs which have been shown to mediate signal transduction in T cells through the negative regulation of SOCs (Feng et al., 2006). Since Golli proteins contain MBP epitopes, we hypothesised that Golli may interact with STIM1 to exert its effect on SOCE. We assessed whether the C-terminus of STIM1 interacts directly with Golli using an *in vitro* binding assay. A recombinant GST-Golli-BG21 fusion protein (~57.5 kD) was expressed in *E. coli* and immobilised on glutathione affinity resin. Immobilised GST-Golli-BG21 or GST control protein (~26 kD) was incubated with PreScission-cleaved STIM1-CT. Western blotting analysis using an antibody directed

Figure 5.6

A

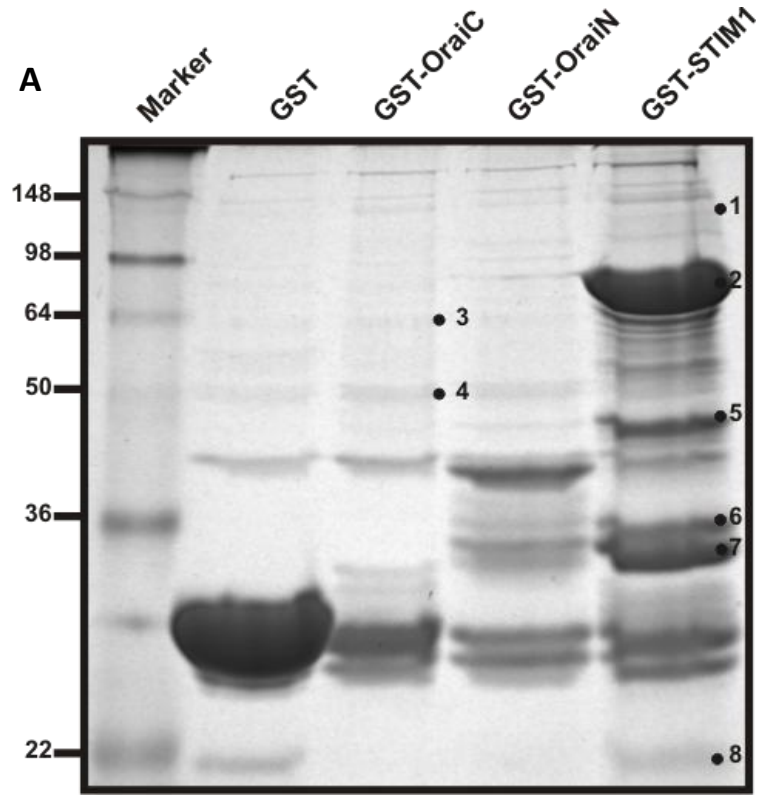

B

No.	Protein	Accession no.	Peptides matched	Coverage (%)	Mr Predicted	Mr Observed
1	Keratin 10	Q8N175	8	15	59 020	120 000
2	STIM1	Q8N382	9	16	77 660	98 000
3	Bovalbumin	AAA51411	11	22	71 274	64 000
4	LanC-like protein	Q1LZH8	8	20	45 976	50 000
5	PP2A, Subunit B'', alpha	Q8BM38	7	18	57 252	43 000
6	GST (Fragment)	AAB59734	10	45	26 374	35 000
7	GST	AAA72682	10	45	26 870	30 000
8	Myelin Basic Protein	MBOBB	8	39	18 312	20 000

Figure 5.6 GST pulldown assays and MALDI-ToF results. (**A**) Coomassie blue stained gel of eluates from GST, GST-Orai1-CT, GST-Orai1-NT and GST-STIM1-CT pulldown assays. GST columns were run in parallel with GST-Orai1-CT, GST-Orai1-NT and GST-STIM1-CT and incubated with bovine brain cytosol extract. Samples were eluted by boiling in Laemmli buffer. Eluted proteins were separated by SDS-PAGE. Subsequently, proteins were excised from gels and analysed by MALDI-ToF. (**B**) Table listing proteins reproducibly identified by MALDI-ToF. Myelin Basic protein (no. 8) was identified as a GST-STIM1-CT binding partner.

Figure 5.7

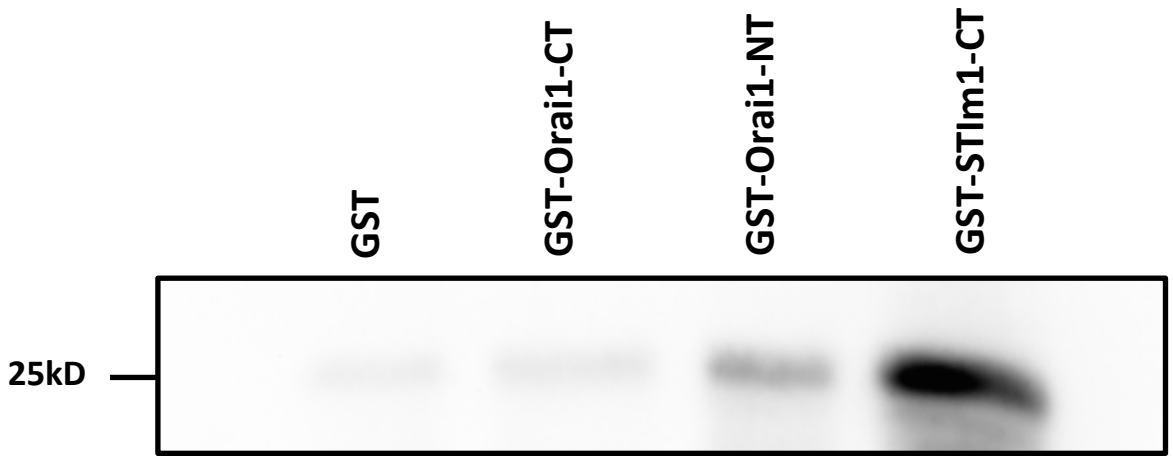

Figure 5.7 Myelin basic protein pulls down specifically with GST-STIM1-CT. Eluates from GST, GST-Orai1-CT, GST-Orai1-NT and GST-STIM1-CT pulldown assays were blotted using an antibody directed against myelin basic protein. A specific band of the correct molecular weight of myelin basic protein (~25kD) is present in the GST-STIM1-CT that is absent from the GST control eluate.

against STIM1 revealed that STIM1-CT bound specifically to the GST-Golli-BG21 protein but not to the GST control (Figure 5.8; n = 4 from 2 independent experiments), demonstrating that the C-terminus of STIM1 does indeed interact with Golli *in vitro*. Note that in these experiments the glutathione beads were incubated with levels of GST or GST-Golli-BG21 that resulted in a 1.4-fold higher level of GST so that lack of binding of STIM1-CT to GST-loaded beads was not a consequence of the relative GST concentration.

To further investigate the possible interaction of STIM1 and Golli-BG21 in a cellular context, these two proteins were expressed in HeLa cells using a Bimolecular Fluorescence Complementation (BiFC) assay (Robida and Kerppola, 2009). This BiFC system involved the fusion of the complementary fragments of EYFP to two proteins of interest. If these proteins interact the EYFP fragments come close enough to fold and form a functional fluorescent EYFP protein (Haynes et al., 2007). In these experiments, complementary fragments of EYFP (YC and YN) were fused to the C-termini of the STIM1-CT (STIM1-CT-YN) and Golli-BG21 (Golli-BG21-YC) proteins and expressed in HeLa cells along with the mCherry-tagged Rit1 tail protein (mCherry-Rit1) described in Chapter 4, as a marker to identify transfected cells. No detectable fluorescence was observed in untreated cells (Figure 5.9, A; n = 21 cells). Transfected cells were treated with thapsigargin for 60 – 90 minutes at room temperature in 2 mM external Ca^{2+} before imaging with a confocal microscope. EYFP fluorescence was detected at the plasma membrane in treated cells expressing STIM1-CT-YN and Golli-BG21-YC ~90 minutes following the addition of thapsigargin (Figure 5.9, B; n = 35 cells) which is consistent with the time-course

Figure 5.8

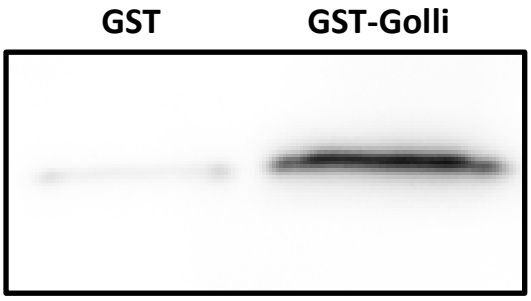

Figure 5.8 The C-terminal domain of STIM1 binds specifically to GST-Golli. GST-Golli or GST as a control immobilised on glutathione beads was incubated with PreScission-cleaved STIM1-CT in binding buffer for 2 hours at 4^{o}C. The beads were then washed, boiled in SDS Laemmli buffer and separated by SDS-PAGE. Bound STIM1-CT was detected by Western blotting with anti-STIM1 antibody.

described for the refolding of EYFP at room temperature (Robida and Kerppola, 2009). EYFP fluorescence was distributed throughout the plasma membrane but no puncta were visible. The uniform plasma membrane EYFP fluorescence observed here is consistent with the previous finding that although STIM1-CT expression gives constitutive activation of the I_{crac} current, it does not form puncta at the plasma membrane (Muik et al., 2008) since it requires an ER localisation to oligomerise prior to translocation to ER-PM junctions (Luik et al., 2008; Muik et al., 2008). No detectable EYFP fluorescence was observed in thapsigargin treated cells expressing either STIM1-YN (Figure 5.9, C; n=12 cells) or Golli-BG21-YC fusion protein alone (Figure 5.9, D; n=20 cells) or along with the appropriate complementary fragment of EYFP (Figure 5.9, E (n=27 cells) and F (n=18 cells)). Similarly, co-expression of both EYFP fragments failed to produce a fluorescent signal and served as a negative control (Figure 5.9, G; n=7 cells). Plasma membrane EYFP fluorescence was also observed in cells which were not cotransfected with mCherry-Rit1 (Figure 5.9, H; n=18 cells), eliminating the possibility that the transfection marker was targeting the BiFC constructs to the plasma membrane.

There are two possibilities to explain why EYFP fluorescence was observed at the plasma membrane following thapsigargin treatment. Firstly, STIM1-CT-YN may associate with endogenous STIM1 puncta enabling it to interact with Golli-BG21-YC at the plasma membrane. It is also possible that a change in cytosolic Ca^{2+} concentration may affect the interaction between STIM1-CT-YN and Golli-BG21-YC. To investigate this, HeLa cells expressing both constructs were treated with 100 µM histamine for 90 minutes in place of thapsigargin. EYFP

Figure 5.9

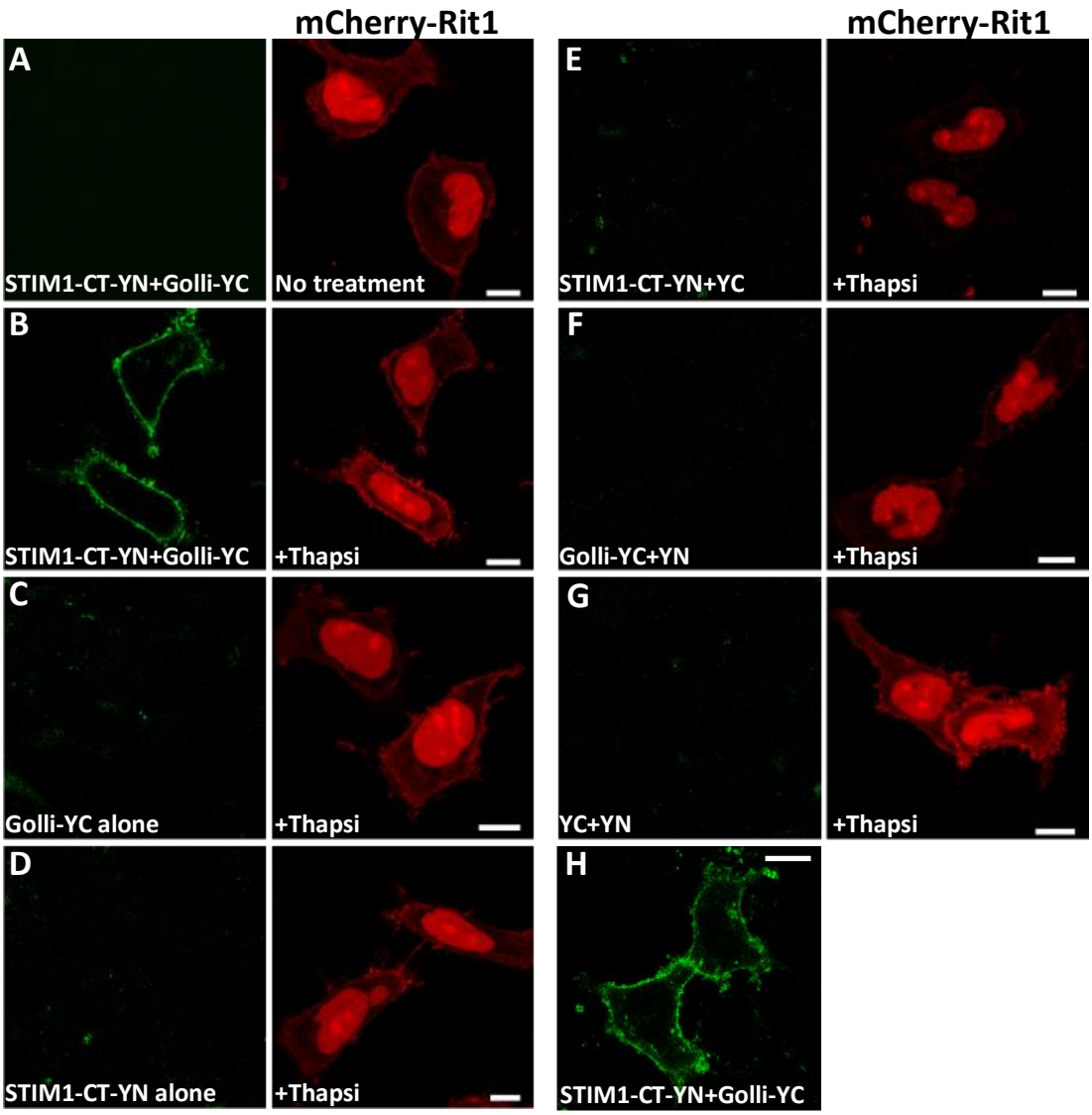

Figure 5.9. STIM1-CT-YN and Golli-BG21-YC fusion proteins reconstitute EYFP fluorescence at the plasma membrane. HeLa cells were cotransfected with mCherry-Rit1 as a transfection marker. 24h post-transfection, cells were treated with 2 µM thapsigargin for 90 min and imaged using a confocal microscope, except in (**A**) where cells were imaged without treatment. (**A**) Co-expression of Golli-YC/STIM1-CT-YN in untreated cells does not result in the formation of EYFP. (**B**) Co-expression of Golli-YC/STIM1-CT-YN results in reconstitution of EYFP fluorescence at the plasma membrane when cells were treated with thapsigargin; n = 35 cells. Expression of either Golli-YC alone (**C**) or with YN (**D**) or STIM1-CT-YN alone (**E**) or with YC (**F**) fails to restore EYFP fluorescence in thapsigargin treated cells. Similarly, co-expression of the YC and YN proteins gives no EYFP fluorescence following thapsigargin treatment (**G**). Plasma membrane EYFP fluorescence is also observed in cells which are not cotransfected with mCherry-Rit1 (**H**).

Figure 5.10

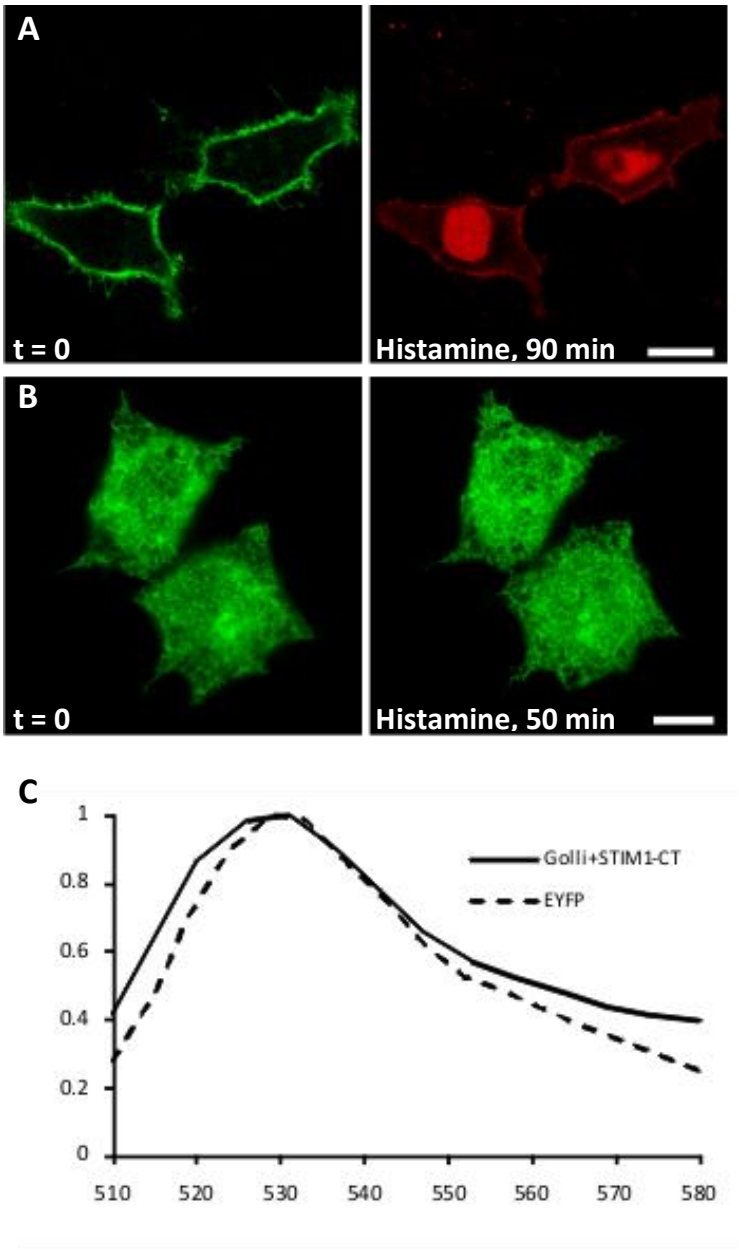

Figure 5.10 Histamine stimulates STIM1-CT-YN and Golli-BG21-YC fusion proteins to reconstitute EYFP fluorescence at the plasma membrane. (**A**) HeLa cells were cotransfected with STIM1-CT-YN, Golli-BG21-YC and mCherry-Rit1 as a transfection marker. 24 hours post-transfection cells were treated with 100 µM histamine in place of thapsigargin to reconstitute EYFP fluorescence (**B**) HeLa cells were transfected with STIM1-EYFP. STIM1 puncta formation was not observed after 50 minutes treatment with histamine. (**C**) EYFP fluorescence from (**A**) was recorded using the Lambda scan mode. Fluorescence intensity after 453 nm excitation was recorded in 5 nm intervals from 510 nm to 590 nm. The emission spectrum was similar to that of EYFP. Scale bars = 10 µm.

fluorescence formation was observed (Figure 5.10, A; n=27) even though full length STIM1-EYFP did not reveal substantial sustained puncta formation under these conditions (Figure 5.10, B; n=11) suggesting that an increase in cytosolic Ca^{2+} from intracellular stores might somehow stimulate the interaction between STIM1-CT and Golli-BG21. A lambda scan of the fluorescence emission observed with STIM1-YN/Golli-BG21-YC was close to that of EYFP (Figure 5.10, C), confirming that the fluorescence observed was due to formation of functional EYFP.

5.2.5 Directed Y2H mating assays

In a separate approach to try to confirm an interaction between Golli-BG21 and STIM1, and to determine whether an interaction could be detected between Golli-BG21 and Orai1, a directed yeast 2-hybrid mating assay was carried out as described in Figure 5.1. MATα haploid cells containing the prey constructs of interest (Golli-BG21, Orai1-CT or Orai1-NT) were spotted in triplicate onto a rich medium plate. MATa yeast transformed with the bait constructs of interest (STIM1-CT, Orai1-CT, Orai1-NT or pGBKT7 control) were spotted on top of these, and were allowed to mate for 24 hours. Mated yeast were velvet replicated onto SD-WL agar plates for diploid yeast selection and grown for 3 days, after which colonies were velvet replicated onto SD-WLA and SD-WLH(3-AT) agar plates to select for interacting partners for 7 days. Positive (p53 bait and T-antigen prey) and negative (pGBKT7 bait with each prey) controls were also spotted onto plates to identify efficient mating and background growth, respectively. Interestingly, no growth was observed on selective plates from mated yeast containing the STIM1-CT bait and the Orai1-CT or Orai1-NT preys (Figure 5.11), when an interaction between STIM1-

Figure 5.11

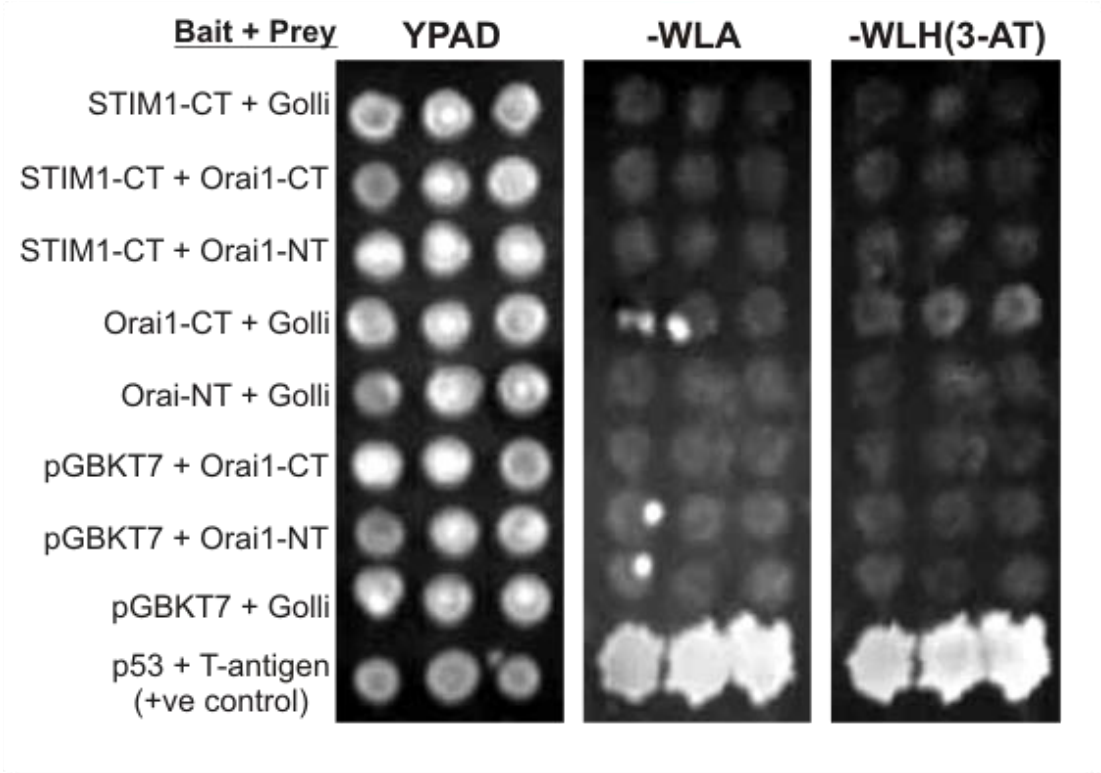

Figure 5.11 Yeast 2-hybrid directed mating assays. MATa yeast were transformed with pGBKT7 bait constructs and MATα yeast with pGADT7 prey constructs. Different preys were spotted in triplicate onto rich medium and yeast transfected with one bait construct was spotted on top of each individual prey spot. Following selection of diploids, yeast on SD-WL plates were replicated onto triple dropout selection plates (-WLH(3-AT) and -WLA), that positively select for interacting partners. Growth was seen only with the positive control bait and prey.

CT and Orai1-CT was expected (Muik et al., 2008). Similarly, diploid yeast containing the STIM1-CT bait and Golli-BG21 prey constructs failed to grow (Figure 5.11), despite the fact that an interaction between these proteins was observed in this study using BiFC and in vitro binding assays. This is consistent with the results from the Y2H library screens using STIM1-CT and confirms that STIM1-CT is not a suitable protein fragment for use in Y2H studies. Additionally, mated yeast containing the Orai1-CT or Orai1-NT bait and Golli-BG21 prey failed to grow on selective plates (Figure 5.11), indicating that Orai1 and Golli-BG21 may not interact with each other. Growth was observed only with yeast containing the p53 bait and T-antigen prey (Figure 5.11) which are known to interact and demonstrate that the yeast mating was successful.

5.2.6 Golli-BG21 and STIM1 colocalise in HeLa cells

Since the biochemical and BiFC assays above suggest that the C-terminal domain of STIM1 along interacts with Golli-BG21 in HeLa cells, we determined whether STIM1-CT and Golli-BG21 colocalise in HeLa cells using confocal microscopy. In order to do this, a STIM1-CT-EYFP protein was constructed and characterised. This protein was diffuse when expressed alone in HeLa cells (Figure 5.12, A), which has been observed previously (Muik et al., 2008). However, when STIM1-CT-EYFP was coexpressed with mCherry-Orai1, it localised at the plasma membrane through an interaction with Orai1, although it did not form puncta (Figure 5.12, B; n=5). The uniform plasma membrane STIM1-CT-EYFP fluorescence and the STIM1-CT-YN/Golli-BG21-YC fluorescence observed here is consistent with the previous finding that although STIM1-CT expression gives constitutive activation of the I_{crac}

Figure 5.12

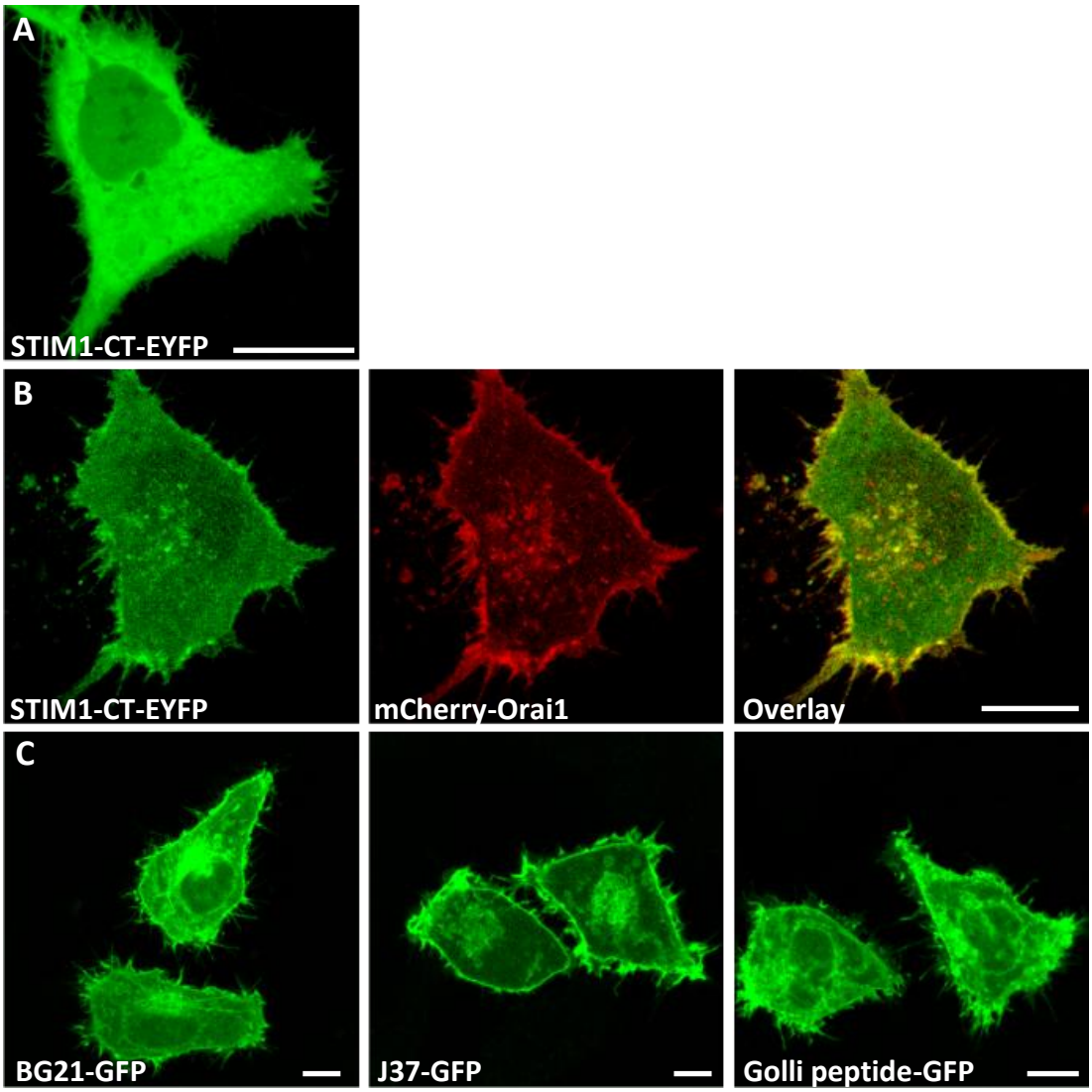

Figure 5.12 Localisation of STIM1-CT-EYFP and Golli proteins in HeLa cells. (**A**) HeLa cells were transfected and imaged 24 hours postransfection. (**A**) Cells transfected with STIM1-CT-EYFP. STIM1-CT-EYFP is diffusely cytosolic when expressed alone. (**B**) Cells cotransfected with STIM1-CT-EYFP and mCherry-Orai1. STIM1-CT-EYFP distribution overlaps with mCherry-Orai1 at the plasma membrane. (**C**) HeLa cells singly transfected with either Golli-BG21-GFP, Golli-J37-GFP or golli peptide (AA1-133)-GFP. Golli proteins localise at the plasma membrane and in intracellular aggregates. Scale bar = 10 µm.

current, it does not form puncta at the plasma membrane (Muik et al., 2008) since it requires an ER localisation to oligomerise prior to translocation to ER-PM junctions (Luik et al., 2008; Muik et al., 2008). To examine the distribution of Golli proteins in HeLa cells for future colocalisation experiments with STIM1 and Orai1, GFP-tagged fusion proteins of the Golli-BG21 and Golli-J37 isoforms, as well as the Golli-specific peptide (AA1-133) were overexpressed in HeLa cells and imaged. All Golli proteins were distributed at the plasma membrane and in intracellular aggregates (Figure 5.12, C), which is consistent with the reported localisation of Golli proteins (Feng et al., 2006).

To determine whether the C-terminal domain of STIM1 and Golli-BG21 colocalise at the plasma membrane, HeLa cells were transfected with STIM1-CT-EYFP and Golli-BG21-mCherry and imaged. Interestingly there was a high degree of colocalisation in the distribution of both proteins at the cytoplasm and also in what appear to be plasma membrane folds (Figure 5.13, A and inlay (taken from bottom right of cell); n=4). The finding that these proteins colocalise in HeLa cells supports the hypothesis that Golli-BG21 interacts with the C-terminal domain of STIM1.

Golli overexpression has been shown to decrease SOCE following store depletion in Jurkat T cells (Feng et al., 2006). If this occurred through an interaction with full length STIM1, the Golli protein would either colocalise with STIM1 in puncta or would prevent STIM1 puncta formation. To test this, full length STIM1-EYFP and a Golli-BG21-mCherry fusion protein were expressed in HeLa cells which had been treated with thapsigargin for 10 minutes before imaging to induce STIM1 puncta

formation. Golli-BG21-mCherry expression was observed predominantly at the plasma membrane where STIM1-EYFP puncta accumulated but was also seen to colocalise with STIM1-EYFP in a subset of puncta (Figure 5.13, B and inlay (taken from top of cell); n = 9). No change was observed in the number of STIM1-EYFP puncta formed in thapsigargin-treated cells overexpressing Golli-BG21-mCherry (Figure 5.13, C; n=19) compared with control cells expressing STIM1-EYFP alone (Figure 5.13, C; n=43) suggesting that Golli does not affect the formation of STIM1 puncta *per se*. The targeting of both proteins to the same punctate structures suggests that Golli and full length STIM1 interact and that Golli may regulate store operated calcium entry through a direct interaction with STIM1 in puncta.

5.2.7 Golli-BG21 colocalises with Orai1 in HeLa cells

Since STIM1 and Golli interact within puncta, it is possible that Golli-BG21 also colocalises with Orai1 and may potentially interact with Orai1. Interestingly, when mCherry-Orai1 was coexpressed with STIM1-CT-YN/Golli-BG21-YC in HeLa cells, the EYFP fluorescence formed between the BiFC proteins clearly overlapped with the mCherry-Orai1 signal following 90 minutes thapsigargin treatment (Figure 5.14, n=18). To determine whether Orai1 itself colocalises with Golli-BG21, Golli-BG21-GFP and mCherry-Orai1 were overexpressed in HeLa cells. An overlay image revealed extensive colocalisation of both proteins at the plasma membrane (Figure 5.15, A; n=21). Cells were treated with thapsigargin for 10 minutes to determine whether store depletion has an effect on the distribution of Golli-BG21 and Orai1. Thapsigargin treatment had little effect on the localisation of both proteins, which remained uniformly distributed throughout the plasma membrane and failed to

Figure 5.13

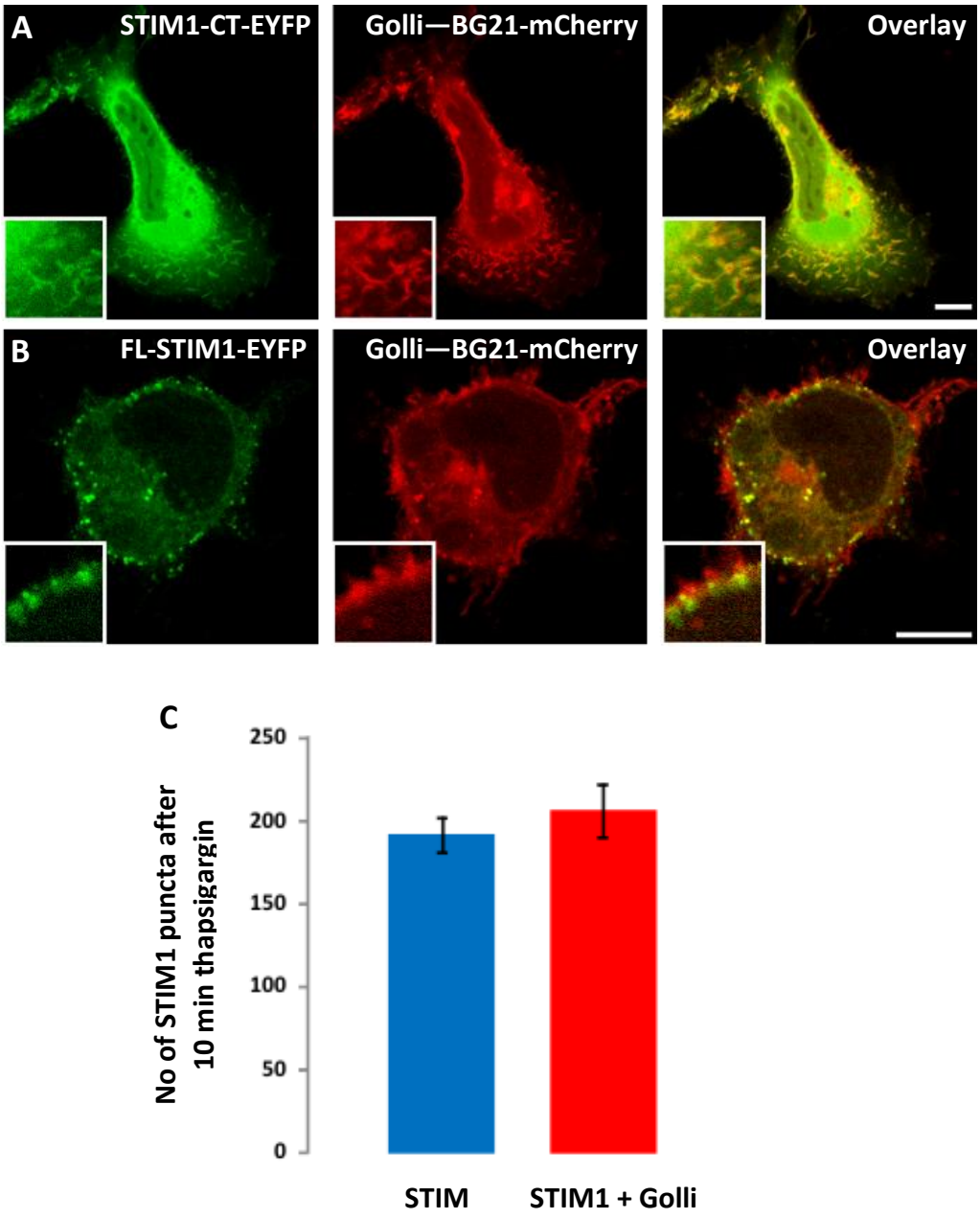

Figure 5.13 STIM1-CT and full length STIM colocalise with Golli in HeLa cells. (A) HeLa cells were cotransfected with STIM1-CT-EYFP or full length STIM1-EYFP and Golli-BG21-mCherry. 24 hours post transfection cells were imaged using a confocal microscope. (**A**) STIM1-CT-EYFP colocalises with Golli-BG21-mCherry cells (inlay taken from botton right of cell). (**B**) Cells were treated with 2 µM thapsigargin for 10 minutes before imaging. Full length STIM1-EYFP puncta colocalise with Golli-BG21-mCherry in thapsigargin-treated HeLa cells (inlay taken from top of cell). (**C**) Number of puncta formed in STIM1-EYFP overexpressing cells versus STIM1-EYFP and Golli-mCherry overexpressing cells. Scale bars = 10 µm.

Figure 5.14

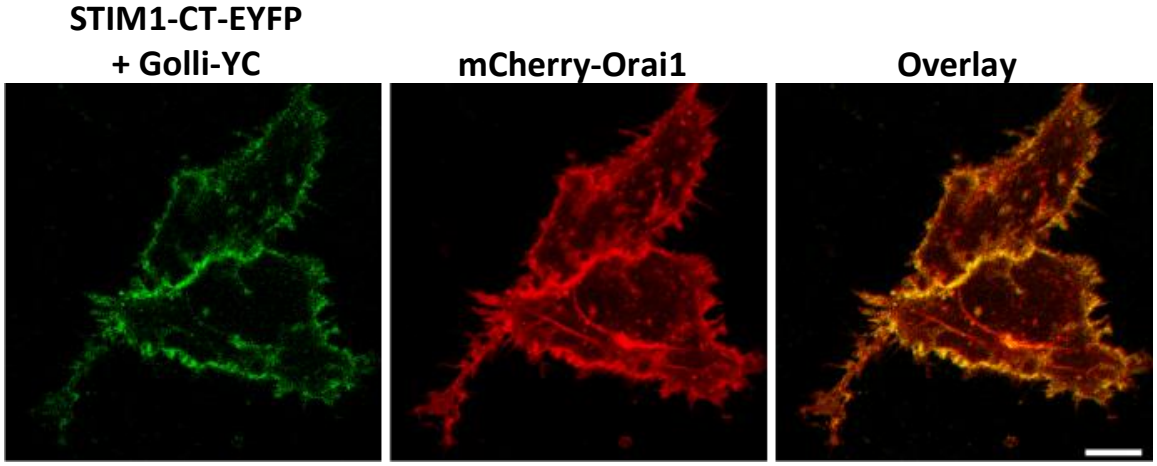

Figure 5.14 mCherry-Orai1 colocalises with reconstituted EYFP fluorescence from STIM1-CT-YN/Golli-YC. HeLa cells were cotransfected with STIM1-CT-YN/Golli-YC and mCherry-Orai1. 24h post-transfection, cells were treated with 2 µM thapsigargin for 90 minutes and imaged using a confocal microscope. Reconstituted EYFP fluorescence from STIM1-CT-YN/Golli-YC colocalises with mCherry-Orai1. Scale bar = 10 µm.

form puncta (Figure 5.15, B). This is consistent with previous reports which show that Orai1 requires STIM1 in order to redistribute into puncta, and suggests that the accumulation of Golli within puncta is also dependent on STIM1.

Since Golli and Orai1 colocalise in HeLa cells, the BiFC assay was used to determine whether Golli interacts with Orai1. For this HeLa cells were transfected with Golli-BG21-YC and Orai1-YN and treated with thapsigargin for 90 minutes before imaging. No EYFP fluorescence was observed under these conditions (Figure 5.16, A; n=16), suggesting that Golli-BG21 and Orai1 may not interact with each other. To determine whether an interact between Golli-BG21 and full length STIM1 could be observed using BiFC, HeLa cells were transfected with Golli-BG21-YC and full length STIM1-YN and treated with thapsigargin for 90 minutes before imaging. No EYFP fluorescence could be observed under these conditions (Figure 5.16, B; n=25).

5.2.8 STIM1, Orai1 and Golli-BG21 colocalise in puncta in HeLa cells

To determine whether Golli-BG21 colocalises with both the C-terminal domain of STIM1 and Orai1, HeLa cells were transfected with Golli-BG21-GFP, STIM1-CT-EYFP and mCherry-Orai1. Cells were imaged 24 hours post transfection. All three proteins colocalised at the plasma membrane and in puncta-like structures (Figure 5.17, A and inlay (taken from bottom left of cell); n=4). Colocalisation experiments described earlier in this chapter revealed that although Golli-BG21 colocalises with Orai1 where it is distributed throughout the plasma membrane, when Golli-BG21 is overexpressed with STIM1, it colocalises within STIM1 puncta. To determine whether Golli-BG21 colocalises with full length STIM1 and Orai1 in puncta, HeLa

Figure 5.15

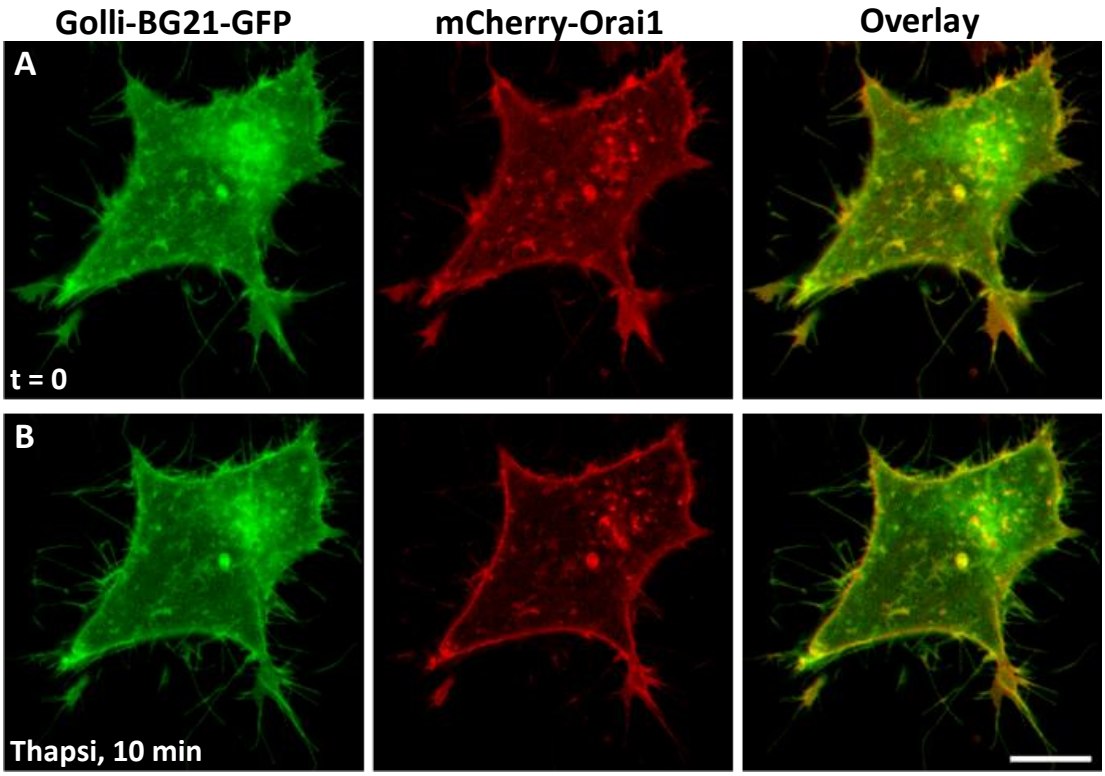

Figure 5.15 Orai1 and Golli-BG21 colocalise in HeLa cells. HeLa cells were transfected with mCherry-Orai1 and Golli-BG21-GFP. 24 hours post-transfection, cells were treated with 2 µM thapsigargin for 10 minutes. Both proteins colocalised extensively before and after treatment (**A & B**) but treatment with thapsigargin did not induce a change in distribution of mCherry-Orai1 or Golli-BG21-GFP expression (**B**) when compared to before treatment (**A**). Scale bar = 10 µm.

Figure 5.16

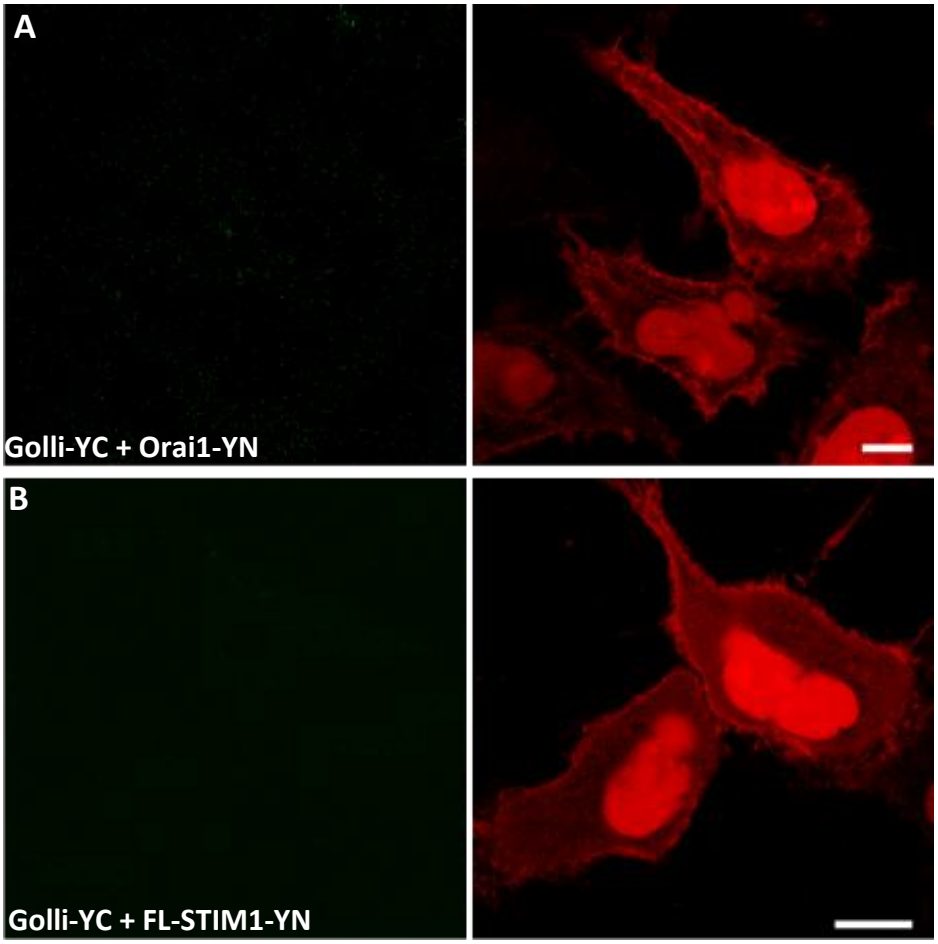

Figure 5.16 An interaction between Golli and FL-STIM1 or Orai1 could not be detected using the BiFC assay. HeLa cells were cotransfected with mCherry-Rit1 as a transfection marker. 24 hours post-transfection, cells were treated with 2 µM thapsigargin for 90 minutes and imaged using a confocal microscope. Co-expression of Golli-BG21-YC/Orai1-YN (**A**) or Golli-BG21-YC/FL-STIM1-YN (**B**) failed to produce EYFP fluorescence. (**B**) Scale bar = 10 µm.

cells were transfected with Golli-BG21-GFP, mCherry-Orai1 and full length STIM1-EYFP. 24 hours post transfection, cells were treated with thapsigargin for 10 minutes and imaged. Under these conditions, Golli-BG21-GFP colocalised with punctate STIM1-EYFP and mCherry-Orai1 complexes (Figure 5.17, B and inlay (taken from left of cell); n=10).

5.2.9 Overexpression of Golli-BG21 affects STIM1-mediated SOCE

To determine whether Golli-BG21 affects SOCE in HeLa cells, cells were transfected with Golli-BG21-mCherry or STIM1-EYFP alone or in combination. Transfected cells were loaded with the cytosolic Ca^{2+} indicator, Fluo-4 AM. Stores were depleted with thapsigargin in Ca^{2+}-free medium for approximately 10 minutes and Ca^{2+} influx was measured upon readdition of Ca^{2+} to the external solution. Untransfected cells in the same field of view as transfected cells were used as internal controls. Golli-expressing cells exhibited a reduced rate and extent of Ca^{2+} influx (Figure 5.18, blue trace) compared with influx in untransfected control cells (Figure 5.18, green trace) which was statistically significant ($p<0.0001$) at the 750 second time-point. This is consistent with previous findings that Golli-deficient T-cells show enhanced SOCE and that overexpression of Golli-BG21 inhibits SOCE (Feng et al., 2006), and suggests that Golli negatively regulates SOCE. In STIM1-overexpressing cells there was an increase in the initial rate of SOCE when compared with untransfected cells (Figure 5.18, red trace), which we have observed previously (Walsh et al., 2010). Interestingly, over-expression of STIM1 abolished the inhibitory effect of Golli-BG21 (Figure 5.18, black trace) when compared with STIM1-overexpressing cells. It is possible that high levels of STIM1 protein expression can directly overcome the

Figure 5.17

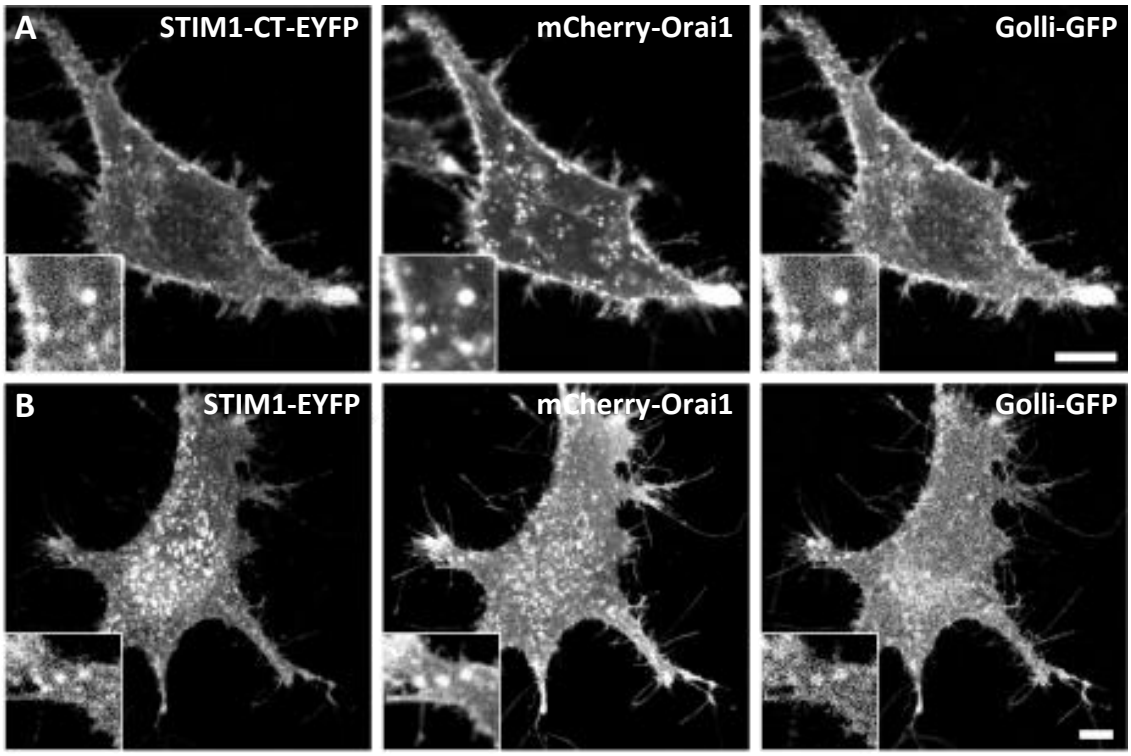

Figure 5.17 STIM1, Orai1 and Golli-BG21 colocalise in HeLa cells. HeLa cells were cotransfected with STIM1-CT-EYFP or STIM1-EYFP along with Golli-BG21-GFP and mCherry-Orai1. STIM1-CT-EYFP, mCherry-Orai1 and Golli-BG21-GFP colocalise in HeLa cells (**A;** inlay (taken from top left of cell). Full length STIM1-EYFP, mCherry-Orai1 and Golli-BG21-GFP colocalise in puncta following thapsigargin treatment in HeLa cells (**B**; inlay (taken from the middle left side of cell)). Scale bars = 10 µm.

Figure 5.18

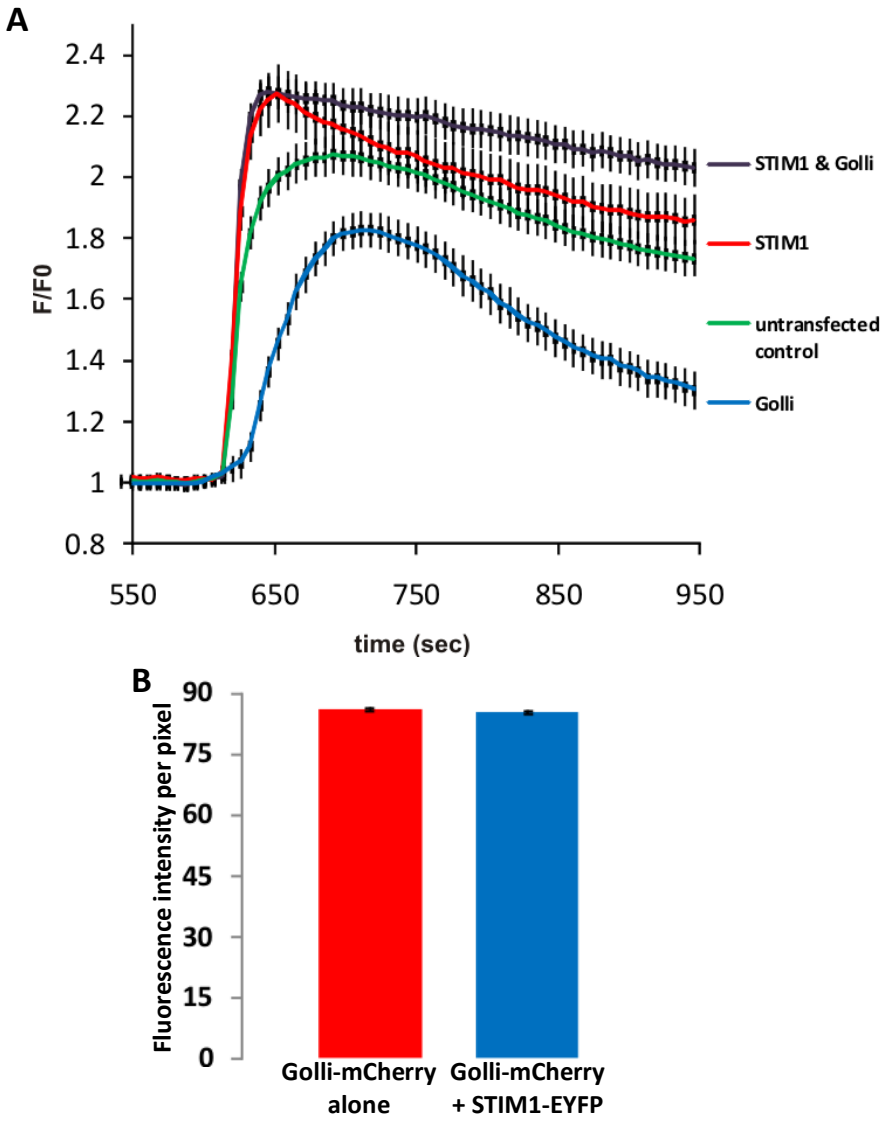

Figure 5.18 Overexpression of Golli reduces store-operated Ca^{2+} influx but this is reversed by overexpression of STIM1. HeLa cells were transfected with Golli-BG21-mCherry, STIM1-EYFP alone or together. 24h post-transfection, cells were loaded with Fluo-4 (5 µM) at room temperature for 30 min. Cells were treated with 2 µM thapsigargin to deplete the stores followed by the readdition of 2 mM Ca^{2+} to the external solution. Changes in $[Ca^{2+}]_i$ were measured and compared in transfected and untransfected cells. The data shown are means ± SEM. For untransfected cells, n = 154. For Golli-BG21-mCherry transfected cells, n = 63. For STIM1-EYFP transfected cells, n = 36. For Golli-BG21-mCherry and STIM1-EYFP transfected cells, n = 55. (**B**) Golli-BG21-mCherry fluorescence was quantified in cells expressing Golli-BG21-mCherry alone (n = 175) or together with STIM1-EYFP (n = 128). Expression levels of Golli-BG21-mCherry were similar in both conditions.

inhibition of SOCE by Golli-BG21. This was not due to differences in the expression of Golli since the level of Golli-BG21-mCherry fluorescence was similar in cells expressing Golli-BG21-mCherry alone or in combination with STIM1-EYFP (Figure 5.18, B). It is possible, therefore, that high levels of STIM1 protein expression can directly overcome the inhibition of SOCE by Golli-BG21.

5.3 Discussion

The aim of this study was to identify novel binding partners for the STIM1 and Orai1 proteins using yeast 2-hybrid screening and GST pulldown approaches. Yeast 2-hybrid library screens using the cytosolic domains of STIM1 and Orai1 as bait proteins resulted in the identification of a small set of potential interacting proteins for the C-terminal domain of Orai1 but not for the N-terminal domain of Orai1 or the C-terminal domain of STIM1. None of the proteins identified are known Orai1 interacting proteins nor have they been previously implicated in SOCE. There are several reasons why the yeast 2-hybrid screening approach was not a suitable method for studying STIM1 and Orai1 protein interactions. Full length transmembrane proteins such as STIM1 and Orai1 are difficult to use as bait proteins because they are retained at cellular membranes and yeast 2-hybrid bait and prey interactions are required to occur in the nucleus in order to activate reporter gene expression. Because of this, cytosolic fragments of transmembrane proteins are generally used. It is possible that these fragments may not fold correctly within the yeast cell and affect the protein's ability to bind other proteins. In addition, the requirement for proteins to interact within the nucleus may not be

optimal since this is not the native compartment for many proteins. For this reason, a GST pulldown approach was used alongside yeast 2-hybrid analysis to try to find potential binding partners for both STIM1 and Orai1 and using this approach, MBP was identified as a potential STIM1 binding protein.

Interestingly, there is a family of MBP isoforms known as Golli proteins which are ubiquitously expressed and of these the Golli-BG21 isoform has been described as a regulator of SOCE. This has been particularly well established for T-cells where knock out of Golli increased SOCE and overexpression of Golli-BG21 decreased SOCE (Feng et al., 2006). It was not clear, however, from these studies whether Golli has a direct effect on the SOC channel itself or another protein or pathway involved in the activation of SOCE. In this study, we suggest that Golli-BG21 directly interacts with the master SOCE regulator, STIM1, to reduce SOCE. The C-terminal domain of STIM1 successfully bound to Golli-BG21 in GST binding assays and BiFC assays. We have not mapped the STIM1-interacting domain within Golli-BG21 but it is possible that this is an epitope which is shared with the classical MBP protein since the C-terminus of STIM1 binds to MBP from bovine brain extract in pulldown assays. We have shown here using a BiFC assay that the interaction between Golli-BG21 and the C-terminus of STIM1 can be detected in cells after stimulation by both thapsigargin and histamine treatment. Both of these compounds should produce changes in cytosolic Ca^{2+} levels but, unlike thapsigargin, histamine elicits transient Ca^{2+} oscillations in HeLa cells (Bootman and Berridge, 1996; Haynes et al., 2004). Since the formation of STIM1-EYFP puncta was not observed under conditions where histamine stimulated BiFC fluorescence between STIM1-CT-YN

and Golli-BG21-YC, it is possible that it is the modulation of the cytosolic Ca^{2+} concentration by both thapsigargin and histamine rather than sustained translocation of endogenous STIM1 that induces an interaction between the C-terminus of STIM1 and Golli-BG21, although this remains to be investigated. The BiFC assay was used in this study since it is a more robust method for investigating protein interactions in live cells than other techniques such as FRET. It is important to note however, that the BiFC assay is not reflective of the kinetics of the interaction, since binding between the YC and YN fragments of EYFP is essentially irreversible and refolding of the full EYFP protein and the reconstitution of fluorescence requires a finite period of time (Robida and Kerppola, 2009), in this case, up to 90 minutes. Irrespective of the lack of information from these experiments on the kinetics of STIM1/Golli-BG21 interaction, this assay provides the most convincing evidence of a direct protein-protein interaction in living cells.

No fluorescence complementation was observed in cells expressing Golli-YC and FL-STIM1-YN or Orai1-YN, suggesting that these proteins may not interact. EYFP fluorescence was also absent in cells expressing Orai1-YC and STIM1-CT-YN (see Chapter 3), even though the STIM1 and Orai1 proteins are known to interact (Muik et al., 2008; Park et al., 2009; Vig et al., 2006a; Yeromin et al., 2006). There are several reasons why this may have occurred. Firstly, fusion of an EYFP fragment to a protein may alter the structure of the protein, thereby abolishing an interaction domain within the protein of interest (Kerppola, 2006). Secondly, the arrangement of the BiFC fusion proteins within a protein complex may sterically hinder an interaction between the complementary EYFP fragments and prevent the formation

of functional EYFP (Kerppola, 2006). The lack of EYFP fluorescence between Orai1-YC/STIM1-CT-YN, Golli-YC/Orai1-YN and Golli-YC/FL-STIM1-YN proteins is therefore not conclusive evidence for the absence of an interaction between these protein pairs.

Despite the large amount of recent research into the activation of SOCs, very few interacting partners have been found for STIM1 and Orai1. One recent study has identified a novel EF-hand containing protein, CRACR2A, which binds to both STIM1 and Orai1 to stabilise their interaction, thereby enhancing SOCE in T-cells (Srikanth et al., 2010a). Additionally, little is known about the Ca^{2+}-dependent inactivation of these channels. One recent study reported that both calmodulin and a short negatively charged region within the STIM1 C-terminus can bind to Orai1 to inactivate SOCE (Mullins et al., 2009). Interestingly, in this study, Golli-BG21 colocalised with STIM1 and Orai1 complexes after store depletion. The ability of Golli-BG21 to bind STIM1 puncta in a Ca^{2+}-dependent manner may be key to its regulation of SOCE. It is possible that Golli-BG21 binds to STIM1-Orai1 complexes when Ca^{2+} levels are already high to reduce the influx of Ca^{2+} into the cell and perhaps may be a further contributor to the Ca^{2+}-dependent inactivation of SOCs. Golli-BG21 does not contain a putative Ca^{2+} binding domain, suggesting that Ca^{2+} probably does not directly influence the STIM1 and Golli interaction. However, Ca^{2+} may be required to recruit a further undiscovered protein into the complex to initiate or stabilise an interaction between STIM1 and Golli, although this remains to be investigated.

To date, studies on MBP and Golli and their regulation of Ca^{2+} channels have focussed exclusively on oligodendrocyte precursor cells and T-cells. Of the three Golli isoforms cloned, the BG21 isoform of Golli is the most widely expressed in many different tissues other than nervous tissues, including the heart, kidney, spleen and lung (Campagnoni et al., 1993) although its function in these tissues has not been elucidated. The widespread distribution of Golli-BG21 suggests that it could be part of a general mechanism for the regulation of SOCE across many tissue types. Hence, this study proposes that Golli-BG21 functions to regulate SOCE via a direct interaction with STIM1 but the exact molecular mechanism underlying this interaction has yet to be defined.

CHAPTER SIX

Discussion

The work described in this thesis characterised several aspects which govern the recruitment of STIM1 to the plasma membrane in HeLa cells. This study was carried out in two separate laboratories which share a common interest in Ca^{2+} signalling. One laboratory had a particular interest in the bioenergetics of SOCE stemming from previous studies performed in the laboratory which investigated the role of ATP in Ca^{2+} influx and extrusion in pancreatic acinar cells (Barrow et al., 2008). The other laboratory utilises a variety of cell based assays in order to investigate the roles of Ca^{2+} sensor proteins, their trafficking and their binding partners (Burgoyne, 2007). This study therefore employed a range of techniques including confocal fluorescence microscopy, live cell Ca^{2+} imaging, immunocytochemistry, in vitro binding experiments and western blotting to reveal a novel mechanism for the regulation of STIM1 translocation to ER-PM junctions, to distinguish the plasma membrane components that target STIM1 to plasma membrane puncta and also to reveal a novel binding partner for STIM1 which may affect the activity of STIM1-dependent SOCE.

Initially, I aimed to characterise the bioenergetics of STIM1 translocation in order to understand whether the trafficking of STIM1 to the plasma membrane was an energy-dependent or diffusional process. To investigate this, ATP production was inhibited in live cells to determine whether ATP is required for STIM1 puncta formation. Surprisingly, it was shown using confocal fluorescence microscopy that

ATP depletion stimulates the translocation of STIM1 to the plasma membrane. Puncta formation occurred over a longer time course than that observed with store depletion, with puncta appearing after approximately 15 minutes following the inhibition of ATP production. Colocalisation experiments revealed that under these conditions, STIM1 and Orai1 complex formation still occurred. Microtubule staining established that microtubules remain intact following ATP depletion, suggesting that STIM1 translocation does not occur as a result of destruction of the microtubule cytoskeleton. These findings suggest that ATP is not required for STIM1 puncta formation or for establishing STIM1-Orai1 complexes at ER-PM junctions and provide support for the hypothesis that STIM1 translocates to ER-PM junctions by diffusion.

It is important to note that although the machinery for SOCE can assemble in the absence of ATP, SOCE itself is attenuated under these conditions (Barrow et al., 2008; Chvanov et al., 2008; Gamberucci et al., 1994; Marriott and Mason, 1995). However, the mechanism by which inhibiting energy production prevents SOCE is unclear. The depletion of ATP may result in the dephosphorylation of many proteins, including proteins required for SOCE. STIM1, STIM2 and Orai1 all contain putative phosphorylation sites (Manji et al., 2000; Smyth et al., 2009; Takahashi et al., 2007). Phosphorylation of STIM1 can affect its ability to activate SOCE and results in suppression of Ca^{2+} influx during mitosis (Smyth et al., 2009). It is possible that the phosphorylation state of Orai1 or another Orai1 or STIM1 interacting protein involved in the SOCE machinery also affects the activation of SOCE under conditions where ATP is depleted. Alternatively, it is also possible that inhibiting ATP

production may affect the ability of mitochondria to buffer Ca^{2+} near the plasma membrane and/or decrease the amount of ATP available for release by mitochondria at the cell periphery to chelate Ca^{2+}. This would increase the amount of Ca^{2+} accumulating in Ca^{2+} microdomains near the plasma membrane and contribute to the feedback inhibition of SOCE.

One of the initial aims was to conclusively determine whether STIM1 inserts into the plasma membrane following translocation and to subsequently define the mechanism by which this occurs. In order to do this, a STIM1 protein was constructed which contained an N-terminal hexahistidine tag and a C-terminal EYFP tag, with the hypothesis that the hexahistidine tag should become exposed to the cell surface following translocation if the protein is secreted into the plasma membrane. A version of this construct has been used previously in a study that concluded that store depletion stimulates the insertion of STIM1 into the plasma membrane (Hauser and Tsien, 2007). However, in the present study this protein was found to be constitutively trafficked to the plasma membrane, possibly an artefact produced by the addition of the N-terminal hexahistidine tag. This result questions the validity of this construct for use in previous investigations into the possible plasma membrane insertion of STIM1 and questions whether untagged STIM1 also inserts into the plasma membrane following translocation. Two studies have independently demonstrated that SOCE activity can be inhibited by suppressing or mutating proteins involved in exocytosis (Yao et al., 1999; Zhang et al., 2006). We therefore hypothesised that STIM1 may insert into the plasma membrane via exocytosis. However, in the present study, inhibition of exocytosis

with an αSNAP(L294A) mutant protein did not prevent the development of STIM1 puncta, suggesting that STIM1 insertion into the plasma membrane is not required for STIM1 puncta formation. In addition, this study has demonstrated that STIM1 puncta can form in cell depleted of ATP, where membrane fusion events would be inhibited. Together these results argue that STIM1 does not insert into the plasma membrane following store depletion. However, further investigations are required in order to determine whether or not this is the case. It would be interesting to determine whether alternative small tags e.g. a myc tag, also affect the distribution of STIM1. Perhaps in future experiments such a tag may be a suitable substitute to the hexahistidine tag.

The mechanism by which STIM1 is anchored to ER-PM junctions needed to be defined in order to further characterise the trafficking of STIM1 to plasma membrane puncta. Live cell confocal fluorescence microscopy revealed that depletion of multiple phosphoinositides inhibits STIM1 puncta formation and reduces SOCE following store depletion, suggesting that phosphoinositide species at the plasma membrane are required for STIM1 puncta formation. From these experiments it seems that PtdIns(4)P, PtdIns(4,5)P_2 and PtdIns(3,4,5)P_3 may all contribute to STIM1 puncta formation, since depletion of any of phosphoinositide species alone has only a small effect on the number of STIM1 puncta formed but simultaneous depletion of all three phosphoinositides results in a complete inhibition of STIM1 puncta formation. These observations mirror those from previous studies which demonstrated that the polybasic tail of STIM1 is involved in puncta formation (Li et al., 2007; Liou et al., 2007; Park et al., 2009; Yuan et al.,

2009) and suggest that this occurs through the binding of the polybasic tail to plasma membrane phosphoinositides. In this study the relative contribution of each phosphoinositide in the establishment of STIM1 puncta was not assessed in detail. It would be interesting to know whether STIM1 binds directly to each phosphoinositide species and also whether STIM1 binds preferentially to specific phosphoinositide species over others. In addition, this study did not focus on the requirement for plasma membrane phosphoinositides in the formation of STIM2 puncta. Following the completion of this study, one group has reported on the specific binding affinities of the STIM1 and STIM2 C-termini for plasma membrane lipids using liposome binding assays (Ercan et al., 2009). Using this approach the authors showed that the C-terminus of STIM1 physically interacts with plasma membrane phosphoinositides, which is consistent with the results found in the present study. They also demonstrated that the C-terminal domain of STIM1 interacts preferentially interacts with PtdIns(4,5)P_2 in PM-like liposomes but, interestingly, binding is reduced in PC liposomes that contain PtdIns(4,5)P_2 (Ercan et al., 2009), suggesting that the C-terminus of STIM1 also interacts with other plasma membrane phosphoinositides, an observation which supports the conclusion from the present study that a combination of phosphoinositide species is required for STIM1 puncta formation. STIM2 on the other hand did not show a preference with respect to binding to specific phosphoinositides (Ercan et al., 2009). It would be of interest to determine using confocal microscopy whether STIM2-EYFP puncta formation can occur in conditions of phosphoinositide depletion and also whether STIM2-dependent SOCE is affected under such conditions. It is likely that since

STIM2 binds to phosphoinositides (Ercan et al., 2009), they will also be involved in the regulation of STIM2 dependent SOCE.

Although the results suggest that a combination of phosphoinositides is involved in the formation of SOCE, I did not investigate the contributory role for each phosphoinositide in SOCE. One recent report has suggested that PI(4)P is the main contributory phosphoinositide for SOCE (Korzeniowski et al., 2009), whereas the data in the present study demonstrates that PI(4)P depletion alone through PI4 kinase inhibition has little affect on the formation of STIM1 puncta, and therefore may not be the major phosphoinositide for SOCE. In order to uncover the individual roles for each phosphoinositide in SOCE activity, SOCE will need to be measured in conditions where each phosphoinositide has been specifically depleted. It is probable that the contribution of each phosphoinositide in SOCE will be dependent on its requirement for STIM1 puncta formation.

Although a vast amount of research has been carried out in recent years to discover the proteins involved in the mediation of SOCE, very few SOCE-regulating proteins have actually been identified. There is an enormous amount of data detailing an interaction between the two crucial SOCE proteins, STIM1 and Orai1, on both a molecular and functional level (Park et al., 2009; Prakriya et al., 2006; Vig et al., 2006b; Yeromin et al., 2006; Yuan et al., 2009). Several other SOCE regulators include the STIM1 homologue, STIM2, which may regulate basal cytosolic Ca^{2+} levels (Brandman et al., 2007) through an interaction with Orai1, and TRPC1 which has been shown to bind to both STIM1 and Orai1 in lipid rafts and is itself a

proposed SOC channel (Huang et al., 2006; Yuan et al., 2009). Another protein shown to bind to STIM1 includes the microtubule plus end tracking protein, EB1, although this interaction seems to be required for remodelling the ER and was not shown to be required for SOCE (Grigoriev et al., 2008). There is also evidence to suggest that calmodulin binds to STIM1 (Bauer et al., 2008) and Orai1 (Mullins et al., 2009) and may be involved in the Ca^{2+}-dependent inactivation of SOCE (Mullins et al., 2009). One of the main aims of this study was to identify a novel interacting partner for STIM1 and/or Orai1 which may be involved in the regulation of SOCE. Pulldown experiments revealed that the C-terminus of STIM1 binds to MBP and further binding experiments determined that STIM1 also binds an MBP splice isoform, Golli-BG21, which has been implicated previously as a negative regulator of SOCE. The interaction between Golli-MBP and STIM1-CT was confirmed using a BiFC assay. Ca^{2+} imaging experiments revealed that overexpression of Golli-BG21 reduced SOCE when compared when untransfected cells and that co-expression of STIM1 reversed this effect.

These results not only confirm a role for Golli-BG21 in the regulation of SOCs, but reports the novel finding that Golli-BG21 may negatively regulate SOCE through a direct interaction with STIM1. Since histamine was shown to stimulate the interaction between STIM1 and Golli, it is possible that changes in cytosolic Ca^{2+} may induce the binding of Golli to STIM1, thereby participating in the Ca^{2+}-dependent inactivation of SOCE. It would be interesting to determine the molecular mechanism behind this inactivation, since Golli-BG21 itself has no Ca^{2+} binding domains. The myristoylation site on the C-terminus of the Golli domain which

anchors it to the plasma membrane is critical for Golli's ability to increase Ca^{2+} influx in oligodendrocytes. It is possible that membrane association of Golli is also required to modulate STIM1-dependent SOCE. Mutation or deletion of the myristoylation site would determine whether this is the case.

I did not examine the molecular mechanism involved in the interaction between the C-terminus of STIM1 and Golli. Since it was initially found that MBP binds to STIM1, it is possible that STIM1 binds an epitope within Golli-BG21 which is shared with MBP. Mutational analysis of the various domains within Golli-BG21 would determine which domain within the protein binds to STIM1 and would also confirm whether or not abolishing the interaction between STIM1 and Golli-BG21 removes the effect of Golli-BG21 on SOCE. Mutational analysis of the domains within the C-terminus of STIM1 would complete the molecular characterisation of the interaction between STIM1 and Golli-BG21. The regulatory region within STIM1 which is required to bind to and activate Orai1 is found within its C-terminus (Mullins et al., 2009) and one recent report has discovered the existence of a second domain within the C-terminus which is involved in Ca^{2+}-dependent inactivation of SOCE (Mullins et al., 2009). It is possible that at high cytosolic Ca^{2+} concentrations, Golli-BG21 may bind the activation domain of STIM1 to partially inhibit its ability to activate Orai1. Alternatively, it may be that Golli binds to the inactivation domain of STIM1 to enhance Ca^{2+}-dependent inactivation of SOCE. It would be interesting to define the interaction between STIM1 and Golli-BG21 on a molecular basis to reveal the exact function that this interaction plays in SOCE.

Recently, a novel cytosolic EF-hand protein, CRACR2A, was discovered as a protein which binds to both STIM1 and Orai1 to stabilise their interaction and thereby enhance SOCE (Srikanth et al., 2010a). Depletion of CRACR2A using RNAi in HEK293 cells resulted in a 50% decrease in SOCE (Srikanth et al., 2010a). Interestingly, CRACR2A is highly expressed in T cells. It would be of interest to determine whether CRACR2A interacts with Golli. It is possible that Golli may competitively interact with STIM1, thereby preventing CRACR2A binding to STIM1 resulting in the destabilisation of the STIM1-Orai1 interaction and a consequent reduction in SOCE.

Conclusion

In conclusion, work in this thesis has identified a novel mechanism for STIM1 translocation to the plasma membrane which supports a model for diffusion of STIM1 to plasma membrane puncta which does not require ATP. In support of this model, I have identified plasma membrane phosphoinositides as the components which target diffusing STIM1 molecules to ER-PM junction. It is probable that STIM1 aggregates become trapped in ER-PM junctions through an electrostatic interaction with phosphoinositides to increase the likelihood of STIM1 binding to diffusing Orai1 molecules in the plasma membrane. Finally, I have revealed a novel STIM1 interacting partner, Golli-BG21 which may negatively regulate the activity of SOCs through a direct interaction with STIM1. Further experimental work is required to map the interacting domains within the STIM1 and Golli-BG21 proteins and to characterise the exact mechanism by which Golli mediates SOCE.

Bibliography

Alicia, S., Angelica, Z., Carlos, S., Alfonso, S., and Vaca, L. (2008). STIM1 converts TRPC1 from a receptor-operated to a store-operated channel: moving TRPC1 in and out of lipid rafts. Cell Calcium *44*, 479-491.

Ashby, M.C., and Tepikin, A.V. (2001). ER calcium and the functions of intracellular organelles. Semin Cell Dev Biol *12*, 11-17.

Baba, Y., Hayashi, K., Fujii, Y., Mizushima, A., Watarai, H., Wakamori, M., Numaga, T., Mori, Y., Iino, M., Hikida, M.*, et al.* (2006). Coupling of STIM1 to store-operated Ca2+ entry through its constitutive and inducible movement in the endoplasmic reticulum. Proc Natl Acad Sci U S A *103*, 16704-16709.

Baba, Y., Nishida, K., Fujii, Y., Hirano, T., Hikida, M., and Kurosaki, T. (2008). Essential function for the calcium sensor STIM1 in mast cell activation and anaphylactic responses. Nat Immunol *9*, 81-88.

Bakowski, D., Burgoyne, R.D., and Parekh, A.B. (2003). Activation of the store-operated calcium current ICRAC can be dissociated from regulated exocytosis in rat basophilic leukaemia (RBL-1) cells. J Physiol *553*, 387-393.

Barnard, R.J., Morgan, A., and Burgoyne, R.D. (1997). Stimulation of NSF ATPase activity by alpha-SNAP is required for SNARE complex disassembly and exocytosis. J Cell Biol *139*, 875-883.

Barr, V.A., Bernot, K.M., Srikanth, S., Gwack, Y., Balagopalan, L., Regan, C.K., Helman, D.J., Sommers, C.L., Oh-Hora, M., Rao, A.*, et al.* (2008). Dynamic movement of the calcium sensor STIM1 and the calcium channel Orai1 in activated T-cells: puncta and distal caps. Mol Biol Cell *19*, 2802-2817.

Barrow, S.L., Voronina, S.G., da Silva Xavier, G., Chvanov, M.A., Longbottom, R.E., Gerasimenko, O.V., Petersen, O.H., Rutter, G.A., and Tepikin, A.V. (2008). ATP depletion inhibits Ca2+ release, influx and extrusion in pancreatic acinar cells but not pathological Ca2+ responses induced by bile. Pflugers Arch *455*, 1025-1039.

Bauer, M.C., O'Connell, D., Cahill, D.J., and Linse, S. (2008). Calmodulin binding to the polybasic C-termini of STIM proteins involved in store-operated calcium entry. Biochemistry *47*, 6089-6091.

Bautista, D.M., and Lewis, R.S. (2004). Modulation of plasma membrane calcium-ATPase activity by local calcium microdomains near CRAC channels in human T cells. J Physiol *556*, 805-817.

Bergmeier, W., Oh-Hora, M., McCarl, C.A., Roden, R.C., Bray, P.F., and Feske, S. (2009). R93W mutation in Orai1 causes impaired calcium influx in platelets. Blood *113*, 675-678.

Berridge, M.J., Lipp, P., and Bootman, M.D. (2000). The versatility and universality of calcium signalling. Nat Rev Mol Cell Biol *1*, 11-21.

Beyersdorf, N., Braun, A., Vogtle, T., Varga-Szabo, D., Galdos, R.R., Kissler, S., Kerkau, T., and Nieswandt, B. (2009). STIM1-independent T cell development and effector function in vivo. J Immunol *182*, 3390-3397.

Bhakta, N.R., Oh, D.Y., and Lewis, R.S. (2005). Calcium oscillations regulate thymocyte motility during positive selection in the three-dimensional thymic environment. Nat Immunol *6*, 143-151.

Bootman, M.D., and Berridge, M.J. (1996). Subcellular Ca2+ signals underlying waves and graded responses in HeLa cells. Curr Biol *6*, 855-865.

Bootman, M.D., Collins, T.J., Peppiatt, C.M., Prothero, L.S., MacKenzie, L., De Smet, P., Travers, M., Tovey, S.C., Seo, J.T., Berridge, M.J.*, et al.* (2001). Calcium signalling--an overview. Semin Cell Dev Biol *12*, 3-10.

Bootman, M.D., and Lipp, P. (1999). Ringing changes to the 'bell-shaped curve'. Curr Biol *9*, R876-878.

Brandman, O., Liou, J., Park, W.S., and Meyer, T. (2007). STIM2 is a feedback regulator that stabilizes basal cytosolic and endoplasmic reticulum Ca2+ levels. Cell *131*, 1327-1339.

Braun, A., Gessner, J.E., Varga-Szabo, D., Syed, S.N., Konrad, S., Stegner, D., Vogtle, T., Schmidt, R.E., and Nieswandt, B. (2009). STIM1 is essential for Fcgamma receptor activation and autoimmune inflammation. Blood *113*, 1097-1104.

Broad, L.M., Braun, F.J., Lievremont, J.P., Bird, G.S., Kurosaki, T., and Putney, J.W., Jr. (2001). Role of the phospholipase C-inositol 1,4,5-trisphosphate pathway in

calcium release-activated calcium current and capacitative calcium entry. J Biol Chem *276*, 15945-15952.

Burgoyne, R.D. (2007). Neuronal calcium sensor proteins: generating diversity in neuronal Ca2+ signalling. Nat Rev Neurosci *8*, 182-193.

Calcraft, P.J., Ruas, M., Pan, Z., Cheng, X., Arredouani, A., Hao, X., Tang, J., Rietdorf, K., Teboul, L., Chuang, K.T.*, et al.* (2009). NAADP mobilizes calcium from acidic organelles through two-pore channels. Nature *459*, 596-600.

Calloway, N., Holowka, D., and Baird, B. (2010). A basic sequence in STIM1 promotes Ca2+ influx by interacting with the C-terminal acidic coiled coil of Orai1. Biochemistry *49*, 1067-1071.

Calloway, N., Vig, M., Kinet, J.P., Holowka, D., and Baird, B. (2009). Molecular clustering of STIM1 with Orai1/CRACM1 at the plasma membrane depends dynamically on depletion of Ca2+ stores and on electrostatic interactions. Mol Biol Cell *20*, 389-399.

Campagnoni, A.T., Pribyl, T.M., Campagnoni, C.W., Kampf, K., Amur-Umarjee, S., Landry, C.F., Handley, V.W., Newman, S.L., Garbay, B., and Kitamura, K. (1993). Structure and developmental regulation of Golli-mbp, a 105-kilobase gene that encompasses the myelin basic protein gene and is expressed in cells in the oligodendrocyte lineage in the brain. J Biol Chem *268*, 4930-4938.

Catterall, W.A. (2000). Structure and regulation of voltage-gated Ca2+ channels. Annu Rev Cell Dev Biol *16*, 521-555.

Catterall, W.A., Cestele, S., Yarov-Yarovoy, V., Yu, F.H., Konoki, K., and Scheuer, T. (2007). Voltage-gated ion channels and gating modifier toxins. Toxicon *49*, 124-141.

Chang, W.C., Nelson, C., and Parekh, A.B. (2006). Ca2+ influx through CRAC channels activates cytosolic phospholipase A2, leukotriene C4 secretion, and expression of c-fos through ERK-dependent and -independent pathways in mast cells. FASEB J *20*, 2381-2383.

Cheng, K.T., Liu, X., Ong, H.L., and Ambudkar, I.S. (2008). Functional requirement for Orai1 in store-operated TRPC1-STIM1 channels. J Biol Chem *283*, 12935-12940.

Chini, E.N., Beers, K.W., and Dousa, T.P. (1995). Nicotinate Adenine-Dinucleotide Phosphate (Naadp) Triggers a Specific Calcium-Release System in Sea-Urchin Eggs (Vol 270, Pg 3216, 1995). Journal of Biological Chemistry *270*, 10359-10359.

Chvanov, M., Walsh, C.M., Haynes, L.P., Voronina, S.G., Lur, G., Gerasimenko, O.V., Barraclough, R., Rudland, P.S., Petersen, O.H., Burgoyne, R.D.*, et al.* (2008). ATP depletion induces translocation of STIM1 to puncta and formation of STIM1-ORAI1 clusters: translocation and re-translocation of STIM1 does not require ATP. Pflugers Arch *457*, 505-517.

Covington, E.D., Wu, M.M., and Lewis, R.S. (2010). Essential role for the CRAC activation domain in store-dependent oligomerization of STIM1. Mol Biol Cell *21*, 1897-1907.

DeHaven, W.I., Jones, B.F., Petranka, J.G., Smyth, J.T., Tomita, T., Bird, G.S., and Putney, J.W., Jr. (2009). TRPC channels function independently of STIM1 and Orai1. J Physiol *587*, 2275-2298.

Delon, J., Bercovici, N., Liblau, R., and Trautmann, A. (1998). Imaging antigen recognition by naive CD4+ T cells: compulsory cytoskeletal alterations for the triggering of an intracellular calcium response. Eur J Immunol *28*, 716-729.

Deng, X., Wang, Y., Zhou, Y., Soboloff, J., and Gill, D.L. (2009). STIM and Orai: dynamic intermembrane coupling to control cellular calcium signals. J Biol Chem *284*, 22501-22505.

Derler, I., Fahrner, M., Muik, M., Lackner, B., Schindl, R., Groschner, K., and Romanin, C. (2009). A Ca2(+)release-activated Ca2(+) (CRAC) modulatory domain (CMD) within STIM1 mediates fast Ca2(+)-dependent inactivation of ORAI1 channels. J Biol Chem *284*, 24933-24938.

Di Capite, J., Ng, S.W., and Parekh, A.B. (2009). Decoding of cytoplasmic Ca(2+) oscillations through the spatial signature drives gene expression. Curr Biol *19*, 853-858.

Dietrich, A., Mederos, Y.S.M., Gollasch, M., Gross, V., Storch, U., Dubrovska, G., Obst, M., Yildirim, E., Salanova, B., Kalwa, H.*, et al.* (2005). Increased vascular smooth muscle contractility in TRPC6-/- mice. Mol Cell Biol *25*, 6980-6989.

Downing, G.J., Kim, S., Nakanishi, S., Catt, K.J., and Balla, T. (1996). Characterization of a soluble adrenal phosphatidylinositol 4-kinase reveals wortmannin sensitivity of type III phosphatidylinositol kinases. Biochemistry *35*, 3587-3594.

Dunlap, K., Luebke, J.I., and Turner, T.J. (1995). Exocytotic Ca2+ channels in mammalian central neurons. Trends Neurosci *18*, 89-98.

Duszynski, J., Koziel, R., Brutkowski, W., Szczepanowska, J., and Zablocki, K. (2006). The regulatory role of mitochondria in capacitative calcium entry. Biochim Biophys Acta *1757*, 380-387.

Ercan, E., Momburg, F., Engel, U., Temmerman, K., Nickel, W., and Seedorf, M. (2009). A conserved, lipid-mediated sorting mechanism of yeast Ist2 and mammalian STIM proteins to the peripheral ER. Traffic *10*, 1802-1818.

Feng, J.M., Fernandes, A.O., Campagnoni, C.W., Hu, Y.H., and Campagnoni, A.T. (2004). The golli-myelin basic protein negatively regulates signal transduction in T lymphocytes. J Neuroimmunol *152*, 57-66.

Feng, J.M., Hu, Y.K., Xie, L.H., Colwell, C.S., Shao, X.M., Sun, X.P., Chen, B., Tang, H., and Campagnoni, A.T. (2006). Golli protein negatively regulates store depletion-induced calcium influx in T cells. Immunity *24*, 717-727.

Feske, S. (2009). ORAI1 and STIM1 deficiency in human and mice: roles of store-operated Ca2+ entry in the immune system and beyond. Immunol Rev *231*, 189-209.

Feske, S., Draeger, R., Peter, H.H., Eichmann, K., and Rao, A. (2000). The duration of nuclear residence of NFAT determines the pattern of cytokine expression in human SCID T cells. J Immunol *165*, 297-305.

Feske, S., Giltnane, J., Dolmetsch, R., Staudt, L.M., and Rao, A. (2001). Gene regulation mediated by calcium signals in T lymphocytes. Nat Immunol *2*, 316-324.

Feske, S., Gwack, Y., Prakriya, M., Srikanth, S., Puppel, S.H., Tanasa, B., Hogan, P.G., Lewis, R.S., Daly, M., and Rao, A. (2006). A mutation in Orai1 causes immune deficiency by abrogating CRAC channel function. Nature *441*, 179-185.

Feske, S., Muller, J.M., Graf, D., Kroczek, R.A., Drager, R., Niemeyer, C., Baeuerle, P.A., Peter, H.H., and Schlesier, M. (1996). Severe combined immunodeficiency due

to defective binding of the nuclear factor of activated T cells in T lymphocytes of two male siblings. Eur J Immunol *26*, 2119-2126.

Fierro, L., and Parekh, A.B. (1999). Fast calcium-dependent inactivation of calcium release-activated calcium current (CRAC) in RBL-1 cells. J Membr Biol *168*, 9-17.

Fill, M., and Copello, J.A. (2002). Ryanodine receptor calcium release channels. Physiol Rev *82*, 893-922.

Freichel, M., Suh, S.H., Pfeifer, A., Schweig, U., Trost, C., Weissgerber, P., Biel, M., Philipp, S., Freise, D., Droogmans, G.*, et al.* (2001). Lack of an endothelial store-operated Ca2+ current impairs agonist-dependent vasorelaxation in TRP4-/- mice. Nat Cell Biol *3*, 121-127.

Frischauf, I., Schindl, R., Derler, I., Bergsmann, J., Fahrner, M., and Romanin, C. (2008). The STIM/Orai coupling machinery. Channels (Austin) *2*, 261-268.

Gagnon, E., Duclos, S., Rondeau, C., Chevet, E., Cameron, P.H., Steele-Mortimer, O., Paiement, J., Bergeron, J.J., and Desjardins, M. (2002). Endoplasmic reticulum-mediated phagocytosis is a mechanism of entry into macrophages. Cell *110*, 119-131.

Galan, C., Woodard, G.E., Dionisio, N., Salido, G.M., and Rosado, J.A. (2010). Lipid rafts modulate the activation but not the maintenance of store-operated Ca(2+) entry. Biochim Biophys Acta *1803*, 1083-1093.

Galione, A., and Petersen, O.H. (2005). The NAADP receptor: New receptors or new regulation? Mol Interv *5*, 73-+.

Gamberucci, A., Innocenti, B., Fulceri, R., Banhegyi, G., Giunti, R., Pozzan, T., and Benedetti, A. (1994). Modulation of Ca2+ influx dependent on store depletion by intracellular adenine-guanine nucleotide levels. J Biol Chem *269*, 23597-23602.

Gamper, N., and Shapiro, M.S. (2007). Regulation of ion transport proteins by membrane phosphoinositides. Nat Rev Neurosci *8*, 921-934.

Glitsch, M.D., Bakowski, D., and Parekh, A.B. (2002). Store-operated Ca2+ entry depends on mitochondrial Ca2+ uptake. EMBO J *21*, 6744-6754.

Gomez, T.M., Robles, E., Poo, M., and Spitzer, N.C. (2001). Filopodial calcium transients promote substrate-dependent growth cone turning. Science *291*, 1983-1987.

Graham, M.E., Washbourne, P., Wilson, M.C., and Burgoyne, R.D. (2001). SNAP-25 with mutations in the zero layer supports normal membrane fusion kinetics. J Cell Sci *114*, 4397-4405.

Grigoriev, I., Gouveia, S.M., van der Vaart, B., Demmers, J., Smyth, J.T., Honnappa, S., Splinter, D., Steinmetz, M.O., Putney, J.W., Jr., Hoogenraad, C.C.*, et al.* (2008). STIM1 is a MT-plus-end-tracking protein involved in remodeling of the ER. Curr Biol *18*, 177-182.

Guermonprez, P., Saveanu, L., Kleijmeer, M., Davoust, J., Van Endert, P., and Amigorena, S. (2003). ER-phagosome fusion defines an MHC class I cross-presentation compartment in dendritic cells. Nature *425*, 397-402.

Gwack, Y., Srikanth, S., Feske, S., Cruz-Guilloty, F., Oh-hora, M., Neems, D.S., Hogan, P.G., and Rao, A. (2007). Biochemical and functional characterization of Orai proteins. J Biol Chem *282*, 16232-16243.

Gwack, Y., Srikanth, S., Oh-Hora, M., Hogan, P.G., Lamperti, E.D., Yamashita, M., Gelinas, C., Neems, D.S., Sasaki, Y., Feske, S.*, et al.* (2008). Hair loss and defective T- and B-cell function in mice lacking ORAI1. Mol Cell Biol *28*, 5209-5222.

Hatsuzawa, K., Tamura, T., Hashimoto, H., Yokoya, S., Miura, M., Nagaya, H., and Wada, I. (2006). Involvement of syntaxin 18, an endoplasmic reticulum (ER)-localized SNARE protein, in ER-mediated phagocytosis. Mol Biol Cell *17*, 3964-3977.

Hauser, C.T., and Tsien, R.Y. (2007). A hexahistidine-Zn2+-dye label reveals STIM1 surface exposure. Proc Natl Acad Sci U S A *104*, 3693-3697.

Haynes, L.P., Sherwood, M.W., Dolman, N.J., and Burgoyne, R.D. (2007). Specificity, promiscuity and localization of ARF protein interactions with NCS-1 and phosphatidylinositol-4 kinase-III beta. Traffic *8*, 1080-1092.

Haynes, L.P., Tepikin, A.V., and Burgoyne, R.D. (2004). Calcium-binding protein 1 is an inhibitor of agonist-evoked, inositol 1,4,5-trisphosphate-mediated calcium signaling. J Biol Chem *279*, 547-555.

Heo, W.D., Inoue, T., Park, W.S., Kim, M.L., Park, B.O., Wandless, T.J., and Meyer, T. (2006). PI(3,4,5)P3 and PI(4,5)P2 lipids target proteins with polybasic clusters to the plasma membrane. Science *314*, 1458-1461.

Hewavitharana, T., Deng, X., Wang, Y., Ritchie, M.F., Girish, G.V., Soboloff, J., and Gill, D.L. (2008). Location and function of STIM1 in the activation of Ca2+ entry signals. J Biol Chem *283*, 26252-26262.

Hofmann, F., Biel, M., and Flockerzi, V. (1994). Molecular basis for Ca2+ channel diversity. Annu Rev Neurosci *17*, 399-418.

Hofmann, T., Obukhov, A.G., Schaefer, M., Harteneck, C., Gudermann, T., and Schultz, G. (1999). Direct activation of human TRPC6 and TRPC3 channels by diacylglycerol. Nature *397*, 259-263.

Hogan, P.G., Chen, L., Nardone, J., and Rao, A. (2003). Transcriptional regulation by calcium, calcineurin, and NFAT. Genes Dev *17*, 2205-2232.

Hogan, P.G., Lewis, R.S., and Rao, A. (2010). Molecular basis of calcium signaling in lymphocytes: STIM and ORAI. Annu Rev Immunol *28*, 491-533.

Hogan, P.G., and Rao, A. (2007). Dissecting ICRAC, a store-operated calcium current. Trends Biochem Sci *32*, 235-245.

Honnappa, S., Gouveia, S.M., Weisbrich, A., Damberger, F.F., Bhavesh, N.S., Jawhari, H., Grigoriev, I., van Rijssel, F.J., Buey, R.M., Lawera, A.*, et al.* (2009). An EB1-binding motif acts as a microtubule tip localization signal. Cell *138*, 366-376.

Hoth, M., Fanger, C.M., and Lewis, R.S. (1997). Mitochondrial regulation of store-operated calcium signaling in T lymphocytes. J Cell Biol *137*, 633-648.

Hoth, M., and Penner, R. (1992). Depletion of intracellular calcium stores activates a calcium current in mast cells. Nature *355*, 353-356.

Hsu, A.L., Ching, T.T., Sen, G., Wang, D.S., Bondada, S., Authi, K.S., and Chen, C.S. (2000). Novel function of phosphoinositide 3-kinase in T cell Ca2+ signaling. A phosphatidylinositol 3,4,5-trisphosphate-mediated Ca2+ entry mechanism. J Biol Chem *275*, 16242-16250.

Huang, G.N., Zeng, W., Kim, J.Y., Yuan, J.P., Han, L., Muallem, S., and Worley, P.F. (2006). STIM1 carboxyl-terminus activates native SOC, I(crac) and TRPC1 channels. Nat Cell Biol *8*, 1003-1010.

Jardin, I., Lopez, J.J., Salido, G.M., and Rosado, J.A. (2008a). Orai1 mediates the interaction between STIM1 and hTRPC1 and regulates the mode of activation of hTRPC1-forming Ca2+ channels. J Biol Chem *283*, 25296-25304.

Jardin, I., Redondo, P.C., Salido, G.M., and Rosado, J.A. (2008b). Phosphatidylinositol 4,5-bisphosphate enhances store-operated calcium entry through hTRPC6 channel in human platelets. Biochim Biophys Acta *1783*, 84-97.

Jardin, I., Salido, G.M., and Rosado, J.A. (2008c). Role of lipid rafts in the interaction between hTRPC1, Orai1 and STIM1. Channels (Austin) *2*, 401-403.

Jenner, S., Farndale, R.W., and Sage, S.O. (1996). Wortmannin inhibits store-mediated calcium entry and protein tyrosine phosphorylation in human platelets. FEBS Lett *381*, 249-251.

Ji, W., Xu, P., Li, Z., Lu, J., Liu, L., Zhan, Y., Chen, Y., Hille, B., Xu, T., and Chen, L. (2008). Functional stoichiometry of the unitary calcium-release-activated calcium channel. Proc Natl Acad Sci U S A *105*, 13668-13673.

Johnson, J.D., Kuang, S., Misler, S., and Polonsky, K.S. (2004). Ryanodine receptors in human pancreatic beta cells: localization and effects on insulin secretion. FASEB J *18*, 878-880.

Kawasaki, T., Lange, I., and Feske, S. (2009). A minimal regulatory domain in the C terminus of STIM1 binds to and activates ORAI1 CRAC channels. Biochem Biophys Res Commun *385*, 49-54.

Kerppola, T.K. (2006). Visualization of molecular interactions by fluorescence complementation. Nat Rev Mol Cell Biol *7*, 449-456.

Kerschbaum, H.H., and Cahalan, M.D. (1999). Single-channel recording of a store-operated Ca2+ channel in Jurkat T lymphocytes. Science *283*, 836-839.

Kim, M.S., Zeng, W., Yuan, J.P., Shin, D.M., Worley, P.F., and Muallem, S. (2009). Native Store-operated Ca2+ Influx Requires the Channel Function of Orai1 and TRPC1. J Biol Chem *284*, 9733-9741.

Komazaki, S., Ikemoto, T., Takeshima, H., Iino, M., Endo, M., and Nakamura, H. (1998). Morphological abnormalities of adrenal gland and hypertrophy of liver in mutant mice lacking ryanodine receptors. Cell Tissue Res *294*, 467-473.

Korzeniowski, M.K., Popovic, M.A., Szentpetery, Z., Varnai, P., Stojilkovic, S.S., and Balla, T. (2009). Dependence of STIM1/Orai1-mediated calcium entry on plasma membrane phosphoinositides. J Biol Chem *284*, 21027-21035.

Laude, A.J., and Simpson, A.W. (2009). Compartmentalized signalling: Ca2+ compartments, microdomains and the many facets of Ca2+ signalling. FEBS J *276*, 1800-1816.

Lee, H.C., and Aarhus, R. (1995). A Derivative of Nadp Mobilizes Calcium Stores Insensitive to Inositol Trisphosphate and Cyclic Adp-Ribose. Journal of Biological Chemistry *270*, 2152-2157.

Levine, T.P., and Munro, S. (2002). Targeting of Golgi-specific pleckstrin homology domains involves both PtdIns 4-kinase-dependent and -independent components. Curr Biol *12*, 695-704.

Li, Z., Lu, J., Xu, P., Xie, X., Chen, L., and Xu, T. (2007). Mapping the interacting domains of STIM1 and Orai1 in Ca2+ release-activated Ca2+ channel activation. J Biol Chem *282*, 29448-29456.

Liao, Y., Erxleben, C., Abramowitz, J., Flockerzi, V., Zhu, M.X., Armstrong, D.L., and Birnbaumer, L. (2008). Functional interactions among Orai1, TRPCs, and STIM1 suggest a STIM-regulated heteromeric Orai/TRPC model for SOCE/Icrac channels. Proc Natl Acad Sci U S A *105*, 2895-2900.

Liao, Y., Erxleben, C., Yildirim, E., Abramowitz, J., Armstrong, D.L., and Birnbaumer, L. (2007). Orai proteins interact with TRPC channels and confer responsiveness to store depletion. Proc Natl Acad Sci U S A *104*, 4682-4687.

Liao, Y., Plummer, N.W., George, M.D., Abramowitz, J., Zhu, M.X., and Birnbaumer, L. (2009). A role for Orai in TRPC-mediated Ca2+ entry suggests that a TRPC:Orai complex may mediate store and receptor operated Ca2+ entry. Proc Natl Acad Sci U S A *106*, 3202-3206.

Lin, S., Fagan, K.A., Li, K.X., Shaul, P.W., Cooper, D.M., and Rodman, D.M. (2000). Sustained endothelial nitric-oxide synthase activation requires capacitative Ca2+ entry. J Biol Chem *275*, 17979-17985.

Liou, J., Fivaz, M., Inoue, T., and Meyer, T. (2007). Live-cell imaging reveals sequential oligomerization and local plasma membrane targeting of stromal interaction molecule 1 after Ca2+ store depletion. Proc Natl Acad Sci U S A *104*, 9301-9306.

Liou, J., Kim, M.L., Heo, W.D., Jones, J.T., Myers, J.W., Ferrell, J.E., Jr., and Meyer, T. (2005). STIM is a Ca2+ sensor essential for Ca2+-store-depletion-triggered Ca2+ influx. Curr Biol *15*, 1235-1241.

Lis, A., Peinelt, C., Beck, A., Parvez, S., Monteilh-Zoller, M., Fleig, A., and Penner, R. (2007). CRACM1, CRACM2, and CRACM3 are store-operated Ca2+ channels with distinct functional properties. Curr Biol *17*, 794-800.

Lopez, J.J., Jardin, I., Bobe, R., Pariente, J.A., Enouf, J., Salido, G.M., and Rosado, J.A. (2008). STIM1 regulates acidic Ca2+ store refilling by interaction with SERCA3 in human platelets. Biochem Pharmacol *75*, 2157-2164.

Lopez, J.J., Salido, G.M., Pariente, J.A., and Rosado, J.A. (2006). Interaction of STIM1 with endogenously expressed human canonical TRP1 upon depletion of intracellular Ca2+ stores. J Biol Chem *281*, 28254-28264.

Luik, R.M., Wang, B., Prakriya, M., Wu, M.M., and Lewis, R.S. (2008). Oligomerization of STIM1 couples ER calcium depletion to CRAC channel activation. Nature *454*, 538-542.

Luik, R.M., Wu, M.M., Buchanan, J., and Lewis, R.S. (2006). The elementary unit of store-operated Ca2+ entry: local activation of CRAC channels by STIM1 at ER-plasma membrane junctions. J Cell Biol *174*, 815-825.

Lur, G., Haynes, L.P., Prior, I.A., Gerasimenko, O.V., Feske, S., Petersen, O.H., Burgoyne, R.D., and Tepikin, A.V. (2009). Ribosome-free terminals of rough ER allow formation of STIM1 puncta and segregation of STIM1 from IP(3) receptors. Curr Biol *19*, 1648-1653.

Ma, H.T., Peng, Z., Hiragun, T., Iwaki, S., Gilfillan, A.M., and Beaven, M.A. (2008). Canonical transient receptor potential 5 channel in conjunction with Orai1 and STIM1 allows Sr2+ entry, optimal influx of Ca2+, and degranulation in a rat mast cell line. J Immunol *180*, 2233-2239.

Manji, S.S., Parker, N.J., Williams, R.T., van Stekelenburg, L., Pearson, R.B., Dziadek, M., and Smith, P.J. (2000). STIM1: a novel phosphoprotein located at the cell surface. Biochim Biophys Acta *1481*, 147-155.

Marriott, I., and Mason, M.J. (1995). ATP depletion inhibits capacitative Ca2+ entry in rat thymic lymphocytes. Am J Physiol *269*, C766-774.

Martin, A.C., Willoughby, D., Ciruela, A., Ayling, L.J., Pagano, M., Wachten, S., Tengholm, A., and Cooper, D.M. (2009). Capacitative Ca2+ entry via Orai1 and stromal interacting molecule 1 (STIM1) regulates adenylyl cyclase type 8. Mol Pharmacol *75*, 830-842.

Maruyama, Y., Ogura, T., Mio, K., Kato, K., Kaneko, T., Kiyonaka, S., Mori, Y., and Sato, C. (2009). Tetrameric Orai1 is a teardrop-shaped molecule with a long, tapered cytoplasmic domain. J Biol Chem *284*, 13676-13685.

Masuyama, R., Vriens, J., Voets, T., Karashima, Y., Owsianik, G., Vennekens, R., Lieben, L., Torrekens, S., Moermans, K., Vanden Bosch, A.*, et al.* (2008). TRPV4-mediated calcium influx regulates terminal differentiation of osteoclasts. Cell Metab *8*, 257-265.

McNally, B.A., Yamashita, M., Engh, A., and Prakriya, M. (2009). Structural determinants of ion permeation in CRAC channels. Proc Natl Acad Sci U S A *106*, 22516-22521.

Mercer, J.C., Dehaven, W.I., Smyth, J.T., Wedel, B., Boyles, R.R., Bird, G.S., and Putney, J.W., Jr. (2006). Large store-operated calcium selective currents due to co-expression of Orai1 or Orai2 with the intracellular calcium sensor, Stim1. J Biol Chem *281*, 24979-24990.

Mignen, O., Thompson, J.L., and Shuttleworth, T.J. (2007). STIM1 regulates Ca2+ entry via arachidonate-regulated Ca2+-selective (ARC) channels without store depletion or translocation to the plasma membrane. J Physiol *579*, 703-715.

Mignen, O., Thompson, J.L., and Shuttleworth, T.J. (2008a). Both Orai1 and Orai3 are essential components of the arachidonate-regulated Ca2+-selective (ARC) channels. J Physiol *586*, 185-195.

Mignen, O., Thompson, J.L., and Shuttleworth, T.J. (2008b). Orai1 subunit stoichiometry of the mammalian CRAC channel pore. J Physiol *586*, 419-425.

Mikoshiba, K. (2007). IP3 receptor/Ca2+ channel: from discovery to new signaling concepts. J Neurochem *102*, 1426-1446.

Muik, M., Fahrner, M., Derler, I., Schindl, R., Bergsmann, J., Frischauf, I., Groschner, K., and Romanin, C. (2009). A Cytosolic Homomerization and a Modulatory Domain within STIM1 C Terminus Determine Coupling to ORAI1 Channels. J Biol Chem *284*, 8421-8426.

Muik, M., Frischauf, I., Derler, I., Fahrner, M., Bergsmann, J., Eder, P., Schindl, R., Hesch, C., Polzinger, B., Fritsch, R.*, et al.* (2008). Dynamic coupling of the putative coiled-coil domain of ORAI1 with STIM1 mediates ORAI1 channel activation. J Biol Chem *283*, 8014-8022.

Mullins, F.M., Park, C.Y., Dolmetsch, R.E., and Lewis, R.S. (2009). STIM1 and calmodulin interact with Orai1 to induce Ca2+-dependent inactivation of CRAC channels. Proc Natl Acad Sci U S A *106*, 15495-15500.

Nakanishi, S., Catt, K.J., and Balla, T. (1994). Inhibition of agonist-stimulated inositol 1,4,5-trisphosphate production and calcium signaling by the myosin light chain kinase inhibitor, wortmannin. J Biol Chem *269*, 6528-6535.

Navarro-Borelly, L., Somasundaram, A., Yamashita, M., Ren, D., Miller, R.J., and Prakriya, M. (2008). STIM1-Orai1 interactions and Orai1 conformational changes revealed by live-cell FRET microscopy. J Physiol *586*, 5383-5401.

Nilius, B., Vriens, J., Prenen, J., Droogmans, G., and Voets, T. (2004). TRPV4 calcium entry channel: a paradigm for gating diversity. Am J Physiol Cell Physiol *286*, C195-205.

Oh-Hora, M., Yamashita, M., Hogan, P.G., Sharma, S., Lamperti, E., Chung, W., Prakriya, M., Feske, S., and Rao, A. (2008). Dual functions for the endoplasmic reticulum calcium sensors STIM1 and STIM2 in T cell activation and tolerance. Nat Immunol *9*, 432-443.

Oka, T., Hori, M., and Ozaki, H. (2005). Microtubule disruption suppresses allergic response through the inhibition of calcium influx in the mast cell degranulation pathway. J Immunol *174*, 4584-4589.

Okada, T., Inoue, R., Yamazaki, K., Maeda, A., Kurosaki, T., Yamakuni, T., Tanaka, I., Shimizu, S., Ikenaka, K., Imoto, K.*, et al.* (1999). Molecular and functional characterization of a novel mouse transient receptor potential protein homologue

TRP7. Ca(2+)-permeable cation channel that is constitutively activated and enhanced by stimulation of G protein-coupled receptor. J Biol Chem *274*, 27359-27370.

Oldenburg, K.R., Vo, K.T., Michaelis, S., and Paddon, C. (1997). Recombination-mediated PCR-directed plasmid construction in vivo in yeast. Nucleic Acids Res *25*, 451-452.

Olivera, B.M., Miljanich, G.P., Ramachandran, J., and Adams, M.E. (1994). Calcium channel diversity and neurotransmitter release: the omega-conotoxins and omega-agatoxins. Annu Rev Biochem *63*, 823-867.

Ong, H.L., Cheng, K.T., Liu, X., Bandyopadhyay, B.C., Paria, B.C., Soboloff, J., Pani, B., Gwack, Y., Srikanth, S., Singh, B.B.*, et al.* (2007). Dynamic assembly of TRPC1-STIM1-Orai1 ternary complex is involved in store-operated calcium influx. Evidence for similarities in store-operated and calcium release-activated calcium channel components. J Biol Chem *282*, 9105-9116.

Orci, L., Ravazzola, M., Le Coadic, M., Shen, W.W., Demaurex, N., and Cosson, P. (2009). From the Cover: STIM1-induced precortical and cortical subdomains of the endoplasmic reticulum. Proc Natl Acad Sci U S A *106*, 19358-19362.

Oritani, K., and Kincade, P.W. (1996). Identification of stromal cell products that interact with pre-B cells. J Cell Biol *134*, 771-782.

Paez, P.M., Fulton, D.J., Spreuer, V., Handley, V., Campagnoni, C.W., and Campagnoni, A.T. (2009a). Regulation of store-operated and voltage-operated Ca2+ channels in the proliferation and death of oligodendrocyte precursor cells by golli proteins. ASN Neuro *1*.

Paez, P.M., Fulton, D.J., Spreuer, V., Handley, V., Campagnoni, C.W., Macklin, W.B., Colwell, C., and Campagnoni, A.T. (2009b). Golli myelin basic proteins regulate oligodendroglial progenitor cell migration through voltage-gated Ca2+ influx. J Neurosci *29*, 6663-6676.

Paez, P.M., Spreuer, V., Handley, V., Feng, J.M., Campagnoni, C., and Campagnoni, A.T. (2007). Increased expression of golli myelin basic proteins enhances calcium influx into oligodendroglial cells. J Neurosci *27*, 12690-12699.

Pani, B., Ong, H.L., Liu, X., Rauser, K., Ambudkar, I.S., and Singh, B.B. (2008). Lipid rafts determine clustering of STIM1 in endoplasmic reticulum-plasma membrane

junctions and regulation of store-operated Ca2+ entry (SOCE). J Biol Chem *283*, 17333-17340.

Parekh, A.B. (2003). Mitochondrial regulation of intracellular Ca2+ signaling: more than just simple Ca2+ buffers. News Physiol Sci *18*, 252-256.

Parekh, A.B. (2007). Functional consequences of activating store-operated CRAC channels. Cell Calcium *42*, 111-121.

Parekh, A.B. (2010). Store-operated CRAC channels: function in health and disease. Nat Rev Drug Discov *9*, 399-410.

Parekh, A.B., and Penner, R. (1995). Depletion-Activated Calcium Current Is Inhibited by Protein-Kinase in Rbl-2h3 Cells. P Natl Acad Sci USA *92*, 7907-7911.

Parekh, A.B., and Putney, J.W., Jr. (2005). Store-operated calcium channels. Physiol Rev *85*, 757-810.

Park, C.Y., Hoover, P.J., Mullins, F.M., Bachhawat, P., Covington, E.D., Raunser, S., Walz, T., Garcia, K.C., Dolmetsch, R.E., and Lewis, R.S. (2009). STIM1 clusters and activates CRAC channels via direct binding of a cytosolic domain to Orai1. Cell *136*, 876-890.

Park, C.Y., Shcheglovitoc, A., and Dolmetsch, R. (2010). STIM1 binds to and inhibits Cav1.2 voltage gated calcium channels. Biophysical society *54th Annual Meeting*.

Parvez, S., Beck, A., Peinelt, C., Soboloff, J., Lis, A., Monteilh-Zoller, M., Gill, D.L., Fleig, A., and Penner, R. (2008). STIM2 protein mediates distinct store-dependent and store-independent modes of CRAC channel activation. FASEB J *22*, 752-761.

Peinelt, C., Lis, A., Beck, A., Fleig, A., and Penner, R. (2008). 2-Aminoethoxydiphenyl borate directly facilitates and indirectly inhibits STIM1-dependent gating of CRAC channels. J Physiol *586*, 3061-3073.

Peinelt, C., Vig, M., Koomoa, D.L., Beck, A., Nadler, M.J., Koblan-Huberson, M., Lis, A., Fleig, A., Penner, R., and Kinet, J.P. (2006). Amplification of CRAC current by STIM1 and CRACM1 (Orai1). Nat Cell Biol *8*, 771-773.

Penna, A., Demuro, A., Yeromin, A.V., Zhang, S.L., Safrina, O., Parker, I., and Cahalan, M.D. (2008). The CRAC channel consists of a tetramer formed by Stim-induced dimerization of Orai dimers. Nature *456*, 116-120.

Perez-Reyes, E. (2003). Molecular physiology of low-voltage-activated t-type calcium channels. Physiol Rev *83*, 117-161.

Petersen, O.H., Michalak, M., and Verkhratsky, A. (2005). Calcium signalling: past, present and future. Cell Calcium *38*, 161-169.

Potier, M., and Trebak, M. (2008). New developments in the signaling mechanisms of the store-operated calcium entry pathway. Pflugers Arch *457*, 405-415.

Prakriya, M., Feske, S., Gwack, Y., Srikanth, S., Rao, A., and Hogan, P.G. (2006). Orai1 is an essential pore subunit of the CRAC channel. Nature *443*, 230-233.

Prakriya, M., and Lewis, R.S. (2003). CRAC channels: activation, permeation, and the search for a molecular identity. Cell Calcium *33*, 311-321.

Ramsey, I.S., Delling, M., and Clapham, D.E. (2006). An introduction to TRP channels. Annu Rev Physiol *68*, 619-647.

Rizzuto, R., and Pozzan, T. (2006). Microdomains of intracellular Ca2+: molecular determinants and functional consequences. Physiol Rev *86*, 369-408.

Robida, A.M., and Kerppola, T.K. (2009). Bimolecular fluorescence complementation analysis of inducible protein interactions: effects of factors affecting protein folding on fluorescent protein fragment association. J Mol Biol *394*, 391-409.

Roos, J., DiGregorio, P.J., Yeromin, A.V., Ohlsen, K., Lioudyno, M., Zhang, S., Safrina, O., Kozak, J.A., Wagner, S.L., Cahalan, M.D., *et al.* (2005). STIM1, an essential and conserved component of store-operated Ca2+ channel function. J Cell Biol *169*, 435-445.

Rosado, J.A., Redondo, P.C., Salido, G.M., Sage, S.O., and Pariente, J.A. (2005). Cleavage of SNAP-25 and VAMP-2 impairs store-operated Ca2+ entry in mouse pancreatic acinar cells. Am J Physiol Cell Physiol *288*, C214-221.

Rosado, J.A., and Sage, S.O. (2000). Phosphoinositides are required for store-mediated calcium entry in human platelets. J Biol Chem *275*, 9110-9113.

Sabbioni, S., Barbanti-Brodano, G., Croce, C.M., and Negrini, M. (1997). GOK: a gene at 11p15 involved in rhabdomyosarcoma and rhabdoid tumor development. Cancer Res *57*, 4493-4497.

Schindl, R., Bergsmann, J., Frischauf, I., Derler, I., Fahrner, M., Muik, M., Fritsch, R., Groschner, K., and Romanin, C. (2008). 2-aminoethoxydiphenyl borate alters selectivity of Orai3 channels by increasing their pore size. J Biol Chem *283*, 20261-20267.

Semple, J.I., Prime, G., Wallis, L.J., Sanderson, C.M., and Markie, D. (2005). Two-hybrid reporter vectors for gap repair cloning. Biotechniques *38*, 927-934.

Smyth, J.T., DeHaven, W.I., Bird, G.S., and Putney, J.W., Jr. (2007). Role of the microtubule cytoskeleton in the function of the store-operated Ca2+ channel activator STIM1. J Cell Sci *120*, 3762-3771.

Smyth, J.T., Petranka, J.G., Boyles, R.R., DeHaven, W.I., Fukushima, M., Johnson, K.L., Williams, J.G., and Putney, J.W., Jr. (2009). Phosphorylation of STIM1 underlies suppression of store-operated calcium entry during mitosis. Nat Cell Biol *11*, 1465-1472.

Snutch, T.P., and Reiner, P.B. (1992). Ca2+ channels: diversity of form and function. Curr Opin Neurobiol *2*, 247-253.

Soboloff, J., Spassova, M.A., Hewavitharana, T., He, L.P., Xu, W., Johnstone, L.S., Dziadek, M.A., and Gill, D.L. (2006a). STIM2 is an inhibitor of STIM1-mediated store-operated Ca2+ Entry. Curr Biol *16*, 1465-1470.

Soboloff, J., Spassova, M.A., Tang, X.D., Hewavitharana, T., Xu, W., and Gill, D.L. (2006b). Orai1 and STIM reconstitute store-operated calcium channel function. J Biol Chem *281*, 20661-20665.

Spassova, M.A., Hewavitharana, T., Fandino, R.A., Kaya, A., Tanaka, J., and Gill, D.L. (2008). Voltage gating at the selectivity filter of the Ca2+ release-activated Ca2+ channel induced by mutation of the Orai1 protein. J Biol Chem *283*, 14938-14945.

Spassova, M.A., Soboloff, J., He, L.P., Xu, W., Dziadek, M.A., and Gill, D.L. (2006). STIM1 has a plasma membrane role in the activation of store-operated Ca(2+) channels. Proc Natl Acad Sci U S A *103*, 4040-4045.

Spitzer, N.C., Lautermilch, N.J., Smith, R.D., and Gomez, T.M. (2000). Coding of neuronal differentiation by calcium transients. Bioessays *22*, 811-817.

Srikanth, S., Jung, H.J., Kim, K.D., Souda, P., Whitelegge, J., and Gwack, Y. (2010a). A novel EF-hand protein, CRACR2A, is a cytosolic Ca2+ sensor that stabilizes CRAC channels in T cells. Nat Cell Biol *12*, 436-446.

Srikanth, S., Jung, H.J., Ribalet, B., and Gwack, Y. (2010b). The intracellular loop of Orai1 plays a central role in fast inactivation of Ca2+ release-activated Ca2+ channels. J Biol Chem *285*, 5066-5075.

Stathopulos, P.B., Li, G.Y., Plevin, M.J., Ames, J.B., and Ikura, M. (2006). Stored Ca2+ depletion-induced oligomerization of stromal interaction molecule 1 (STIM1) via the EF-SAM region: An initiation mechanism for capacitive Ca2+ entry. J Biol Chem *281*, 35855-35862.

Stathopulos, P.B., Zheng, L., and Ikura, M. (2009). Stromal interaction molecule (STIM) 1 and STIM2 calcium sensing regions exhibit distinct unfolding and oligomerization kinetics. J Biol Chem *284*, 728-732.

Stathopulos, P.B., Zheng, L., Li, G.Y., Plevin, M.J., and Ikura, M. (2008). Structural and mechanistic insights into STIM1-mediated initiation of store-operated calcium entry. Cell *135*, 110-122.

Strange, K., Yan, X., Lorin-Nebel, C., and Xing, J. (2007). Physiological roles of STIM1 and Orai1 homologs and CRAC channels in the genetic model organism Caenorhabditis elegans. Cell Calcium *42*, 193-203.

Striessnig, J. (1999). Pharmacology, structure and function of cardiac L-type Ca(2+) channels. Cell Physiol Biochem *9*, 242-269.

Suh, B.C., Inoue, T., Meyer, T., and Hille, B. (2006). Rapid chemically induced changes of PtdIns(4,5)P2 gate KCNQ ion channels. Science *314*, 1454-1457.

Takahashi, Y., Murakami, M., Watanabe, H., Hasegawa, H., Ohba, T., Munehisa, Y., Nobori, K., Ono, K., Iijima, T., and Ito, H. (2007). Essential role of the N-terminus of

murine Orai1 in store-operated Ca2+ entry. Biochem Biophys Res Commun *356*, 45-52.

Takeshima, H., Iino, M., Takekura, H., Nishi, M., Kuno, J., Minowa, O., Takano, H., and Noda, T. (1994). Excitation-contraction uncoupling and muscular degeneration in mice lacking functional skeletal muscle ryanodine-receptor gene. Nature *369*, 556-559.

Takeshima, H., Komazaki, S., Hirose, K., Nishi, M., Noda, T., and Iino, M. (1998). Embryonic lethality and abnormal cardiac myocytes in mice lacking ryanodine receptor type 2. EMBO J *17*, 3309-3316.

Terasaki, M., Chen, L.B., and Fujiwara, K. (1986). Microtubules and the endoplasmic reticulum are highly interdependent structures. J Cell Biol *103*, 1557-1568.

Touret, N., Paroutis, P., Terebiznik, M., Harrison, R.E., Trombetta, S., Pypaert, M., Chow, A., Jiang, A., Shaw, J., Yip, C.*, et al.* (2005). Quantitative and dynamic assessment of the contribution of the ER to phagosome formation. Cell *123*, 157-170.

Trebak, M., Lemonnier, L., DeHaven, W.I., Wedel, B.J., Bird, G.S., and Putney, J.W., Jr. (2009). Complex functions of phosphatidylinositol 4,5-bisphosphate in regulation of TRPC5 cation channels. Pflugers Arch *457*, 757-769.

Varnai, P., Thyagarajan, B., Rohacs, T., and Balla, T. (2006). Rapidly inducible changes in phosphatidylinositol 4,5-bisphosphate levels influence multiple regulatory functions of the lipid in intact living cells. J Cell Biol *175*, 377-382.

Varnai, P., Toth, B., Toth, D.J., Hunyady, L., and Balla, T. (2007). Visualization and manipulation of plasma membrane-endoplasmic reticulum contact sites indicates the presence of additional molecular components within the STIM1-Orai1 Complex. J Biol Chem *282*, 29678-29690.

Vig, M., Beck, A., Billingsley, J.M., Lis, A., Parvez, S., Peinelt, C., Koomoa, D.L., Soboloff, J., Gill, D.L., Fleig, A.*, et al.* (2006a). CRACM1 multimers form the ion-selective pore of the CRAC channel. Curr Biol *16*, 2073-2079.

Vig, M., DeHaven, W.I., Bird, G.S., Billingsley, J.M., Wang, H., Rao, P.E., Hutchings, A.B., Jouvin, M.H., Putney, J.W., and Kinet, J.P. (2008). Defective mast cell effector functions in mice lacking the CRACM1 pore subunit of store-operated calcium release-activated calcium channels. Nat Immunol *9*, 89-96.

Vig, M., Peinelt, C., Beck, A., Koomoa, D.L., Rabah, D., Koblan-Huberson, M., Kraft, S., Turner, H., Fleig, A., Penner, R.*, et al.* (2006b). CRACM1 is a plasma membrane protein essential for store-operated Ca2+ entry. Science *312*, 1220-1223.

Walsh, C.M., Chvanov, M., Haynes, L.P., Petersen, O.H., Tepikin, A.V., and Burgoyne, R.D. (2010). Role of phosphoinositides in STIM1 dynamics and store-operated calcium entry. Biochem J *425*, 159-168.

Wang, Y., Deng, X., Zhou, Y., Hendron, E., Mancarella, S., Ritchie, M.F., Tang, X.D., Baba, Y., Kurosaki, T., Mori, Y.*, et al.* (2009). STIM protein coupling in the activation of Orai channels. Proc Natl Acad Sci U S A *106*, 7391-7396.

Wang, Y., Mancarella, S., Hendron, E., Eguchi, E., Deng, X., and Gill, D.L. (2010). STIM1 mediates control over Cav1.2 channels as well as Orai channels. Biophysical society *54th Annual Meeting*.

Watanabe, H., Takahashi, R., Zhang, X.X., Kakizawa, H., Hayashi, H., and Ohno, R. (1996). Inhibition of agonist-induced Ca2+ entry in endothelial cells by myosin light-chain kinase inhibitor. Biochem Biophys Res Commun *225*, 777-784.

Williams, R.T., Manji, S.S., Parker, N.J., Hancock, M.S., Van Stekelenburg, L., Eid, J.P., Senior, P.V., Kazenwadel, J.S., Shandala, T., Saint, R.*, et al.* (2001). Identification and characterization of the STIM (stromal interaction molecule) gene family: coding for a novel class of transmembrane proteins. Biochem J *357*, 673-685.

Williams, R.T., Senior, P.V., Van Stekelenburg, L., Layton, J.E., Smith, P.J., and Dziadek, M.A. (2002). Stromal interaction molecule 1 (STIM1), a transmembrane protein with growth suppressor activity, contains an extracellular SAM domain modified by N-linked glycosylation. Biochim Biophys Acta *1596*, 131-137.

Wu, M.M., Buchanan, J., Luik, R.M., and Lewis, R.S. (2006a). Ca2+ store depletion causes STIM1 to accumulate in ER regions closely associated with the plasma membrane. J Cell Biol *174*, 803-813.

Wu, Y., Borde, M., Heissmeyer, V., Feuerer, M., Lapan, A.D., Stroud, J.C., Bates, D.L., Guo, L., Han, A., Ziegler, S.F.*, et al.* (2006b). FOXP3 controls regulatory T cell function through cooperation with NFAT. Cell *126*, 375-387.

Wuttke, A., Sagetorp, J., and Tengholm, A. (2010). Distinct plasma-membrane PtdIns(4)P and PtdIns(4,5)P2 dynamics in secretagogue-stimulated beta-cells. J Cell Sci *123*, 1492-1502.

Xu, P., Lu, J., Li, Z., Yu, X., Chen, L., and Xu, T. (2006). Aggregation of STIM1 underneath the plasma membrane induces clustering of Orai1. Biochem Biophys Res Commun *350*, 969-976.

Yamashita, M., Navarro-Borelly, L., McNally, B.A., and Prakriya, M. (2007). Orai1 mutations alter ion permeation and Ca2+-dependent fast inactivation of CRAC channels: evidence for coupling of permeation and gating. J Gen Physiol *130*, 525-540.

Yao, Y., Ferrer-Montiel, A.V., Montal, M., and Tsien, R.Y. (1999). Activation of store-operated Ca2+ current in Xenopus oocytes requires SNAP-25 but not a diffusible messenger. Cell *98*, 475-485.

Yeromin, A.V., Zhang, S.L., Jiang, W., Yu, Y., Safrina, O., and Cahalan, M.D. (2006). Molecular identification of the CRAC channel by altered ion selectivity in a mutant of Orai. Nature *443*, 226-229.

Yuan, J.P., Zeng, W., Dorwart, M.R., Choi, Y.J., Worley, P.F., and Muallem, S. (2009). SOAR and the polybasic STIM1 domains gate and regulate Orai channels. Nat Cell Biol *11*, 337-343.

Yuan, J.P., Zeng, W., Huang, G.N., Worley, P.F., and Muallem, S. (2007). STIM1 heteromultimerizes TRPC channels to determine their function as store-operated channels. Nat Cell Biol *9*, 636-645.

Zagranichnaya, T.K., Wu, X., and Villereal, M.L. (2005). Endogenous TRPC1, TRPC3, and TRPC7 proteins combine to form native store-operated channels in HEK-293 cells. J Biol Chem *280*, 29559-29569.

Zhang, S.L., Kozak, J.A., Jiang, W., Yeromin, A.V., Chen, J., Yu, Y., Penna, A., Shen, W., Chi, V., and Cahalan, M.D. (2008). Store-dependent and -independent modes regulating Ca2+ release-activated Ca2+ channel activity of human Orai1 and Orai3. J Biol Chem *283*, 17662-17671.

Zhang, S.L., Yeromin, A.V., Zhang, X.H., Yu, Y., Safrina, O., Penna, A., Roos, J., Stauderman, K.A., and Cahalan, M.D. (2006). Genome-wide RNAi screen of Ca(2+) influx identifies genes that regulate Ca(2+) release-activated Ca(2+) channel activity. Proc Natl Acad Sci U S A *103*, 9357-9362.

Zhang, S.L., Yu, Y., Roos, J., Kozak, J.A., Deerinck, T.J., Ellisman, M.H., Stauderman, K.A., and Cahalan, M.D. (2005). STIM1 is a Ca2+ sensor that activates CRAC channels and migrates from the Ca2+ store to the plasma membrane. Nature *437*, 902-905.

Zheng, L., Stathopulos, P.B., Li, G.Y., and Ikura, M. (2008). Biophysical characterization of the EF-hand and SAM domain containing Ca2+ sensory region of STIM1 and STIM2. Biochem Biophys Res Commun *369*, 240-246.

Zhou, Y., Meraner, P., Kwon, H.T., Machnes, D., Oh-hora, M., Zimmer, J., Huang, Y., Stura, A., Rao, A., and Hogan, P.G. (2010). STIM1 gates the store-operated calcium channel ORAI1 in vitro. Nat Struct Mol Biol *17*, 112-116.

Zhu, M.X., Ma, J.J., Parrington, J., Calcraft, P.J., Galione, A., and Evans, A.M. (2010). Calcium signaling via two-pore channels: local or global, that is the question. Am J Physiol-Cell Ph *298*, C430-C441.